Comparison of techniques to reconstruct palaeoclimates of China

Zhiyong Zhang

Doctor of Philosophy

(Co-tutelle Program)

Department of Biological Sciences

Faculty of Science and Engineering

Macquarie University

And

State Key Laboratory of Systematic and Evolutionary Botany

Institute of Botany, the Chinese Academy of Sciences

June 2016

This thesis is presented as a partial fulfillment to the requirements for the degree of

Doctor of Philosophy

Certificate of candidate

I, Zhiyong Zhang, herewith certify that the work in this thesis entitled 'Comparison of techniques to reconstruct palaeoclimates of China' has not been previously submitted for a degree, nor has it been submitted as part of the requirements for a degree to any university or institution other than Macquarie University and the co-tutelle partner institute – Institute of Botany, the Chinese Academy of Sciences.

I also certify that this is an original piece of research and has been written by me. Any help and assistance that I have received in my research and the preparation of this thesis has been appropriately acknowledged.

In addition I certify that all information sources and literature are indicated in the thesis.

Zhiyong Zhang
Final Submitted Date: 20th June 2016

Table of contents

List of figures

List of tables

Abstract

Investigating the past climate is helpful to distinguish humankind's contribution on present climate change, and also helpful to understand the historic or geological evolution of global environmental conditions. A number of different types of records provide information about past climate changes, including petrology, sedimentology, glaciology, dendrochronology, palynology and others. Various different techniques can be used to make quantitative reconstructions from palaeodata. All of these methods have their shortcomings and advantages. In this thesis, I examine two reconstruction methods, which have been widely applied to make reconstructions of climate during pre-Quaternary times, specifically the coexistence approach and leaf traits analysis.

The coexistence approach (CoA) assumes that the climate of a fossil assemblage can be defined from the overlap between the climate ranges of the individual taxa, where the climate range of each taxon is defined by the climate range under which it grows today. For taxa that are no longer extant, the range is defined as that of the nearest living relative (NLR). The method assumes that it is possible to define the modern climate tolerance accurately and also that taxa were physically present at the site. In Chapter 2, I test the impact of these two assumptions on CoA reconstructions of mean annual precipitation (MAP), mean annual temperature (MAT), mean temperature of the warmest month (MTWA) and mean temperature of the coldest month (MTCO) using modern pollen data from the Qinghai-Tibetan Plateau. I find that the data quality of NLRs and the exotic pollen seriously affect the reconstructed MAP, MAT, MTWA and MTCO. The uncertainties are also relatively large, especially for those three temperature parameters, even those two factors considered. Thus the complementary method should be explored.

Methods based on the correlation between leaf physiognomy and climate variables provide an alternative approach to reconstructing past climate. The two most widely used methods are like leaf margin analysis (LMA) and the climate leaf analysis multivariate program (CLAMP). The disadvantages of these methods are identified in various studies, such as using the limited leaf traits and the problem of correlation within traits. Hence, we are exploring our leaf traits-climate model method.

I first establish the modern relationships between leaf traits and climates (Chapter 3) based on a large data set of modern trait observations from China. I used logistic regression techniques to investigate the relationships between summer temperature (measured by the accumulated temperature sum above 0°C), plant-available moisture (measured by the ratio of actual to equilibrium transpiration) and seasonality (measured by the daily mean growing season temperature when temperatures are >5°C) and the frequencies of 25 leaf morphometric traits, collected from 98 sites sampling the range of climate and vegetation types found in China. Results show that these morphometric traits vary along climate gradients in a predictable and understandable way. Different traits combination can outline the specific climate space. Leaf traits responding to one or more climate variables indicate that traits could play multiple functions on the adaptation for the moisture and temperature. Many specific relationships between traits and bioclimate variables are conservative across all woody life forms. These findings lay a stronger foundation for using morphometric traits to reconstruct past climates.

In Chapter 4, I apply the independent relationships between specific leaf traits and individual climate variables to build predictive models for estimating the length of the growing season (GDD_0: growing degree days above a baseline of 0°C) and plant-available moisture (α: the ratio of actual to equilibrium evapotranspiration). I then apply these models to predict the paleoclimate of four fossil leaf floras: from the Fushun Basin (Eocene), from

Shanwang Basin (Middle Miocene), from Xiaolongtan Basin (Late Miocene), and from Shengzhou (Pliocene) in China. These geological times are examples of climate intervals when CO_2 was higher than today, and as such provide opportunities to examine how the climate system has responded to enhanced greenhouse gas concentrations. Results show that our models have relatively small reconstruction biases under modern conditions. The reconstructed paleoclimates by the modified models are comparable with previous reconstructions, but our results show more constraints rather than large uncertainties like previous reconstructions. Paleoclimate changes for these four sites are consistent with the evolution of climates in this region and compatible with enhanced monsoon conditions during these high CO_2 intervals.

In summary, my thesis makes three important contributions to the field of palaeoclimate reconstruction. Firstly, by quantifying the impact of extra-local pollen on climate reconstructions for the Tibetan Plateau, I demonstrate the unreliability of the coexistence approach when applied in open vegetation. This work suggests that the coexistence approach should only be used when pollen samples can be combined with e.g. macrofossil evidence that would demonstrate the local presence of individual species. Secondly, through applying generalised linear modelling (GLM) technique to establish the independent relationships between multiple climate variables and leaf morphometric traits, after removing the influence of interactions between these variables, I have shown why univariate correlations as used in standard methods such as leaf margin analysis (LMA) and the climate leaf analysis multivariate program (CLAMP) are noisy and unreliable. The GLM methodology provides a better way to use leaf traits to reconstruct climate. Finally, I have developed a new multi-model technique based on these independent trait-climate relationships to reconstruct palaeoclimates in China from fossil leaf floras, and demonstrated that this provides well-constrained estimates of temperature and moisture variables.

Acknowledgements

For their expertise, help and encouragement to me as a doctoral researcher, I would like to thank the following people:

Professors Sandy P. Harrison, Volker Mosbrugger, David K. Ferguson, Khum N. Paudayal, Anjali Trivedi, and Cheng–Sen Li as co-authors of my first published paper "Evaluation of the realism of climate reconstruction using the Coexistence Approach with modern pollen samples from the Qinghai-Tibetan Plateau" with their agreement.

I thank Prof. Sandy Harrison and Prof. Colin Prentice for collecting data used in Chapters 3 and 4. I am also grateful to Post-doctor Wang Han for her extraordinary amount of help in the analyses for Chapters 3 and 4.

I thank my supervisor Professor Sandy P. Harrison for her valuable comments and contributions, which made the completion of this thesis possible.

List of publications

Zhang ZY, Harrison SP, Mosbrugger V, Ferguson DK, Paudayal KN, Trivedi A, Li CS (2015) Evaluation of the realism of climate reconstruction using the Coexistence Approach with modern pollen samples from the Qinghai-Tibetan Plateau. *Rev. Palaeobot. Palyno* 219, 172-182.

Chapter 1 Introduction

1. The motivation of reconstructing past climate

There is much concern about ongoing and potential future changes in climate and their impacts on society (Collins et al., 2013; Hartmann et al., 2013; Kirtman et al., 2013; Denton et al., 2014; Kunreuther et al., 2014; Smith et al., 2014). According to the Intergovernmental Panel on Climate Change (IPCC) fifth assessment (Hartmann et al., 2013), anthropogenic emissions have increased the level of greenhouse gases, carbon dioxide (CO_2), methane, nitrous oxide (N_2O), and three groups of fluorinated gases (sulfur hexafluoride, hydroflurocarbons, and perflurocarbons), in the atmosphere to levels that are unprecedented since the pre-industrial era (Joos and Spahni, 2008; Schilt et al., 2010). Current climate changes have had widespread influences on human and natural systems (Hartmann et al., 2013; Jiménez Cisneros et al., 2014; Porter et al., 2014). Climate change has altered the patterns of the global hydrological cycle including runoff (Labat et al., 2004; Gedney et al., 2006; Krakauer and Fung, 2008). In the 20th century, river discharge has decreased in parts of Africa, central/southern Asia and south-eastern Europe, and increased especially in parts of North America and western Asia (Gerten et al., 2008). The amount and seasonality of river discharge also has been altered in many regions (Kundzewicz et al., 2007; Jiménez Cisneros et al., 2014). Global warming has caused glacier shrinkage in the European Alps, which has led to the yield of the glacial melt water greater in 1910–1940 than in 1980–2000 (Collins, 2008). Almost all glaciers in the tropical Andes and Himalayan have been shrinking rapidly due to climate change (Rabassa, 2009; Bolch et al., 2012; Gardner, 2013; Rabatel et al., 2013). The impacts of climate change on human systems are also distinguishable. Climate change has already influenced the global crop production, such as wheat, maize, rice and soybean, although the estimated negative impacts on wheat and maize are larger than on rice and soybean (Lobell et al., 2011). At a regional scale, the

impacts of climate change are most noticeable in low-lying coastal regions that are at risk from sea-level rise and coastal flooding (Losada et al., 2013). This has already caused serious economic damage over the period 1995-2010 in Florida (Morris, 2010). Coastal flooding is also a major problem in SE Asia, particularly Bangladesh where there has been a major impact on both protected habitats (Agrawala et al., 2003) and local economies (Murty et al., 1986) while major floods in 1970 and 1991 claimed many thousand lives (Haque, 1997; Karim and Mimura, 2008). Coastal flooding has been exacerbated by increased frequency of major storm events (e.g. Barras et al., 2008). The combined effects of sea-level rise, coastal flooding and storms have led changes in coastal wetlands, increased coastal erosion, and saltwater intrusion in many regions around the world (e.g. Morton et al., 2005; Saito et al., 2007; McLeod et al., 2010). The regional impacts of climate change are also registered in inland areas. Regional droughts have increased in recent decades, leading to reductions in surface water and groundwater availability particularly in subtropical regions (Piao et al., 2010; Jiménez Cisneros et al., 2014). Increased flooding e.g. the United Kingdom has also been attributed to regional climate changes (Pall et al., 2011). Although the attribution of regional climate changes is subject to large uncertainties, taken together the evidence strongly indicates that anthropogenic climate change is being manifested increasingly through regional impacts.

It is important to determine whether current climate change is normal relative to the natural variability of the climate system. It is also important to determine how the climate system responds to large changes in climate forcing, and whether state-of-the-art climate models can simulate these responses accurately. The palaeoclimate record provides an opportunity to determine the natural variability of climate system, identify the large changes of climate forcing and test the performance of climate models because there have been large changes in forcing during periods prior to the development of meteorological instruments. We know

what the response to these changes in forcing was because of various kinds of environmental records, which can be used to derive reconstructions of past climate.

1.1 Current climate change and climate change projections

Warming of the current climate system is unequivocal and our Earth is experiencing extremely large changes in the atmosphere, land surface, ocean and cryosphere (Hartmann et al., 2013; Rhein et al., 2013; Vaughan et al., 2013). There are four sources of global temperature data for the post-industrial period, including the Berkeley data set (Rohde et al., 2013), the Climatic Research Unit (CRU) temperature database (Jones et al., 2012), the Global Historical Climatology Network Version 3 (Lawrimore et al., 2011) and the Goddard Institute of Space Studies data sets (Hansen et al., 2010). Although they differ in details, they all show that global land-surface air temperature has increased between around 0.65 and 1.06 °C over the instrumental period. Among these different estimates of land-surface air temperature, the long-term variations and trends generally agree, especially after 1900; a warming of around 0.7-0.8 °C has been particularly marked since the 1970s (Hartmann et al., 2013). Geographically, Europe, North America, and Asia have experienced higher warming with a greater rate of 0.01-0.02 °C per decade and Antarctica has a lower warming with the slowest rate of warming with 0.006 °C per decade (Rohde et al., 2013). According to Rohde et al. (2013), it is almost 100% certain that the upper ocean (above 700 m) has warmed between 1971 and 2010, with a increasing rate of 0.11 [0.09 to 0.13] °C per decade in the upper 75 m, down to about 0.015°C per decade at 700 m (Rhein et al., 2013). The ocean warming is more significant in the Northern Hemisphere, especially the North Atlantic, than the Southern Hemisphere (Levitus et al., 2009). During the same period, the globally averaged temperature difference between the ocean surface and 200 m has increased by around 0.25°C, which corresponds to a 4% increase in density stratification (Levitus et al., 2009).The annual Arctic sea ice extent decreased over the period 1979–2012,

with a rate of very likely between 3.5 and 4.1% per decade (0.45 to 0.51 million km^2 per decade) (Vaughan et al., 2013). The average decrease in decadal extent of Arctic sea ice has been most rapid in summer and autumn. For example, there was a decrease in ice extent at the end of the summer (September) of 0.5×10^6 km^2 between 1979–1988 and 1989–1998, followed by a further decrease of 1.2×10^6 km^2 between 1989–1998 and 1999–2008 (Comiso et al., 2008; Comiso, 2012). Almost all glaciers worldwide have continued to shrink, especially the period of 2003-2009 (Vaughan et al., 2013), during which most of the ice lost was from glaciers in Alaska, the Canadian Arctic, the periphery of the Greenland ice sheet, the Southern Andes and the Asian Mountains (Gardner et al., 2013). The loss from these regions accounts for more than 80% of the total ice loss that was very likely 226 ± 135 Gt yr^{-1} (sea level equivalent, 0.62 ± 0.37 mm yr^{-1}) in the period 1971–2009, 275 ± 135 Gt yr–1 (0.76 ± 0.37 mm yr^{-1}) in the period 1993–2009, and 301 ± 135 Gt yr–1 (0.83 ± 0.37 mm yr^{-1}) between 2005 and 2009 (Gardner et al., 2013). The rate of ice loss from the Greenland ice sheet has accelerated since 1992 with an average rate of very likely from 34 [–6 to 74] Gt yr^{-1} over the period 1992–2001 (sea level equivalent, 0.09 [–0.02 to 0.20] mm yr^{-1}), to 215 [157 to 274] Gt yr^{-1} over the period 2002–2011 (0.59 [0.43 to 0.76] mm yr^{-1}) (Vaughan et al., 2013).

The principal driver of current climate warming is emissions of anthropogenic greenhouse gases (GHGs) since the pre-industrial era (Collins et al., 2013; Myhre et al., 2013). The globally averaged abundance of atmospheric carbon dioxide (CO_2) in 1750 was 278 ± 2 ppm (Etheridge et al., 1996), which is reconstructed from measurements on air bubbles extracted from ice cores and from firn. The globally averaged methane (CH_4) and nitrous oxide (N_2O) in 1750 were 722 ± 25 ppb (Etheridge et al., 1998; Dlugokencky et al., 2005) and 270 ± 7 ppb (Prather et al., 2012). While in 2011, the atmospheric abundance of CO_2, N_2O and CH_4 was 390.5 ppm (390.3 to 390.7, 90% confidence intervals), 324.2 ppb (324.0 to 324.4) and 1803.2 ppb (1801.2 to 1805.2), which is 40%, 20% and 150% respectively

greater than in 1750 (Hartmann et al., 2013). Anthropogenic GHG emissions in 2010 have reached 49 ± 4.5 $GtCO_2$-eq/yr (quantified as CO_2-equivalent per year) (IEA, 2012; JRC/PBL, 2013). Emissions of CO_2 from fossil fuel combustion and industrial processes contributed almost 80% of the total GHG emissions increase from 1970 to 2010 and the percentage contribution was similar for the increase from 2000 to 2010 (Macknick, 2011; Blanco et al., 2014). Global economic and population growth are the most important drivers for the increases of CO_2 emissions from fossil fuel combustion; population growth between 2000 and 2010 was approximately equal to the previous three decades, however economic growth contributed with a sharp rise (Blanco et al., 2014).

For decades, climate changes have caused impacts on natural and human systems on all continents and across the oceans. The evidence of observed climate change impacts is strongest and most comprehensive for natural systems. In many regions, changing precipitation is altering hydrological systems, which affects water resources in terms of quantity and quality. Analysis of observed annual maximum 1-day precipitation over global land areas with a global dataset of 8326 high-quality land-based observing stations with more than 30 years of record over the period from 1900 to 2009 indicates a significant increase in extreme precipitation globally (Westra et al., 2013). However, there are significant precipitation variations between regions and seasons (Seneviratne, 2012; Westra et al., 2013). It is very likely that the sea level rise of 0.6 ± 0.2 mm per year since 1971, which is equivalent to 30% of the observed rate of global mean sea level rise for the same period, can be attributed to the warming of the upper 700 m of the ocean (Jevrejeva et al., 2008; Church and White, 2011; Ray and Douglas, 2011; Rohde et al., 2013). Global warming is speeding up the snow and ice melting and causing permafrost warming and thawing in high-latitude regions and in high-elevation regions (Vaughan et al., 2013). This deglaciation has altered the risk of glacier lake outburst floods in the Alps of Europe, Himalayas, Andes, and other mountain regions (Huggel et al., 2011; Carey et al., 2012).

However, some regions of the world have experienced more intense and longer droughts since the 1950s (Seneviratne, 2012).

The impacts of climate change on human systems are often geographically heterogeneous. In China, farmers need to adapt the irrigation systems during the low flows of Yellow River (Liu et al., 2008). In the United States, northward shifts in fisheries match the patterns of northward shifts in species distributions in response to warming climates (Perry et al., 2005; Dulvy et al., 2008; Nye et al., 2009; Pinsky and Fogarty, 2012). In Mexico, more and more people migrate to the US due to the reduction in crop yields driven by climate (Feng et al., 2010). In Indonesia and Africa, population migration also has occurred more frequently by the impact of the climate change (Marchiori and Schumacher, 2012; Bohra-Mishra et al., 2014).

Projections of the likely trajectory of future climate have been made using state-of-the-art climate models in the framework of the Coupled Model Intercomparison Project Phase 5 (CMIP5). These simulations are driven by the Representative Concentration Pathways (RCPs) scenarios, which specify the concentrations and corresponding emissions of the full suite of greenhouse gases, aerosols and chemically active gases (Moss et al., 2008). These pathways provide internally consistent sets of time-dependent forcings up to 2100 consistent with a specific underlying socioeconomic scenario. RCP2.6 is the lowest pathway where radiative forcing peaks at approximately 3 W m^{-2} before 2100 and then declines (the corresponding Extended Concentration Pathway, ECP, assumes constant emissions after 2100); RCP4.5 and RCP6.0 are two intermediate stabilization pathways in which radiative forcing is stabilized at approximately 4.5 W m^{-2} and 6.0 W m^{-2} after 2100 (the corresponding ECPs assume constant concentrations after 2150); and RCP8.5 is the highest pathway for which radiative forcing reaches more than 8.5 W m^{-2} by 2100 and continues to

rise for some amount of time (the corresponding ECP assuming constant emissions after 2100 and constant concentrations after 2250).

Under the four RCP scenarios (RCP2.6, RCP4.5, RCP6.0 and RCP8.5), the projected change in global mean surface air temperature will likely be in the range of 0.3 to 0.7°C for the period of 2016-2035, assuming there are no major volcanic eruptions or secular changes in total solar irradiance during this period (Kirtman et al., 2013). Globally averaged sea surface temperatures (SSTs) are projected under all RCP forcing scenarios to be warmer by 0.2 to around 2.0°C over the near term (present through mid-century) relative to 1986–2005 (Meehl et al., 2007). For the sea ice change in the near term future, the ice-free (sea ice extent less than 1×10^6 km^2 for at least 5 consecutive years) Arctic Ocean in September is predicted by five CMIP5 models. Results from four CMIP5 models indicate that an ice-free ocean would likely occur before 2050 for RCP8.5, with the earliest and latest years of near disappearance of the sea ice pack being about 2040 and about 2060, respectively (Kirtman et al., 2013). Under the highest representative concentration pathway scenario, 11 CMIP5 Earth System Models (ESMs) with interactive carbon cycle estimate, on average, a 50 ppm (min to max range –140 to +210 ppm) larger atmospheric CO_2 concentration and 0.2°C (min to max range –0.4 to +0.9°C) larger global surface temperature increase by 2100 (Collins et al., 2013). The global ocean will warm in all RCP scenarios, from about 0.6°C [0.1-1.0°C] (RCP2.6) to 2.0°C [0.5-2.5°C] (RCP8.5) in the top 100 m, and from about 0.3°C [0.1-0.5°C] (RCP2.6) to 0.6°C [0.2-1.0°C] (RCP8.5) at about 1 km depth by the end of the 21st century (Collins et al., 2013).

Climate models are the only tool to investigate the response of climate system to different forcings, and to make projections of the short-term or long-term future changes, and are continually being developed and improved. According to the IPCC report (Flato et al., 2013), the ability of climate models to simulate both surface temperature and precipitation

has improved in many important ways compared to the generation of models assessed in the last Assessment Report (AR4). However, model performance for surface temperature is generally much better than for precipitation (Flato et al., 2013). There is high confidence that the latest models can reproduce many features of the observed global and Northern Hemisphere (NH) mean temperature variance on interannual to centennial times scales. Model ability to assess variability from millennial simulations has improved since the AR4, which allows the climate-change signal to be distinguished from internal variability (Flato et al., 2013). However improvements in simulating the modern climate do not necessarily mean that the models can simulate large climate changes accurately. This is where evaluation using the palaeoclimate record can be helpful.

1.2 The role of palaeoclimate record

Climate model evaluation can be made using palaeodata because the paleoclimate data provide evidence of the response to past changes in forcing, changes which can be as large as those expected over the 21st century (Braconnot et al., 2012; Harrison et al., 2015). Climate models usually underestimate the magnitude of regional changes in climate, but shed light on the direction and large-scale patterns of past climate changes (Joussaume et al., 1999; Wohlfahrt et al., 2004; Braconnot et al., 2012; Zhao and Harrison, 2012; Izumi et al., 2013; Li et al., 2013; Perez-Sanz et al., 2014; Schmidt et al., 2014; Harrison et al., 2015). Paleoclimate studies increase confidence in the models' ability to forecast a future climate and lead to improved reconstructions on the basis of paleodata (Robinson and Dowsett, 2010). In addition to the fundamental function of paleorecords providing qualitative and quantitative climate reconstructions of the past climates, paleorecords also provide boundary conditions, such as sea ice distribution, vegetation cover, sea level, ice sheet extent and topography, for climate model simulations.

1.3 Natural variability of climate in Eocene, Miocene and Pliocene

The Earth has experienced three periods with climate warmer than today in the past 65 Ma: the Eocene, Miocene and Pliocene (Figure 1-1). The high temperature during these three periods is most likely associated with higher atmospheric CO_2 levels than that of

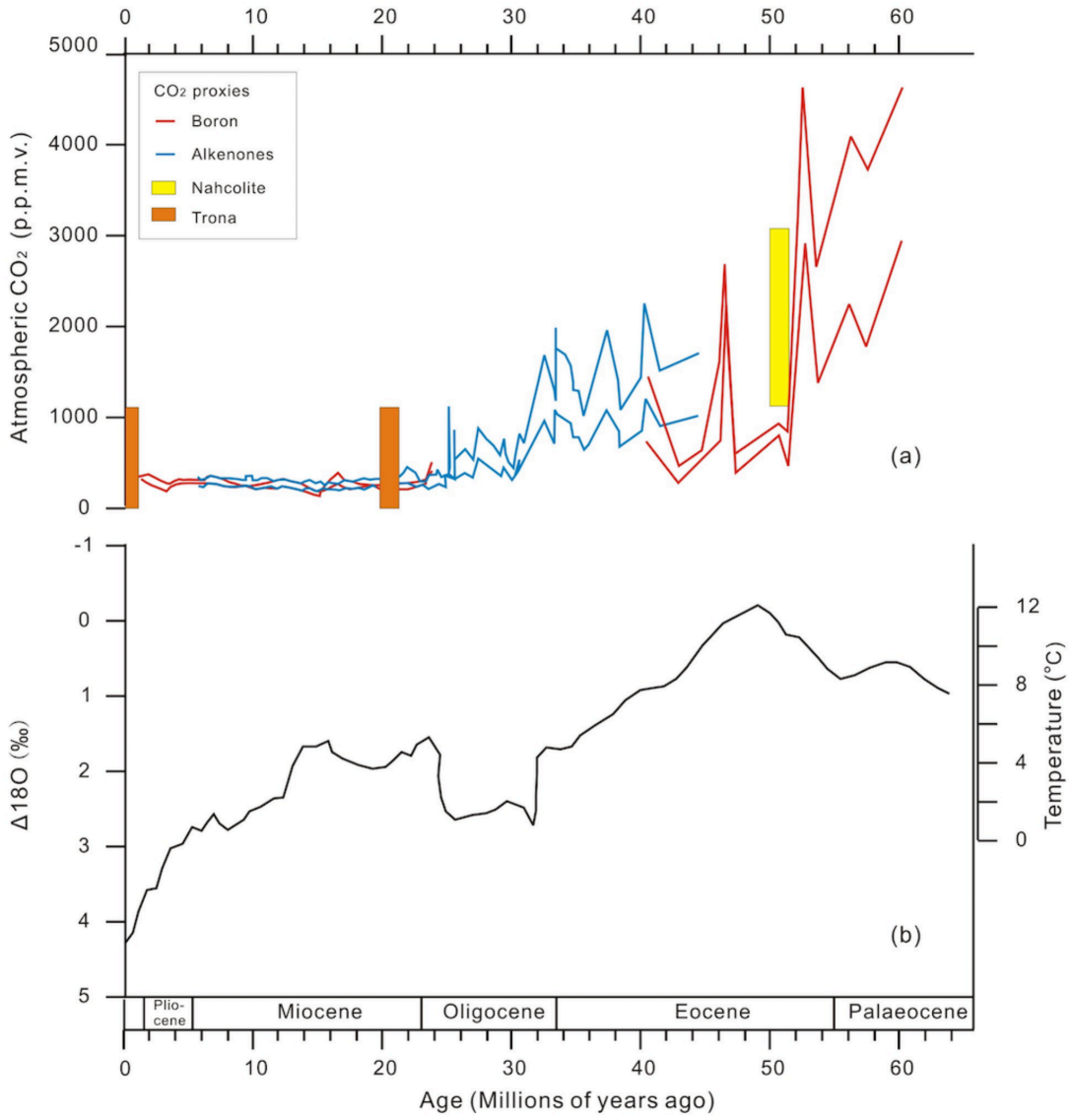

Figure 1-1 Natural variability of climate since the last 65 Ma (redrawn from Zachos, et al. 2008). **a**, Cenozoic pCO_2 estimations based on the different carbon dioxide proxy, including Boron, Alkenones, Nahcolite and Trona (Lowenstein and Demicco, 2006; Royer, 2006). **b**, the climate for the period of 65 Ma to 0 year ago. The oxygen-isotope curve and temperature scale is based on deep-sea benthic foraminiferal records (Zachos et al., 2001).

pre-industrial times (Budyko and Sedunov, 1988; Zubakov and Borzenkova, 1988; Masson-Delmotte et al., 2013). This potentially gives us the opportunities of testing how the climate system will be changed due to the constantly increasing the CO_2 levels in the next few decades.

The Eocene, which occurred between 56 to 33.9 Ma ago, encompassed a wide diversity of different climate conditions including the Early Eocene Climatic Optimum (EECO) and the expansion of the Antarctic ice sheet in the end. The land-sea distribution and continental topography at that time was different from today (Herold et al., 2011). The early Eocene was characterised by a high frequency of volcanism on a global scale; at the same time, the atmospheric temperature rose to peak levels at 50.7 to 52.9 Ma (Tsukui and Clyde, 2012). The relation between frequent volcanic eruptions and peak air temperature (Zachos et al., 2008) suggests that CO_2 venting associated with Late Paleocene and Early Eocene volcanism, including the North Atlantic Igneous Province and the Siletzia terrane, might be the cause of the high temperatures during the EECO (Reagan et al., 2013). Another source of CO_2 may have been the oxidation of methane released from storage in wetlands in the early Eocene, although it is just a speculation based on indirect evidence (Sloan et al., 1992). Atmospheric CO_2 is estimated more than 1125 ppm based upon the proxy of the sodium carbonate mineral nahcolite from the lake sediments aged around 50 Ma (Lowenstein and Demicco, 2006). However, this is inconsistent with lower estimates based on stomatal density measurements and paleosoils (Masson-Delmotte et al., 2013).

The EECO is thought to be the warmest period of the last 65 Ma (Zachos et al., 2008), characterized by the absence of substantial polar ice sheets, and different vegetation type and distribution from today (Masson-Delmotte et al., 2013). Because of the coupled CO_2-climate response during the Early Eocene Climatic Optimum, the atmospheric pCO_2 values rapidly increased up to around 1700 ppm, which is indicated by the isotopic analysis; in

some regions, the climate was remarkably warmer (~7 °C) and significantly wetter (~750 mm yr^{-1}) suggested by the geochemical and isotopic proxies from the terrestrial sources (Hyland and Sheldon, 2013). The warmer climates in EECO shown by terrestrial observations (Sloan and Barron, 1990; Sloan et al., 1992; Sloan, 1994) are not easily reproduced by climate models (Huber and Sloan, 2001; Heinemann et al., 2009; Lunt et al., 2010; Tindall et al., 2010; Winguth et al., 2010). This problem is known as the early Eocene 'equable climate problem' i.e. warm extratropical annual mean and above-freezing winter temperatures evidenced by environmental records.

The Miocene, between 23.03 to 5.333 Ma ago, is characterized by a moderately warm climate, with a pronounced warmer period (the Middle Miocene Climatic Optimum, MMCO) between 17-15 Ma. The MMCO was the warmest period during the Neogene. The continents were already close to their present position, although the Central American seaway still was open (Duque-Caro, 1990; Butzin et al., 2011). The uplift of the Tibetan Plateau in Asia started to accelerate during the early Miocene, and the Plateau further increased in altitude about 10 to 8 Ma ago (An et al., 2001). The uplift of this massive area caused a notable increase in the intensity of the Asian summer and winter monsoons, with the development of wetter climates to the southern and eastern margin and drier climates to the northern and western margin of the Tibetan Plateau (Kutzbach et al., 1989; Kutzbach et al., 1993). One of the major driving forces causing the MMCO was most likely the large volume of CO_2 venting from Columbia River volcanism (Hodell and Woodruff, 1994; Kurschner et al., 2008). The absolute level of CO_2 during the MMCO has been estimated based on stomatal density data as 350–400 ppm, but fluctuated between 300 and 600 ppm (Kurschner et al., 2008). The Antarctic Ice Sheet is thought to have been reduced in size by 10-25% compared to its modern volume (De Boer et al., 2010). Evidence, from the boron isotope record from deep ocean sites, for a linear relationship between CO_2 levels and ice

volume suggests atmospheric CO_2 concentration was one of the major forcings of climate (Foster et al., 2012).

The Pliocene, 5.333 to 2.58 Ma, was characterized by a climate generally warmer than that of today. Tectonic activity during this interval led to the enhanced uplift of the northern and eastern margins of the Qinghai-Tibetan Plateau after 3.6 Ma ago (An et al., 2001), inferred both from tectonic and sedimentary evidence (Burchfiel et al., 1991; Li et al., 1997; Métivier et al., 1998; Zheng et al., 2000). For example, around 3.5 Ma, there was a sharp increase in the elevation of northern Tibet reflected by the increase of grain size and accumulation rate of sediments both from the southwestern Tarim Basin and the Loess Plateau (Qiang et al., 2001). Uplift during this time interval could have had a significant influence on atmospheric circulation in the Northern Hemisphere (Fauquette et al., 1999), on the distribution patterns of moisture and temperatures on continents, especially in Asia (Sun and Wang, 2005), and on the strength of the Asian Monsoon (An et al., 2001). However, the regional climatic differences between the Pliocene and the modern day could also be explained by other factors, such as global-scale climatic forcing due to increased ocean heat transport (Rind and Chandler, 1991). However, in Eurasia, the mechanism behind the climate difference between the Pliocene and present is most likely to have been altered atmospheric circulation with more accentuated waves (Fauquette et al., 1999), which was most likely caused by the continuous uplift of the Tibetan Plateau (Kutzbach et al., 1993).

The Mid-Pliocene Warm Period (MPWP, *ca*. 3.3 to 3.0 Ma) is the most recent extended period in the past significantly warmer than today (Dowsett et al., 1992; Dowsett et al., 2010; Haywood et al., 2010). During this period, the CO_2 concentration has been estimated to have been in the range of 350 to 450 ppm based on marine evidence (Pagani et al., 2010; Seki et al., 2010; Bartoli et al., 2011). However, there are large uncertainties associated with

these estimates. Boron and ice core records have uncertainties of around 25 ppm, while the alkenone estimates have even larger uncertainties (Foster, 2008; Hönisch et al., 2009).

Model simulations made as part of the Pliocene Model Intercomparison Project (PlioMIP) shed light on the large-scale features of Pliocene climate (Dowsett et al., 2010; Haywood et al., 2010; Haywood et al., 2011; Dowsett et al., 2012; Haywood et al., 2013). The Pliocene climate was mainly due to the forcing of CO_2 and the cryosphere, rather than the insignificant changes in atmospheric and oceanic heat transports. According to the PlioMIP simulations, the Mid-Pliocene global annual mean temperature was more than 3°C [1-5°C] warmer than present-day (Haywood et al., 2013). There are large differences in the observed climate from region to region. For example, geological data indicates the climate of European and Mediterranean region ca. 3 Ma was warmer (by 5 °C), wetter (by 400–1000 mm/yr), and less seasonal than present both in temperature and precipitation (Suc, 1995; Morzadec-Kerfourn, 1997; Fauquette et al., 1998; Fauquette et al., 1999). However, a cold-wet episode occurred in the Yushe and Taigu Basins, Shanxi of China between 3.6 and 2.5 Ma with mean annual temperature being possibly 2 to 6 °C lower than today on the basis of the pollen assemblages from the Pliocene sediments (Li et al., 2004). This indicates that middle latitude Pliocene climate was not uniformly warm in China.

2. Approaches to reconstructing past climates

There are a large number of methods to reconstruct the various aspects of paleoclimates from paleobiological records for the different geological timescales. As summarized by Birks et al. (2010), these methods for quantitatively reconstructing past climate can be categorized into three groups: assemblage approaches such as modern analogue techniques (MAT) and response surfaces, indicator-species approaches involving bioclimate-envelope modeling, e.g. the coexistence approach (CoA, Mosbrugger and Utescher, 1997); and multivariate calibration-function approaches, e.g. the climate leaf analysis multivariate

program (CLAMP). The MAT (Overpeck et al., 1985; Thompson et al., 2008) and response surface approaches (Bartlein et al., 1986; Guiot, 1990; Prentice et al., 1991; Huntley et al., 1993) have been most frequently used for more recent times (e.g. since the last glacial maximum), during which sedimentary environments were relatively unchanged with minimal variation of taphonomy, basin size, relevant source areas, etc. (Fletcher et al., 2010). This approach is less suitable for the deep geological time because of the difficulty of finding good modern analogues or because there are multiple modern analogues for a fossil assemblage (e.g. Ortu et al., 2006; Minckley et al., 2008; Ortu et al., 2010). The CoA and CLAMP methods have been widely applied to make paleoclimate reconstructions for earlier periods during the last 65 Ma (e.g. Mosbrugger and Utescher, 1997; Wilf et al., 1998; Gregory-Wodzicki, 2000; Sun et al., 2002; Liang et al., 2003; Uhl et al., 2007; Yang et al., 2007; Li et al., 2009; Xia et al., 2009; Tomsich et al., 2010; Jacques et al., 2011b; Qin et al., 2011; Fletcher, 2012; Thiel et al., 2012; Breedlovestrout et al., 2013; Tang et al., 2014). Because they have been widely used to reconstruct climates in the pre-Quaternary era, the CoA and CLAMP approaches were the starting point for the investigations presented in this thesis. However, the many of the conclusions about the reliability of the reconstructions are applicable to other methods of palaeoclimate reconstruction. In particular, sources of reconstruction uncertainties are likely to increase with time and the reliability of reconstructions to lessen; this is true whatever statistical reconstruction techniques are used to reconstruct climate on the basis of plant attributes.

2.1 Taxon-based method: CoA

2.1.1 Definition and source

The CoA is a plant-based paleoclimate reconstruction method first developed by Mosbrugger and Utescher (1997). Paleoclimates are reconstructed as the overlap of the climatic tolerances of all the taxa within a fossil assemblage (Figure 1-2), where the climatic

tolerances of each fossil taxon are derived from the modern climatic tolerances of their nearest living relative (NLR, Mosbrugger and Utescher, 1997; Utescher et al., 2014).

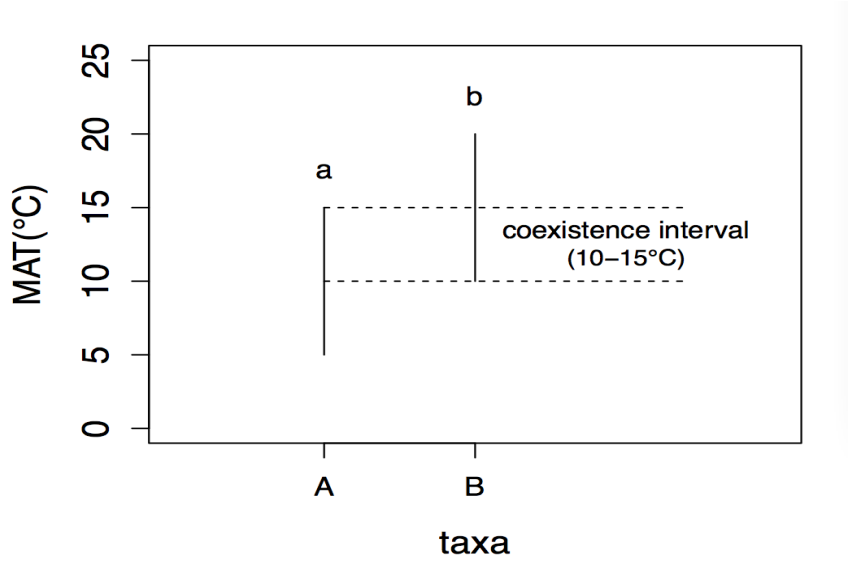

Figure 1-2 The theory of the CoA, using the reconstruction of mean annual temperature as an example. Uppercase A and B indicate the fossil taxa. Lowercase a and b indicate the nearest living relatives (NLRs) of fossil taxa A and B, respectively. Vertical bars indicate the range of mean annual temperature of NLR a or b.

The CoA is similar to the indicator taxa (Iversen, 1944; Birks and Birks, 1980) and mutual climatic range (Grichuk, 1969; Atkinson et al., 1987) approaches. The difference is that the indicator taxa method uses relatively few representative taxa to make the paleoclimate reconstruction, whereas all of the taxa in an assemblage can be incorporated in the framework of the mutual climatic range and the CoA approaches. The basic difference between mutual climatic range and CoA is that CoA has been applied to assemblages, which contain species that are extinct because of the use of the NLR. A common assumption made in all indicator taxa approaches is that the fossil taxon and its nearest living relatives have identical climatic requirements (Birks et al., 2010).

2.1.2 Basic assumptions of the CoA

Following the illustrations provided by Mosbrugger and Utescher (1997) and guidelines summarized by Utescher et al. (2014), the following assumptions are made:

(1) A species that is taxonomically related to the fossil taxon can be identified;

(2) The climatic requirements of this nearest living relative are similar to those of the fossil taxon;

(3) The climatic requirements of a nearest living relative can be determined from its current distribution;

(4) The modern climate data corresponding to the distribution dataset for a given nearest living relative is of good quality.

2.1.3 Procedures of the CoA

The following procedures are followed in order to generate the final coexistence interval (Mosbrugger and Utescher, 1997; Utescher et al., 2014):

(1) The nearest living relative (NLR) is determined for every fossil taxon in the sample assemblage.

(2) The modern distribution area is obtained for each NLR.

(3) The range of a given climatic variable is established from the data of the distribution information.

(4) The coexistence interval is generated by overlapping the ranges of the NLRs for a specific climate variable.

More detailed guidelines are given on the application of classical CoA (Utescher et al., 2014; Grimm et al., 2015). These include, for example, how to choose the most reasonable NLR for a fossil taxon. Procedures (1) to (3) of the approach can readily be followed using information from the Palaeoflora database (Utescher and Mosbrugger, 2013). However, situations can arise in which some observations lie outside the common climate range of the majority of taxa in a fossil flora. In this situation, providing the identification of the fossil taxon is secure, the coexistence interval is generally obtained by ignoring the outlier since

Mosbrugger and Utescher (1997) indicated that the coexistence concept does not necessarily force 100% taxa in a fossil assemblage to have a common coexistence interval. This provides a pragmatic solution to the problem, but ignores the larger problem of the cause of such outliers, particular when they represent a key taxon at a specific geologic time. The distribution of plant taxa generally reflects multiple climate controls, including seasonal temperature and moisture availability. The presence of outliers in a univariate relationship, and indeed the general noisiness of such relationships, is a reflection of the fact that plant distribution must be considered in terms of a multivariate representation of the climate environment. Another situation is when multiple potential coexistence intervals are obtained, leading to ambiguous reconstructions (Utescher et al., 2014; Grimm et al., 2015). Multiple coexistence intervals can be obtained when the sample contains pollen transported from outside the catchment (long-distance transport), when the sample is from a very large catchment, or when there is pronounced relief in the catchment (Ivanov et al., 2002; Hoorn et al., 2012; Utescher et al., 2014; Zhang et al., 2015). Again, providing the procedure has otherwise been carefully checked, the solution to this case is to combine the coexistence intervals to provide a single final range (Mosbrugger and Utescher, 1997). However, this could lead to very large uncertainties on the final reconstructions.

Since the CoA approach is based on considering the overlap in the climate range on NLRs, more accurate reconstructions should be obtained as the number of taxa included in the analyses increases. It is generally recommended that reconstructions be based on at least 10 taxa (Mosbrugger and Utescher, 1997; Utescher et al., 2014). This is an improvement over the indicator species approach (Iversen, 1944; Birks and Birks, 1980) where only a single taxon or few selected taxa are used to infer the paleoclimate (Mosbrugger and Utescher, 1997). However, the number of taxa can vary according to ecosystem represented by a given fossil sample. In samples from subtropical ecosystems, like the Eocene specimens from Hainan Island, China, as many as 36 taxa could be used in CoA (Yao et al., 2009).

However, samples from arid or semi-arid regions, might have considerably fewer than 10 taxa because of the depauperate nature of the original ecosystem and poor preservation in dry climates. Thus, it is considered acceptable to use less than 10 taxa in a CoA reconstruction if necessary (Utescher et al., 2014).

2.1.4 Identification of nearest living relatives (NLRs)

The identification of a nearest living relative is fundamental to the application of CoA, and inaccurate designations can seriously affect the reliability and precision of this method. A NLR or several NLRs could be designated for a fossil taxon, depending on the organ type preserved, the morphometric traits displayed, and mutual phylogenetic closeness (Utescher et al., 2014). The designation could be at the species, genus or family level.

The identification of fossil pollen grains and assignment of their taxonomic affinity is a challenge for palynologists. Through the considerable efforts of many researchers, monographs or atlases of pollen identification are available (e.g. Stuchlik, 2001, 2002; Collinvaux et al., 2003; Punt et al., 2003; Stuchlik, 2009; Grímsson and Zetter, 2011). The major sources of information for the Chinese pollen flora are e.g. Xi and Ning (1994), Wang et al. (1995) and Song (1999). These guides are mostly based on the light microscopy technique for pollen identification. Combining light microscopy with scanning electron microscopy (SEM) improves the reliability of the identification of individual microfossils (Ferguson et al., 2007). There are a number of guides to pollen identification on the basis of SEM technique (Wei et al., 2003; Grímsson and Zetter, 2011; Li, 2011). The detailed description of pollen micromorphology in a more standardized way improves the resolution of the identification (Moore et al., 1991; Punt et al., 2007; Hesse et al., 2009) and increases the reliability of the choice of NLR for the fossil taxon used in CoA (Li et al., 2009; Qin et al., 2011; Zhang et al., 2012; Tang et al., 2014; Li et al., 2015b).

Leaf anatomy, wood physiognomy and comparative morphology have played major roles in identifying NLRs for leaf, wood and seed macrofossils (Wang et al., 2003; Sun et al., 2005; Cheng et al., 2006; Kovar-Eder et al., 2006; Erdei et al., 2007; Teodoridis et al., 2009). The NLRs of around 5800 macrobotanical and 2500 microbotanical taxa are documented in the Palaeoflora Database by Neogene Climate Evolution in Eurasia (NECLIME) group (Utescher et al., 2014).

The taxonomic level of the NLR assignment definitely affects the quality of reconstructions made using the CoA approach. Assigning NLRs to species or genus level will generally make the coexistence interval narrower than when assignments are made to genus or family level. As an example, there have been two studies of the Xiaolongtan formation: in one most of the taxa were assigned to species or genus level (Xia et al., 2009), while in the other (Yao et al., 2011) almost all of the taxa were assigned to the genus or family level (Table 1-1). This difference in assignment led to reconstructions of the mean temperature of the warmest month of 25.4 to 26.0°C in the former case (Xia et al., 2009) and 5.6 to 14.8°C in the latter case (Yao et al., 2011). Assigning erroneous NLRs also affects the reconstructed climates (Mosbrugger and Utescher, 1997). As Grimm et al. (2015) critically pointed out, the assignment of Engelhardia and *Castanea* in the study by Quan et al. (2011) as the NLRs of Engelhardioideae and Cupuliferoipollenites was inappropriate because of the different taxonomic affinities of the modern and fossil groups and differences in their climatic requirements, and this led to a substantial reconstruction bias when the coexistence analysis was rerun after correcting the NLR assignments (Grimm et al., 2015). This incorrect assignment is not a single case, since the same erroneous identification of NLRs has also been made in other studies (Wang et al., 2010).

According to the rules stated by (Mosbrugger and Utescher, 1997; Utescher et al., 2014; Grimm et al., 2015), extinct, cosmopolitan, and aquatic taxa must be removed from

Table 1-1 NLRs comparisons at genera and family level.

Fossil taxon from Xiaolongtan Formation of Yunnan, China	Nearest Living Relative (NLR)	
	Xia et al. 2009	Yao et al. 2011
Desmos kaiyuanensis	*Desmos*	Annonaceae
Machilus americana	*Machilus*	Lauraceae
Machilus ugoana	*Machilus*	Lauraceae
Nothaphoebe precavaleriei	*Nothaphoebe*	Lauraceae
Castanea miomollissima	*Castanea mollissima*	*Castanea sp.*
Cyclobalanopsis mandraliscae	*Cyclobalanopsis myrsinaefolia*	Fagaceae
Cyclobalanopsis praegilva	*Cyclobalanopsis gilva*	Fagaceae
Lithocarpus sp.	*Lithocarpus harlandii*	Fagaceae
Castanopsis miocuspidata	*Castanopsis echinocarpa / Castanopsis carlesii*	*Castanopsis chrysophylla*
Quercus lahtenoisii	*Cyclobalanopsis glauca*	*Quercus sp.*
Quercus sinomiocenica	*Quercus variabilis*	*Quercus sp.*
Desmodium pulchellum	*Phyllodium*	Leguminosae
Erythrophleum ovatifolium	*Erythrophleum*	Fabaceae
Ormosia xiaolongtanensis	*Ormosia*	Fabaceae

the analysis in order to get reliable reconstructions. However, different studies may differ in which species are removed. For example, Xia et al. (2009) removed *Salix miosinica*, *Lespedeza sp*., *Sophoramio japonica, Sophora paraflavescens* and *Typha lesquereuxii* in their analyses, because they were considered either extinct, cosmopolitan or aquatic taxa. However, these taxa were included in the reconstructions of the climate of Xiaolongtan by Yao et al. (2011).

2.1.5 Determination of climatic tolerances of modern plant taxa

The basic assumption that the fossil and modern taxon should have identical climatic requirements means that the CoA has mostly been applied to Quaternary and Neogene floras because evolutionary change in environmental requirements is thought to be minimal over these geological times (MacGinitie, 1941; Hickey, 1977; Chaloner and Creber, 1990; Mosbrugger and Utescher, 1997; Utescher et al., 2014).

Identification of the climatic tolerance, or climatic envelope (Pearson and Dawson, 2003), of a modern taxon is an important step in the CoA method. The theory of determining the climatic tolerances by approximating the regions of plant distribution in climate space is in the ecological and species distribution modeling literature (Franklin; Pearson and Dawson, 2003; Araujo and Pearson, 2005; Bond et al., 2005; Sexton et al., 2009). The climatic tolerance of a taxon can be easily derived providing the complete climate range of that taxon has been sampled.

There are different ways that have been used to obtain the minimum and maximum tolerances of a given NLR. The original developers of the approach simply selected 6 'extreme' meteorological stations within the modern distribution area of the taxon, taking care to include stations representing altitudinal variation (Mosbrugger and Utescher, 1997). Other researchers (e.g. Sun and Li, 2012) have refined this approach by selecting six meteorological stations at the northern, southern, eastern and western boundaries of the distribution area and then included stations from the highest and lowest elevation within this area. In both cases, the minimum and maximum climatic values of the meteorological data are assigned as the tolerances of a given NLR.

An alternative method of determining the climate tolerances of an NLR is to match the distribution of the NLR and climate data from the same area. There have been several attempts to do this in China. The distribution of different taxa across China information can be derived from the distribution of seed plants at county level compiled by Wu and Ding (1999). The long-term (generally 30 years) mean climate for each county from the compilation published by the Information Department of Beijing Meteorological Center (1983), are then attributed to all taxa occurring in the county. Fang et al. (2011) have compiled county-level distributions for 11,405 woody plants of China and used the climatic variables with longitude-latitude-altitude interpolation on the basis of the gridded spatial

database from the world climate website (http://www.worldclim.org/) to calculate the climate tolerances for 12 climatic variables.

Another method of defining the tolerances of an NLR is to use fine-gridded distributions of both plant taxa and climate data or statistical derivation (e.g. weighted averaging regression), which makes the tolerance reconstructions more realistic. For example, the climatic envelopes of a large number of North American trees and shrubs have been defined for nine climatic and bioclimatic variables based on this gridded data (Thompson et al., 1999; Thompson, 2006). A similar approach has been made in China: Lu et al. (2011) used climate data and an extensive modern pollen surface-sample data set to estimate the tolerance range and optimum of 9 environmental variables for 215 taxa, of which 153 taxa are seed plants, found on the Qinghai-Tibetan Plateau.

The first method of defining the climatic range of NLRs is less satisfactory than the other two, because there is no guarantee that the six 'extreme' stations are the best method of deriving the climatic tolerances of the modern taxon (Mosbrugger and Utescher, 1997). The second method is better, but, as Grimm and Denk (2012) demonstrated, climate data obtained in this way could be wrong by more than 1°C. However, this approach introduces a certain amount of uncertainty because of the difference in size of counties and the large range of topography in western China, so that in reality the climate could vary considerably across the county (see Chapter 2). The counties in the Qinghai-Tibetan Plateau, for example, have an area ranging from 11,000 km^2 to 199,200 km^2 and topography ranging from 300-4800m. The third method of defining the tolerances of a NLR can be constrained by statistical procedures, such as 'capping' the climate range in order to eliminate extreme climates where plants do not thrive (Greenwood et al., 2005; Thompson et al., 2012) (Grimm et al., 2015; Li et al., 2015b).

2.1.6 Data quality of biogeographical distribution and climate tolerances of NLRs

The third assumption of the Coexistence Approach is that the current biogeographical distribution of modern taxa (NLRs) corresponding to fossil taxa is known and can be used to derive the climatic tolerances for NLRs. The theory behind this assumption is that the distribution range of a specific plant taxon mirrors its climatic requirements (Mosbrugger and Utescher, 1997). However, this assumption is flawed because factors, such as competition, may limit species distribution (Austin et al., 1990).

The determination of the distribution of NLRs usually requires a massive study of the literature on the vegetation. The Atlas of Woody Plants in China: Distribution and Climate (Fang et al., 2011) has compiled information about plant distribution based on a large number of field surveys and various national floras. Another source of plant distribution information is the China-wide data set of the distribution of seed plants at county level compiled by Wu and Ding (1999). However, both sources only provides data aggregated at the county level; there is no information on the within-county distribution of different plants.

Although there are surveys on plant distribution, the data for many modern taxa are incomplete and needs to be updated. Herbarium data could be used to complement other sources of information on plant distribution. Online platforms, such as the Chinese Virtual Herbarium and Muséum National d'Histoire Naturelle in France, provide an opportunity to gather relative distribution information (Utescher et al., 2014), but there may be inconsistencies about the geographical record of individual cases. For example, the GPS coordinates for single herbarium specimen may not be consistent with the county-level location record. Maps of plant distribution, such as the Atlas of United States Trees (http://esp.cr.usgs.gov/data/atlas/little/) or the Flora Europaea (http://www.luomus.fi/english/botany/afe/index.htm), could provide another source of information on the distribution of NLRs.

2.1.7 Disadvantages of the Coexistence Approach

The CoA is a species-based method, which focuses on occurrence information (i.e. the presence or absence of a taxon) rather than the abundance of a specific taxon. However, the method discards information because the relative abundance of a taxon may also be informative about the climate (Mosbrugger and Utescher, 1997) because the probability of occurrence of a taxon will peak near the optimal conditions for that taxon (Guiot, 1994). Including information on relative abundance could therefore increase the precision of reconstructions based on coexistence (Zhang et al., 2015). This could be done within the CoA framework by using an abundance threshold to determine which taxa are included in the analysis.

The application of the CoA to make reconstructions for pre-Neogene intervals is limited because of the fundamental assumption that the fossil taxon and the corresponding nearest living relative have similar climatic requirements. The environmental requirements of species are not thought to have changed very much during the Neogene and Quaternary, but this may not be true further back in time.

Although the CoA has been applied using data on many different organs, including leaves, seeds, wood, charcoal and pollen (Mosbrugger and Utescher, 1997; Pross et al., 2000; Yang et al., 2007; Yao et al., 2009; Sun and Li, 2012; Bondarenko et al., 2013), the precision of the CoA is not dependent on what organ is used, but is really strongly dependent on the quality of the modern climate data used for the NLRs of the fossil taxa (Grimm and Denk, 2012; Zhang et al., 2015a).

2.2 Leaf physiognomy-climate reconstruction methods

Leaves are the organs of plants that conduct the photosynthesis and respiration under the physical laws governing heat and mass transfer between plants and environment (Parkhurst and Loucks, 1972). For a specific plant community, the leaf architecture should reflect a trade-off between resources invested and photosynthetic return (Givnish, 1984; Bloom et al., 1985) constrained by the surrounding environment, although phenotypic plasticity (Ryser and Eek, 2000; Pigliucci, 2003; Royer et al., 2009) and flexibility in the aspect of leaf development (Pien et al., 2001; Bharathan et al., 2002) could explain partial variation. Leaves adapt themselves to having a combination of form and function optimal for plant growth and reproduction in the environments in which they live (Rosen, 1967; Parkhurst and Loucks, 1972; Givnish and Vermeij, 1976) or the adaptive mechanisms in biology (Mc Millen and Mc Clendon, 1979; Nicotra et al., 2011). Keddy (1992) suggested that the hierarchic environmental filters play various roles in selecting the association of plant characteristics at different spatial scales, with climatic factors being most important at the broad regional scale. It was noticed before the end of the 19th century that external forces might influence certain leaf physiognomic traits (Stahl, 1880; Schimper, 1898). This led to attempts to quantify the relationships between leaf characteristics and climates (Wolfe, 1979; Wilf, 1997; Traiser et al., 2005; Meng et al., 2009; Peppe et al., 2011; Peppe et al., 2014; Meng et al., 2015). The existence of such relationships forms the basis for two well-known methods for climate reconstruction based on leaf morphometry: leaf margin analysis (LMA) and the Climate Leaf Analysis Multivariate Program (CLAMP).

Plant traits are observable and measurable characteristics that are thought to be the response to external conditions (McIntyre et al., 1999; Lavorel and Garnier, 2002; Lavorel et al., 2007). Many studies have shown that the abundance of a variety of leaf traits, including characteristics such as the leaf margin, leaf size and shape, varies along climatic gradients within a region or at a continental scale (Bailey and Sinnott, 1916; Werger and Ellenbroek,

1978; Dolph and Dilcher, 1980; Woodward, 1987; Díaz et al., 2001; Niinemets, 2001; Barboni et al., 2004; Royer et al., 2005; Wright et al., 2005b; Meng et al., 2009; Moles et al., 2014; Meng et al., 2015). The relationships between climate and traits have widespread applications in models to predict vegetation responses to climate change (Woodward and Cramer, 1996; Lavorel and Garnier, 2002; Friedlingstein et al., 2006; Wang et al., 2011), in studies on plant functional types for large-scale mapping (DeFries et al., 2000) and in paleoclimate reconstructions (Wolfe, 1979, 1993, 1995; Wilf, 1997; Prentice and Jolly, 2000; Greenwood et al., 2005; Miller et al., 2006; Yang et al., 2007; Peppe et al., 2010; Peppe et al., 2011).

2.2.1 Leaf margin analysis (LMA)

The essential assumption behind the LMA method is that environmental convergence rather than phylogeny is the most important explanation for the variation of leaf form (Bailey and Sinnott, 1916) and thus the distribution of leaf physiognomic traits in the modern-day world should be similar to that of the past. The observed relationship between leaf-margin percentage (the percentage in a flora of woody dicots angiosperm species that have toothed leaf margins) and mean annual temperature (MAT) is the basis for the Leaf Margin Analysis (LMA) approach (Bailey and Sinnott, 1916; Wolfe, 1978, 1979) to reconstruct mean annual temperature. LMA is easy to apply since it only requires measuring the percentage of toothed margin versus untoothed margin in woody dicots. LMA has been applied to infer paleotemperature from fossil floras ranging from Late Cretaceous to Tertiary (Bailey and Sinnott, 1916; Wolfe, 1978, 1979; Davis and Taylor, 1980; Spicer and Parrish, 1986; Upchurch Jr and Wolfe, 1987; Wolfe and Upchurch, 1987; Parrish and Spicer, 1988; Wolfe, 1990; Greenwood, 1992; Gregory and Chase, 1992; Wing and Greenwood, 1993; Wolfe, 1993; Greenwood, 1994; Greenwood and Wing, 1995; Wolfe, 1995; Utescher et al., 2000; Wing et al., 2000; Jacobs, 2002; Liang et al., 2003; Uhl et al., 2003; Wilf et al., 2003; Fricke

and Wing, 2004; Roth-Nebelsick et al., 2004; Miller et al., 2006; Su et al., 2010; Peppe et al., 2011).

The correlation between the leaf-margin percentage and mean annual temperature has been shown to differ between regions. For example, the correlation between the percentage of untoothed leaves of woody dicots plants and MAT in mesic forests of East Asia is ca. 0.98 (Wolfe, 1979; Wing and Greenwood, 1993), whereas the correlation between the percentage of untoothed leaves of woody dicots and MAT in South America is 0.89 (Gregory-Wodzicki, 2000) and this correlation is only 0.79 in China (Su et al., 2010). Chen et al. (2014) compared almost all of the studies of the relationships between MAT and the proportion of woody dicots with untoothed leaves from East Asia, Europe, South America, Australia and China and showed that the strength of this correlation varies from 0.53 to 0.98. As the correlation varies from region to region, a regionally-specific training dataset for modern leaf flora has to be used to make palaoeclimate reconstructions for each region.

LMA is based on an empirical statistical relationship. However, the actual physiological mechanism why there is a strong correlation between the proportions of untoothed leaves and mean annual temperature was not explained explicitly (Wolfe, 1993; Roth et al., 1995) until the hypothesis that this is related to gas exchange at leaf margins put forward by Royer and Wilf (2006). According to this hypothesis, leaf teeth are thought to play an important role in carbon uptake during the early growing season when temperature is limiting but nutrient availability and moisture are not. Specifically, it is argued that toothed leaves enhance photosynthesis and transpiration more than untoothed leaves do in cold climates (Royer and Wilf, 2006). This functional explanation of the role of leaf teeth strengthens the theoretical basis of the LMA method for estimating MAT.

If the basic assumption of LMA is correct, how well does it reconstruct mean annual temperature? The minimum standard error of 0.8°C for MAT estimation comes from the linear equation given by Wing and Greenwood (1993). However, the LMA approach overestimated observed MAT for Australia and New Zealand (11.3°C, 7.5°C respectively) by an average of about 8.2°C (Jordan, 1997). When the same equation is applied to the paleoclimate prediction in Xiaolongtan fossil flora of China, the MAT error is up to 2.05°C (Xia et al., 2009). Regional differences in the correlation of temperature and leaf-margin percentage, described above, show the relationship is not stable and uniform, and could be affected by other factors (Davis and Taylor, 1980). Because of this changing relationship (both slope and intercept), there is also a problem in choosing a calibration set to compare to the fossil assemblage. Other traits, such as the number of acute based leaves have been found to exhibit a stronger correlation with MAT than leaf margin type (Traiser et al., 2005).

2.2.2 Climate Leaf Analysis Multivariate Program (CLAMP)

The Climate Leaf Analysis Multivariate Program (CLAMP) is a development from LMA that uses 31 categorical leaf states, with the inclusion of leaf-margin and leaf-size categories (Wolfe, 1993, 1995). Because CLAMP uses more than one leaf character, it was expected to result in more accurate climate estimation than LMA. This expectation led to extensive application of the method for reconstructing paleoclimate (Wilf et al., 1998; Gregory-Wodzicki, 2000; Sun et al., 2002; Liang et al., 2003; Uhl et al., 2007; Yang et al., 2007; Xia et al., 2009; Tomsich et al., 2010; Jacques et al., 2011b; Fletcher, 2012; Thiel et al., 2012; Breedlovestrout et al., 2013; Su et al., 2013).

Canonical correspondence analysis (CCA) (ter Braak, 1986) is used in CLAMP to investigate the relationships between leaf characteristics and climate (Wolfe, 1993, 1995). The site means of each characteristic are calculated and used to position each sample in

multidimensional climate space based on its physiognomic signature (Wolfe, 1993, 1995; Spicer, 2012; Yang et al., 2015). This method has been used to estimate 13 different climate variables including MAT, humidity, enthalpy, and variables related to thermal and moisture seasonality (Yang et al., 2007; Royer, 2012), although most studies only focus on 11 of these climate variables.

Both LMA and CLAMP are based on establishing univariate relationship between a trait and a single climate variable. This underlying assumption may be invalidated either when there are strong correlations between climate variables, such that it is difficult to determine which is controlling trait variation, or when multiple climate factors influence trait expression (Jordan, 1997; Royer, 2012). This could help to explain why CLAMP, despite using information on multiple traits, does not necessarily produce better estimations of climate parameters than LMA (Wilf, 1997; Wiemann et al., 1998; Gregory-Wodzicki, 2000; Kowalski and Dilcher, 2003; Royer et al., 2005; Peppe et al., 2011; Royer, 2012). Green (2006) has also argued that the assumption of a linear relationship between specific traits and climate is not valid, since CCA plots often show arched or parabolic relationships. Finally, although CLAMP uses many different morphological measurements, many of the morphological traits are highly correlated with one another (or indeed aspects of the same basic trait) and this could also affect the reliability of the climate reconstructions (Yang et al., 2015).

The "taxon-free" approach used in both LMA and CLAMP, in which phylogenetic history is ignored as a cause of variability in trait abundance, has been challenged by some scientists (Little et al., 2010; Hinojosa et al., 2011). The role of phylogeny needs to be tested further, including sampling a wider variety of vegetation from different continents. Increasing the geographic area sampled by training datasets has been advocated as one way of avoiding

phylogenetic bias on multivariate leaf form–climate relationships (Wolfe, 1979; Wright et al., 2004; Traiser et al., 2005; Jacques et al., 2011a; Peppe et al., 2011; Yang et al., 2015).

3. Philosophy and approach in this thesis

One goal of my thesis is to explore some of the problems associated with common techniques used to reconstruct past climates, particularly pre-Quaternary climates. The success of the CoA method is critically dependent on assuming that the fossil assemblage represents the local climate at the site, and being able to derive good estimates of the climate tolerance of NLRs. The limited amount of information on plant distribution in China, and the reliance on county-level data compilations, could represent a challenge for the application of the CoA method. The use of pollen assemblages to represent fossil plant distribution could also introduce some uncertainties, because the pollen assemblage at a site might represent both local and extra-local vegetation because of long-distance transport by wind. In Chapter 2, I investigate the impact of both of these issues on pollen-based climate reconstructions using CoA, based on analyses of climate reconstructions based on modern pollen samples from the Qinghai-Tibetan Plateau.

The CLAMP and LMA approaches are both based statistical relationships between leaf traits and climate, and both approaches have been used to reconstruct paleoclimates in China (Sun et al., 2002; Yang et al., 2007; Xia et al., 2009; Su et al., 2013; Spicer et al., 2014). However, studies in many regions suggest that there are large uncertainties associated with CLAMP and LMA reconstructions. There are large differences between the reconstructions made using LMA and CLAMP for classic sites in China (e.g. Xiaolongtan) and no way of distinguishing, on theoretical grounds, which values are likely to be more realistic. This problem propelled me to explore an alternative and more robust way of reconstructing paleoclimate from morphometric traits.

In Chapter 3, I use a data set based on extensive field sample across China, which provides information on a much larger range of leaf morphometric traits than used in LMA and CLAMP, to build relationships between individual traits and key bioclimatic variables. I focus on summer temperature, plant-available moisture and seasonality, since these bioclimatic variables have been shown to be sufficient to predict vegetation distribution across the country (Wang et al., 2013). The independent and statistically insignificant relationships between leaf morphometric traits and these bioclimatic variables form the basis for developing a more robust method for paleoclimate reconstruction. In chapter 4, I build a suite of models using the independent individual relationships between specific leaf traits and climatic variables derived from Chapter 3 and use these models to reconstruct paleoclimates during the Eocene, Miocene and Pliocene on the basis of fossil leaves for four classic paleobotanical sites (Fushun, Shanwang, Xiaolongtan, and Shengzhou) in China. The palaeoclimate reconstructions obtained for each site have smaller uncertainties than those obtained using LMA and CLAMP approaches, which suggests this new technique may have advantages over other methods.

Chapter 2 Evaluation of the realism of climate reconstruction using the Coexistence Approach with modern pollen samples from the Qinghai-Tibetan Plateau

1. Introduction

Fossil pollen or plant macrofossil assemblages are widely used to reconstruct past climates (e.g. Cheddadi et al., 1996; Davis et al., 2003; Viau et al., 2006; Wu et al., 2007; Thompson et al., 2008), and a variety of statistical methods have been developed for this purpose (see review in Bartlein et al., 2011). These methods all draw on the basic principle that the geographic distributions of plant species can be approximated by ‘‘envelopes’’ representing contiguous regions in climate space, a situation which arises because the distribution of any plant taxon is defined by bioclimatic limits to growth and reproduction (Harrison et al., 2010). The Coexistence Approach (Mosbrugger and Utescher, 1997), or mutual climatic range approach, was originally applied to Tertiary floras. It has been widely used to reconstruct pre-Quaternary climates (e.g. Gebka et al., 1999; Pross et al., 2000; Böhme et al., 2007; Yang et al., 2007; Grein et al., 2011; Yao et al., 2011) but has also been used to reconstruct Quaternary climates particularly in China (e.g. Sun and Li, 2012; Tang et al., 2014). In this approach, the climatic envelopes for each species found in a fossil assemblage are superimposed and the climate interval common to all the species is assumed to represent the climate of the sampling site (Atkinson et al., 1987; Mosbrugger and Utescher, 1997).

Pollen samples in arid and semi-arid regions frequently contain considerable quantities of tree pollen, even though the surrounding vegetation does not include trees. Long-distance transport of tree pollen into more open vegetation (e.g. tundra, semi-arid shrublands and steppe) result in a significant contamination of the local pollen signal (e.g. Hjelmroos and Franzen, 1994; Carrión, 2002; Pan et al., 2013). The presence of a large amount of

contamination through long-distance transport could substantially affect the reconstruction of climate variables whatever method is used. However, its impact on CoA reconstructions has not been evaluated.

The aim of the present study is to test the realism of climate reconstructions made using the CoA, using a set of modern pollen samples from the central part of the Qinghai-Tibetan Plateau. This region is characterized by open vegetation, chiefly subalpine shrub, alpine meadow, alpine steppe, and alpine desert. Previous studies of modern pollen samples from the Plateau (Huang et al., 1993; Cour et al., 1999; Yu et al., 2001; Lu et al., 2006; Shen et al., 2006; Herzschuh, 2007; Lu et al., 2008; Shen et al., 2008; Zheng et al., 2008; Zhao and Herzschuh, 2009; Herzschuh et al., 2010; Lu et al., 2010; Lu et al., 2011) show significant amounts of arboreal pollen (AP) in the surface samples, chiefly brought in by long-distance transport from surrounding regions. A second aim is to examine the impact of this contamination on CoA reconstructions.

2. Materials and Methods

2.1 The study area

The Qinghai-Tibetan Plateau covers over 2.3 million square kilometers with an average elevation of 4000 m a.s.l., but is divided by a series of east-west oriented mountain ranges which, from south to north, are the Himalayas, Kailash–Nyainqentanglha, Karakorum–Nyainqentanglha, southern Kunlun–Bayan Har, and northern Kunlun–Altyn Tagh–Qilian mountains. The Plateau experiences intense solar radiation which helps to create a regional heat source that intensifies the Pacific summer monsoon circulation, resulting in warm, wet conditions in the southeastern part of the Plateau during summer. However, the Pacific monsoon winds do not penetrate into the interior and, as the mountain ranges block penetration of the Indian Monsoon from the south, the northern and northwestern part of the

Plateau is arid. During winter, the whole of the Plateau is influenced by upper-level westerly airflow associated with cold, dry conditions. These climate patterns are reflected in the vegetation patterns (Zhang et al., 2007): deserts occur in northern part of the Plateau, the central part is characterized by alpine vegetation, while subtropical broad-leaved evergreen forest region occurs to the west and south, and tropical monsoon and tropical rainforests occur on the southern slopes of the Himalayas (Figure 2-1). The alpine region, which is the focus of the current study, can be subdivided from east to west into three types: subalpine shrub and alpine meadow in the east, alpine steppe, and alpine desert in the northwest.

2.2 Pollen sample collection and processing

Forty-four surface soil samples were collected along a transect from Qinghai Lake, across the central part of the Qinghai-Tibetan Plateau towards Lhasa (Figure 2-1, Table 2-1). Bagged samples were opened under sterile conditions in the laboratory. Each 30g sample was processed using heavy liquid separation (Li and Du, 1998) and acetolysis (Moore et al., 1991). Fifty-percent glycerol solution was used for storage and preparation of microscopic slides. The spores and pollen were examined under a Leica DM 2500 microscope and identified using the Pollen Flora of China (Wang et al., 1995) and Sporae Pteridophytorum Sinicorum (Zhang et al., 1976). At least 200 pollen grains were counted for each sample. This comparatively low number is characteristic of soil samples, but the pollen sum is comparable to other surface samples taken from this region (see e.g. Yu et al., 2001). The relative abundance of each pollen taxon was calculated relative to the sum of all taxa present.

We separate the pollen into three groups: non-arboreal pollen (NAP), shrubs, and strictly arboreal pollen (AP). The vegetation of the Tibetan Plateau is characterized by a small number of shrubby plants, many of which are dwarf shrubs (e.g. *Nitraria*, *Salix*, *Tamarix*). The threefold division of the pollen types was created in order to distinguish this group from

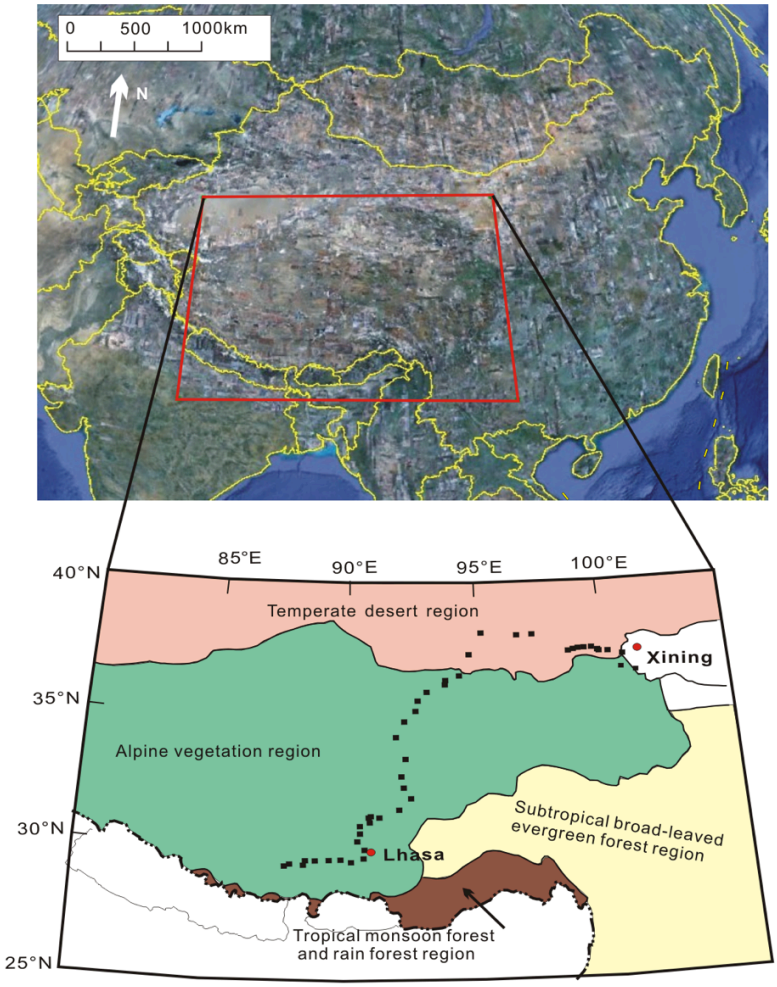

Figure 2-1 The location of the study area and sampling sites. The map in the upper panel is from Google (2012), while the vegetation map in the lower panel is redrawn from Zhang (2007).

trees, sensu stricto, which may be present as tree-line species but also may be non-local contaminants.

2.3 Derivation of climate of the pollen sites

The observed climate at each of the pollen sites is the target against which we measure the validity of the CoA reconstructions. There are no meteorological stations at the pollen sites. We therefore used a 1-km resolution gridded climate data set constructed from mean monthly values of temperature, precipitation derived from 1814 meteorological stations across China (China Meteorological Administration, unpublished data). Of these, 740 stations have observations from 1971–2000 and the remaining stations have observations

Table 2-1 Information on the modern pollen sampling sites from the Qinghai-Tibetan Plateau

Sample No.	Lat. (N/°)	Lon. (E/°)	Alt. (m)	Vegetation type	No. of pollen taxa represented			Observed climate			
					total	>1%	No-trees >1%	MAP (mm)	MAT (°C)	MTWA (°C)	MTCO (°C)
Td1	36.42	101.12	3359	Temperate desert	9	9	8	459.5	0.3	10.9	-12.1
Td2	36.57	100.16	3217	Temperate desert	20	14	12	409.8	0.5	11.5	-12.3
Td3	36.63	100.89	3194	Temperate desert	9	9	6	471.4	-0.9	9.7	-13.6
Td4	36.64	100.86	3195	Temperate desert	16	11	9	455	-0.1	10.7	-13
Td5	36.78	99.86	3387	Temperate desert	19	14	11	360.6	1	12.3	-12.1
Td6	36.75	99.37	3810	Temperate desert	13	13	8	338.3	-0.6	10.9	-13.6
Td7	36.68	99.38	3148	Temperate desert	14	8	6	305.6	0.9	12.6	-12.4
Td8	36.71	99.09	3078	Temperate desert	12	7	4	250.3	2.2	14.2	-11.5
Td9	36.66	99.53	3203	Temperate desert	9	9	8	384.5	-1.9	9.2	-14.5
Td10	37.35	97.85	3091	Temperate desert	16	6	5	209.6	2.1	14.3	-11.9
Td11	37.32	96.16	2813	Temperate desert	7	3	3	116.6	1.5	14.3	-13.2
Td12	37.46	95.29	3179	Temperate desert	9	4	4	79.3	2.2	15.5	-12.9
Td13	36.67	95.33	2717	Temperate desert	9	9	7	52.4	5.7	18.7	-9.2
Av14	35.9	94.98	3509	Alpine vegetation	7	2	2	294.5	-6.1	4.8	-17.7
Av15	35.72	94.2	4503	Alpine vegetation	17	17	12	218	-3.5	7.8	-15.7
Av16	35.61	94.74	4722	Alpine vegetation	17	9	8	372.5	-8.5	1.9	-19.6
Av17	35.35	93.05	4521	Alpine vegetation	12	9	7	262.5	-5.7	5.3	-17.1
Av18	35.03	93.53	4621	Alpine vegetation	19	16	13	308.7	-5.9	4.9	-17.1
Av19	34.65	92.06	4822	Alpine vegetation	12	12	9	277.4	-5.6	5.8	-17.8
Av20	34.29	92.61	4546	Alpine vegetation	9	4	2	292.3	-4.1	7.4	-16.5
Av21	33.74	92.75	4653	Alpine vegetation	6	6	5	349.1	-3.7	7.6	-16
Av22	33.26	91.62	4821	Alpine vegetation	19	19	15	425.2	-7.2	3.6	-18.8
Av23	32.67	91.37	5015	Alpine vegetation	19	19	13	411.8	-4	6.8	-15.8
Av24	32.22	91.66	4652	Alpine vegetation	15	6	4	424	-2.3	8.3	-14.2
Av25	31.8	91.26	4802	Alpine vegetation	3	3	2	419.7	-1.8	8.5	-13.4
Av26	31.42	91.88	4471	Alpine vegetation	17	12	8	454.3	-1.2	8.9	-12.7
Av27	31.02	91.45	4693	Alpine vegetation	9	9	6	480.2	-2.7	6.8	-13.7
Av28	30.85	91.95	4796	Alpine vegetation	16	12	7	573	-5.7	3.1	-15.7
Av29	30.84	91.27	4765	Alpine vegetation	8	8	4	476.9	-2.6	6.6	-13.5
Av30	30.74	91.6	4809	Alpine vegetation	13	10	9	490.5	-1.7	7.4	-12.6
Av31	30.68	91.85	5190	Alpine vegetation	17	13	9	561.5	-4.9	3.7	-14.8
Av32	30.54	91.29	4394	Alpine vegetation	10	10	9	450	1.2	10.4	-10
Av33	30.28	90.28	4390	Alpine vegetation	17	10	6	515.3	-6	1.4	-14.2
Av34	30	90.09	4705	Alpine vegetation	14	9	6	498.8	-4.7	2.3	-12.6
Av35	29.68	90.22	3710	Alpine vegetation	10	7	4	461.7	-1.7	5.5	-9.7
Av36	29.38	90.31	3573	Alpine vegetation	14	6	3	426.8	0.9	8.1	-7.4
Av37	29.26	90.24	3659	Alpine vegetation	9	4	2	390.2	3	10.5	-5.7
Av38	29.34	90.86	3785	Alpine vegetation	8	8	5	381.4	7	14.6	-2
Av39	29.34	89.28	3796	Alpine vegetation	13	9	6	347.4	6.7	14.9	-3.2
Av40	29.32	89.42	3810	Alpine vegetation	27	11	9	341.8	6.7	14.8	-3.2
Av41	29.33	88.58	3879	Alpine vegetation	23	9	6	357.6	6.6	14.8	-2.9
Av42	29.16	88.84	3923	Alpine vegetation	14	8	4	375.2	5.8	13.8	-3.7
Av43	29.22	88.67	3998	Alpine vegetation	19	11	8	374.3	4.5	12.4	-4.6
Av44	29.15	88.36	4185	Alpine vegetation	12	8	7	375.7	3.4	11.2	-5.2

between 1981–1990. The climate data were interpolated to the 1-km resolution grid using smoothing spline interpolation (ANUSPLIN version 4.36; Hancock and Hutchinson, 2006) and the STRM 1-km digital elevation model (Farr et al., 2007). Elevationally-sensitive smoothing spline interpolation is the standard technique to construct gridded climate data sets (see e.g. Harris et al., 2014). The climate of each pollen sampling site was taken as that of the 1km×1km gridcell in which the site occurred. We calculated mean annual precipitation (MAP), mean annual temperature (MAT), mean temperature of the warmest month (MTWA), and mean temperature of the coldest month (MTCO) for each pollen site. These bioclimatic parameters are closely related to the physiological controls on plant growth (Harrison et al., 2010).

2.4 Application of the Coexistence Approach

We use the Coexistence Approach (CoA) to reconstruct MAP, MAT, MTWA and MTCO for each sampling site based on the pollen data. CoA assumes that the reconstructed climate at a site is the area of climate space given by the overlap between the climate ranges of each taxon present. The ranges of the selected climate variables for each taxon are superimposed, and the estimate is given as the climate interval common to all taxa. Thus, the final reconstruction is generally expressed as range. The calculation can be made for any climate variable, but the reconstruction is made separately for each of the selected climate variable.

It is generally recommended that a minimum of 10 taxa be used to obtain the climate range for a site (Mosbrugger and Utescher, 1997; Utescher et al., 2014). However, many of the taxa represented in our samples are present in very low abundance, and this opens up the possibility that they represent highly localized environmental or climate conditions. Since inclusion of rare taxa could bias the reconstructions of regional climate, we excluded taxa that comprised less than 1% of the pollen assemblage. The CoA was performed on the remaining taxa.

Our initial analysis was based on information about the presence/absence of plant taxa within counties on the Qinghai-Tibetan Plateau. The distribution information was derived from a China-wide data set of the distribution of seed plants at county level compiled by Wu and Ding (1999). Although this data set was based on data from vegetation surveys and mapping, it only provides aggregated data at the county level and there is no information on within-county distribution. Wu and Ding (1999) did not include information on the distribution of ferns, and we therefore ignored the fern spores present in the pollen assemblages. We obtained 30-year climate averages (1951-1980) for each county from the compilation published by the Information Department of Beijing Meteorological Center (1983) and attributed these values to all taxa occurring in the county. This introduces a certain amount of uncertainty, because the counties can be quite large (average area: 21,700 km^2; ranging from 11,000 km^2 to 199,200 km^2) as well as having a range of topography (300-4800m), both of which mean that in reality the climate could vary considerably across the county. Nevertheless, we used this information to derive a reconstruction of MAP, MAT, MTWA and MTCO for each pollen assemblage. The reconstructions for each climate variable were made independently. The final value for each pollen assemblage is the median of the full range of the overlap of the values of the component taxa. These reconstructions are referred to as "unweighted reconstructions" in further discussions.

Lu et al. (2011) used climate data and an extensive modern surface sample data set to estimate the tolerance range and optimum for 215 taxa, of which 153 taxa are seed plants, found on the Qinghai-Tibetan Plateau in terms of MAP, MAT, MTWA and MTCO. The surface pollen data set consists of 1320 samples. The climate at each sampling site was derived by interpolating climate data from 996 meteorological stations covering the Qinghai-Tibetan Plateau and surrounding areas of India, Nepal, Pakistan, Afghanistan, Kazakhstan, Kirghizia, and Mongolia. We use these estimates to derive an alternative reconstruction of MAP, MAT, MTWA and MTCO for each of our pollen assemblages,

based only on the seed taxa present for comparability with our "unweighted reconstructions". Again, the reconstructions for each climate variable were made independently, and the final value for each pollen assemblage is the median of the full range of the overlap of the values of the component taxa. These reconstructions are referred to as "weighted reconstructions" in further discussions.

Finally, we made a reconstruction using the climate optimum and tolerance range information from Lu et al. (2011) but based only on non-arboreal (NAP) and shrub pollen types. The reconstructions for each climate variable (MAP, MAT, MTWA, MTCO) were made independently, and the final value for each pollen assemblage is the median of the full range of the overlap of the values of the component taxa. These reconstructions are referred to as "non-trees reconstructions" in further discussions.

2.5 Statistical analyses

The number of taxa used to make climate reconstructions varied between sites for any one reconstruction method and between the three different reconstruction methods. In particular, the number of taxa used in the no-trees reconstructions was much lower than in the unweighted reconstruction (which drew on both AP and NAP taxa). Comparisons between the three sets of reconstructions are only made on sites where the assemblage used for any of the reconstructions included more than 5 taxa. In practice, this meant comparisons were confined to sites with more than 5 NAP and shrub taxa. Only 32 samples (out of the original 44 samples) satisfied the criterion of having more that 5 NAP and shrub taxa represented at >1%.

The CoA provides a range for the reconstructed value of each climate variable, but the observed climate at a site is a single value derived from the gridded climate dataset. To facilitate quantitative comparisons between observed and reconstruction climate, we derived

a single summary climate value for each pollen assemblage given by the median of the full range of the overlap of the values of the component taxa. The median value is more robust than the mean and effectively weights the estimate towards values favoured by more taxa (see e.g. Gavin and Hu, 2006). We compared the observed and reconstructed values of MAP, MAT, MTWA and MTCO using root mean square error (RMSE) to assess the goodness of fit.

3. Results

3.1 Modern pollen assemblages

Seventy pollen types were identified from the central Qinghai-Tibetan Plateau. The pollen assemblages (Figure 2-2), are dominated by non-arboreal pollen (NAP) (Mean±SD = 73.1±16.4%) and shrubs (5.5±14.2%). Arboreal pollen (AP) comprise 15.9±11.9% of the assemblages. Fern spores and other non-fern spores are a minor component of the assemblages, comprising 3.9±8.2% and 1.6±9.1% of the assemblages respectively.

The non-arboreal and shrub component of the pollen assemblages reflects the local vegetation (Table 2-2). Chenopodiaceae and *Nitraria* dominate the spectra from the temperate desert region (Figure 2-1), while other Asteraceae and Ephedra are well represented. In contrast, samples from the alpine vegetation (Figure 2-1) are dominated by Chenopodiaceae and Cyperaceae, while *Artemisia*, other Asteraceae and Caryophyllaceae are well represented. Although *Nitraria* and Ephedra can be present in samples from this region, they are not abundant. Poaceae pollen is rare in both regions. Tree pollen is present in most of the samples, but occurs in greater abundance in the alpine vegetation region than the temperate desert region (18.3±12.2% compared to 10.1±9.1%, see Table 2-2). *Populus* and *Picea* occur at high elevations in the temperate desert region, however, *Populus* are not represented in the pollen samples. *Pinus* and *Castanea* are recorded at relatively high

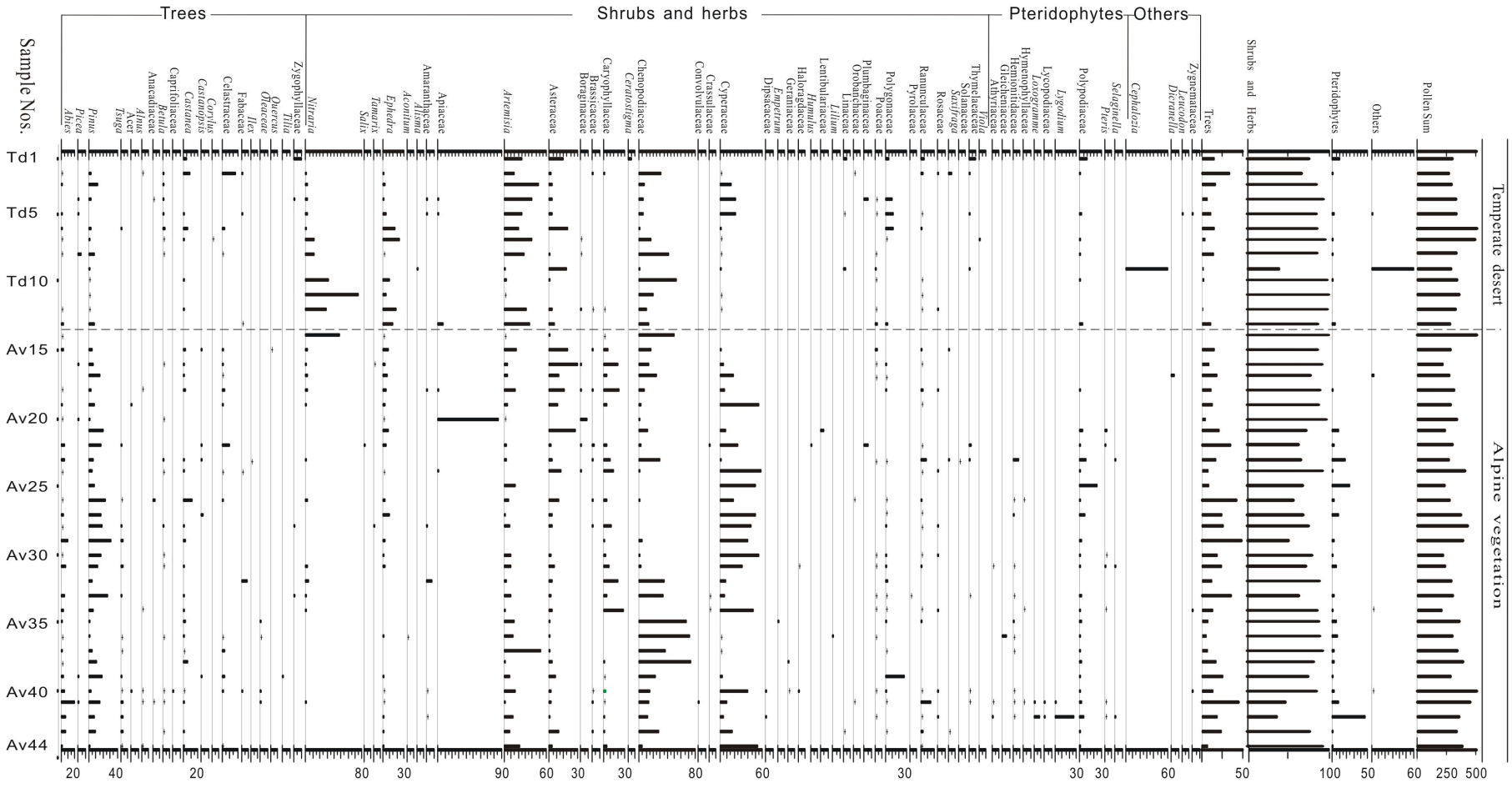

Figure 2-2 Modern pollen samples from the Qinghai-Tibetan Plateau. The samples are arranged by vegetation type (temperate desert: Td, alpine vegetation: Av) and named sequentially (Td1 to Td10, Av1 to Av44).

abundances, and *Abies*, *Picea*, *Tsuga*, *Alnus*, *Betula*, *Corylus* are present in these samples, despite the fact that no trees are found in the immediate vicinity of the sampling sites. *Pinus* and *Abies* are moderately abundant at sampling sites from the alpine vegetation region, and several other tree species are also recorded. The treeline in this region occurs at ca. 4500m and there are no trees present in the immediate vicinity of the sampling sites. Thus, the representation of tree pollen in the assemblages must reflect long-distance pollen transport.

3.2 Climate reconstructions

The observed MAP at the sampling sites varies from 52-573 mm (Table 2-1). The reconstructed range of the median values obtained in the unweighted CoA is much larger, from 304.0-1198.4 mm (Table 2-3). The RMSE is correspondingly large: 345 mm (Table 2-4). The reconstructed value is larger than observed at 72% of the sites, and in 83% of these cases the reconstructed MAP is at least 50% larger than the observed MAP. However, the errors involved at sites where the reconstructed MAP is less than the observed MAP are generally much smaller than the positive biases (Figure 2-3). The reconstructions of MAP based on the weighted CoA show a range from 331.0 to 552.5 mm compared to observed values of 52 to 573 mm. Use of the weighted approach clearly reduces the overall biases (RMSE: 126 mm), by reducing the very high estimates of precipitation obtained using the unweighted approach. The reconstructions overestimate observed MAP at a similar number of sites than the unweighted CoA, however the reconstructed MAP is only more than 50% of the observed MAP at 22% of these sites. Excluding AP sensu stricto in the "non-trees" reconstructions expands the range (308.0-472.5mm) and generally reduces the reconstructed MAP compared to the weighted CoA reconstructions. The overall RMSE (98 mm) is much better than for the other two reconstructions. However, even this method fails to reproduce extremely low values of MAP (e.g. site 10, Figure 2-3). The observed MAT at the sampling sites varies from -8.5 to 7°C (Table 2-1). The reconstructed range of the median values

Table 2-2 Comparison of pollen assemblages from sampling sites in the temperate desert and alpine vegetation regions of the Qinghai-Tibetan Plateau

Pollen taxa	Temperate desert Mean±SD %	Alpine vegetation Mean±SD %
NAP	**70.6 ± 19**	**74.2 ± 15.4**
Ephedra	7.9 ± 8.2	2.4 ± 2.7
Aconitum	0	0.0± 0.0
Alisma	0.1 ± 0.5	0
Amaranthaceae	0.1 ± 0.2	0.3 ± 1.4
Apiaceae	0.7 ± 2	2.8 ± 15.3
Artemisia	24.2 ± 15.5	8.9 ± 10.2
Asteraceae	7.4 ± 9.3	8.1 ± 10.4
Boraginaceae	0.1 ± 0.1	0.4 ± 1.6
Brassicaceae	0.1 ± 0.1	0.3 ± 0.6
Caryophyllaceae	0.2 ± 0.5	5.9 ± 7.6
Ceratostigma	0.4 ± 1.4	0
Chenopodiaceae	16.3 ± 16.4	19 ± 21.8
Convolvulaceae	0	0 ± 0.1
Crassulaceae	0	0.1 ± 0.3
Cyperaceae	5.1 ± 8.6	21.3 ± 21.3
Dipsacaceae	0	0 ± 0.1
Empetrum	0	0 ± 0.1
Geraniaceae	0	0.1 ± 0.2
Haloragdaceae	0	0.1 ± 0.3
Humulus	0	0 ± 0.2
Lentibulariaceae	0	0.1 ± 0.7
Lilium	0	0.0± 0.0
Linaceae	0.7 ± 1.6	0 ± 0.1
Orobanchaceae	0 ± 0.1	0 ± 0.1
Poaceae	0.7 ± 1	0.3 ± 0.8
Plumbaginaceae	0.4 ± 1.5	0.2 ± 1
Polygonaceae	3.4 ± 4.9	1.7 ± 4.9
Pyrolaceae	0	0 ± 0.1
Ranunculaceae	1.1 ± 1.7	1.6 ± 2.9
Rosaceae	0.1 ± 0.3	0.1 ± 0.3
Saxifraga	0.4 ± 1.4	0.1 ± 0.4
Solanaceae	0	0 ± 0.2
Thymelaeaceae	1.2 ± 2.8	0.2 ± 0.5
Viola	0.1 ± 0.4	0
Shrub	**13.1 ± 21.4**	**2.3 ± 8.5**
Nitraria	13.1 ± 21.4	2.2 ± 8.5
Salix	0	0 ± 0.2
Tamarix	0	0.1 ± 0.4
AP	**10.1 ± 9.1**	**18.3 ± 12.2**
Abies	0.9 ± 1.1	3.4 ± 3.9
Picea	0.5 ± 1.2	0.1 ± 0.2
Pinus	3.2 ± 3.8	10.5 ± 8.3
Tsuga	0.1 ± 0.4	0.9 ± 1.3
Acer	0	0 ± 0.2
Anacardiaceae	0 ± 0.2	0.1 ± 0.7
Alnus	0 ± 0.1	0.1 ± 0.3
Betula	0.7 ± 1	0.2 ± 0.3
Caprifoliaceae	0	0 ± 0.1
Corylus	0 ± 0.1	0
Castanea	1.9 ± 3	1.3 ± 2.3
Castanopsis	0	0.2 ± 0.6
Celastraceae	1.6 ± 4.9	0.9 ± 1.8
Fabaceae	0.3 ± 0.7	0.3 ± 1.4
Ilex	0	0 ± 0.2
Oleaceae	0	0.1 ± 0.3
Quercus	0	0 ± 0.2
Tilia	0	0 ± 0.1
Zygophyllaceae	0.8 ± 2.8	0 ± 0.2
others	**6.2 ± 16.4**	**5.2 ± 9.4**

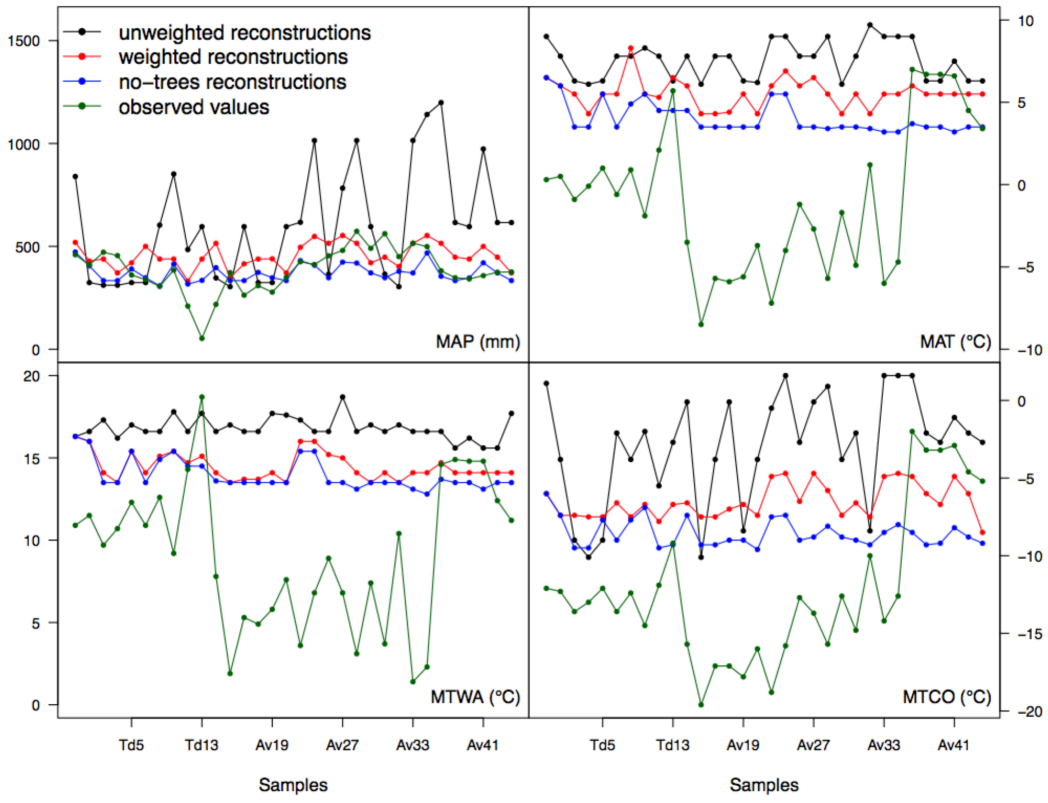

Figure 2-3 Comparison of observed and reconstructed climates at modern surface sample sites on the Qinghai-Tibetan Plateau. The reconstructions are based on county-level plant distribution and climate data (unweighted), climate ranges determined using climate information at pollen sites (weighted) and the same climate range information but for no-trees only. MAP, mean annual precipitation; MAT, mean annual temperature; MTWA, mean temperature of the warmest month; MTCO, mean temperature of the coldest month.

obtained in the unweighted CoA goes from 6.1 to 9.7°C, and thus the reconstructions shows a positive bias (Table 2-3, Figure 2-3).The RMSE is correspondingly large: 9.7°C (Table 2-4). Only two of the sites (Av39, Av41) have reconstructed MAT similar to the observed MAT, and both of these occur at the warmer end of the observed temperature gradient. The reconstructions of MAT based on the weighted CoA show a range from 4.3 to 8.3°C, i.e. the overestimation of temperature is reduced at most sites although the method still fails to reproduce observed MAT in the colder part of the temperature range. Although the use of the weighted CoA reduces the biases, the RMSE is still very large (7.7°C). Excluding AP sensu stricto allows reconstruction of somewhat colder temperatures (range 3.2 to 6.5°C) in the non-trees reconstruction but does not improve the ability to reconstruct observed MAT at sites where the MAT is negative.

Table 2-3 Reconstructed MAP, MAT, MTWA and MTCO at the sampling sites, using three variants of the Coexistence Approach (unweighted, weighted, non-trees) as described in the text.

	Mean Annual Precipitation (mm)									
	unweighted reconstructions			weighted reconstructions			non-trees reconstructions			
Sample No.	Number of coexisting taxa (Number of potential taxa)	Coexistence interval	Median	Number of coexisting taxa (Number of potential taxa)	Coexistence interval	Median	Number of coexisting taxa (Number of potential taxa)	Coexistence interval	Median	observed value
Td1	9 (9)	730—950	840	9 (9)	478—561	520	7 (7)	384—561	473	460
Td2	13 (20)	279—368	324	12 (20)	401—456	429	10 (13)	401—409	405	410
Td3	9 (9)	254—368	311	5 (9)	421—456	439	6 (6)	286—381	334	471
Td4	11 (16)	254—368	311	10 (16)	286—456	371	9 (11)	286—381	334	455
Td5	14 (19)	279—368	324	11 (19)	384—456	420	11 (13)	371—409	390	361
Td6	12 (13)	279—368	324	11 (13)	439—561	500	8 (8)	286—409	348	338
Td7	8 (14)	254—952	603	5 (14)	421—456	439	5 (8)	207—409	308	306
Td9	9 (9)	240—1464	852	9 (9)	421—456	439	8 (8)	371—456	414	385
Td10	6 (16)	17—952	485	5 (16)	253—409	331	5 (12)	253—381	317	210
Td13	9 (9)	240—952	596	6 (9)	421—456	439	7 (7)	288—381	335	52
Av15	13 (17)	325—368	347	13 (17)	478—522	515	11 (11)	384—409	397	218
Av16	9 (17)	240—368	304	8 (17)	286—409	348	8 (12)	286—381	334	373
Av17	9 (12)	240—952	596	8 (12)	409—421	415	7 (9)	286—381	334	263
Av18	14 (19)	279—368	324	12 (19)	421—456	439	13 (14)	338—409	374	309
Av19	12 (12)	279—368	324	9 (12)	423—456	440	8 (8)	286—409	348	277
Av21	6 (6)	240—952	596	6 (6)	286—456	371	5 (5)	286—381	334	349
Av22	19 (19)	614—620	617	17 (19)	439—522	496	12 (14)	405—456	431	425
Av23	17 (19)	362—1667	1015	15 (19)	522—544	548	13 (13)	408—409	409	412
Av26	12 (17)	362—368	365	9 (17)	478—522	515	8 (11)	286—409	348	454
Av27	9 (9)	614—952	783	7 (9)	544—561	553	6 (6)	286—561	424	480
Av28	12 (16)	362—1667	1015	12 (16)	478—522	515	6 (10)	286—552	419	573
Av30	10 (13)	240—952	596	9 (13)	384—456	420	9 (10)	286—456	371	491
Av31	13 (17)	362—368	365	9 (17)	439—456	448	9 (11)	286—409	348	562
Av32	10 (10)	240—368	304	10 (10)	348—456	402	8 (8)	348—409	379	450
Av33	10 (17)	362—1667	1015	9 (17)	478—522	515	6 (11)	286—456	371	515
Av34	9 (14)	614—1667	1141	8 (14)	544—561	553	6 (10)	384—552	468	499
Av38	8 (8)	730—1667	1199	7 (8)	478—522	515	5 (5)	253—456	355	381
Av39	9 (13)	279—952	616	7 (13)	439—456	448	6 (7)	286—381	334	347
Av40	11 (27)	240—952	596	9 (27)	421—456	439	9 (16)	312—381	347	342
Av41	9 (23)	279—1667	973	9 (23)	439—561	500	6 (13)	384—456	420	358
Av43	11 (19)	279—952	616	9 (19)	439—456	448	8 (11)	286—456	371	374
Av44	8 (12)	279—952	616	7 (12)	286—456	371	7 (7)	286—381	334	376

Table 2-3 (continued)

Sample No.	Mean Annual Temperature (°C)									observed value
	unweighted reconstructions			weighted reconstructions			non-trees reconstructions			
	Number of coexisting taxa (Number of potential taxa)	Coexistence interval	Median	Number of coexisting taxa (Number of potential taxa)	Coexistence interval	Median	Number of coexisting taxa (Number of potential taxa)	Coexistence interval	Median	
Td1	9 (9)	3.0—15.0	9	9 (9)	4.6—8.3	6.5	7 (7)	4.6—8.3	6.5	0.3
Td2	14 (20)	3.0—12.6	7.8	14 (20)	4.6—7.4	6	10 (13)	4.6—7.4	6	0.5
Td3	9 (9)	-0.1—12.6	6.3	9 (9)	4.6—6.3	5.5	6 (6)	0.6—6.3	3.5	-0.9
Td4	9 (16)	-0.4—12.6	6.1	11 (16)	2.2—6.3	4.3	9 (11)	0.6—6.3	3.5	-0.1
Td5	14 (19)	-0.1—12.6	6.3	14 (19)	4.6—6.3	5.5	10 (13)	4.6—6.3	5.5	1
Td6	13 (13)	3.0—12.6	7.8	13 (13)	4.6—6.3	5.5	8 (8)	0.6—6.3	3.5	-0.6
Td7	8 (14)	3.0—12.6	7.8	8 (14)	7.9—8.6	8.3	6 (8)	1.1—8.6	4.9	0.9
Td9	9 (9)	1.5—15.1	8.3	9 (9)	4.6—6.3	5.5	8 (8)	4.6—6.3	5.5	-1.9
Td10	6 (16)	3.0—12.6	7.8	6 (16)	2.2—8.3	5.3	5 (12)	0.6—8.3	4.5	2.1
Td13	9 (9)	-0.1—12.6	6.3	9 (9)	4.6—8.3	6.5	7 (7)	0.6—8.3	4.5	5.7
Av15	17 (17)	3.0—12.6	7.8	16 (17)	4.6—7.4	6	11 (11)	2.6—6.3	4.5	-3.5
Av16	9 (17)	-0.4—12.6	6.1	9 (17)	2.2—6.3	4.3	8 (12)	0.6—6.3	3.5	-8.5
Av17	9 (12)	3.0—12.6	7.8	9 (12)	2.2—6.3	4.3	7 (9)	0.6—6.3	3.5	-5.7
Av18	16 (19)	3.0—12.6	7.8	16 (19)	2.4—6.3	4.4	13 (14)	0.6—6.3	3.5	-5.9
Av19	12 (12)	-0.1—12.6	6.3	12 (12)	4.6—6.3	5.5	8 (8)	0.6—6.3	3.5	-5.6
Av21	6 (6)	-0.2—12.6	6.2	6 (6)	2.2—6.3	4.3	5 (5)	0.6—6.3	3.5	-3.7
Av22	19 (19)	5.4—12.6	9	18 (19)	4.6—7.4	6	14 (14)	4.6—6.3	5.5	-7.2
Av23	19 (19)	3.0—15.0	9	17 (19)	6.4—7.4	6.9	13 (13)	4.6—6.3	5.5	-4
Av26	12 (17)	3.0—12.6	7.8	12 (17)	4.6—7.4	6	8 (11)	0.6—6.3	3.5	-1.2
Av27	9 (9)	3.0—12.6	7.8	9 (9)	4.6—8.3	6.5	6 (6)	0.6—6.3	3.5	-2.7
Av28	12 (16)	3.0—15.0	9	12 (16)	4.6—6.3	5.5	6 (10)	0.5—6.3	3.4	-5.7
Av30	10 (13)	-0.4—12.6	6.1	10 (13)	2.2—6.3	4.3	9 (10)	0.6—6.3	3.5	-1.7
Av31	13 (17)	3.0—12.6	7.8	13 (17)	4.6—6.3	5.5	9 (11)	0.6—6.3	3.5	-4.9
Av32	10 (10)	-0.4—19.8	9.7	10 (10)	2.2—6.3	4.3	9 (8)	0.4—6.3	3.4	1.2
Av33	10 (17)	3.0—15.0	9	10 (17)	4.6—6.3	5.5	6 (11)	0.0—6.3	3.2	-6
Av34	9 (14)	3.0—15.0	9	9 (14)	4.6—6.3	5.5	6 (10)	0.1—6.3	3.2	-4.7
Av38	8 (8)	3.0—15.0	9	8 (8)	4.6—7.4	6	5 (5)	0.0—7.4	3.7	7
Av39	9 (13)	-0.1—12.6	6.3	9 (13)	4.6—6.3	5.5	6 (7)	0.6—6.3	3.5	6.7
Av40	11 (27)	-0.1—12.6	6.3	11 (27)	4.6—6.3	5.5	9 (16)	0.6—6.3	3.5	6.7
Av41	9 (23)	-0.1—15.1	7.5	9 (23)	4.6—6.3	5.5	6 (13)	0.1—6.3	3.2	6.6
Av43	11 (19)	-0.1—12.6	6.3	11 (19)	4.6—6.3	5.5	8 (11)	0.6—6.3	3.5	4.5
Av44	8 (12)	-0.1—12.6	6.3	8 (12)	4.6—6.3	5.5	7 (7)	0.6—6.3	3.5	3.4

Table 2-3 (continued)

Sample No.	Mean Temperature of the Warmest Month (°C)									observed value
	unweighted reconstructions			weighted reconstructions			non-trees reconstructions			
	Number of coexisting taxa (Number of potential taxa)	Coexistence interval	Median	Number of coexisting taxa (Number of potential taxa)	Coexistence interval	Median	Number of coexisting taxa (Number of potential taxa)	Coexistence interval	Median	
Td1	9 (9)	11.8—20.8	16.3	9 (9)	15.2— 17.4	16.3	7 (7)	15.2— 17.4	16.3	10.9
Td2	13 (20)	11.8—21.3	16.6	14 (20)	15.2— 16.8	16	10 (13)	15.2— 16.8	16	11.5
Td3	9 (9)	9.8—24.8	17.3	9 (9)	12.5— 15.6	14.1	6 (6)	11.3— 15.6	13.5	9.7
Td4	11 (16)	7.6—24.8	16.2	11 (16)	11.4— 15.6	13.5	9 (11)	11.3— 15.6	13.5	10.7
Td5	14 (19)	9.8—24.2	17	14 (19)	15.2— 15.6	15.4	10 (13)	15.2— 15.6	15.4	12.3
Td6	13 (13)	11.8—21.3	16.6	13 (13)	12.5— 15.6	14.1	8 (8)	11.3— 15.6	13.5	10.9
Td7	8 (14)	11.8—21.3	16.6	8 (14)	11.7— 18.4	15.1	6 (8)	11.3— 18.4	14.9	12.6
Td9	9 (9)	14.2—21.4	17.8	9 (9)	15.2— 15.6	15.4	8 (8)	15.2— 15.6	15.4	9.2
Td10	6 (16)	11.8—21.3	16.6	6 (16)	11.7— 17.7	14.7	5 (12)	11.3— 17.7	14.5	14.3
Td13	8 (9)	9.8—25.6	17.7	9 (9)	12.5— 17.7	15.1	7 (7)	11.3— 17.7	14.5	18.7
Av15	17 (17)	11.8—21.3	16.6	16 (17)	12.5— 15.6	14.1	11 (11)	11.6— 15.6	13.6	7.8
Av16	9 (17)	7.6—26.4	17	9 (17)	11.4— 15.6	13.5	8 (12)	11.3— 15.6	13.5	1.9
Av17	9 (12)	11.8—21.3	16.6	9 (12)	11.7— 15.6	13.7	7 (9)	11.3— 15.6	13.5	5.3
Av18	16 (19)	11.8—21.3	16.6	16 (19)	11.7— 15.6	13.7	13 (14)	11.3— 15.6	13.5	4.9
Av19	12 (12)	9.8—25.6	17.7	12 (12)	12.5— 15.6	14.1	8 (8)	11.3— 15.6	13.5	5.8
Av21	6 (6)	10.5—24.6	17.6	6 (6)	11.4— 15.6	13.5	5 (5)	11.3— 15.6	13.5	7.6
Av22	18 (19)	13.2—21.3	17.3	19 (19)	15.2— 16.8	16	14 (14)	15.2— 15.6	15.4	3.6
Av23	19 (19)	11.8—21.3	16.6	17 (19)	15.2— 16.8	16	13 (13)	15.2— 15.6	15.4	6.8
Av26	12 (17)	11.8—21.3	16.6	12 (17)	14.8— 15.6	15.2	8 (11)	11.3— 15.6	13.5	8.9
Av27	9 (9)	11.8—25.6	18.7	9 (9)	12.5— 17.4	15	6 (6)	11.3— 15.6	13.5	6.8
Av28	12 (16)	11.8—21.3	16.6	12 (16)	12.5— 15.6	14.1	7 (10)	10.5— 15.6	13.1	3.1
Av30	10 (13)	7.6—26.4	17	10 (13)	11.4— 15.6	13.5	9 (10)	11.3— 15.6	13.5	7.4
Av31	13 (17)	11.8—21.3	16.6	13 (17)	12.5— 15.6	14.1	9 (11)	11.3— 15.6	13.5	3.7
Av32	10 (10)	7.6—26.4	17	10 (10)	11.4— 15.6	13.5	8 (8)	11.3— 15.6	13.5	10.4
Av33	10 (17)	11.8—21.3	16.6	10 (17)	12.5— 15.6	14.1	6 (11)	10.5— 15.6	13.1	1.4
Av34	9 (14)	11.8—21.3	16.6	9 (14)	12.5— 15.6	14.1	6 (10)	10.0— 15.6	12.8	2.3
Av38	8 (8)	11.8—21.3	16.6	8 (8)	12.5— 16.8	14.7	5 (5)	10.5— 16.8	13.7	14.6
Av39	9 (13)	9.8—21.3	15.6	9 (13)	12.5— 15.6	14.1	6 (7)	11.3— 15.6	13.5	14.9
Av40	11 (27)	9.8—22.6	16.2	11 (27)	12.5— 15.6	14.1	9 (16)	11.3— 15.6	13.5	14.8
Av41	9 (23)	9.8—21.3	15.6	9 (23)	12.5— 15.6	14.1	6 (13)	10.5— 15.6	13.1	14.8
Av43	11 (19)	9.8—21.3	15.6	11 (19)	12.5— 15.6	14.1	8 (11)	11.3— 15.6	13.5	12.4
Av44	8 (12)	9.8—25.6	17.7	8 (12)	12.5— 15.6	14.1	7 (7)	11.3— 15.6	13.5	11.2

Table 2-3 (continued)

Sample No.	Mean Temperature of the Coldest Month (°C)									observed value
	unweighted reconstructions			weighted reconstructions			non-trees reconstructions			
	Number of coexisting taxa (Number of potential taxa)	Coexistence interval	Median	Number of coexisting taxa (Number of potential taxa)	Coexistence interval	Median	Number of coexisting taxa (Number of potential taxa)	Coexistence interval	Median	
Td1	9 (9)	-6.0— 8.2	1.1	9 (9)	-9.0— -3.0	-6	7 (7)	-9.0— -3.0	-6	-12.1
Td2	14 (20)	-13.5— 5.9	-3.8	14 (20)	-8.5— -6.3	-7.4	10 (13)	-8.5— -6.3	-7.4	-12.3
Td3	9 (9)	-11.3— -6.7	-9	8 (9)	-8.7— -6.0	-7.4	6 (6)	-12.6— -6.3	-9.5	-13.6
Td4	11 (16)	-13.5— -6.7	-10.1	11 (16)	-8.7— -6.3	-7.5	9 (11)	-12.6— -6.3	-9.5	-13
Td5	14 (19)	-11.3— -6.7	-9	13 (19)	-8.9— -6.0	-7.5	10 (13)	-9.0— -6.3	-7.7	-12.1
Td6	13 (13)	-10.0— 5.9	-2.1	12 (13)	-7.2— -6.0	-6.6	8 (8)	-11.6— -6.3	-9	-13.6
Td7	8 (14)	-13.5— 5.9	-3.8	8 (14)	-8.7— -6.3	-7.5	6 (8)	-9.0— -6.3	-7.7	-12.4
Td9	9 (9)	-12.6— 8.7	-2	9 (9)	-8.7— -4.7	-6.7	8 (8)	-12.6— -4.7	-6.9	-14.5
Td10	6 (16)	-16.9— 5.9	-5.5	6 (16)	-9.3— -6.3	-7.8	5 (12)	-12.6— -6.3	-9.5	-11.9
Td13	9 (9)	-11.3— 5.9	-2.7	9 (9)	-8.7— -4.7	-6.7	7 (7)	-12.6— -6.0	-9.3	-9.2
Av15	16 (17)	-6.0— 5.9	-0.1	16 (17)	-8.4— -4.7	-6.6	11 (11)	-8.4— -6.3	-7.4	-15.7
Av16	9 (17)	-13.5— -6.7	-10.1	9 (17)	-8.7— -6.3	-7.5	8 (12)	-12.3— -6.3	-9.3	-19.6
Av17	9 (12)	-13.5— 5.9	-3.8	9 (12)	-8.7— -6.3	-7.5	7 (9)	-12.3— -6.3	-9.3	-17.1
Av18	16 (19)	-6.0— 5.9	-0.1	16 (19)	-7.7— -6.3	-7	13 (14)	-11.6— -6.3	-9	-17.1
Av19	12 (12)	-10.0— -6.7	-8.4	11 (12)	-7.3— -6.0	-6.7	8 (8)	-11.6— -6.3	-9	-17.8
Av21	6 (6)	-13.5— 5.9	-3.8	6 (6)	-8.7— -6.0	-7.4	5 (5)	-13.1— -6.0	-9.6	-16
Av22	19 (19)	-3.8— 2.8	-0.5	17 (19)	-5.1— -4.7	-4.9	14 (14)	-9.0— -6.0	-7.5	-18.8
Av23	19 (19)	-6.0— 9.1	1.6	16 (19)	-5.1— -4.3	-4.7	13 (13)	-8.5— -6.3	-7.4	-15.8
Av26	12 (17)	-11.3— 5.9	-2.7	9 (17)	-8.7— -4.3	-6.5	8 (11)	-11.6— -6.3	-9	-12.7
Av27	9 (9)	-6.0— 5.9	-0.1	7 (9)	-5.1— -4.3	-4.7	6 (6)	-11.6— -6.0	-8.8	-13.7
Av28	12 (16)	-6.0— 7.8	0.9	12 (16)	-7.2— -4.3	-5.8	6 (10)	-11.9— -4.3	-8.1	-15.7
Av30	10 (13)	-13.5— 5.9	-3.8	10 (13)	-8.7— -6.0	-7.4	9 (10)	-11.6— -6.0	-8.8	-12.6
Av31	13 (17)	-10.0— 5.9	-2.1	12 (17)	-7.2— -6.0	-6.6	9 (11)	-11.6— -6.3	-9	-14.8
Av32	10 (10)	-10.0— -6.7	-8.4	10 (10)	-8.7— -6.3	-7.5	8 (8)	-12.3— -6.3	-9.3	-10
Av33	10 (17)	-6.0— 9.1	1.6	10 (17)	-5.1— -4.7	-4.9	6 (11)	-12.3— -4.7	-8.5	-14.2
Av34	9 (14)	-6.0— 9.1	1.6	9 (14)	-5.1— -4.3	-4.7	6 (10)	-11.6— -4.3	-8	-12.6
Av38	8 (8)	-6.0— 9.1	1.6	8 (8)	-5.1— -4.7	-4.9	5 (5)	-12.3— -4.7	-8.5	-2
Av39	9 (13)	-10.0— 5.9	-2.1	9 (13)	-7.2— -4.7	-6	6 (7)	-12.6— -6.0	-9.3	-3.2
Av40	11 (27)	-11.3— 5.9	-2.7	11 (27)	-8.7— -4.7	-6.7	9 (16)	-12.3— -6.0	-9.2	-3.2
Av41	9 (23)	-11.3— 9.1	-1.1	9 (23)	-5.1— -4.7	-4.9	6 (13)	-11.6— -4.7	-8.2	-2.9
Av43	11 (19)	-10.0— 5.9	-2.1	11 (19)	-7.2— -4.7	-6	8 (11)	-11.6— -6.0	-8.8	-4.6
Av44	8 (12)	-11.3— 5.9	-2.7	8 (12)	-12.3— -4.7	-8.5	7 (7)	-12.3— -6.0	-9.2	-5.2

Table 2-4 Comparison of observed and reconstructed climate variables, and assessment of goodness-of-fit using root mean squared error (RMSE)

Climatic parameters	Reconstructions	RMSE	observed range	RMSE as % of observed range
MAP (mm)	unweighted	344.5	52.4—573.0	66%
	weighted	125.5		24%
	no-trees	97.9		19%
MAT (/°C)	unweighted	9.7	-8.5—7.0	63%
	weighted	7.7		50%
	no-trees	6.6		43%
MTWA (/°C)	unweighted	8.9	1.4—18.7	51%
	weighted	6.9		40%
	no-trees	6.4		37%
MTCO (/°C)	unweighted	10.7	-19.6— -2.0	61%
	weighted	7.4		42%
	no-trees	6.2		35%

The RMSE remains large (6.6°C). Reconstructions of both MTWA and MTCO (Figure 2-3) show similar error patterns as the reconstructions of MAT. The reconstructed range is somewhat larger than observed and shifted towards warmer temperatures in the unweighted CoA, both for MTWA (15.6 to 18.7°C compared to observed values of 1.4 to 18.7°C) and for MTCO (-10.1 to 1.6°C compared to observed values of -19.6 to -2.0°C). The use of the weighted CoA reduces the range at the warmer end but nevertheless the RMSE remains large (6.9°C from MTWA and 7.4°C for MTCO). Exclusion of AP sensu stricto reduces the RMSE in the non-trees reconstructions by *ca.* 0.5°C in the case of MTWA and about 1.2°C in the case of MTCO (Table 2-4), but although the warm-end biases are negligible the method still fails to reproduce the observed values of MTWA or MTCO at the cold-end sites.

These analyses show that the performance of CoA can be significantly improved by using a data set with more accurate attributions of the climate distribution of individual taxa (weighted versus unweighted reconstructions). They also suggest that the removal of possible extra-local contaminants improves the reconstructions (weighted versus non-trees reconstructions). The errors associated with the reconstruction of MAP are reasonable. The

RMSE for the non-tree reconstruction is 98 mm, approximately equivalent to between 20-100% of the observed values of MAP. However, the errors associated with the reconstruction of temperature are very large, *ca.* 8°C on observed temperatures ranging from -8.5 to 7°C.

The warm biases in the temperature reconstructions do not appear to be attributable to the presence/absence of specific taxa (Appendix A). Even in the weighted reconstructions, the lowest values of the range for MAT are only -1.6 (Apiaceae) and -1.5 (Cyperaceae) and the minimum value of the ranges is only negative for 9 taxa altogether. In contrast, about 86% of the taxa in the weighted data set have minimum ranges of MAP within the observed range at the sampling sites. Thus, the quality of the reconstructions of individual climate variables is clearly a function of the quality of the underlying climate data set.

4. Discussion and Conclusions

We have shown that there are differences in the patterns of non-arboreal and shrub pollen abundance between the temperate desert and alpine vegetation zones. Similar patterns have been observed in previous studies (e.g. Yu et al., 2001; Shen et al., 2006; Herzschuh, 2007; Zhao and Herzschuh, 2009). Strictly arboreal pollen is present in most of the samples, despite the fact that trees do not occur in the vicinity of the sampling sites. We assume that the arboreal pollen is transported by the Asian summer monsoon winds from the southeastern part of the Plateau, where trees do occur. Tree pollen has been recovered from pollen traps in the northwestern part of Tibet (Cour et al., 1999) and in the Nam Co Basin (Lu et al., 2010). Multiple authors have suggested that tree pollen is brought into the central part of the Plateau by the Asian summer monsoon (e.g. Cour et al., 1999; Jiang and Ding, 2009; Lu et al., 2010), which coincides with the flowering period of most tree species. Yu et al. (2001) showed that the abundance of tree pollen in modern pollen samples increased

towards the southeastern part of the Plateau, which is again consistent with transport from the east or south by monsoon winds.

We have used the CoA approach to make reconstructions of modern climate from pollen surface samples from the temperate desert and alpine regions of the Plateau. The accuracy of the reconstruction depends on the accuracy with which plant distributions can be described in climate space. In our unweighted reconstructions, the climate space of various plant taxa was taken from observations of the whether a taxon was present anywhere in the county. We used a single value of MAP, MAT, MTWA and MTCO for the county, although some of the counties on the Qinghai-Tibetan Plateau are large and encompass a considerable range of elevations, and thus potentially a range of different ecosystems. It is not surprising that reconstructions using estimates of the climate range of specific pollen taxa derived by Lu et al. (2011) based on climate data for individual pollen sampling sites provide better constrained reconstructions, even though the sampling-site climate was derived by interpolation. The fact that the number of taxa used in the weighted reconstruction is often less than in the non-weighted reconstructions provides further support for the idea that the use of county level data obscures the relationship between climate and plant distribution. Although this only affects a small percentage of the temperature reconstructions (between 6-13% depending on the variable), it occurs in 81% of the MAP reconstructions. Thus, as is the case for any other modern-analogue based climate-reconstruction methodology (Salonen et al., 2013), the size and representativeness of the modern analogue data set is crucial in order to be able to derive robust reconstructions using the CoA approach. We have shown that excluding tree pollen in the non-tree reconstructions results in better reconstructions of observed climates at our sampling sites. Given that AP is presumed to be of extra-local origin, this was to be expected.

The CoA reconstructions of temperature are poor: there is a systematic warm bias, observed MAT below 0°C are not reproduced at any of the sites, and the RMSE is large (*ca.* 7-8°C) even when potentially extra-local contaminants are removed. However, the reconstructions of MAP are much better constrained than those of any of the temperature variables. Studies in other regions of open-vegetation have shown difficulties in reconstructing cold climates and a tendency for a reconstruction bias towards warmer temperatures (see e.g. Guiot et al., 1999; Jost et al., 2005). This is because, while long-lived tree species display frost-tolerance (or frost-avoidance) mechanisms (Woodward, 1987; Harrison et al., 2010) and thus are sensitive recorders of winter temperature, the short-lived plants largely represented in the NAP fraction rarely display such adaptations and are therefore less sensitive recorders. At the same time, the abundance of many of the NAP taxa are strongly controlled by water availability and these taxa are distributed in a wide range of temperature regimes (see e.g. Minckley et al., 2008).

Our analyses indicate that CoA is an appropriate technique for the reconstruction of recent and Holocene climates. Its application to the Qinghai-Tibetan Plateau requires detailed information on the distribution of plant species and good quality climate data at the species-sampling sites. The development of such data sets could improve the ability to make reconstructions of past climate changes in this region.

Chapter 3 Relationships between leaf morphometric traits and climate

1. Introduction

Functional leaf traits are observable characteristics of plants that reflect adaptive physiological responses to environmental stressors such as disturbance or climate (Lavorel et al., 2007). There is a growing body of work that documents coherent relationships between specific climate variables and leaf traits, focusing particularly on quantitative measures such as specific leaf area and dry matter content, and chemical properties such as leaf carbon or nitrogen content (e.g. Werger and Ellenbroek, 1978; Diaz et al., 1998; Fonseca et al., 2000; Niinemets, 2001; Wright and Westoby, 2002; Wright et al., 2004; Wright et al., 2005a; Swenson and Enquist, 2007; Meng et al., 2009; Poorter et al., 2009; Prentice et al., 2011). The observed statistical relationships have been explained in terms of the economics of leaf growth under a specific set of environmental constraints, with contrasting traits reflecting fast or slow returns on plant investments in leaf mass and nutrients (Wright et al., 2004, 2005).

There is a much wider range of leaf traits that appear to vary in abundance in different climates, including leaf type and phenology (e.g. Harrison et al., 2010), leaf shape (e.g. Nicotra et al., 2011), leaf orientation (e.g. Shaver, 1978), the degree to which the leaf margin is dissected (e.g. Peppe et al., 2011; Royer et al., 2012), the presence of a terminal drip tip or notch (e.g. Ellenberg, 1985), leaf colour (e.g. Archetti et al., 2013), and characteristics of the leaf surface such as the presence of a waxy coating, trichomes or surface patterning (e.g. Wiegand, 1910; Johnson, 1975; Neinhuis and Barthlott, 1997). Several of these traits have been associated with strategies both to promote water conservation in water-limited environments and to provide protection against high leaf

temperatures. Some of these traits have also been associated with strategies to promote water removal in very wet climates. However, there has been considerably less exploration of the statistical relationships between such traits and climate gradients, perhaps because many of these traits are recorded simply in terms of presence/absence or using categorical, qualitative descriptive classes. As a result, possible adaptive explanations for the apparent differences in the frequency of these traits remain largely unexplored by quantitative methods. Quantification of the relationships between climate and specific morphometric traits would promote (a) the explicit simulation of traits affecting the water- and energy-budgets in land-surface models (Dong et al., 2016a), (b) the use of morphometric traits to improve the definition of plant functional types (PFTs) in global vegetation models (Lavorel et al., 2007), and (c) improve techniques currently used to reconstruct past climates on the basis of morphometric traits (Royer, 2012).

Here, we draw on work that has established that the vegetation patterns of China can be explained in terms of responses to gradients in summer temperature, plant-available moisture and seasonality (Wang et al., 2013) and an exceptionally large data set of observations of leaf traits from 92 sites sampling most of these vegetation types, to explore and quantify the climate controls on the frequencies of leaf morphometric traits. We first examine patterns in leaf type with climate, then relationships between morphometric traits related to leaf economics, and finally traits that have been associated with strategies to conserve or remove water and to protect against high leaf temperatures.

2. Methods

2.1 Sampling sites

Ninety-two sites (Appendix B) were selected to represent variation along the major gradients in summer temperature, aridity and seasonality (Figure 3-1). These sites include

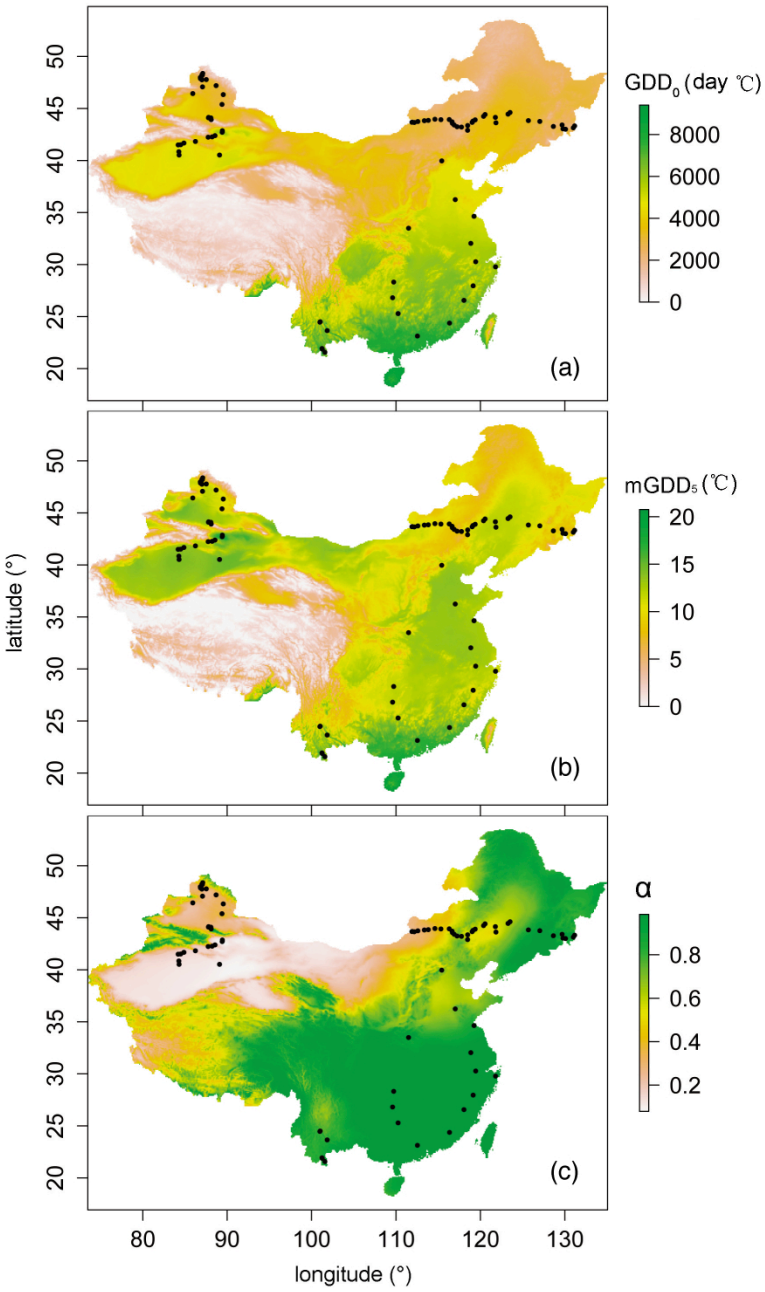

Figure 3-1 Location of the study sites. The sites (shown as closed black circles) are superimposed on maps showing the geographic gradients in (a) growing degree days above a baseline of 0°C (GDD_0), (b) mean temperature of the period above 5°C ($mGDD_5$) and (c) the Cramer–Prentice index (α) of plant-available moisture (Prentice et al., 1993), which is equivalent to the ratio between actual and equilibrium evapotranspiration.

representatives of all the major vegetation types in China, except those found at high elevations. Thirty-three sites along the Northeast China Transect (NECT: Ni and Wang, 2004; Prentice et al., 2011) sample an aridity gradient from closed forests with annual rainfall > 700 mm in the east, through grasslands to desert with annual rainfall of < 150 mm

in the west. Thirty-five sites in the Xinjiang Autonomous Region sample the extreme dry end of this gradient, with annual rainfall between 12 and 468 mm/year (160 mm on average). Fourteen sites located in forest reserves on the North-South Transect of Eastern China (NSTEC: Gao et al., 2003) have much higher annual rainfall and sample a range from temperate climates in the north to warm-temperate/subtropical climates in the south. The NSTEC sites are also differentiated in terms of aridity, the sites in the east at any given latitude being wetter than those in the west. Ten sites in Yunnan provide data from tropical rain forest, through subtropical evergreen broadleaved forest, to savanna and shrubland vegetation.

All sites were occupied by visually homogeneous uncultivated vegetation with minimal signs of recent disturbance. Species composition and vegetation structure were surveyed at each site. A checklist of vascular species at each site was created and field assessments of selected morphometric traits were made on a representative sample of the most abundant species. The species were initially classified into 14 life forms (tree, small tree, shrub, erect dwarf shrub, prostrate dwarf shrub, liana, climber, forb, geophyte, bamboo, other graminoid, succulent, fern or fern ally, epiphyte or parasite) and care was taken to sample each life form, when an example was present at a site. Although the sampling was carried out in several different years (Xinjiang: 2005; NECT: 2006; NSTEC: 2007; Yunnan: 2012 and 2013), the assessments were made by the same people using standard crib sheets for each traits to ensure consistency in reporting.

2.2 Leaf morphometric trait data

Measurements were made of 25 morphometric leaf traits (Appendix C). The recognition of each trait followed standard definitions. Some traits were recorded in terms of presence/absence (e.g. presence of a drip tip); others as a specified number of sub-categories

(e.g. leaf size, where leaves were classified as picophyll, leptophyll, nanophyll, microphyll, notophyll, mesophyll, or macrophyll using the CLAMP system: http://clamp.ibcas.ac.cn/CLAMP_Home.html). In some cases (e.g. the presence of hairs or the presence of spines), the position on the leaf was recorded in the field but this information was subsequently combined for the statistical analyses because there were insufficient records in some of the sub-categories. The field descriptors, and the subsequent amalgamation of these sub-categories, are given in Appendix C. The frequency of each trait (or trait category) was calculated for each site as a percentage of the total number of observations (i.e. the total number of species). Fifteen of the sites from Xinjiang were relatively depauperate (5 species or less), and these sites were omitted from subsequent analyses. Thus, the trait analyses were performed on data from 77 sites.

2.3 Climate data

We used a baseline 1-km resolution gridded climatology constructed from mean monthly values of temperature, precipitation and percentage of possible sunshine hours, derived by an elevationally-sensitive spline interpolation from 1814 meteorological stations across China (Wang et al., 2013). Wang et al. (2013) have shown that a reasonable description of vegetation patterns across China can be produced using three bioclimatic variables: accumulated temperature sum during the growing season defined as the period when interpolated daily temperatures above 0°C (GDD_0), the daily mean during the growing season when temperatures are >5°C ($mGDD_5$) and the Cramer-Prentice plant-available moisture index, α (the ratio between actual and equilibrium evapotranspiration: AET/EET). We derived these variables following the methods described by Prentice et al. (1993) and Gallego-Sala et al. (2010). The climate data for each of the sampling sites was assumed to be that of the nearest 1-km grid cell.

2.4 Generalised linear modeling

Our analysis is based on a special case of the generalised linear model (GLM) known as logistic regression. GLM enables underlying relationships with several predictor variables to be determined even in the presence of moderate correlations among the predictors (Wang et al., 2013). Logistic regression fits an underlying relationship between logit-transformed probability (y) and a linear combination of predictors:

$$\ln [y/(1-y)] = b_0 + b_1x_1 + b_2x_2 + \ldots \quad (1)$$

where b_0 is the intercept and b_i are the slope coefficients for each variable i. The predictand was taken as the abundance of a given trait at each site as a function of the total number of possible observations at the site. The use of percentage abundance data implies maximization of a quasi-likelihood function instead of a true likelihood (Papke and Wooldridge, 1996). Implicitly, the frequencies of traits are treated as estimates of an underlying probability. The logarithm on the left-hand side of equation (1) implies that the predictors combine multiplicatively, so the model is 'linear' only in the sense that the terms on the right-hand side are added together. If a given predictor has a statistically significant effect on the predictand, this shows that *there is a relationship that remains after the effects of the other predictors have been taken into account*. This is particularly important for the interpretation of $mGDD_5$ where, given that $mGDD_5$ will be maximal both in warm climates and in climates with short but warm summers, the occurrence of a relationship independent of GDD_0 is a measure of the degree of concentration of summer warm and hence of seasonality.

Logistic regression was implemented using the glm package in R. Goodness-of-fit of the complete model was quantified using the proportion of explained deviance, also known as MacFadden's R2 (McFadden, 1974) with significance assessed at the 95% confidence level. Partial residual plots were used to display the fitted underlying relationship between each

variable and the predicted probabilities. These plots are analogous to x-y plots in bivariate regression, except that the y-coordinate of each data point in each plot is shifted so as to remove the fitted partial effects of all the other predictors (Larsen and McCleary, 1972). Z values (slope coefficients normalized by their respective standard errors) were used to quantify the importance of each partial relationship. Z values are the most appropriate statistics for this purpose because they express the strength of the signal relative to noise, and are independent of the units of measurement. We did not include any interactions among predictors.

We applied the logistic regression in two stages. We first examined the relationships across all the observations. In order to determine whether the observed relationships were robust across different plant functional types (PFTs), we then repeated the analyses using six broadly defined PFTs: woody (W), non-woody (NW), deciduous broadleaf tree (DBT), evergreen broadleaf tree (EBT), evergreen broadleaf shrub (EBS), and evergreen needleleaf tree (ENT). The abundance of a specific trait at a site was recalculated based on the total number of representative of the PFTs present at the site.

3. Results

All results from the analyses using generalised linear regression modelling, please see Appendix D and E.

3.1 Leaf type

Broadleaved plants occur throughout the climate range examined, and therefore show no significant overall gradient with any of the climate variables (Figure 3-2). The frequency of broadleaved woody plants is positively related with GDD_0 (Figure 3-3) but shows no significant relationship with either of the other climate variables. Needle and scale leaves are confined to woody plants. The frequency of needle leaves shows a significant negative

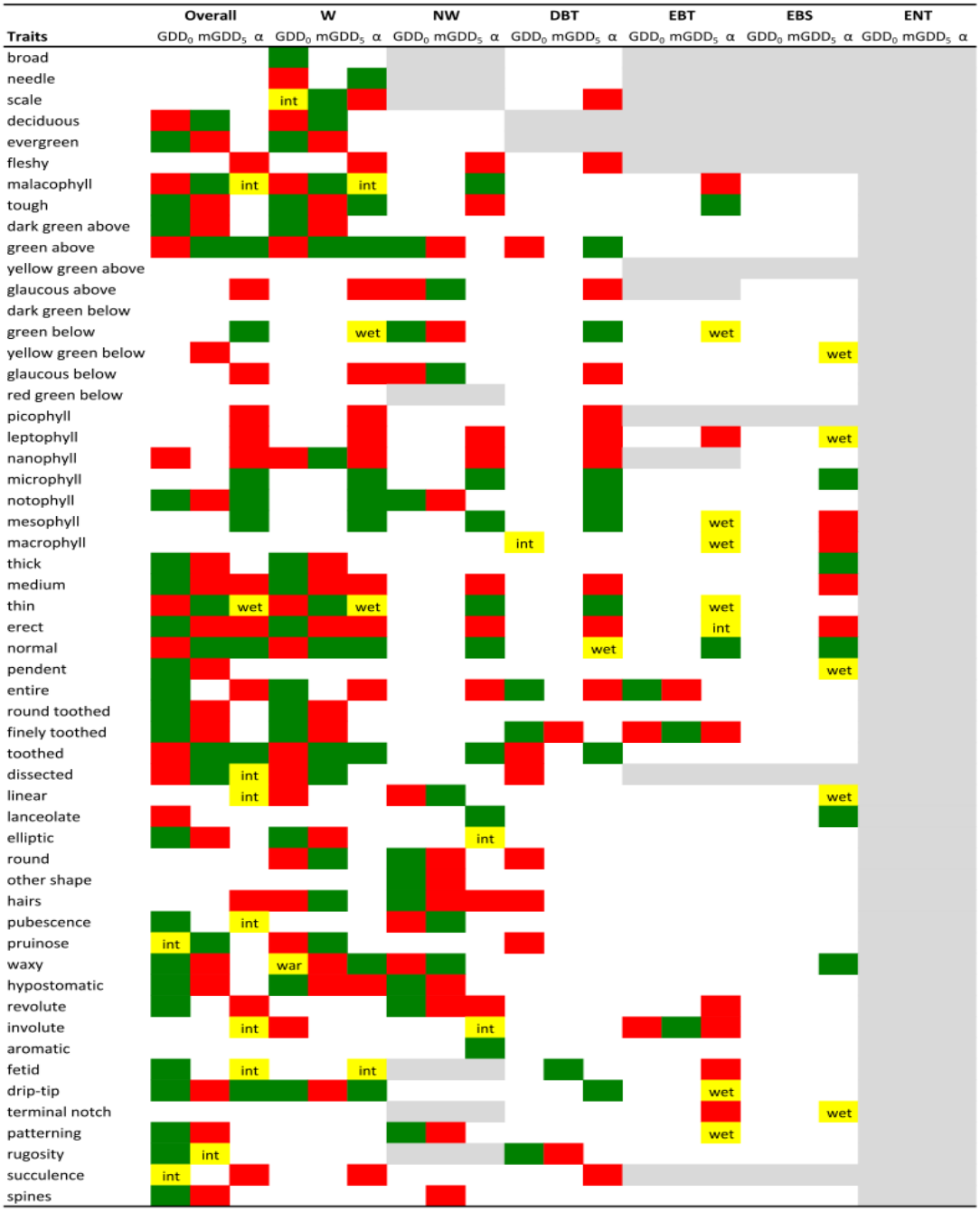

Figure 3-2 Relationships between traits and climate for the data set as a whole (overall) and within individual plant functional types. Positive relationships that are significant at the 95% confidence level are shown in green, negative relationships that are significant at the 95% confidence level are shown in red; non-linear relationships that are significant at the 95% confidence level are shown in yellow; grey shading indicates that the analysis was not made because there were insufficient observations to derive a meaningful relationship. The climate variables are: growing degree days above a baseline of 0°C (GDD_0), mean temperature of the period above 5°C ($mGDD_5$) and the Cramer–Prentice index (α) of plant-available moisture. For non-linear relationships (yellow boxes), the location of maximum abundance in climate space is indicated, where maximum abundance can be warm, intermediate (int) or cold in terms of temperature (GDD_0), low, intermediate or high in terms of seasonality ($mGDD_5$), and wet, intermediate (int) or dry in terms of moisture (α). The plants functional types (PFTs) are woody (W), non-woody (NW), deciduous broadleaf tree (DBT), evergreen broadleaf tree (EBT), evergreen broadleaf shrub (EBS), and evergreen needleleaf tree (ENT).

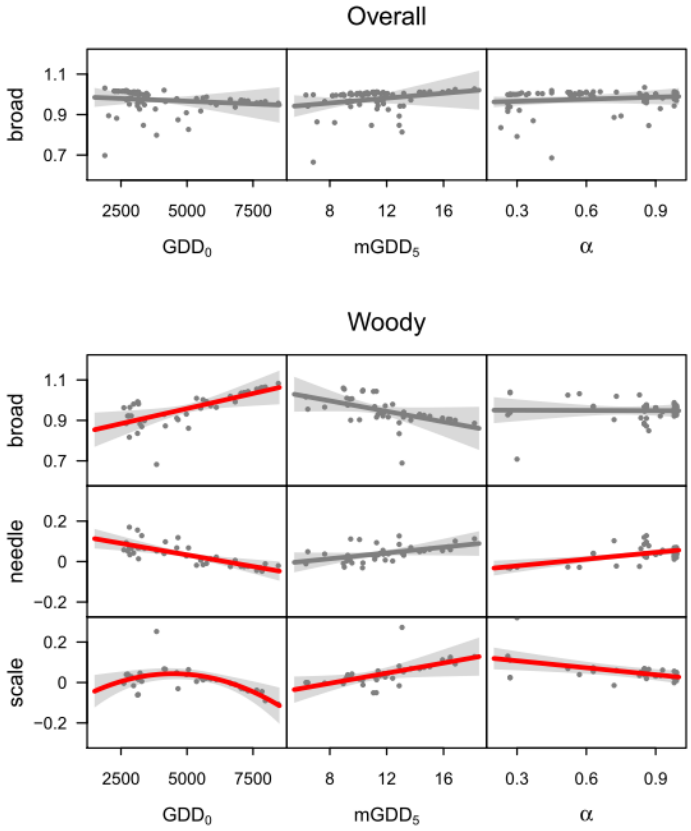

Figure 3-3 Relationships between the frequency of different leaf types (broad, needle, scale) and climate. The climate variables are: growing degree days above a baseline of 0°C (GDD_0), mean temperature of the period above 5°C ($mGDD_5$) and the Cramer–Prentice index (α) of plant-available moisture. The plots show the partial residuals from the generalised linear model, which shows the relationship between the leaf type and the specific climate variable after taking into account the influence of the other climate variables. Needle and scale-leaved only occur in woody species in our data set and so the climate- frequency relationships within this group are shown. Broad leaves characterise both woody and non-woody species, and so we show the overall relationship and that for woody species. Significant relationships are shown in red, non-significant relationships in grey.

relationship with GDD_0 and a significant positive relationship with α. There is no overall relationship with $mGDD_5$. Scale leaves show a non-linear relationship with GDD_0 (Figure 3-2), with peak abundances when GDD_0 <6000 day °C, and a significant negative relationship with α. Scale leaves also show a positive relationship with $mGDD_5$, increasing in frequency as the season of high summer temperature becomes shorter. Effectively, needle-leaved woody plants are characteristic of cold, wet environments, scale-leaved plants are characteristic of dry, relatively warm, and highly seasonal climates, and broadleaved woody plants dominate in warm, wet and non-seasonal climates.

3.2 Leaf economic traits

Evergreen leaves, because of the relatively large carbon and nutrient investment in leaf production, tend to display a number of traits that facilitate leaf longevity, including traits associated with size, thickness, and toughness. The frequency of evergreens increases with GDD_0 (Figure 3-4), and is associated with an increase in size (marked by a decrease in e.g. nanophylls and an increase in notophylls), toughness (and a corresponding decrease in malacophylls) and thickness (and a corresponding decrease in thinness). There is also a positive relationship with dark green leaf colour, which likely reflects the increase in photosynthetic pigments in thick leaves. Conversely, all of these traits show negative relationships with $mGDD_5$ (Figure 3-4) as might be expected given that evergreen species are not favoured in climates with high temperature seasonality. The change in size with $mGDD_5$ is only significant in notophylls, although changes in smaller size classes are coherent with the shift to smaller leaf sizes with increased temperature seasonality.

The positive relationships of size, thickness, toughness and dark green colour with GDD_0 are significant when only woody plants are considered (Figure 3-2; Appendix F) but are not significant for any of the individual woody PFTs. The relationship between these traits and GDD_0 in non-woody plants is positive but not significant, except for size where there is a significant increase in the frequency of notophylls that corresponds to a (non-significant) decrease in several smaller leaf categories. Similarly, the negative relationships with $mGDD_5$ are apparent and significant in woody plants (although not significant for any individual PFTs) and apparent but not significant for non-woody plants. The results support the idea that there are a group of traits associated with being evergreen in woody plants, but suggest that some of these traits may also be advantageous to non-woody plants in warm and non-seasonal climates.

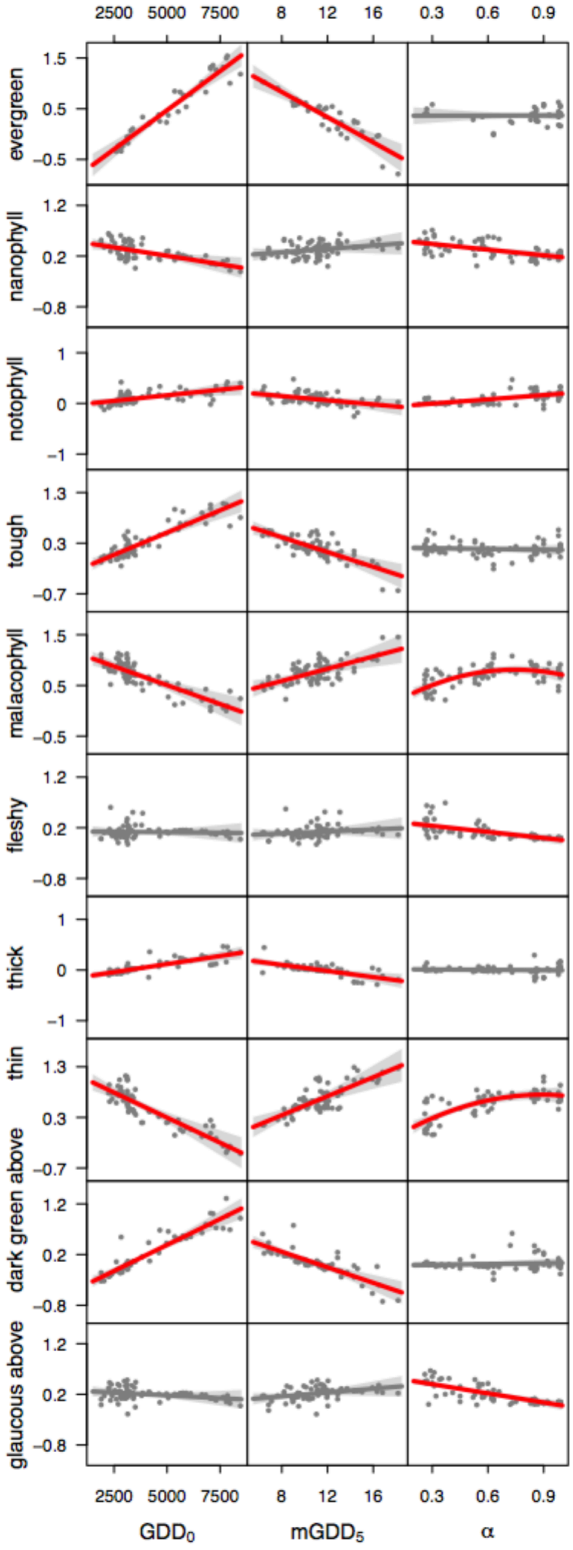

Figure 3-4 Relationships between the frequency of different traits related to quantitative leaf economics traits (evergreen, nanophyll, notophyll, tough, malacophyll, fleshy, thick, thin, dark green above, glaucous above) and climate. The climate variables are: growing degree days above a baseline of 0°C (GDD_0), mean temperature of the period above 5°C ($mGDD_5$) and the Cramer–Prentice index (α) of plant-available moisture. The plots show the partial residuals from the generalized linear model, which shows the relationship between a given trait and the specific climate variable after taking into account the influence of the other climate variables. Significant relationships are shown in red, non-significant relationships in grey.

Relationships between leaf economic traits and α are not strictly parallel with the relationships between these traits and temperature variables. There is no overall relationship between the frequency of evergreen plants and α (Figure 3-4). Leaf size increases with α, as illustrated by the decrease in nanophylls and the increase in notophylls. Malacophyll leaves are most abundant at intermediate moisture levels, and are replaced by tougher leaves in wetter environments and fleshy leaves in drier environments. The frequency of thin leaves shows a positive relationship with α, although there is no corresponding change in thickness. Leaf colour also shows significant relationships with α, with glaucous leaf colour decreasing and green leaves (though not dark green leaves) increasing with increased α.

The relationship between leaf size and α is shown by both woody and non-woody plants (Figure 3-2; Appendix F). The peak in frequency of malacophyll leaves at intermediate levels of moisture in the overall relationship is clearly driven by woody plants; non-woody plants show a significant positive relationship with α. The increase in fleshy-leaved plants at low α is shown by both woody and non-woody plants, although the response in non-woody plants seems to be less marked (Appendix F). However, non-woody and woody plants show contrasting changes in toughness with woody plants showing increasing toughness (presumably reflecting environments where the number of evergreen plants also increases) and non-woody plants showing decreasing toughness with increasing α. The frequency of thin leaves increases with α in both woody and non-woody plants, and the relationship is also significant for deciduous broad-leaved trees and evergreen broad-leaved trees (Figure 3-2). The opposite signal is seen in leaves of intermediate thickness (medium), and in the case of evergreen broad-leaved shrubs there is an increase in thick leaves as α increases. The overall relationships between α and leaf colour appear to be largely driven by woody plants, and significant relationships are also shown for individual woody PFTs.

Our analyses of leaf types and leaf economic traits basically suggest that there are three broad syndromes of behavior, which apply for both woody and non-woody plants. In warm, wet climates with low seasonality, broad leaves that are evergreen, large, tough, thick, and dark in colour are favoured. In dry climates, with short but warm summers, small, fleshy, glaucous leaves of intermediate thickness are favoured. In cold, wet climates of high temperature seasonality, evergreen needle-leaves trees are favoured.

3.3 Leaf margin dissection

Entire, round and finely toothed leaves all increase in frequency with GDD_0, while toothed and dissected decrease with GDD_0. The positive relationship between entire leaves and GDD_0 (and finely toothed) is significant in woody, deciduous and evergreen broadleaved tree, and present though not significant in evergreen broadleaved shrub. The positive relationship between round leaves and GDD_0 is present in multiple PFTs but only significant for woody. The negative relationship between GDD_0 and toothed and dissected leaves is only significant for woody and woody deciduous PFTs. Thus, these analyses support the idea of a strong correlation between the degree of dissection and temperature. However, these leaf margin types show a different relationship with seasonal concentration as measured by $mGDD_5$. Although there is no overall relationship for entire leaves, both round and finely toothed leaves decrease in frequency as the summer season becomes shorter (Figure 3-5), while toothed and dissected leaves become more abundant. These relationships are only found in woody plants (Appendix G). Thus, whereas the degree of marginal dissection broadly reflects summer temperature, less dissected leaves are replaced by more dissected leaves in areas with short, hot summers.

The frequency of entire leaves is negatively correlated with α, whereas the frequency of toothed leaves is positive correlated with α (Figure 3-5). These relationships are significant for both woody and non-woody PFTs, although the slope is steeper for woody plants

(Appendix G). However, amongst the woody PFTs, only deciduous trees show a significant relationship between dissection and α (Figure 3-2).

Our analyses suggest that, at least for woody plants, entire leaves are most common in environments that are warm and wet year round. The frequency of dissected leaves increases in colder climates, in wet but seasonal climates characterized by deciduous trees, and in climates with short, hot summers.

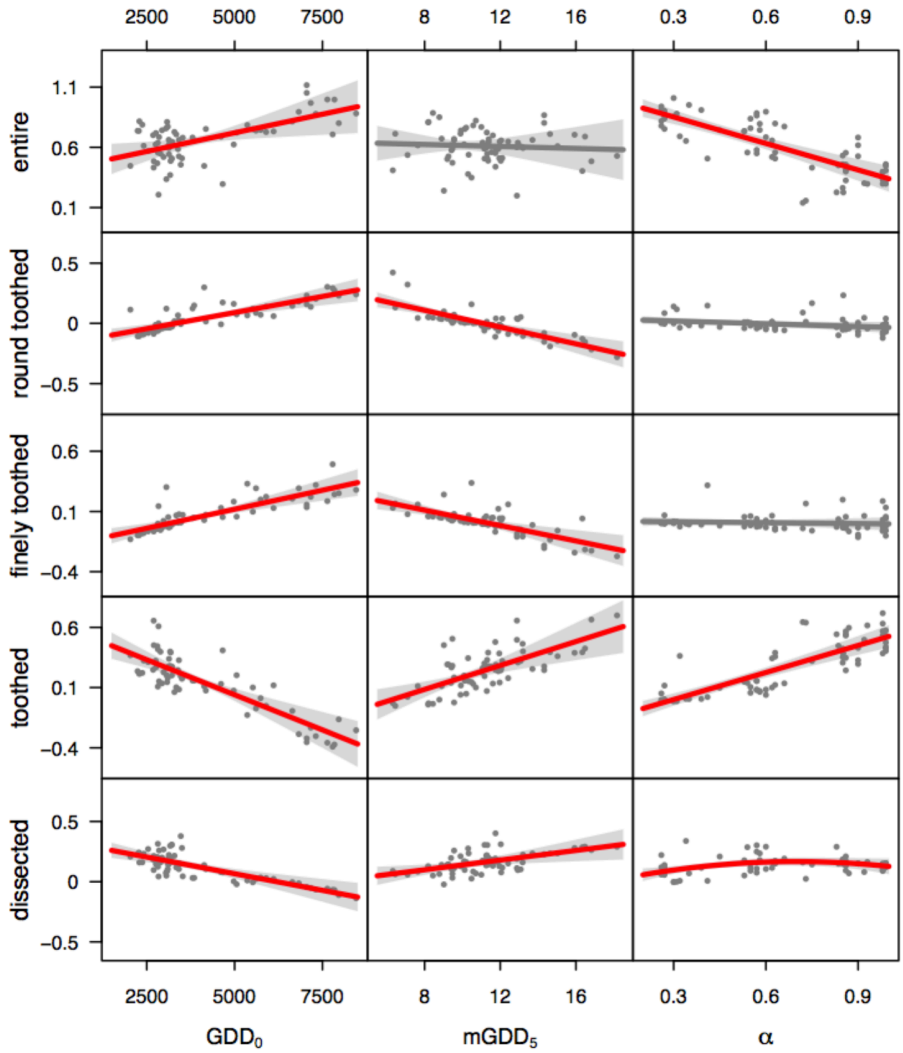

Figure 3-5 Relationships between leaf margin categories (entire, round toothed, finely toothed, toothed, dissected) and climate. The climate variables are: growing degree days above a baseline of 0°C (GDD_0), mean temperature of the period above 5°C ($mGDD_5$) and the Cramer–Prentice index (α) of plant-available moisture. The plots show the partial residuals from the generalised linear model, which shows the relationship between a given trait and the specific climate variable after taking into account the influence of the other climate variables. Significant relationships are shown in red, non-significant relationships in grey.

3.4 Traits associated with water or temperature stress

Waxiness, conspicuous hypostomatism, surface patterning and rugosity all show positive relationships with GDD_0 but no overall relationship with α (Figure 3-6). In the case of conspicuous hypostomatism, surface patterning and rugosity, the relationship with GDD_0 is seen in both woody and non-woody plants (Appendix H), but is not always significant (e.g. surface patterning in woody plants) or only significant for one woody PFT (e.g. rugosity in deciduous trees). However, in the case of waxiness, the relationship is only positive for woody plants; non-woody plants show a significant negative relationship between the frequency of waxy leaves and GDD_0. This presumably reflects the fact that non-woody plants only occur in the understorey in regions with the highest GDD_0 (Figure 3-1). Despite the absence of an overall relationship between waxiness and α, there is a significant positive relationship for woody plants and evergreen broadleaved shrubs. Similarly, despite the absence of an overall relationship with α, the frequency of hypostomatic leaves decreases significantly with α in woody plants. Surface patterning shows a significant non-linear increase with α in evergreen broadleaf trees.

The presence of a waxy cuticle is associated with an increase in surface reflectance, while surface patterning and rugosity affects boundary-layer conductance and thus the rate at which heat is transferred between the leaf and the atmosphere. Thus, the positive relationship between these traits and GDD_0 could be seen as mechanisms to protect against heat stress. However, the fact that the relationship between waxy and surface patterning with α is positive, at least in some woody PFTs, argues that these traits also play a role in removal of excess moisture. The increase in hypostomatism with temperature, accompanied by a decrease with α, in woody plants argues that this reflects an adaptation to high temperatures that is only present under water-limited conditions.

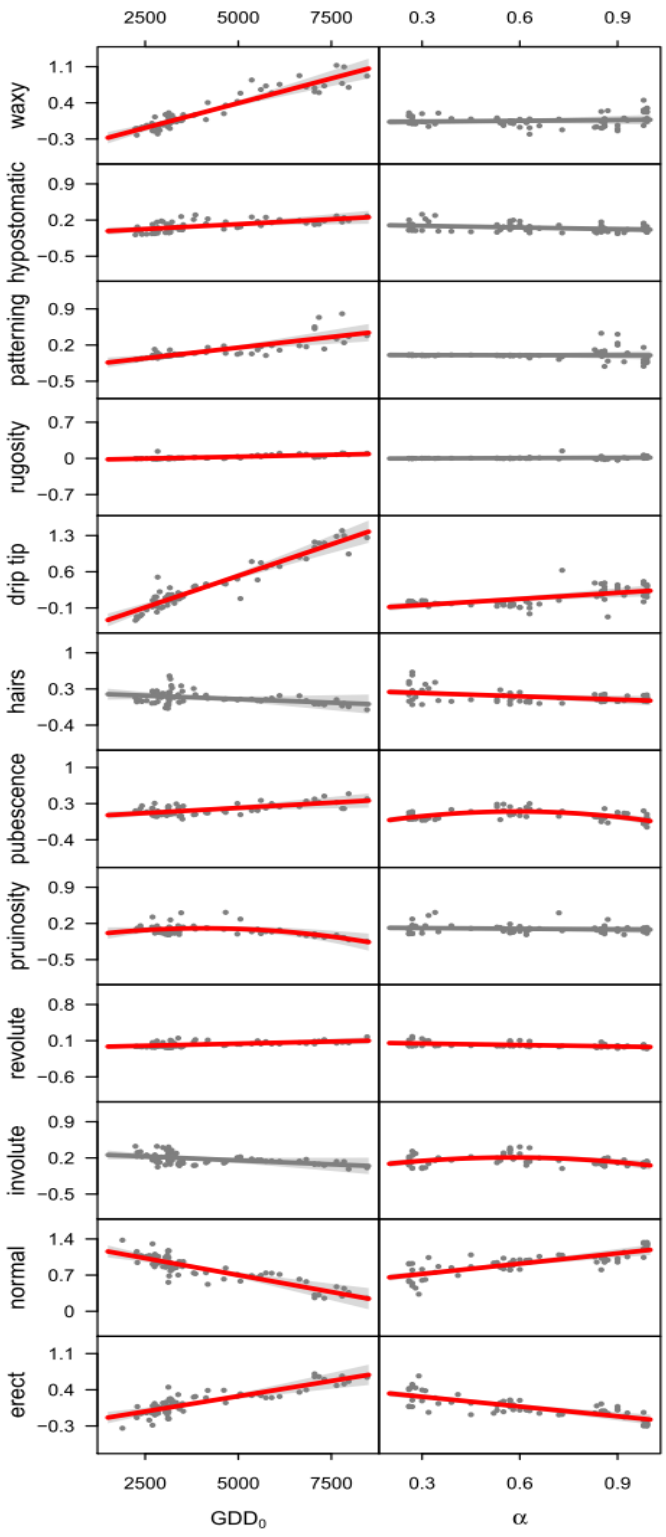

Figure 3-6 Relationships between the frequency of different leaf traits related to protection against high levels of radiation and/or water conservation (waxy, hypostomatic, surface patterning, rugosity, drip tip, hairs, pubescence, pruinosity, revolute, involute, normal orientation, erect orientation) and climate. The climate variables are: growing degree days above a baseline of 0°C (GDD_0), and the Cramer–Prentice index (α) of plant-available moisture. The plots show the partial residuals from the generalised linear model, which shows the relationship between a given trait and the specific climate variable after taking into account the influence of the other climate variables. Significant relationships are shown in red, non-significant relationships in grey.

A number of traits show significant overall relationships with both GDD_0 and α. Both erect and pendant leaves increase in frequency with GDD_0, and as a corollary the frequency of leaves of normal orientation decreases (Figure 3-6). The frequency of normally oriented leaves increases with α, while erect and pendant leaves become less frequent. These relationships are significant for both woody and non-woody plants (Appendix H) and, in the case of normal or erect leaves also for some individual woody PFTs (Figure 3-2). The significant but opposite relationships with GDD_0 and α argue that leaf orientation serves double function in getting rid of water (with increased α) and protecting against excess heating (with increased GDD_0).

The frequency of revolute leaves also shows a positive relationship with GDD_0 and a negative relationship with α. The positive relationship with GDD_0 is significant in non-woody plants and present, but non-significant in woody plants. The negative relationship with α is significant in non-woody plants and also in evergreen broadleaved trees. Again, the opposite relationships with GDD_0 and α suggest that revolute leaves have double function, protecting against excess heating in warm environments and conserving water in dry environments. However, involute leaves do not appear to have similar functions. The frequency of involute leaves peaks at intermediate levels of α, but this relationship is only significant for non-woody plants. Although the relationship in woody plants is not significant, there is a significant negative trend with α for evergreen broadleaved trees. This suggests that involute leaves may also represent an adaptation for water conservation in drier environments. However, although there is no overall relationship between the frequency of involute leaves with GDD_0, there are significant negative relationships for woody plants and evergreen broadleaved trees – i.e. the opposite relationship with temperature from revolute leaves.

Some traits show basically the same form of relationship with both GDD_0 and α. Thus, the presence of drip tips is positively correlated with both GDD_0 and α, particularly in woody plants. The positive relationship with α is also seen in both deciduous and evergreen tree PFTs. The presence of drip tips is usually considered to be a mechanism for removing excess water. The independent relationship with GDD_0 argues that drip tips also serve a function with respect to heat stress.

Pruinosity has a significant negative relationship with GDD_0, which is only manifested in woody deciduous trees. There is no significant relationship with α, either overall or for any individual PFT. The absence of a relationship with α argues that this trait is a protection against cool summer temperatures (given that it is characteristic of deciduous trees). Pubescence shows positive overall relationship with GDD_0, but this relationship is not seen in any individual PFT. In fact there is a significant and negative relationship with GDD_0 in non-woody plants. Pubescence peaks at intermediate levels of α, but the relationship for any individual PFT is non-significant. The presence of leaf hairs has a significant negative overall relationship with α, and this is also the case for non-woody plants. Although there is no overall relationship with temperature, there is a significant negative relationship between the frequency of hairs at GDD_0 for woody plants and deciduous trees, and a significant positive relationship for non-woody plants.

4. Discussion and Conclusions

We have shown many coherent relationships between morphometric leaf traits and specific aspects of climate. Many studies of climate-trait relationships use classic bivariate analyses as an exploratory tool (Kattge et al., 2011; Price et al., 2014). This approach is problematic when there are multiple potential controls on the abundance of a trait or when there are correlations between predictor variables (Wang et al., 2013). Logistic regression, a special case of generalised linear modelling, provide a powerful tool to separate out the influence of

different predictor variables even in the presence of moderate correlations (see e.g. Prentice et al., 2011; Bistinas et al., 2014; Li et al., 2015a; Meng et al., 2015). The use of logistic regression here has allowed us to demonstrate that some traits show independent variation with both moisture and temperature (e.g. leaf dissection, surface patterning) while others respond to only temperature (e.g. the presence of a waxy cuticle) or moisture (e.g. marginal involution) variation.

In our analyses, we have focused on the role of morphometric traits at three different levels: phenological syndromes, traits that relate to the economics of leaf growth, and traits that might affect the leaf energy and water balance. We recognize distinct syndromes of morphometric traits associated with the cost of leaf formation: warm, wet climates with low seasonality favour broad leaves that are evergreen, large, tough, thick, and dark in colour; dry, warm climates with high seasonality favour small, fleshy, glaucous leaves of intermediate thickness; cold, wet climates of high seasonality favour needle leaves that are evergreen.

The leaf economic spectrum describes correlations between leaf traits, such as carbon assimilation rate, leaf lifespan, leaf mass per unit area and nitrogen content, that define different growth strategies reflecting fast or slow returns on plant investment in leaf mass and nutrients (Reich et al., 1997; Wright et al., 2004; Wright et al., 2005a; Shipley et al., 2006; Reich, 2014). Our analyses show patterns in the frequencies of morphometric traits that are consistent with the predictions of the leaf economic spectrum. Specifically, as is shown by relationships with GDD_0, environmental conditions that promote an increase in the frequency of long-lived evergreen leaves are also associated with increases in size, toughness, thickness and the amount of photosynthetic pigment present (as reflected by colour). Environmental conditions that promote an increase in short-lived deciduous leaves,

as shown by relationships with $mGGD_5$ and α, are associated with decreases in size, toughness, thickness and dark leaf colour.

Both excessively high and excessively low temperatures inhibit photosynthesis and can cause tissue damage. There is extensive evidence that the temperature of leaves is less variable than the temperature of the surrounding air, such that leaves are warmer than air at when daytime air temperatures are low, but cooler than air when daytime air temperatures are high (Lange, 1959; Linacre, 1964; Campbell and Norman, 1998; Michaletz et al., 2015). This phenomenon is a result of biophysical homeostasis, whereby transpiration acts to cool leaves when air temperature is high (Dong et al., 2016b). Leaf size, shape and the degree of leaf margin dissection affect the leaf energy balance, through changing boundary-layer conductance (Linacre, 1964; Gates, 1968; Parkhurst and Loucks, 1972; Taylor, 1975) (Givnish and Vermeij, 1976; Smith, 1978; Zangerl, 1978; Upchurch and Mahan, 1988). We have shown that other traits that increase boundary-layer conductance, such as surface patterning, rugosity, and the presence of a drip tip show a strong, positive correlation with GDD_0. Traits that decrease boundary-layer conductance, such as pruinosity, show a negative correlation with GDD_0. However, the positive correlation between waxiness and the frequency of erect or pendant leaves and GDD_0 indicates that adaptations to minimize heat stress operate through mechanisms other than altering boundary-layer conductance, specifically through increasing surface reflectance in the case of waxiness (Holmes and Keiller, 2002; Bell, 2012) and of minimizing direct heating in the case of leaf orientation. The fact that the frequency of erect or pendant leaves decreases with increasing α is consistent with the idea that this mechanism is less necessary under well-water conditions, when transpiration promotes leaf cooling. A similar situation pertains for the expression of conspicuous hypostomatism, which also increases with GDD_0 and decreases with α, again suggesting that whereas reducing the number of stomata helps to limit transpiration such protection is not required in well-watered conditions. The only traits that show independent

positive relationships with both GDD_0 and α across all life forms are the presence of a drip tip and of revolute margins. However, waxiness and surface patterning show positive relationships with α for some woody PFTs, especially evergreen broadleaf shrubs and trees. This supports the idea that these traits play a role in water-shedding in warm, wet climates.

The idea that leaf shape and degree of leaf margin dissection varies with temperature is not new (see e.g. Bailey and Sinnott, 1915). Indeed, it forms the basis for two widely used methods to reconstruct mean annual temperature from measurements of leaf dissection on fossil floras: Leaf margin analysis (LMA, Bailey and Sinnott, 1916; Wolfe, 1978, 1979) and The Climate Leaf Analysis Multivariate Program (CLAMP, Wolfe, 1993; Wolfe, 1995). These approaches have been widely used to infer paleotemperature from fossil floras ranging from Late Cretaceous to Tertiary in age (e.g. Bailey and Sinnott, 1915; Wolfe, 1978, 1979; Wing and Greenwood, 1993; Wilf, 1997; Utescher et al., 2000; Liang et al., 2003; Uhl et al., 2003; Greenwood et al., 2004; Greenwood et al., 2005; Miller et al., 2006; Peppe et al., 2011). However, the discovery that the strength of the correlation between mean annual temperature and dissection varies between continents and regions (Gregory-Wodzicki, 2000; Su et al., 2010; Chen et al., 2014) has raised some concern about the use of these techniques. Our results shed light on this problem since they show that while the degree of marginal dissection is negatively correlated with summer warmth (as measured by GDD_0), it is also affected by temperature seasonality – less dissected leaves are replaced by more dissected leaves in areas with short, hot summers. Thus, differences in temperature seasonality between different regions could contribute to the observed differences in the strength of the relationship with mean annual temperature. We have also shown that the frequency of toothed leaves is positive correlated with α. This supports suggestions that differences in moisture availability are partially responsible for differences in the strength of the correlation between leaf dissection and temperature in different regions (Davis and Taylor, 1980; Chen et al., 2014).

Many of the relationships between traits and climate variables are generic (i.e. displayed across all PFTs) or generic across woody PFTs. The lack of such strong relationships in non-woody PFTs, primarily understorey PFTs, may be a result of under-sampling of these taxa in our data set. It could also reflect the fact that the climate data used in our analyses does not necessarily represent environmental conditions in the understorey. Both issues should be addressed in future work. Nevertheless, the existence of strong independently significant relationships with specific climate variables demonstrates the utility of using quantitative and categorical trait data to explore variation along climate gradients.

Our focus in this paper has been on examining whether the differences in trait frequency with gradients in specific climate variables are consistent with potential adaptive explanations for these traits. The quantification of these relationships could be useful in other contexts. There has been a considerable effort expended on the definition of PFTs for global modelling (Bonan et al., 2002; Lavorel and Garnier, 2002; Pillar and Sosinski, 2003; Lavorel et al., 2007; Prentice et al., 2007; Lapola et al., 2008; Sun et al., 2008; Poulter et al., 2011). While bottom-up classification approaches are equivocal, top-down approaches are limited by the degree to which they are process-informed. Quantification of key relationships that reflect plant adaptations to environmental gradients offers an opportunity to develop more process-based PFT classifications for global modelling. Quantification of climate-trait relationships may also offer the opportunity to go beyond the use of PFT classification to explicitly modelling traits related to water- and energy-balance. There are now a number of studies suggesting that trait-based modelling can capture broad-scale patterns of plant behavior (e.g. Scheiter and Higgins, 2009; Van Bodegom et al., 2012; Verheijen et al., 2013), and a growing body of theory that supports the idea that climate-trait relationships are an expression of the optimisation of resource use by plants (Medlyn et al., 2011; Prentice et al., 2014; Dong et al., 2016a; Dong et al., 2016b). Finally, the demonstration that it is possible to separate out the influences of different climate variables

on trait abundance in a quantitative way opens up the possibility of explaining apparent inconsistencies in the use of climate-trait relationships to reconstruct past climate changes (e.g. Wolfe, 1993; Greenwood, 2005; Royer, 2012)and to develop improved techniques for doing so.

Chapter 4 Reconstruction of Eocene, Miocene and Pliocene climates in China using plant morphometric traits

1. Introduction

Marine oxygen-isotope records indicate that the Cenozoic, the last *ca.* 65 Ma, has been characterized by a shift from a warm ice-free state to a predominantly cold state (Zachos et al., 2001). This interval provides several examples of natural climate states that were globally warmer than today associated with atmospheric CO_2 levels above that of pre-industrial times (Masson-Delmotte et al., 2013), including the Early Eocene Climatic Optimum (EECO, ca 52-50 Ma, Zachos et al., 2008), the middle Miocene Climatic Optimum (MCO, ca 17-15.2 Ma, Foster et al., 2012) and the Mid-Pliocene Warm Period (MPWP, ca 3.3-3.0 Ma, Dowsett et al., 2012). Although none of these intervals are analogues for future climates, because tectonics and changes in the biological contribution to the carbon cycle over this interval also impacted the relationship between climate and atmospheric CO_2 concentration, they nevertheless provide an opportunity to examine how the climate system has responded to enhanced greenhouse gas concentrations comparable to the range that might be experienced during the 21st century. As such, and despite the large uncertainties associated with CO_2 reconstructions prior to the well-constrained records from polar ice cores (Beerling and Royer, 2011; Masson-Delmotte et al., 2013), these three intervals have been foci for palaoclimate analysis (Pearson et al., 2001; Dowsett et al., 2010; Herold et al., 2010; Huber and Caballero, 2011; Dowsett et al., 2012; Lunt et al., 2012) and climate modeling (Herold et al., 2011; Lunt et al., 2012; Goldner et al., 2013; Haywood et al., 2013).

Reconstructions of the Eocene, Miocene and Pliocene climate of China have been made based on fossil leaf assemblages from a number of sites and using several different reconstruction techniques (Sun et al., 2002; Hu, 2007; Yang et al., 2007; Xia et al., 2009; Wang et al., 2010; Quan et al., 2011; Yao et al., 2012). However, the uncertainties associated with the reconstructions for any one site are relatively large, both for individual reconstruction techniques and especially when different techniques are compared. For example, reconstructions of mean temperature of the warmest month (MTWA) during the EECO at Fushun range from 19 to 27°C (Wang et al., 2010; Quan et al., 2011). A similarly large range (2 to 13°C) was obtained for the mean temperature of the coldest month (MTCO), while the range for mean annual precipitation (MAP) was from 730 to 1650 mm.

Pre-Quaternary climate reconstructions from China, including Fushun, have been based on two broad types of techniques: the coexistence approach (CA: Mosbrugger and Utescher, 1997) or the closely-related overlapping distribution analysis (ODA: Yang et al., 2007), and leaf trait-based techniques such as leaf margin analysis (LMA: Wolfe and Hopkins, 1967; Wolfe, 1971) and the Climate-Leaf Analysis Multivariate Program (CLAMP: Wolfe, 1993; Yang et al., 2011; Spicer, 2012). The CoA method reconstructs palaeoclimate from the overlap of the climatic tolerances of the nearest living relatives (NLRs) of the fossil taxa, assuming that the climatic requirements of fossil taxa are the same as the corresponding NLRs. The ODA method is similar to CoA, but identifies the overlap in the distribution of NLRs first and then derives an estimate of the palaeoclimate from the common distribution area. Uncertainties arise with both methods because of difficulties in identifying NLRs, which may not be possible to better than genus or even family level, and in assuming that the NLR occupies the same climate range as an extinct fossil species. Additional uncertainties arise because the climate data used to derive climate tolerances for the modern

NLR is often too coarse for adequate characterization of the tolerance range (Zhang et al., 2015).

LMA and CLAMP are statistical reconstruction techniques based on empirical correlations between leaf characteristics and mean annual temperature (MAT). LMA uses information on the degree of dissection of the leaf margin to derive MAT. CLAMP uses a larger number of measurements to characterize leaf size, shape and margin dissection, on the assumption that the use of more traits would lead to more accurate prediction although in reality this does not seem to be the case. Wilf (1997), for example, used both methods to estimate temperature at nine western hemisphere forest sites and showed that the maximum error in MAT estimated using LMA was only 2.5°C while the maximum error estimated using CLAMP was over 3°C. Similarly, in a global analysis of the performance of the two methods at 144 sites, the slopes of the predicted versus observed MAT for LMA and CLAMP (0.93 versus 0.95 respectively) were statistically indistinguishable (Royer, 2012). Both approaches have similar sources of uncertainty, related to the underpinning assumptions about the trait-climate relationship. Several studies have shown that the empirical relationship between leaf dissection and MAT varies between different regions (Wing and Greenwood, 1993; Wilf, 1997; Gregory-Wodzicki, 2000; Greenwood et al., 2004; Greenwood, 2005; Miller et al., 2006; Su et al., 2010; Peppe et al., 2011). This is a situation that can arise when either (a) the reconstructed climate variable is not causally related to the trait in question but is correlated with the controlling variable in a given region, or (b) when variation in the trait is a response to more than one climate variable (Harrison et al., 2010; Wang et al., 2013). Finally, although CLAMP uses many different morphological measurements, many of the morphological traits are highly correlated with one another (or indeed aspects of the same basic trait) and this could also affect the reliability of the climate reconstructions (Yang et al., 2015). There are a variety of techniques that could be used to

disentangle correlations between traits, between climate variables, and to interpret multi-dimensional trait-climate relationships, including factor analysis (Jackson, 1991; Jobson, 1992), correspondence analysis (Leps and Smilauer, 2003) and generalized linear modelling (Larsen and McCleary, 1972; this thesis Chapter 3). However, these approaches would still require the selection of appropriate bioclimatic factors (Trninic et al., 2012, 2013) in order to make meaningful reconstructions.

Nevertheless, there are strong and explicable patterns of variation in many plant traits along climate gradients (Barboni et al., 2004; Wright et al., 2004; Wright et al., 2005b; Poorter and Bongers, 2006; Meng et al., 2009; Prentice et al., 2011; Atkin et al., 2015; Maire et al., 2015; Meng et al., 2015). Thus, it should be possible to exploit plant traits for climate reconstruction, providing care is taken to identify a suite of traits that are display mutually independent relationships with climate variables. A number of recent studies have shown that generalized linear modeling (Nelder and Wedderburn, 1972) techniques provide a powerful means of establishing the nature of independent controls on biological properties (e.g. Wang et al., 2013; Bistinas et al., 2014; Li et al., 2015a). In Chapter 3, I used this approach to establish to explore the relationships between a large number of leaf morphometric traits and the three most important gradients of climate variability in China, using a very large data set of modern observations, and were able to demonstrate that there were a substantial number of traits that displayed significant and independent relationships with one or more of these climate variables.

Here, we exploit Chapter 3's analyses to develop predictive models of climate based on multiple leaf morphometric traits. After testing these models under modern climate conditions, we apply them to reconstruct the climate at four classic fossil sites in China.

Finally, we compare these reconstructions with earlier reconstructions based on CoA, ODA, LMA and CLAMP.

2. Materials and Methods

2.1 Constructing trait-climate models

In Chapter 3, I analysed leaf trait abundances from 66 sites that sample the major gradients in summer temperature (GDD_0, defined by the accumulated temperature sum during the growing season defined as the period when interpolated daily temperatures above 0°C), temperature seasonality ($mGDD_5$, the daily mean during the growing season when temperatures are >5°C) and plant-available moisture (α, defined as the ratio of actual and equilibrium evapotranspiration). I found that 44 leaf morphometric traits showed independent significant relationships with one or more of these climate variables (Figure 4-1). However, the number of individual traits that could be considered as diagnostic, and therefore be used for reconstruction purposes, varies between the three climate variables. There are 28 traits that show a significant and independent relationship with GDD_0, 27 with α, and only 23 with $mGDD_5$.

Combining information derived from several traits will refine the estimate of the climate. However, it is not inherently obvious how many or which combination of traits will yield the best estimates for each variable. We therefore built additive linear models for each climate variable separately, with all trait combinations possible for a given number of traits varying from a single trait to the maximum number of significant traits for each variable. This results in the creation of a large number of models depending on the number of significant traits used. We tested how well each of the resulting models reproduced the observed climate at each of the 66 modern sites, using the root mean square error (RMSE) as a measure of the fit and the Akaike information criterion (AIC) to assess the optimal

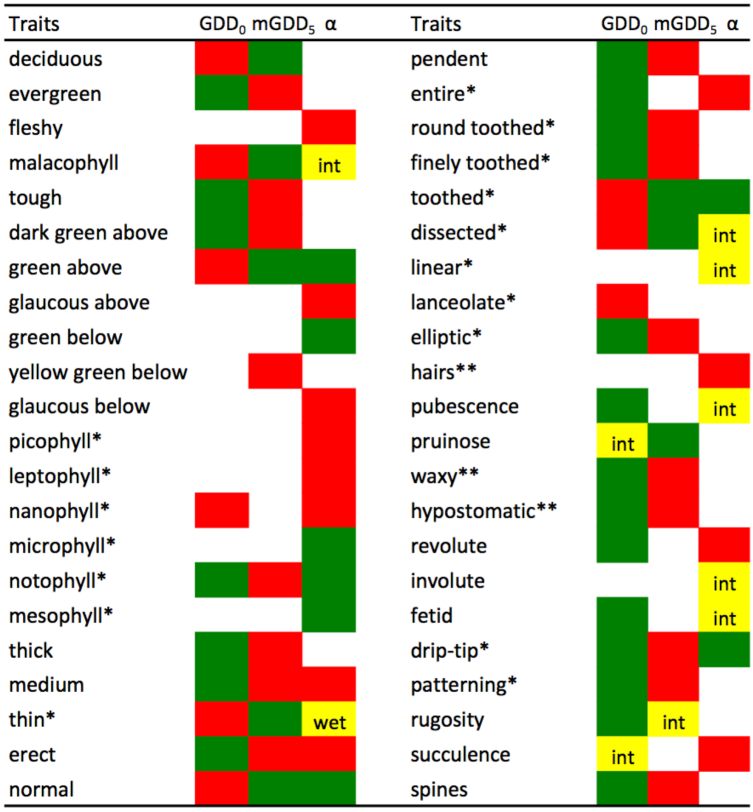

Figure 4-1 Modern trait-climate relationships (derived from Chapter 3). The climate variables are: growing degree days above a baseline of 0°C (GDD_0), mean temperature of the period above 5°C ($mGDD_5$) and the Cramer–Prentice index (α) of plant-available moisture. Only traits that show a significant relationship with one or more climate variables under modern conditions are shown. Traits used to build the fossil relationships are marked with a star; traits that are only used at Zhejiang are marked with two stars. The cells are colour coded to show the nature of the relationship: red indicates a significant negative relationship, green a significant positive relationship, yellow a unimodal relationship where the position of the peak is indicated, where int means at intermediate levels of the climate variable and wet means towards the upper end of the range in α.

number of traits to avoid over-fitting (Burnham and Anderson, 2002). The final climate reconstruction is given by the mean of the ten best models (as identified by the RMSE values) using the optimal number of traits (as identified by AIC); reconstruction uncertainty is estimated as the standard deviation of these 10 models. The choice of the exact number of models to use necessarily arbitrary, but 10 was chosen because this resulted in RMSE values for the final reconstructions of <10% of the observed range for each variable while at the same time providing a statistically robust basis for the estimates of reconstruction uncertainty.

2.2 Paleobotanical sites and fossil leaf traits

Fossil leaf assemblages were obtained from the published literature for four sites in China: Fushun, Shanwang, Xiaolongtan, and Shengzhou (Figure 4-2).

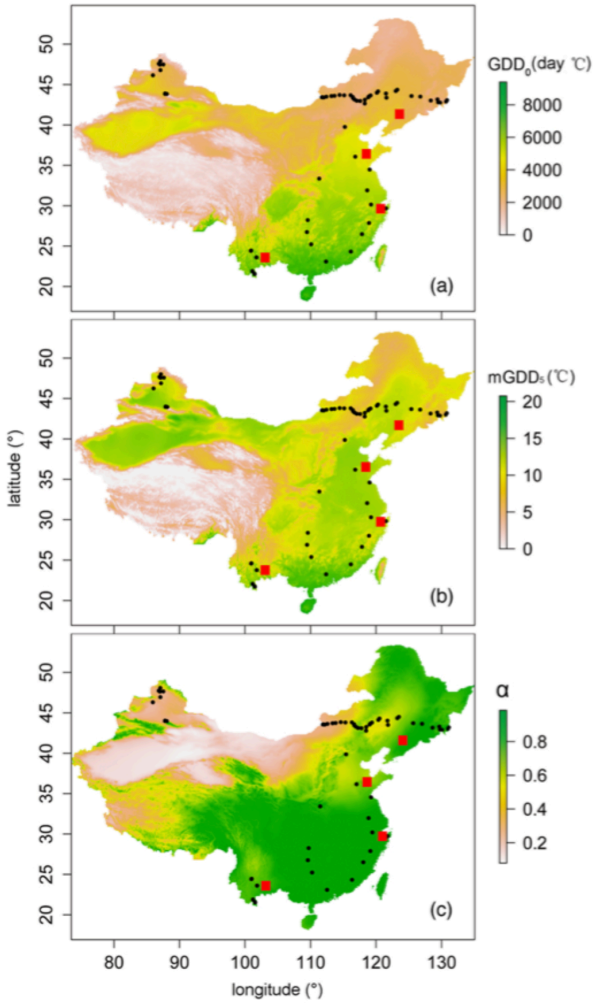

Figure 4-2 Location of the modern sites (shown as closed black circles) used for development of the statistical relationships between traits and climate variables, and subsequently for testing the trait-based models. The four leaf fossil sites are shown as closed red squares. The sites are superimposed on maps showing the geographic gradients in growing degree-days above a baseline of 0°C (GDD_0), mean temperature of the period above 5°C ($mGDD_5$) and the Cramer–Prentice index (α) of plant-available moisture.

The Fushun Basin (41.83°N, 123.90°E, Figure 4-2) is a strike-slip basin on the DunMI fault zone in northeastern China filled with Eocene sediments (Johnson, 1990). The fossil leaf assemblage was obtained from the lower part of the Jijuntun formation (WGCPC, 1978). The Jijuntun Formation consists of oil and black shales, and has been assigned an age of 51-

45 Ma, spanning the interval of the EECO, based on the vegetation and insect assemblages (Hong et al., 1974; Hong et al., 1980; Hong, 1983; Hong et al., 2000).

The Shanwang basin (36.55°N, 118.73°E, Figure 4-2) is in Shandong Province, eastern China. The Shanwang Formation consists of diatomaceous lacustrine sediments and interbedded basalts (Yang et al., 2007). The fossil leaf assemblage was obtained from the lacustrine sediments. Mammalian faunas co-occurring with the leaves have been assigned to MN5 (Qiu, 1989; Steininger et al., 1996) dated to *ca.* 17-15.2 Ma, and thus equivalent to the MCO. K-Ar dating for the underlying basalt (Yang and Yang, 1994) also suggests the age of Shanwang Formation ranges from 18–16 Ma, while the upper basalt suggests the age of 10–9 Ma (Chen and Pen, 1985; Zhu et al., 1985; Wang and Jin, 1986).

The Xiaolongtan Basin (23.50°N, 103.20°E, Figure 4-2) is in Yunnan Province, southern China. The fossil leaf assemblage was obtained from the upper layers of Tertiary lignite deposits in the basin. Co-occurring mammalian fossils are assigned to the late Miocene, equivalent to the Tortonian (11.6-7.2Ma) in Europe (Dong, 2001) This is an interval in the Late Miocene when CO_2 levels were at levels similar to the pre-industrial period (i.e. *ca.* 280 ppm). The pollen assemblage from the site is consistent with a late Miocene age (Wang, 1996).

The Pliocene formation in Shengzhou, Zhejiang (29.60 °N, 120.73°E, Figure 4-2) is characterized by alternating basalts and diatomaceous mudstone, shale and argillaceous siltstone (Hu, 2007). The fossil leaf assemblage was obtained from the diatomaceous mudstone. These sediments have been dated to 3.5-3.0 Ma using ^{40}Ar–^{39}Ar (RegionalGeologyofZhejiangProvince, 1982; Ho et al., 2003), and thus date to the MPWP.

Information on the leaf size, thickness, texture, shape, and margin for each taxon in the fossil assemblage was obtained from the published reports on each of the sites (WGCPC, 1978; Tao et al., 2000; Hu, 2007). Additional information on the occurrence of a drip-tip or surface patterning was obtained by examination of photographs of each taxon in these publications. Table 4-1 provides a summary of the number of samples, the number of species identified, and the trait abundances at each site. More detailed information on plant taxa and leaf traits information is given in Table S1.

Table 4-1 Summary of the samples and species number and the abundance of traits at each fossil site.

Items	Shengzhou	Xiaolongtan	Shanwang	Fushun
Samples No.	69	50	327	136
Species identified	34	22	116	62
Traits				
picophyll	2.6	0.0	0.0	0.0
leptophyll	1.7	0.0	0.0	0.0
nanophyll	9.5	5.9	3.2	4.5
microphyll	43.1	64.7	19.4	31.8
notophyll	29.3	14.7	37.1	40.9
mesophyll	13.8	11.8	40.3	22.7
macrophyll	0.0	2.9	0.0	0.0
thin	56.0	60.0	28.6	100.0
entire	43.0	42.4	21.3	19.0
round toothed	3.5	12.1	3.3	4.8
finely toothed	7.0	3.0	6.6	0.0
tooth	42.6	39.4	67.2	57.1
dissected	1.8	3.0	1.6	9.5
linear	8.7	3.0	1.6	4.8
lanceolate	13.9	15.2	17.7	14.3
elliptic	18.3	24.2	24.2	14.3
hairs	67.6	NA	NA	NA
waxy	18.2	NA	NA	NA
hypostomatic	84.4	NA	NA	NA
drip-tip	63.6	58.6	85.0	38.1
patterning	90.4	100.0	96.8	100.0

2.3 Application to the fossil leaf assemblages

Some of the traits identified as showing a significant correlation with climate, such as leaf phenology and colour, cannot be identified from fossil specimens. The definitions of leaf

toughness and leaf thickness used in the description of the fossil leaf assemblages differed from those employed by Chapter 3 and thus information about these traits could not be used in our analyses. Some of the traits identified as showing a significant correlation with climate, specifically the presence of hairs, waxy cuticle and hypostomatism, were identified in the Shengzhou fossil flora, but were not recorded in the other three sites. Thus, only 20 of the traits used for the modern analysis could be used for the climate reconstruction at Shengzhou and only 17 traits for the other three sites.

We used the same procedure to build models based on the more limited number of traits available at the fossil sites. We first tested whether the use of a more limited number of traits compromised the reconstructions by applying these models to the modern data set. We then used the ten best models (based on the RMSE values) for the optimal number of traits (based on the AIC values) to reconstruct the climate at each fossil site, using the standard deviation of the inter-model difference in the reconstructions as a measure of the reconstruction uncertainty.

3. Results

3.1 Evaluation of trait-based models

We tested many thousands of individual models for each of the climate variables. The total number of models between the three climate variables varies and fewer potential models were fitted for $mGDD_5$ (Figure 4-3). As the number of traits increase, the RMSE of the fitted models decreases (Figure 4-4). The ten-best models converge very quickly at intermediate number of traits, whereas there is no convergence of the worst models even for those based on the maximum number of traits. The AIC values indicate that the optimal number of traits is 15, 11 and 12 for GDD_0, $mGDD_5$ and α respectively. We then use the

ten-best models with these numbers of traits for the reconstructions of each variable (i.e. 15 for GDD_0, 11 for $mGDD_5$ and 12 for α) to avoid over-fitting.

The RMSE of the optimal GDD_0 reconstruction is 491 day °C with a reconstruction uncertainty between the ten-best models of 58 day °C (Table 2). The potential reconstruction error as measured by the RMSE is relatively small, equivalent to only 7.5%

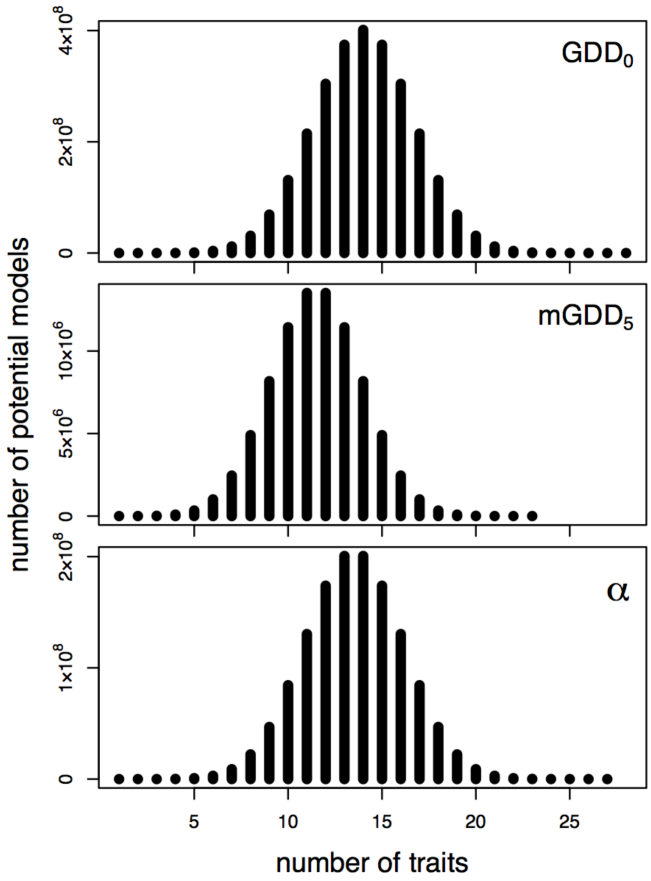

Figure 4-3 The number of potential models with different numbers of traits for growing degree days above a baseline of 0°C (GDD_0), mean temperature of the period above 5°C ($mGDD_5$) and the Cramer–Prentice index (α) of plant-available moisture.

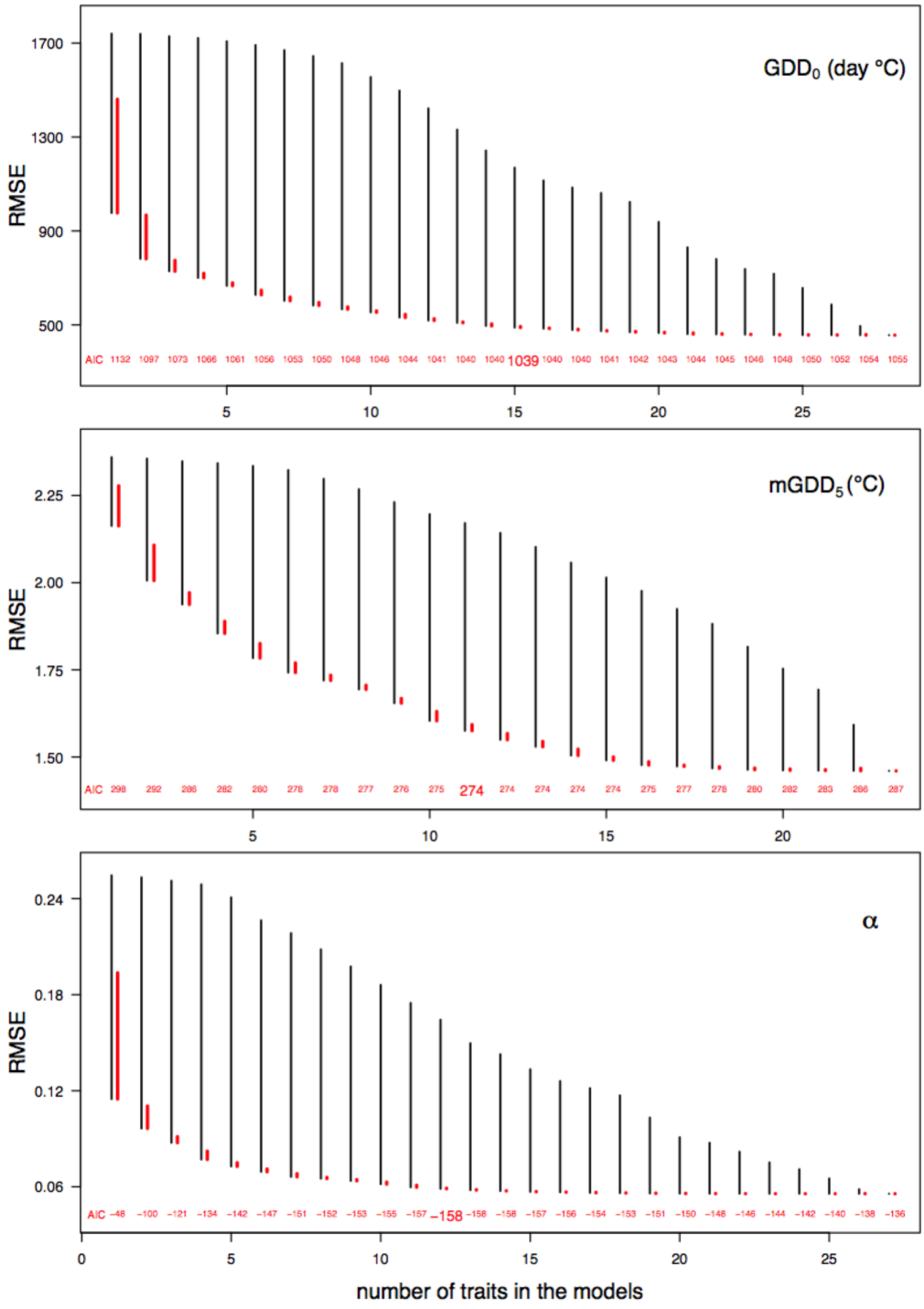

Figure 4-4 RMSE of the modern reconstructions, for all models (black bars) and for the 10 best models (red bars), for different numbers of traits. The climate variables are: growing degree days above a baseline of 0°C (GDD_0), mean temperature of the period above 5°C ($mGDD_5$) and the Cramer–Prentice index (α) of plant-available moisture. Values for the Akaike information criterion (AIC) for the 10 best models are given in red on each plot. The AIC value defining the optimum number of traits is given in a larger font.

of the sampled climate range. The RMSE of the optimal $mGDD_5$ reconstruction is 1.58°C, with a reconstruction uncertainty of 0.3°C, equivalent to *ca.* 13.3% of the sampled climate range. The RMSE for α is 0.06±0.01, again representing about 7.2% of the sampled climate range. There is no systematic difference in the magnitude of the reconstruction errors along the climate gradient in GDD_0 and α (Figure 4-5). However, there is a systematic bias in the $mGDD_5$ reconstructions, with a systematic underestimation when $mGDD_5$ is low (i.e. when temperature seasonality is low) and overestimation when $mGDD_5$ is high (i.e. in highly seasonal climates).

Table 4-2 Summary of model tests: number of traits and uncertainties for final models based on all modern traits and fossil traits only.

	Models based on modern traits			Models based on fossil traits		
Climatic variable	Traits No.	Uncertainty	Proportion of full climatic range in China	Traits No.	Uncertainty	Proportion of full climatic range in China
GDD_0 (day °C)	15	58	0.6 %	7(8)	147 (62)	1.6% (0.7 %)
$mGDD_5$ (°C)	11	0.3	1.4 %	5(5)	0.4 (0.3)	1.9% (1.4 %)
α	12	0.01	1.1 %	7(7)	0.01 (0.01)	1.1% (1.1 %)

Although there are 20 traits altogether that can be recognized in the fossil samples (Figure 4-1), the number of traits that show a significant and independent relationship for individual climate variables varies for the different fossil sites. There are 11, 9 and 12 traits available to build models for GDD_0, $mGDD_5$ and α respectively for Fushun, Shanwang and Xiaolongtan, while there are 13, 11 and 13 traits for these three climate variables for Shengzhou. The AIC indicates that the optimal number of traits is 8, 5 and 7 traits for GDD_0, $mGDD_5$ and α respectively at the first three sites, and 7, 5 and 7 traits for Shengzhou (Table 4-2).

Using the reduced number of traits that are identifiable from the fossil samples degrades the reconstructions of the modern climate (Table 4-2) compared to using all available traits.

Thus, the RMSE for GDD_0 is 839 day °C, with a reconstruction uncertainty of 147 day °C, using the traits available for the Shengzhou assemblage, and 846 day °C and the reconstruction uncertainty is 62 day °C for the more limited set of traits available for the other three sites (*ca.* 12.8% of the sampled climate range). The RMSE for $mGDD_5$ is 1.89°C,

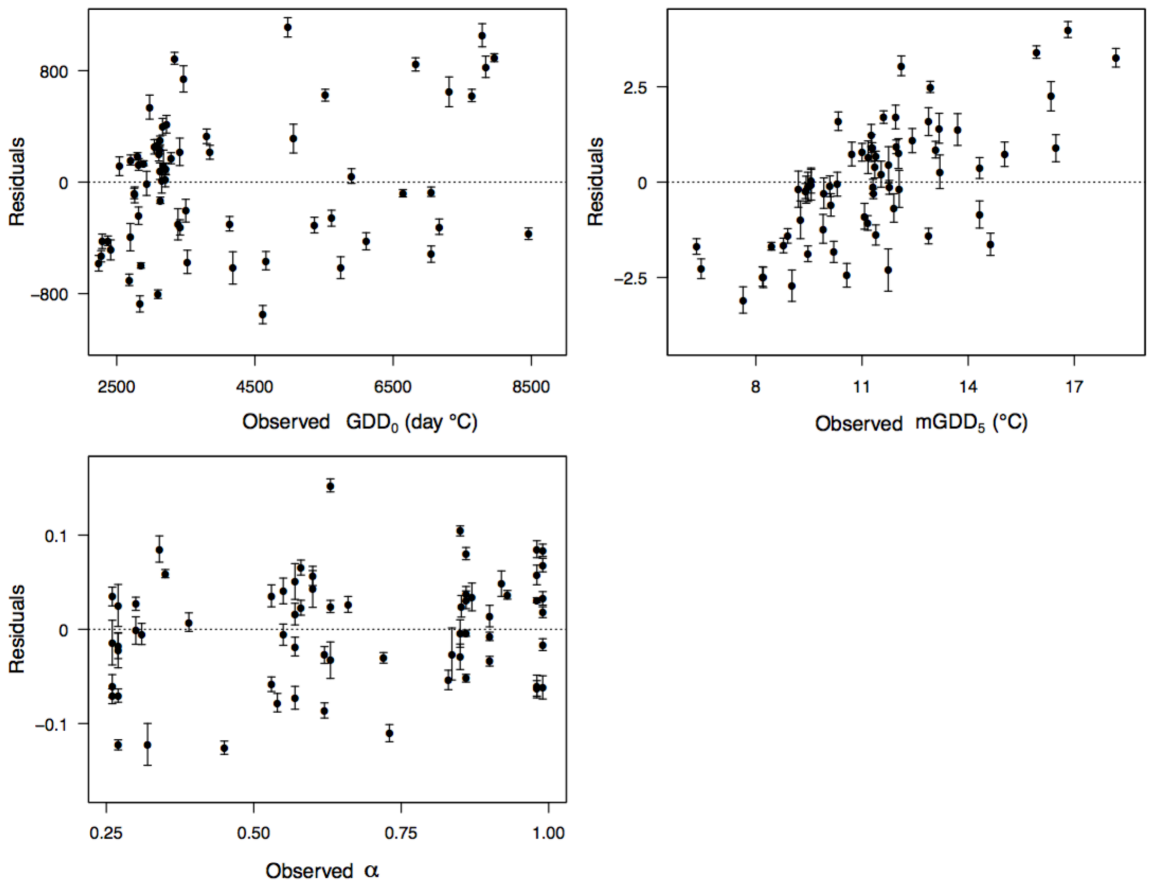

Figure 4-5 Assessment of model performance by comparing the model residuals versus observations. The climate variables are: growing degree days above a baseline of 0°C (GDD_0), mean temperature of the period above 5°C ($mGDD_5$) and the Cramer–Prentice index (α) of plant-available moisture.

with a reconstruction uncertainty of 0.4°C (*ca.* 16% of the sample climate range). The RMSE for α is 0.08 or 0.07 for the reduced sets of traits, with a reconstruction uncertainty of both 0.01 (*ca.* 9.6 or 8.4% of the sampled climate range).

Nevertheless, even using the reduced set of traits, the correlations between reconstructed and observed climate at the modern sites remains reasonable for GDD_0 and α: 0.88

compared to 0.96 with the full set of traits for GDD_0, and 0.96 compared to 0.97 for α (Figure 4-6). The degradation is more substantial for $mGDD_5$, where the correlation goes

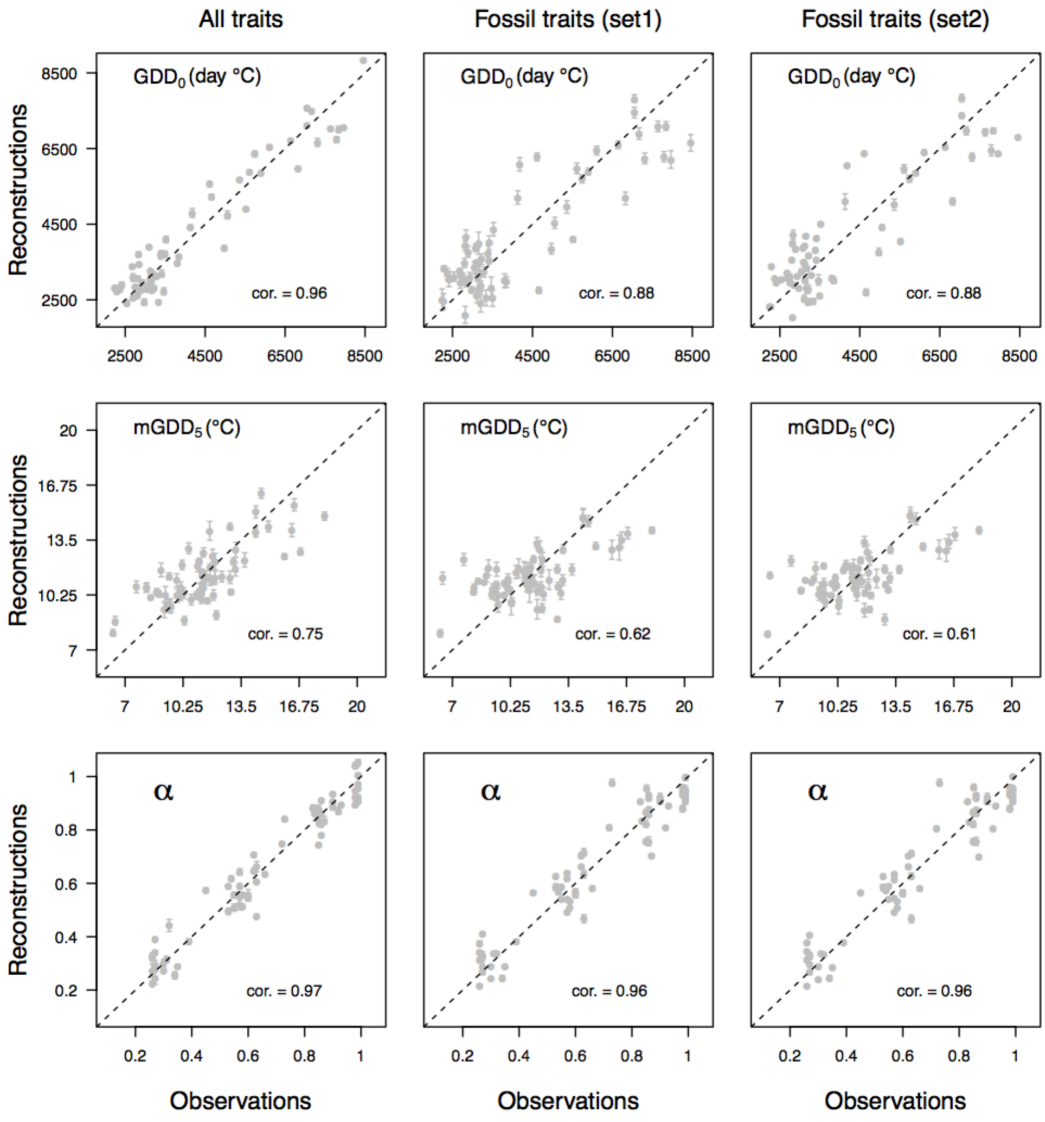

Figure 4-6 The correlations between reconstructed and observed climate at the modern sites based on all traits, fossil traits (set 1, traits with single asteroid in Figure 4-1) and fossil traits (set 2, traits with single asteroid and double asteroids in Figure 4-1).

down from 0.75 to 0.61 with the most reduced number of traits. The relatively poor correlation against modern observations for $mGDD_5$, and the presence of a significant systematic bias in the reconstructions, suggests that reconstructions of this variable will be much less reliable than those of GDD_0 and α, and we therefore make no attempt to reconstruct seasonality at the fossil sites.

3.2 Paleoclimate reconstructions

The EECO flora at Fushun yields a reconstructed value for GDD_0 of 2935±393 day °C, which is slightly lower than the modern value of 3667 day °C (Figure 4-7). While the difference is larger than the reconstruction uncertainty, it does not exceed the RMSE for the modern reconstructions and thus this change is unlikely to be significant. The reconstructed value for α is 0.94±0.01, slightly higher than the modern value of 0.91. However, although the change is larger than the palaeo-reconstruction uncertainty, it does not exceed the RMSE for the modern reconstruction.

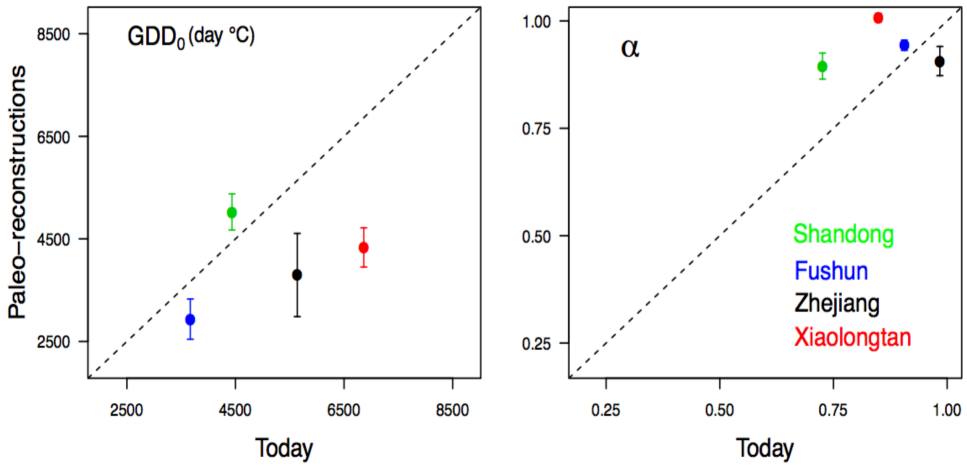

Figure 4-7 Reconstructed palaeoclimates at the fossil sites versus climate of today. Dashed line is 1:1 line. The palaeoclimates values (the coloured points) are indicated by mean of the reconstructions obtained by ten best models. The error bars are indicated the standard deviation. The colours of names of fossil sites correspond to the colours of the reconstructed palaeoclimates.

The MCO flora at Shanwang yields a reconstructed value for GDD_0 of 5024±353 day °C, slightly higher than the modern value of 4436 day °C (Figure 4-7). However, although the change in GDD_0 is larger than the palaeo-reconstruction uncertainty, it does not exceed the modern RMSE and thus is unlikely to be significant. In contrast, the reconstructed value of α is 0.89±0.03, compared to a modern value of 0.73. The change in α exceeds both the

reconstruction uncertainty and the modern reconstruction error, and thus the reconstruction of wetter conditions at Shanwang is likely to be robust.

The Late Miocene flora from Xiaolongtan yields a reconstructed value for GDD_0 of 4334±382 day °C, much lower than the modern value of 6863 day °C (Figure 4-7). The change in GDD_0 is larger than either the palaeo-reconstruction uncertainty or the RMSE for the modern reconstructions, and thus this reduction in growing season temperature is likely to be robust. In contrast, the reconstruction of wetter conditions, as indicated by a reconstructed α value of 1.01 compared to the modern value of 0.85, does exceed the modern reconstruction error.

The MPWP flora from Shengzhou yields a reconstructed value for GDD_0 of 3795±811 day °C, which is lower than modern value of 5639 day °C (Figure 4-7). The difference is larger than the palaeo-reconstruction uncertainty and exceeds the RMSE for the modern reconstructions. Thus this reconstructed reduction in growing season temperature is likely to be robust. However, the reconstructed change in α, from a modern value of 0.98 to a palaeo-value of 0.91±0.03, does not exceed the modern reconstruction error.

4. Discussions

During the Eocene, Miocene and Pliocene era, the carbon dioxide level is higher than today where gives the opportunity of investigating the responding mechanism, under which enhanced greenhouse gas concentrations has played an important role in the climate system. Our results show that the Eocene climate of Fushun is slightly colder and wetter than that of today in terms of GDD_0 and α. The continental cooling period after the Early Eocene Climatic Maximum has been revealed both by the evidence of isotope of oxygen and fossil plants from the Bighorn Basin, Wyoming (Wing et al., 2000). The extent of temperature dropping varied from 3.5 to 4°C (Wing et al., 2000), from 3 to 5°C (Jolley and Widdowson,

2005), or even more approximately 7.5°C (Wing et al., 2000) depending on the different paleorecords employed. This long-term cooling during the Early Eocene was mostly likely to be the result of frequently massive volcanic eruptions occurred along the North Atlantic rift around the Paleocene to Eocene boundary (Zachos et al., 2001; Jolley and Widdowson, 2005). The relatively cooler climate of Eocene Fushun seems attributed to the same reason because the cooling effect on Earth might have been on a global scale, as evidences of mean annual temperature declining found not only on the continent (Jolley and Widdowson, 2005), but also sea surface temperature dropping in the ocean (Zachos et al., 2001). Previous studies reconstructed the higher MTCO and MAT than those of today with over 14.5-25.1°C and 4.1-13.4°C, while for MTWA it seems very similar or at most 4.6°C (Figure 4-8) lower depending on whether the fossil pollen or leaves employed in the analysis (Wang et al., 2010; Quan et al., 2011). The uncertainties related to these temperature reconstructions are about 10%, 9.5% and 7.2% of the full range of MTCO, MAT and MTWA in China. These uncertainty percentages are bigger than that of GDD_0 with 4%. If MTWA was indeed cooler than that of today, then that means the growing seasons for plants were very likely with relatively lower temperature (i.e. relatively lower GDD_0, around 700 °C day lower than today). MAP in Eocene Fushun was very likely higher than that of today by around 910mm at most (Wang et al., 2010; Quan et al., 2011). Such higher precipitation with warmer winters eventually led to the higher actual evapotranspiration in whole-year round, which is in agreement with the slightly higher α in this study. The uncertainty related to MAP in previous studies is about 20%, which is much bigger than the uncertainty (1%) related to α in this study. However, these seemingly abnormal temperatures (for GDD_0 and MTWA) could be arose by other factors, such as quite different paleogeography, much higher CO_2 level or higher sea level in Eocene. Nevertheless, the paleoclimate in Fushun was most likely wetter than today both in terms of α and MAP.

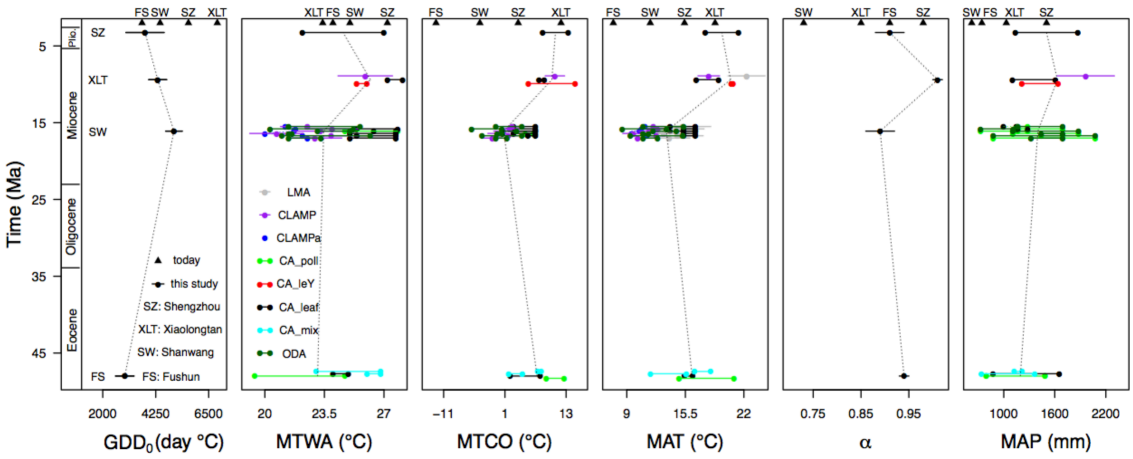

Figure 4-8 Comparisons of the reconstructed palaeoclimates at the fossil sites in this study to climate of today and previous reconstructions. The climate variables are: growing degree days above a baseline of 0°C (GDD_0), the mean temperatures of the warmest month (MTWA), the coldest month coldest month (MTCO), mean annual temperature (MAT), the Cramer–Prentice index of plant-available moisture (α), mean annual precipitation (MAP). LMA = leaf margin analysis, CLAMP = Climate-Leaf Analysis Multivariate Program, CA_Poll = reconstructions based on the coexistence approach by using the fossil pollen records, CA_leY = reconstructions based on the coexistence approach by using the fossil leaf records in Yao et al. (2011), CA_leaf = reconstructions based on the coexistence approach by using the fossil leaf records, CA_mix = reconstructions based on the coexistence approach by using the fossil leaf and pollen records, ODA = overlapping distribution analysis. Black triangles indicate the climates of today at Shengzhou (SZ), Xiaolongtan (XLT), Shanwang (SW) and Fushun (FS).

The Mid-Miocene climate of Shanwang was slightly warmer and much wetter than that of today in terms of GDD_0 and α. The Mid-Miocene Climatic Optimum (MMCO 17–14.50 Ma), as one of the remarkable warmer period, has been reported on the basis of the deep-sea stable isotope record (Zachos et al., 2008). During this geological time, temperatures on Earth were significantly warmer both in the ocean and in mid-to-high latitudes (Böhme et al., 2007; Shevenell et al., 2008; Zachos et al., 2008; Pound et al., 2012). In Europe, this optimum is reflected by increases of temperature records of Cenozoic Lower Rhine, Weisselster and Molasse Basins (Mosbrugger et al., 2005). Moreover, combined herpetological, palaeobotanical and bauxite formation data suggested Central Europe experienced a high MAT (at least 20-22°C) and MAP (Böhme, 2003). In fact, previous studies already showed that the Mid-Miocene Shanwang is characteristic of higher MAT and MAP (Figure 4-8), around 2-5°C higher and almost doubled precipitation than today by

using the methods of the coexistence approach (Yang et al., 2007), which supports our results of warmer and wetter climates. The uncertainties related to MAT and MAP by CoA are about 3.4% and 7% of the total range. However, CLAMP results (Yang et al., 2007) seem to underestimate the temperature variables, except MTCO, compared to CoA results and our GDD_0 reconstruction (Figure 4-8). This may be attributed to preferential selection of leaves produced by plants near to the lake bank with physiognomies adapted to the lakeside microclimate (Sun et al., 2002), or could be caused by reasons we described in introduction. Given the warmer growing seasons, the actual evapotranspiration eventually was large (i.e. reflected by higher α) as the precipitation is sufficient. ODA results show wetter climates with the warmer winters, but are indicating the cooler summer like the CLAMP (Yang et al., 2007). Collectively, the total uncertainties related to the previous reconstructions for MTWA, MTCO, MAT and MAP are around 8.5%, 11%, 10% and 29%, which are also much bigger than the uncertainties of the reconstructed GDD_0 and α with 3.7% and 3.3%. The warmer and wetter climate in Mio-Miocene Shanwang was seriously related to the already-existed East Asian Monsoon established during the latest Oligocene (Sun and Wang, 2005).

Our results also show that the Late Miocene climates in Xiaolongtan of Yunnan are colder and wetter than that of today in terms of GDD_0 and α. Since at least the Middle Miocene the southern and central Tibetan Plateau has been elevated with an established geomorphological feature (Coleman and Hodges, 1995; Blisniuk et al., 2001), during which is probably equivalent to the second stage of uplift for the Tibetan Plateau modeled by An et al. (2001), the warm and wet air current from Indian Ocean started to be diverted along the southern slope of the plateau (Kutzbach et al., 1993). Consequently, the warmer and wetter monsoon storms made the summertime warmer and the wintertime colder, and in the meantime, a larger amount of precipitation than usual had fallen in the southern part of the plateau where the Xiaolongtan basin is located today. This is reflected by the higher MTWA,

lower MTCO, lower MAT and higher MAP obtained by the previous studies (Xia et al., 2009; Yao et al., 2011), except for a little higher MAT by CoA in Yao et al. (2011) and really higher MAT by LMA in Xia et al. (2009) (Figure 4-8). The total uncertainties of these climatic variables in previous studies are about 3.7%, 8.2%, 7.8% and 29%, separately. During the monsoon time the cloudiness brought by the monsoonal storms would be increased (Kutzbach et al., 1993), which caused the relatively lower temperature for plant growth. This cloudiness effect could be the reason of GDD_0 lower than today in this study. For the moisture index, i.e. higher α, the heavy precipitation and warmer summer temperature very likely accelerated the actual evapotranspiration rate in the monsoon seasons. The uncertainties related to GDD_0 and α are around 4% and 1%. Then, around 8 Ma ago, a much larger area of plateau elevated and extended especially towards to the northern and eastern margins (An et al., 2001), and this led to alter the thermally forced circulation significantly. At present, accompanying with the continued uplift of plateau, the current Indian Monsoon could not penetrate the uplifted mountains (here specifically indicate the Wuliang and Ailaoshan mountains) or only partially penetrated, although Asian Monsoon (here the branch of Indian Monsoon) intensified around 8 Ma from the carbon isotopic evidence from Siwalik formation (Harrison et al., 1995). Thus the rain shadow side of the mountains is formed and the climates would be hotter and drier as today. This phenomenon is called hotter-drier valley in Yunnan created following the identical mechanism described above, also identified by Yao et al. (2012) in Yuanmou of Yunnan.

For Shengzhou fossil flora, the Pliocene climate is colder and slightly drier than today for GDD_0 and α with ca. 8% and 3.3% uncertainties. Around 3.6-2.6 Ma, both the Asian summer and winter monsoon intensified reflected by the magnetic susceptibility, Rb/Sr ratio, >19um grain size and Al flux records from the Loess Plateau of China (An et al., 2001). The lack of thermophiles and the high percentages of *Picea* and *Abies* in pollen assemblages from the formation in Taigu and Yushe Basins also suggest MAT probably 2-

6 °C lower than in the middle to late Pliocene than today (Li et al., 2004). These results may indicate that the strength of the intensification of winter monsoon is stronger than that of the intensification of the summer monsoon during Pliocene in Shengzhou. However, previous reconstruction got the lower MTWA (Figure 4-8) and higher MTCO having around 4.7% and 4.4% uncertainties (Hu, 2007), which do not show any signal of capturing the intensification of Asian Monsoon both for summer and winter. Higher MAT along with ca. 3.8% uncertainty might indicate the quite warmer winter (Hu, 2007), while plants growth still would slow down for wintertime. This means the growing days for plants would be reduced. The mean value of MAP along with nearly 16% uncertainties reconstructed by Hu (2007) is accidently the same as MAP of today. Given the reduced growing days (i.e. cool temperature), the actually evapotranspiration most likely was decelerated. Thus, the climate in Shengzhou would be slightly drier during Pliocene than today.

5. Conclusions

Independently significant relationships between multiple leaf traits and specific bioclimatic variables provide an opportunity to reconstruct palaeoclimates based on multiple trait-climate models. The models built in this study are quite promising and showing that the uncertainties of reconstructed results by models using only fossil traits degrade little (not over 1%) comparing to the reconstruction uncertainties yielded by the models using all modern traits. With the application of our modified models to four fossil floras in China, it approves the reconstructed results generally reflect the climate evolution of this region during those high CO_2 geological time intervals. More importantly, our results are showing that the uncertainties of reconstructions are much more constrained (mostly 1-4%) in contrast to the previous reconstructions.

Chapter 5 Conclusions

The increasing concern about the current climate change and the need to project the trajectory of future climate with less uncertainty motivates the use of palaeoclimate records to document natural climate variability and evaluate the performance of state-of-the-art climate models (Joussaume et al., 1999; Wohlfahrt et al., 2004; Robinson and Dowsett, 2010; Braconnot et al., 2012; Zhao and Harrison, 2012; Collins et al., 2013; Hartmann et al., 2013; Izumi et al., 2013; Kirtman et al., 2013; Li et al., 2013; Denton et al., 2014; Kunreuther et al., 2014; Perez-Sanz et al., 2014; Schmidt et al., 2014; Smith et al., 2014; Harrison et al., 2015). There are many methods to reconstruct palaeoclimates on the basis of the statistical correlations between climate variables and biological information under modern day conditions, such as the presence/absence of different species and their abundance (Iversen, 1944; Grichuk, 1969; Birks and Birks, 1980; Atkinson et al., 1987; Mosbrugger and Utescher, 1997) or the presence/absence of particular plant traits (e.g. Bailey and Sinnott, 1916; Wolfe, 1978, 1979, 1993, 1995). The reliability of each method needs to be tested and assessed in order to assess the robustness of reconstructions of past climates. A major goal of my thesis has been to examine and evaluate techniques that have been used to reconstruct pre-Quaternary climates.

The coexistence approach (CoA) is one of the most widely used methods of reconstructing the pre-Quaternary climate (Mosbrugger and Utescher, 1997; Ivanov et al., 2002; Liang et al., 2003; Uhl et al., 2003; Erdei and Bruch, 2004; Bruch et al., 2006; Kou et al., 2006; Utescher et al., 2007; Yang et al., 2007; Chirilă and Ţabără, 2008; Li et al., 2009; Qin et al., 2011; Quan et al., 2011; Yao et al., 2011; Sun and Li, 2012; Tang et al., 2014). Although this method has been applied to reconstruct past climates for many different regions or continents, it has never been used to reconstruct past climates of the Qinghai-Tibetan

Plateau in China. This region poses some specific challenges for reconstructing palaeoclimate, most noticeably the fact that it is characterized by open vegetation, mostly alpine meadow and tundra (Zhang et al., 2007), but pollen assemblages taken from sites across the Plateau contain abundant arboreal pollen which is brought in by long-distance transport from lower elevation sites outside the Plateau (Huang et al., 1993; Cour et al., 1999; Yu et al., 2001; Lu et al., 2006; Shen et al., 2006; Herzschuh, 2007; Lu et al., 2008; Shen et al., 2008; Zheng et al., 2008; Zhao and Herzschuh, 2009; Herzschuh et al., 2010; Lu et al., 2010; Lu et al., 2011). In my first publication (Chapter 2), I examine the impact of contamination by long-distance transport of pollen on reconstructions of climate using the coexistence approach. I show that including arboreal pollen (AP) when making reconstructions lead to an overestimate of the actual seasonal temperatures and precipitation, while removing the potential AP contaminants lead to more accurate climate reconstructions. The problem of AP contamination affecting climate reconstructions is likely to be of importance in all areas of open vegetation. It was recognized as a problem, for example, in a study by Tang et al. (2014) where they indicated that reconstruction of climate of Tuyoq, Xinjiang in the 5th century probably overestimated mean annual precipitation (MAP) by *ca.* 30mm and temperature by between 0.5-1.2°C. In this study, the coexistence intervals for both precipitations were largely determined by *Castanea* or *Betula,* although this is a region where the modern vegetation is largely temperate desert and steppe vegetation and was unlikely to have been substantially different during the historical epoch (Tang et al. 2014). AP pollen could be brought to Xinjiang from considerable distances because the wind patterns in this region are dominated by the westerly jet, which is routed to the north of the Qinghai-Tibetan Plateau (Zhao and Yu, 2012).

Another problem in applying the coexistence approach to sites on the Qinghai-Tibetan Plateau is lack of detailed information about the distribution of plant taxa and their climatic tolerance. This is a generic problem for China. In applying CoA for paleoclimate

reconstruction in China, most studies have used county-level climate data to derive the climate tolerances of the nearest living relatives (NLR) (e.g. Li et al., 2009; Yao et al., 2009; Hao et al., 2010; Li et al., 2010; Wang et al., 2010; Qin et al., 2011; Zhang et al., 2012; Tang et al., 2014; Zhang et al., 2016). In Chapter 2, I tested this problem and found that there are systematic biases in the climate reconstructions based on county-level climate data, especially warm biases for temperature variables. This strongly suggests that it is necessary to take account of the large variations in climate within counties in China when determining the climatic tolerances of NLR. This problem has been tackled by using weighted averaging of the NLR climate tolerances (Lu et al., 2011) or by using the climatic envelopes (10th and 90th percentiles to delimit the extreme value) recommended by Thompson et al. (2012). However, the best solution would be to use high-resolution climate and species distribution data as a basis for CoA reconstructions.

I was able to obtain plausible reconstructions of MAP and seasonal temperature (mean temperature of the warmest month and mean temperature of the coldest month) for 44 sites on the Qinghai-Tibetan Plateau (Chapter 2), after removing arboreal taxa and by using the most detailed information of the optimum and range of specific taxa. The uncertainty on the temperature reconstructions, as measured by root mean square error, was large (e.g. 6.6 °C for MAT). The root mean square error on the precipitation reconstructions was smaller (*ca.* 98 mm for MAP). This suggests that MAP is the most important control of vegetation distribution on the Qinghai-Tibetan Plateau, rather than temperature. This is in agreement with the finding that the zonal pattern of vegetation distribution is controlled by gradients in summer monsoon rainfall on the Qinghai-Tibetan Plateau (Chang, 1981; Lu et al., 2011).

My analyses (Chapter 2) suggest that three things need to be improved in order to use the CoA to derive reliable estimates of past climate in open-vegetation environments, particularly in China: (1) deriving high-resolution plant distribution information, (2) using

more detailed climate data from meteorological stations, and (3) trying to identify extra-local contaminants in the fossil pollen records in order to remove their influence. There are now several major publications that provide more detailed plant distribution information (e.g. Wu and Ding, 1999; Fang et al., 2011; Cao et al., 2015). A high-resolution gridded climate data set has been created with a baseline 1-km resolution using an elevationally-sensitive spline interpolation of mean monthly values of temperature, precipitation and percentage of possible sunshine hours from, 1814 meteorological stations across China (Wang et al., 2013). (This data set is used in Chapter 3 of my thesis). So, using these new data sources would make it possible to develop better quality datasets of climatic tolerances of modern taxa, which would improve the accuracy of paleoclimate reconstruction by CoA. Unfortunately, the problem of contaminants in palaeo-records is more difficult to solve since we cannot assume that the climate and vegetation patterns have not changed over longer periods. The only way of dealing with this would be to use other sources of information, such as the presence/absence of tree macrofossils at a site to determine whether the AP signal was a result of long-distance transport.

An alternative approach to reconstructing pre-Quaternary palaeoclimates is based on relationships between climate and leaf physiognomy. There are two widely used methods: Leaf margin analysis (LMA, Bailey and Sinnott, 1916; Wolfe, 1978, 1979) and The Climate Leaf Analysis Multivariate Program (CLAMP, Wolfe, 1993; Wolfe, 1995). LMA uses information on the degree of dissection of the leaf margin to derive mean annual temperature (MAT). CLAMP uses a larger number of measurements to characterize leaf size, shape and margin dissection to reconstruct temperature. Unfortunately, the relationship between leaf dissection and MAT has been shown to vary between regions (Wing and Greenwood, 1993; Wilf, 1997; Gregory-Wodzicki, 2000; Greenwood et al., 2004; Greenwood et al., 2005; Miller et al., 2006; Su et al., 2010; Peppe et al., 2011). This implies either that MAT is not the controlling variable although it is partially correlated to the

controlling variable or that multiple climate factors influence leaf dissection. It has been argued that CLAMP should provide better reconstructions than LMA because it uses more traits. However, many of these traits are highly correlated to one another (Yang et al., 2015) and are related to leaf dissection in some way and so the same issue applies to the CLAMP methodology. Furthermore, comparisons have not shown that CLAMP provides more accurate reconstructions than LMA, and the reconstruction uncertainties for both methods are large. These challenges with the existing techniques led me to develop a new trait-based way of reconstructing the paleoclimates using a wider range of leaf traits and a more sophisticated approach to determining the independent relationship between leaf traits and climate (Chapter 3).

In Chapter 3, I exploit the existence of a large database on modern plant traits from China. This database includes samples from 92 sites, which sample almost all the major vegetation types in China and a wide range of different climates. The sampled climate range for GDD_0 (GDD_0, accumulated temperature sum during the growing season defined as the period when interpolated daily temperatures above 0°C) is from 1890 to 8459 day °C, of $mGDD_5$ ($mGDD_5$, the daily mean during the growing season when temperatures are >5°C) is from 6.3 to 18.2°C, and of α (the ratio between actual and equilibrium evapotranspiration: AET/EET) is from 0.16 to 0.99. This database has been used to explore the relationships between quantitative leaf traits and climate (Prentice et al., 2011; Meng et al., 2015). It also includes the types of information used in the LMA and CLAMP approaches, but provides data on many more aspects of leaf morphometry including e.g. the presence/absence of waxiness, surface patterning and hairs.

In Chapter 3, I use generalised linear modelling (GLM) to analyse trait-climate relationships. This approach allows the underlying relationships with several predictor variables to be determined even in the presence of correlations among the predictors (Wang et al., 2012).

The GLM approach has been used to characterize the independent relationships between multiple climate and environmental controls of burnt area (Bistinas et al., 2014) and annual tree growth (Li et al., 2015a). In Chapter 3, by separating out the relationship between the individual leaf trait and bioclimates, I have established the correlations between individual leaf morphometric traits and GDD_0, $mGDD_5$ and α under modern conditions. These three bioclimatic variables were chosen for the analysis because have been shown to be good predictors of vegetation patterns across China (Wang et al., 2013).

The explorations of trait-climate relationships in Chapter 3 also shed light on the function of specific leaf traits. More importantly, the physiological mechanisms behind the leaf traits-climate relationships are readily understandable in terms of the maintenance of leaf water and/or temperature balance during photosynthesis and transpiration. This physiological understand builds a firm foundations for the application of leaf physiognomy method in paleoclimates reconstructions.

I have used the significant relationships between a wide range of leaf traits and GDD_0, $mGDD_5$ and α to develop a new approach to reconstructing palaeoclimate using additive linear modelling of multiple leaf traits (Chapter 4). The specific traits, and optimal number of traits, to include in such a model cannot be determined from first principles. I therefore built additive linear models for each climate variable separately, with all trait combinations possible for a given number of traits varying from a single trait to the maximum number of significant traits for each variable. These multivariate models have different predictive powers in terms of the precision and accuracy of the reconstructed climates. However, the root mean square values for those ten-best models converge quickly when the number of traits increases. This means that the predictions by these ten-best models can yield the good reconstructions with the least uncertainties.

Many diagnostic traits are lost during fossilization (e.g. leaf colour) or are difficult to recognize in fossil floras (e.g. presence of hairs, marginal involution). However, I have shown that reconstructions that are based only on traits that are visible in fossil specimens does not result in a major degradation of the climate estimates. The correlation between observed and reconstructed GDD0 using the reduced set of fossil traits is 0.88 compared to 0.96 for the full set of traits, while the correlation between observed and reconstructed alpha is 0.96 for the fossil traits compared to 0.97 for the full set of traits. The reconstruction uncertainty for alpha is the same in both reconstructions, whereas the reconstruction uncertainty for GDD0 only increases from ±58 to ±147 day °C. This finding suggests that the loss of information caused by fossilization is not a major issue in the application of the new trait-climate reconstruction technique.

I have applied the aforementioned multivariate trait-based models for GDD_0 and α, to reconstruct the paleoclimate of four classic sites from China (Fushun, Shanwang, Xiaolongtan, and Shengzhou), which have been dated to the Eocene, Miocene and Pliocene (Chapter 4). The reconstructed climates in paleo-Fushun, Shanwang, Xiaolongtan, and Shengzhou for GDD_0 and α are 2935±393 day °C and 0.94±0.01, 5024±353 day °C and 0.89±0.03, 4334±382 day °C and 1.01±0.01 and 3795±811 day °C and 0.91±0.03, respectively. The Eocene Fushun, Middle Miocene Shanwang and Late Miocene Xiaolongtan were wetter than today, while Pliocene Shengzhou were drier than today. The paleo-GDD_0 for these sites could be closely related to the moisture due to the high concentration of carbon dioxide. These changes between paleoclimates and modern climates are consistent with the evolution of climates in this region and compatible with enhanced monsoon conditions during these high CO_2 intervals. The reconstructed GDD_0 and α have more constrained uncertainty in contrast to the previous reconstructions based on other methods (Sun et al., 2002; Hu, 2007; Yang et al., 2007; Xia et al., 2009; Wang et al., 2010;

Quan et al., 2011; Yao et al., 2011), such as the coexistence approach, LMA and CLAMP, although the different climatic variables are reconstructed.

In summary, I have shown that there are limits to the reliability of using CoA to reconstruct the paleoclimate in the Qinghai-Tibetan Plateau, and have suggested ways to improve the precision of climate reconstructions using this method in open environments. I have also shown that there are significant relationships between a wide range of leaf morphometric traits and bioclimatic variables and that these can be used to build leaf traits-based models for climate reconstruction. These leaf traits-climate relationships are not only readily understandable in terms of the plant physiology, but also meaningful in the retrodiction of paleoclimate. The multivariate trait-based modelling approach developed in my thesis is novel but capitalizes on the growing knowledge of the physiological role of specific morphometric traits.

The application of these multivariate trait-based models to reconstruct paleoclimates for four classic paleobotanical sites from China is quite promising because the results are plausible and the reconstruction uncertainties are smaller than those using other methods. However, there is still considerable work to be done before this new approach can be more widely applied to paleoclimate reconstruction. Firstly, it would be useful to explore the statistical approach more rigorously. I used the 10 “best” models in part because this is widely considered an acceptable number in other multi-model reconstruction approaches (e.g. Krawchuk et al., 2009) and in part because this number of models resulted in a reconstruction uncertainty of <10% of the observed range of each climate variable. However, given the arbitrary nature of this choice, it would be useful to find a more objective way to determine the number of models used to make the final reconstruction. Perhaps more importantly, the impact of reducing the number of traits used in the reconstruction needs to be explored more systematically given that the number of

observable traits in fossil samples is always going to be less than those for modern samples. However, the description of traits in fossil floras is also often incomplete. An analysis of which traits are crucial in ensuring reliable palaeoclimate reconstructions could help to inform better descriptions of fossil floras in the future. Finally, I have based my analysis of a large data set of modern trait-climate relationships from China. Large compilations of morphometric traits are now available from many other regions of the world, thanks to efforts such as the TRY database (Kattge et al., 2011), making it possible both to test the relationships established in the Chinese analysis and ultimately to extend the application of these relationships to fossil floras from other regions.

The main conclusions of my thesis, and their significance for the field can be summarized as:

1. The application of CoA to reconstruct palaeoclimates is crucially dependent on the quality of the climate and plant distribution data used to determine the climatic tolerances of NLRs. The use of county-level information, which is widespread in China, results in a degradation of the reconstructions of MAT of e.g. up to 5°C at some sites on the Tibetan Plateau compared to reconstructions made using more highly resolved climate and species distribution data. The RMSE of the MAT reconstructions based on county-level data is 9.7°C, whereas the RMSE of the reconstructions using more highly resolved data is 7.7°C. This finding suggests the need for great caution in using CoA based reconstructions from China.

2. The application of CoA to reconstruct palaeoclimates using pollen in regions characterized by open vegetation is compromised by long-distant transport of tree pollen from forested areas. Climate reconstructions for sites in the Tibetan Plateau made after excluding tree pollen results in more realistic estimates of the range of MAT across sites (3.2 to 6.5 °C compared to an observed range of −8.5 to 7 °C) but the RMSE of the reconstructions is still very large (6.6 °C). This finding is problematic because it implies that

CoA could only be used to reconstruct palaeoclimates in such regions if there is information on the local occurrence of species (e.g. from macrofossils) which could be used to determine which taxa should be excluded from the pollen samples as representing extra-local contaminants.

3. A large number of leaf morphometric traits show systematic variation along major climatic gradients in summer temperature, plant-available moisture and temperature seasonality across China. Similarly strong relationships have been demonstrated between photosynthetic traits and climate, but this is the first systematic analysis of morphometric traits. These predictable relationships can be explained in terms of physiological adaptations to environmental conditions, including key aspects of the leaf water- and temperature-balance. This finding provides a strong basis for developing new palaeoclimate reconstruction techniques based on plant traits.

4. The trait-climate analysis demonstrates that very few morphometric traits are controlled by a single climate variable. A unique climatic control was found in only 29% of the 44 individual classes which showed a significant relationship to climate across all plant functional types; the remaining classes all showed independent relationships with more than one climate variable (growing season temperature, temperature seasonality and moisture). This finding helps to explain why attempts to reconstruct individual climate variables through univariate correlation approaches are noisy and subject to large uncertainties.

5. Multi-model estimates based on trait-climate relationships provide reasonably accurate reconstructions of modern climate across China. The RMSE of the optimal GDD_0 reconstruction is 491 day °C with a reconstruction uncertainty between the ten-best models of 58 day °C. The RMSE of the optimal $mGDD_5$ reconstruction is 1.58°C, with a reconstruction uncertainty of 0.3°C. The RMSE for α is 0.06±0.01. These findings suggest

that the multi-model approach should yield reconstructions that are at least as accurate as most modern analogue approaches to climate reconstructions, and more accurate than CoA.

6. Many diagnostic traits are lost during fossilization (e.g. leaf colour) or are difficult to recognize in fossil floras (e.g. presence of hairs, marginal involution). However, I have shown that reconstructions that are based only on traits that are visible in fossil specimens does not result in a major degradation of the climate estimates. The correlation between observed and reconstructed GDD_0 using the reduced set of fossil traits is 0.88 compared to 0.96 for the full set of traits, while the correlation between observed and reconstructed alpha is 0.96 for the fossil traits compared to 0.97 for the full set of traits. The reconstruction uncertainty for alpha is the same in both reconstructions, whereas the reconstruction uncertainty for GDD_0 only increases from ±58 to ±147 day °C. This finding suggests that the loss of information caused by fossilization is not a major issue in the application of the new trait-climate reconstruction technique.

7. The multi-model palaoeclimate reconstructions indicate wetter climates at Fushan during the Eocene, Shanwang during the Middle Miocene, and Xiaolongtan during the Late Miocene. Drier climates were recorded at Shengzhou during the Pliocene. Reconstructed values of GDD_0 were 2935±393 day °C, 5024±353 day °C, 4334±382 day °C and 3795±811 day °C respectively. These reconstructions are qualitatively similar to previous inferences about the regional climate at each time, based on CoA and CLAMP methods, but the uncertainties on the multi-model reconstructions are much less than previous reconstructions. Thus, they provide a firmer and more reliable basis for interpreting regional climate changes in China through geologic time.

Appendix A Climatic tolerances for pollen taxa

Pollen Taxon	Max. MAP (mm)		Min. MAP (mm)		Max. MAT (°C)		Min. MAT (°C)	
	unweighted	weighted	unweighted	weighted	unweighted	weighted	unweighted	weighted
Abies	1667.4	878	112.7	544	16.2	11.2	-0.1	4.6
Picea	1667.4	734	25.2	358	17	9.8	-5.6	2
Pinus	1667.4	865	239.8	421	21.9	12	-0.4	2.2
Tsuga	1667.4	919	279.4	439	15.1	11.2	-0.4	2.6
Acer	1922.8	923	279.4	423	19.8	10.6	-0.4	3.8
Alnus	1922.8	1022	617.9	486	15	12.6	3	2.4
Anacardiaceae	1922.8	1082	115	740	21.9	15	-1.2	6.4
Betula	1922.8	911	254.2	467	17	9.6	-3.8	2
Caprifoliaceae	1922.8	980	38.9	642	21.9	12	-4.9	6
Castanea	1922.8	844	729.7	478	15	12.4	3	2.2
Castanopsis	1922.8	1387	613.8	829	21.9	18.5	3	7.9
Corylus	1922.8	980	361.5	642	17	10	-0.4	1.6
Celastraceae	1922.8	na.	279.4	na.	21.9	na.	-2.4	na.
Fabaceae	1922.8	744	17.4	312	21.9	8.5	-4.9	-0.3
Ilex	1922.8	1010	308.3	624	19.8	13.6	-1.2	6.4
Oleaceae	1922.8	992	279.4	392	19.8	14.5	-0.4	3.1
Quercus	1922.8	825	324.7	487	21.9	10.2	-0.4	2.6
Tilia	1667.4	na.	588.2	na.	15.1	na.	4.1	na.
Zygophyllaceae	949.5	na.	17.4	na.	21.9	na.	-5.6	na.
Nitraria	368.2	409	17.4	133	19.8	8.6	-4.9	0.4
Salix	1922.8	787	17.4	405	21.9	9.1	-5.6	0.9
Tamarix	1922.8	544	17.4	250	18	7.1	0.9	-0.1
Ephedra	951.6	381	17.4	105	12.6	9.2	-5.6	0.6
Aconitum	1922.8	na.	254.2	na.	15.6	na.	-4.9	na.
Alisma	1463.8	697	176.1	195	16.3	9.1	1.5	0.9
Amaranthaceae	1922.8	556	17.4	348	21.9	7.8	-0.4	-1
Apiaceae	1922.8	728	17.4	288	21.9	8.4	-4.9	-1.6
Artemisia	1922.8	561	17.4	207	21.9	8.6	-5.6	0
Asteraceae	1922.8	635	17.4	253	21.9	8.3	-5.6	-0.7
Boraginaceae	1922.8	na.	17.4	na.	21.9	na.	-5.6	na.
Brassicaceae	1922.8	721	17.4	239	21.9	10.1	-5.6	0.5
Caryophyllaceae	1922.8	552	17.6	252	21.9	7.4	-4.9	-0.4
Ceratostigma	1922.8	na.	279.4	na.	15.6	na.	3	na.
Chenopodiaceae	1667.4	456	17.4	134	21.9	8.9	-5.6	-0.1
Convolvulaceae	1922.8	926	25.2	366	21.9	12.5	-5.6	1.5
Crassulaceae	1922.8	na.	17.4	na.	21.9	na.	-5.6	na.
Cyperaceae	1922.8	622	17.4	286	21.9	6.3	-5.6	-1.5
Dipsacaceae	1922.8	na.	324.7	na.	15.1	na.	-3.8	na.
Empetrum	1332.6	na.	180.8	na.	4	na.	-7.3	na.
Geraniaceae	1922.8	na.	30.2	na.	18	na.	-4.1	na.
Haloragdaceae	1922.8	na.	201.1	na.	17	na.	-4.1	na.
Humulus	619.9	923	474.6	425	14.5	11.7	5.4	2.7
Lentibulariaceae	1922.8	na.	176.1	na.	19.8	na.	-0.2	na.
Lilium	1774.3	na.	129	na.	18	na.	-2.4	na.
Linaceae	1667.4	na.	176.1	na.	15.1	na.	-3.8	na.
Orobanchaceae	1922.8	na.	18.1	na.	17	na.	-4.9	na.
Plumbaginaceae	1922.8	na.	25.2	na.	15.6	na.	-5.6	na.
Poaceae	1922.8	675	17.4	241	21.9	9.4	-5.6	-0.4
Polygonaceae	1922.8	na.	17.4	na.	21.9	na.	-5.6	na.
Pyrolaceae	1667.4	na.	254.2	na.	15.1	na.	0.6	na.
Ranunculaceae	1922.8	814	17.4	384	21.9	8.9	-5.6	0.1
Rosaceae	1922.8	772	17.4	338	21.9	8.6	-5.6	0.2
Saxifraga	1922.8	931	38.9	401	18	9.1	-4.1	2.3
Solanaceae	1922.8	914	17.4	408	21.9	11.8	-5.6	2
Thymelaeaceae	1922.8	649	17.4	371	21.9	14.2	-4.9	4.6
Viola	1922.8	992	254.2	476	18	11.5	-3.8	1.1

Appendix A (continued)

Pollen Taxon	Max. MTWA (°C)		Min. MTWA (°C)		Max. MTCO (°C)		Min. MTCO (°C)	
	unweighted	weighted	unweighted	weighted	unweighted	weighted	unweighted	weighted
Abies	25.6	19.3	9.8	12.5	9.1	2.5	-11.3	-5.1
Picea	24.2	18.6	5.4	11.8	9.5	0.4	-18.3	-11.2
Pinus	26.4	19.4	7.6	11.4	15.2	3.3	-13.5	-8.7
Tsuga	21.3	18.4	7.6	11.2	9.1	2.8	-10	-7.2
Acer	26.9	19.1	7.6	11.9	12.1	1.3	-10	-7.3
Alnus	21.3	19.6	10.5	11.6	9.1	3.9	-6	-7.7
Anacardiaceae	26.4	23.4	7.6	14.8	15.2	5.8	-11.3	-3.4
Betula	24.8	17.8	7.5	11.2	9.5	0.7	-18.3	-8.9
Caprifoliaceae	26.9	19.5	6.4	13.5	15.2	3.7	-18.3	-3.1
Castanea	21.3	19.7	11.8	11.7	9.1	4.5	-6	-9.3
Castanopsis	26.4	24.8	11.8	16.4	15.2	10.6	-6	-1.8
Corylus	24.8	18.2	7.6	11.4	9.5	1.3	-10.4	-10.1
Celastraceae	26.9	na.	7.6	na.	15.2	na.	-14.8	na.
Fabaceae	27.4	17.6	6.4	10	15.2	-1.5	-17	-12.7
Ilex	26.9	21.2	7.6	14.4	12.1	5.4	-11.3	-4
Oleaceae	26.9	21.9	7.6	13.1	12.1	6	-10	-9
Quercus	26.4	18.3	7.6	11.5	15.2	1.2	-10.4	-8.4
Tilia	21.3	na.	11.7	na.	8.7	na.	-6.9	na.
Zygophyllaceae	27.4	na.	5.4	na.	15.2	na.	-16.9	na.
Nitraria	27.4	21	5.4	11	-6.7	-6.3	-16.9	-13.1
Salix	27.4	18.1	5.4	10.5	15.2	-0.8	-18.3	-11
Tamarix	27.4	18.4	11.8	10.2	7.8	-6	-12.4	-13.2
Ephedra	27.4	21.3	5.4	11.3	5.9	-6	-18.3	-13.2
Aconitum	25.3	na.	6.4	na.	9.1	na.	-18.3	na.
Alisma	26	21.3	14.2	10.7	8.7	-4.1	-12.6	-11.1
Amaranthaceae	27.4	17.3	7.6	11.3	15.2	-2.6	-10	-16
Apiaceae	27.4	17.7	6.4	8.5	15.2	-1.9	-18.3	-13.7
Artemisia	27.4	18.4	5.4	10	15.2	-3	-16.9	-12.6
Asteraceae	27.4	17.7	5.4	9.3	15.2	-2.5	-18.3	-13.1
Boraginaceae	27.4	na.	5.4	na.	15.2	na.	-18.3	na.
Brassicaceae	27.4	19.3	5.4	10.5	15.2	0.1	-18.3	-11.9
Caryophyllaceae	26.9	16.8	6.4	9	15.2	-3.1	-18.3	-12.3
Ceratostigma	20.8	na.	11.7	na.	8.2	na.	-6	na.
Chenopodiaceae	27.4	19.9	5.4	10.5	15.2	-4.7	-18.3	-13.5
Convolvulaceae	26.4	19.5	5.4	10.7	15.2	3.5	-16.9	-9.1
Crassulaceae	27.4	na.	5.4	na.	15.2	na.	-17	na.
Cyperaceae	27.4	15.6	5.4	8.6	15.2	-4.3	-18.3	-13.5
Dipsacaceae	21.7	na.	7.5	na.	9.1	na.	-16.5	na.
Empetrum	22.1	na.	8.6	na.	-17	na.	-27.8	na.
Geraniaceae	26.9	na.	7.5	na.	9.1	na.	-16.8	na.
Haloragdaceae	22.6	na.	7.5	na.	9.5	na.	-16.8	na.
Humulus	24.8	20.2	13.2	12	2.8	2.3	-3.8	-9.1
Lentibulariaceae	24.6	na.	10.5	na.	12.1	na.	-13.5	na.
Lilium	26.9	na.	8.7	na.	9.5	na.	-14.8	na.
Linaceae	21.4	na.	7.5	na.	8.7	na.	-14	na.
Orobanchaceae	25.6	na.	6.4	na.	9.5	na.	-17	na.
Plumbaginaceae	25	na.	5.4	na.	8.2	na.	-18.3	na.
Poaceae	27.4	18.7	5.4	9.7	15.2	-1.5	-18.3	-12.9
Polygonaceae	27.4	na.	5.4	na.	15.2	na.	-18.3	na.
Pyrolaceae	21.3	na.	11.7	na.	8.7	na.	-13.5	na.
Ranunculaceae	27.4	17.4	5.4	9.8	15.2	-0.6	-18.3	-11.6
Rosaceae	27.4	17.1	5.4	10.1	15.2	-0.9	-18.3	-11.7
Saxifraga	26.9	17.4	7.5	11.6	9.1	0.5	-16.8	-8.5
Solanaceae	27.4	19.8	5.4	11.4	15.2	2.8	-18.3	-8.8
Thymelaeaceae	27.4	26	6.4	15.2	15.2	2.6	-17	-9
Viola	26.9	19.8	7.5	10	9.1	2.2	-18.3	-9

Appendix B Information on location, vegetation and climate of the sampling sites.

Latitude and longitude are given in decimal degrees. The climate variables are: growing degree days above a baseline of 0°C (GDD_0), mean temperature of the period above 5°C ($mGDD_5$) and the Cramer–Prentice index (α) of plant-available moisture.

site name	latitude (N/°)	longitude (E/°)	elevation (m)	vegetation type	species number	GDD_0 (day °C)	$mGDD_5$ (°C)	α
Ailaoshan Dwarf	24.54	101.03	2637	subtropical montane forest	20	4180.46	6.45	0.85
Ailaoshan Flux	24.54	101.03	2394	subtropical evergreen broadleaved forest	36	4132.71	6.32	0.85
Ailaoshan Mid	24.50	100.99	2056	subtropical montane forest	35	4613.18	7.64	0.84
Long Ling 1	21.62	101.58	1034	tropical broadleaved evergreen forest	37	7050.32	14.32	0.90
Mandan Shrub	23.69	101.85	758	subtropical shrubland	32	7963.98	16.82	0.63
Mandan Wood	23.69	101.86	772	subtropical woodland	39	8458.78	18.18	0.63
Mengla 1 rain forest	21.61	101.58	668	tropical broadleaved evergreen forest	42	7166.55	14.63	0.90
Mengla 2 Midslope	21.62	101.58	828	tropical broadleaved evergreen forest	19	7050.32	14.32	0.90
NECTS01	42.88	118.48	1024	steppe	19	2816.21	9.56	0.60
NECTS02	43.64	119.02	781	steppe	43	2976.44	10.33	0.57
NECTS03	43.02	129.78	136	deciduous broadleaved forest	24	3164.18	10.30	0.83
NECTS04	42.98	130.08	114	mixed evergreen conifer and deciduous broadleaved forest	26	3125.96	10.09	0.85
NECTS05	43.30	131.15	289	mixed evergreen conifer and deciduous broadleaved forest	42	2800.54	9.20	0.86
NECTS06	43.12	131.00	244	mixed evergreen conifer and deciduous broadleaved forest	49	2890.67	9.42	0.86
NECTS07	43.39	129.67	224	mixed evergreen conifer and deciduous broadleaved forest	40	2818.01	9.47	0.86
NECTS08	43.25	128.64	601	mixed evergreen conifer and deciduous broadleaved forest	39	2701.51	9.26	0.93
NECTS09	43.73	127.03	390	mixed evergreen conifer and deciduous broadleaved forest	55	2753.35	9.56	0.98
NECTS10	43.81	125.68	252	mixed evergreen conifer and deciduous broadleaved forest	39	3286.53	11.29	0.86
NECTS11	44.59	123.51	146	meadow steppe	19	3417.53	11.97	0.62
NECTS12	44.43	123.27	150	meadow steppe	18	3412.90	11.95	0.62

NECTS13	43.60	121.84	203	meadow steppe	20	3522.61	12.05	0.53
NECTS14	44.12	121.77	202	meadow steppe	7	3500.21	12.03	0.54
NECTS15	44.39	120.55	448	steppe	21	3212.54	11.17	0.57
NECTS16	44.22	120.37	372	steppe	18	3337.06	11.61	0.55
NECTS17	43.88	119.38	601	steppe	15	3078.25	10.71	0.57
NECTS18	43.76	119.12	729	steppe	23	2933.15	10.20	0.58
NECTS19	43.34	118.49	707	steppe	12	3097.60	10.57	0.55
NECTS20	43.19	117.76	889	steppe	23	2850.40	9.90	0.58
NECTS21	43.22	117.24	1259	steppe	23	2275.71	8.19	0.66
NECTS22	43.39	116.89	1267	steppe	13	2239.48	8.21	0.63
NECTS23	43.55	116.68	1261	steppe	22	2289.82	8.44	0.60
NECTS24	43.69	116.64	1211	steppe	20	2373.15	8.78	0.57
NECTS25	43.91	116.31	1199	steppe	24	2413.50	8.90	0.53
NECTS26	43.90	115.32	1196	steppe	27	2539.05	9.40	0.45
NECTS27	43.94	114.61	1123	desert steppe	19	2681.43	9.92	0.39
NECTS28	43.83	113.83	1166	desert steppe	14	2760.69	10.12	0.35
NECTS29	43.80	113.36	1017	desert steppe	11	3045.03	11.00	0.30
NECTS30	43.72	112.59	974	desert steppe	21	3127.67	11.27	0.27
NECTS31	43.63	112.17	999	desert steppe	16	3110.69	11.26	0.27
NECTS32	43.66	111.92	1005	desert steppe	15	3124.11	11.39	0.26
NECTS33	43.65	111.89	1017	desert steppe	16	3131.76	11.31	0.26
NSTEC01	36.24	117.02	368	mixed conifer-deciduous broadleaved forest	9	4659.66	12.88	0.72
NSTEC02	34.64	119.24	59	mixed conifer-deciduous broadleaved forest	13	5057.38	12.88	0.87
NSTEC03	32.05	118.86	76	mixed conifer-deciduous broadleaved forest	35	5518.49	13.18	0.98
NSTEC04	30.29	119.44	299	evergreen broad-leaved forest	21	5360.95	12.42	0.98
NSTEC05	29.80	121.79	231	evergreen broad-leaved forest	41	5741.25	11.16	0.98
NSTEC06	27.98	119.14	294	evergreen broad-leaved forest	57	6109.67	11.74	0.98
NSTEC07	26.59	118.05	239	evergreen broad-leaved forest	59	6641.81	13.20	0.99
NSTEC08	24.41	116.34	195	evergreen broad-leaved forest	35	7638.99	15.93	0.99

NSTEC09	23.17	112.54	240	evergreen broad-leaved forest	45	7840.27	16.48	0.99
NSTEC10	25.32	110.25	199	mixed conifer-deciduous broadleaved forest	29	6825.13	13.70	0.99
NSTEC11	26.84	109.60	390	mixed conifer-deciduous broadleaved forest	53	5608.62	11.90	0.99
NSTEC12	28.34	109.73	220	mixed conifer-deciduous broadleaved forest	39	5897.15	11.54	0.99
NSTEC13	33.50	111.49	449	deciduous broadleaved forest	27	4975.52	12.11	0.92
NSTEC14	39.95	115.42	1253	deciduous broadleaved forest	14	2835.32	9.02	0.73
Unholy Mt	21.98	101.24	1075	tropical broadleaved evergreen forest	41	7309.74	15.03	0.86
X001	48.19	87.02	272	desert	8	2336.91	8.34	0.37
X002	46.40	85.94	701	desert	18	3386.71	11.77	0.27
X003	47.04	87.09	620	desert steppe	10	3177.40	11.36	0.27
X004	47.83	86.85	499	desert steppe	20	3152.10	11.07	0.27
X005	47.94	86.83	481	desert	11	3144.10	11.03	0.28
X006	48.17	87.08	709	desert steppe	15	2697.47	9.47	0.32
X007	48.11	87.01	1100	shrubland	6	1889.65	6.84	0.45
X008	48.33	87.12	1595	meadow	13	1889.65	6.84	0.45
X009	47.72	87.02	498	desert steppe	23	3220.65	11.39	0.26
X010	47.74	87.54	521	desert steppe	13	3202.97	11.32	0.26
X011	47.16	88.70	750	desert	8	3122.83	11.11	0.29
X012	46.30	89.55	885	desert	10	2985.09	10.63	0.31
X013	45.36	89.40	1068	desert	7	2863.20	10.19	0.37
X014	44.12	87.81	513	desert	11	3848.11	13.08	0.30
X015	44.08	87.79	583	desert steppe	16	3802.48	12.93	0.31
X016	44.07	88.08	852	desert steppe	10	3466.81	11.75	0.34
X017	43.99	88.06	1060	meadow	12	3057.33	10.48	0.41
X018	43.93	88.11	1430	shrubland	9	2609.37	8.95	0.52
X019	42.84	89.44	-91	shrubland	2	5763.53	17.68	0.09
X020	42.73	89.44	-136	desert	2	5929.28	18.07	0.08
X021	42.69	89.42	-146	desert	2	5975.05	18.17	0.08
X022	42.37	88.57	1721	desert	5	3199.92	10.81	0.26

X023	42.22	87.76	1445	desert	9	3350.05	10.93	0.23
X024	41.81	86.25	1444	desert	3	3983.63	12.23	0.17
X025	40.51	84.32	931	desert	1	4895.69	14.23	0.12
X026	40.83	84.29	921	desert	4	4892.88	14.20	0.13
X027	41.48	84.21	928	desert	3	4660.33	13.66	0.15
X028	41.50	84.51	919	desert	3	4627.47	13.62	0.15
X029	41.66	84.89	902	desert	5	4520.68	13.48	0.16
X030	42.25	88.23	966	desert	2	4221.62	13.56	0.14
X031	43.90	88.12	1935	desert	9	2033.05	7.10	0.75
X032	40.83	84.29	26	desert	1	4892.88	14.20	0.13
X033	40.51	89.11	70	shrubland	3	4862.58	14.86	0.09
X034	43.93	88.11	1430	evergreen conifer forest	3	2395.03	8.27	0.60
X035	48.33	87.12	1595	deciduous woodland	1	1594.50	5.78	0.51
XTBG rain forest	21.92	101.27	502	tropical broadleaved evergreen forest	45	7789.31	16.34	0.85

Appendix C The morphometric traits recorded in the field.

Some traits were defined by presence/absence (yes/no); pre-defined sub-categories were used for other traits. There were insufficient records available in some of the sub-categories and so several sub-categories were amalgamated (and renamed) for the statistical analyses.

Leaf trait	Categories used in field description	Categories used in analyses
Type	broad	broad
	needle	needle
	scale	scale
Phenology	deciduous	deciduous
	semi-deciduous	
	leaf exchanger	evergreen
	evergreen	
Texture	fleshy	fleshy
	malacophyll	malacophyll
	papery	tough
	leathery	
	coriaceous	
	rigidly coriaceous	
Colour upper surface	dark green	dark green
	mottled green	
	green	green
	bright green	
	pale green	
	yellow-green	yellow-green
	yellow	
	glaucous	glaucous
	grey-green	
	silvery-grey	
Colour lower surface	dark green	dark green
	mottled green	
	green	green
	bright green	
	pale green	
	brown-green	yellow-green
	pale brown	
	yellow-green	
	yellow	
	glaucous	glaucous
	grey-green	
	silvery-grey	
	white	
	red-green	red-green
	purple	
Size class	picophyll	picophyll
	leptophyll	leptophyll
	nanophyll	nanophyll
	microphyll	microphyll
	notophyll	notophyll
	mesophyll	mesophyll
	macrophyll	macrophyll
Thickness class	thick	thick
	medium	medium
	thin	thin
Orientation	erect	erect
	semi-erect	

	normal	normal
	reclinate	pendent
	pendent	
Shape	elliptic	elliptic
	falcate-elliptic	
	obovate-elliptic	
	ovate-elliptic	
	cordate-lanceolate	lanceolate
	elliptic-lanceolate	
	lanceolate	
	linear-lanceolate	
	oblanceolate	
	ovate-lanceolate	
	spathulate	
	linear	linear
	cordate	roundish
	cordate-trilobate	
	deltoid	
	obcordate	
	oblong	
	obovate	
	obovate-decurrent	
	orbicular	
	ovate	
	ovoid	
	hastate	
	ovate-decurrent	
	rhomboid	
	rhomboid-ovate	
	lobate	
	flavate	
	ovate-trilobate	
	bifid	other
	bipinnate	
	five lobate	
	five lobate-cordate	
	palmate	
	fishtail	
	triffid	
	pinnatiphid	
	septemlobate	
	trilobite	
Margin incision	entire	entire
	lobed	round toothed
	crenate	
	crenulate	
	finely toothed	finely toothed
	toothed	toothed
	dissected	dissected
	highly dissected	
	incised	
	pinnate	
	pinnatifid	
Hairs	hairs on top	yes/no
	hairs on bottom	
	hairs on midrib/veins	
	marginal hairs	
	basal hairs	
Pubescence	pubescent: top	yes/no
	pubescent: bottom	
	pubescent: marginal	
	pubescent: midrib/veins	
Pruinosity	upper surface	yes/no
	lower surface	
	on veins, midrib or petiole	
	tomentose	
Waxy	waxy	yes/no

	slightly waxy or glossy	
Conspicuous hypostomatic		yes/no
Revolute	revolute	yes/no
	slightly revolute	
Involute	involute	yes/no
	slightly involute	
Aromatic		yes/no
Fetid		yes/no
Drip-tip		yes/no
Terminal notch		yes/no
Surface patterning	marked surface patterning	yes/no
	slight surface patterning	
Rugosity	rugose above	yes/no
	rugose below	
Leaf succulence		yes/no
Presence of spines or thorns	on upper surface	yes/no
	on lower surface	
	on midrib	
	on veins	
	marginal	
	terminal	
	thorn	

Appendix D Results from the analyses using generalized linear regression modelling.

The intercept and the slope values for each partial relationship between a given trait and climate variable are given. Significant linear terms are shown in bold. The quadratic term is shown only when this is significant and used in the final model. We show the overall relationship, and for woody (W) and non-woody (NW) separately. The climate variables are: growing degree days above a baseline of 0°C (GDD_0), mean temperature of the period above 5°C ($mGDD_5$) and the Cramer–Prentice index (α) of plant-available moisture. Grey shading indicates that the analysis was not made because there were insufficient observations to derive a meaningful relationship.

	Overall							W							NW						
		linear term			quadratic term				linear term			quadratic term				linear term			quadratic term		
		GDD_0	$mGDD_5$	α	GDD_0	$mGDD_5$	α		GDD_0	$mGDD_5$	α	GDD_0	$mGDD_5$	α		GDD_0	$mGDD_5$	α	GDD_0	$mGDD_5$	α
Traits	intercept	slope	slope	slope	slope	slope	slope	intercept	slope	slope	slope	slope	slope	slope	intercept	slope	slope	slope	slope	slope	slope
broad	0.91	-0.00	0.01	0.03	–	–	–	0.96	**0.00**	-0.01	-0.00	–	–	–							
needle	-0.00	-0.00	-0.00	0.05	–	–	–	-0.03	**-0.00**	0.01	**0.11**	–	–	–							
scale	0.10	0.00	-0.01	-0.08	–	–	–	-0.20	**0.00**	**0.01**	**-0.11**	-0.00	–	–							
deciduous	0.62	**-0.00**	**0.12**	-0.01	–	–	–	0.62	**-0.00**	**0.12**	-0.01	–	–	–	0.82	-0.00	0.04	0.08	–	–	–
evergreen	0.38	**0.00**	**-0.12**	0.01	–	–	–	0.38	**0.00**	**-0.12**	0.01	–	–	–	0.18	0.00	-0.04	-0.08	–	–	–
fleshy	0.26	-0.00	0.01	**-0.40**	–	–	–	0.51	0.00	-0.00	**-0.57**	–	–	–	-0.03	0.00	0.00	**-0.23**	–	–	–
malacophyll	-0.25	**-0.00**	**0.06**	**2.30**	–	–	-1.55	-0.51	**-0.00**	**0.05**	**3.55**	–	–	-2.61	0.07	-0.00	0.15	**0.68**	–	–	–
tough	0.47	**0.00**	**-0.07**	-0.05	–	–	–	0.06	**0.00**	**-0.05**	**0.39**	–	–	–	0.95	0.00	-0.15	**-0.45**	–	–	–
dark green above	0.19	**0.00**	**-0.08**	0.05	–	–	–	0.33	**0.00**	**-0.08**	0.03	–	–	–	0.02	0.00	-0.01	-0.02	–	–	–
green above	0.36	**-0.00**	**0.06**	**0.56**	–	–	–	-0.16	**-0.00**	**0.08**	**0.93**	–	–	–	0.96	**0.00**	**-0.21**	0.13	–	–	–
yellow green above	0.02	0.00	-0.00	-0.01	–	–	–	-0.00	0.00	0.00	-0.01	–	–	–	0.12	0.00	-0.02	-0.03	–	–	–
glaucous above	0.44	-0.00	0.02	**-0.60**	–	–	–	0.83	-0.00	0.01	**-0.95**	–	–	–	-0.11	**-0.00**	**0.24**	-0.08	–	–	–
dark green below	0.05	0.00	-0.01	-0.01	–	–	–	0.09	0.00	-0.01	-0.03	–	–	–	0.02	0.00	-0.01	-0.02	–	–	–
green below	0.45	-0.00	0.00	**0.55**	–	–	–	-0.52	-0.00	0.01	**3.00**	–	–	-1.64	0.91	**0.00**	**-0.23**	0.09	–	–	–
yellow green below	0.04	0.00	**-0.00**	-0.01	–	–	–	0.04	0.00	-0.00	-0.01	–	–	–	0.12	0.00	-0.02	-0.03	–	–	–
glaucous below	0.46	-0.00	0.01	**-0.54**	–	–	–	0.82	0.00	0.00	**-0.86**	–	–	–	-0.05	**-0.00**	**0.26**	-0.04	–	–	–
red green below	-0.00	0.00	-0.00	0.00	–	–	–	-0.01	0.00	-0.00	0.01	–	–	–							

picophyll	0.25	0.00	-0.01	**-0.27**	–	–	–	0.27	-0.00	0.00	**-0.32**	–	–	–	-0.01	-0.00	0.10	-0.08	–	–	–
leptophyll	0.38	0.00	0.00	**-0.42**	–	–	–	0.37	-0.00	0.00	**-0.41**	–	–	–	0.04	-0.00	0.09	**-0.24**	–	–	–
nanophyll	0.57	**-0.00**	0.02	**-0.37**	–	–	–	0.35	**-0.00**	**0.02**	**-0.32**	–	–	–	1.02	0.00	-0.06	**-0.52**	–	–	–
microphyll	-0.00	-0.00	0.01	**0.57**	–	–	–	0.21	0.00	-0.03	**0.37**	–	–	–	-0.13	-0.00	0.07	**0.56**	–	–	–
notophyll	0.00	**0.00**	**-0.02**	**0.28**	–	–	–	0.09	0.00	-0.02	**0.38**	–	–	–	0.11	**0.00**	**-0.16**	0.08	–	–	–
mesophyll	-0.14	0.00	0.00	**0.19**	–	–	–	-0.20	-0.00	0.01	**0.28**	–	–	–	-0.71	0.00	0.12	**0.16**	–	-0.01	–
macrophyll	-0.06	0.00	-0.00	0.02	–	–	–	-0.10	0.00	0.00	0.02	–	–	–	0.02	0.00	-0.02	0.01	–	–	–
thick	0.15	**0.00**	**-0.03**	-0.02	–	–	–	0.13	**0.00**	**-0.03**	0.02	–	–	–	0.17	0.00	-0.02	-0.07	–	–	–
medium	1.15	**0.00**	**-0.07**	**-0.76**	–	–	–	1.15	**0.00**	**-0.05**	**-0.53**	–	–	–	1.12	-0.00	-0.02	**-0.73**	–	–	–
thin	-0.73	**-0.00**	**0.09**	**2.37**	–	–	-1.33	-0.84	**-0.00**	**0.08**	**2.56**	–	–	-1.61	-0.29	-0.00	0.04	**0.81**	–	–	–
erect	0.68	**0.00**	**-0.05**	**-0.63**	–	–	–	0.87	**0.00**	**-0.07**	**-0.72**	–	–	–	0.18	-0.00	0.01	**-0.31**	–	–	–
normal	0.27	**-0.00**	**0.06**	**0.66**	–	–	–	0.04	**-0.00**	**0.07**	**0.78**	–	–	–	0.78	-0.00	0.00	**0.36**	–	–	–
pendent	0.05	**0.00**	**-0.01**	-0.03	–	–	–	0.10	0.00	-0.01	-0.06	–	–	–	0.03	0.00	-0.02	-0.05	–	–	–
entire	0.92	**0.00**	-0.00	**-0.73**	–	–	–	0.74	**0.00**	-0.02	**-0.76**	–	–	–	0.96	-0.00	0.16	**-0.57**	–	–	–
round toothed	0.26	**0.00**	**-0.03**	-0.08	–	–	–	0.31	**0.00**	**-0.04**	-0.09	–	–	–	0.26	0.00	-0.08	-0.10	–	–	–
finely toothed	0.18	**0.00**	**-0.03**	-0.03	–	–	–	0.22	**0.00**	**-0.04**	-0.02	–	–	–	-0.01	0.00	-0.01	-0.01	–	–	–
toothed	-0.41	**-0.00**	**0.05**	**0.75**	–	–	–	-0.42	**-0.00**	**0.07**	**0.90**	–	–	–	-0.30	0.00	-0.02	**0.63**	–	–	–
dissected	-0.10	**-0.00**	**0.02**	**0.61**	–	–	-0.44	0.15	**-0.00**	**0.03**	-0.04	–	–	–	0.07	0.00	-0.05	0.06	–	–	–
linear	-0.03	-0.00	0.02	**1.69**	–	–	-1.56	0.04	**-0.00**	0.01	0.02	–	–	–	-0.05	**-0.00**	**0.37**	1.61	–	–	-1.62
lanceolate	0.05	**-0.00**	0.02	0.12	–	–	–	0.22	-0.00	0.00	-0.09	–	–	–	-0.41	-0.00	0.19	**0.45**	–	–	–
elliptic	0.24	**0.00**	**-0.08**	0.01	–	–	–	0.41	**0.00**	**-0.09**	0.01	–	–	–	-0.40	-0.00	0.02	**0.72**	–	–	-0.49
round	0.22	-0.00	0.03	0.02	–	–	–	0.24	**-0.00**	**0.08**	0.12	–	–	–	1.02	**0.00**	**-0.52**	-0.31	–	–	–
other shape	0.01	-0.00	0.00	0.03	–	–	–	0.09	-0.00	0.00	-0.06	–	–	–	0.13	**0.00**	**-0.08**	0.01	–	–	–
hairs	0.21	-0.00	0.01	**-0.21**	–	–	–	0.14	**-0.00**	**0.02**	0.02	–	–	–	0.49	**0.00**	**-0.22**	**-0.36**	–	–	–
pubescence	-0.34	**0.00**	-0.00	**1.28**	–	–	-1.09	0.04	0.00	0.00	-0.14	–	–	–	-0.12	**-0.00**	**0.17**	0.20	–	–	–
pruinose	-0.33	**0.00**	**0.02**	-0.04	-0.00	–	–	-0.01	**-0.00**	**0.02**	0.06	–	–	–	0.31	0.00	-0.08	-0.20	–	–	–
waxy	0.38	**0.00**	**-0.09**	0.05	–	–	–	-0.51	**0.00**	**-0.06**	**0.29**	-0.00	–	–	0.18	**-0.00**	**0.12**	-0.11	–	–	–
hypostomatic	0.31	**0.00**	**-0.03**	-0.11	–	–	–	0.41	**0.00**	**-0.04**	**-0.16**	–	–	–	0.42	**0.00**	**-0.14**	-0.16	–	–	–
revolute	0.07	**0.00**	-0.00	**-0.09**	–	–	–	0.08	0.00	-0.00	-0.07	–	–	–	0.15	**0.00**	**-0.04**	**-0.09**	–	–	–
involute	-0.01	-0.00	0.00	**0.99**	–	–	-0.85	0.09	**-0.00**	0.01	-0.02	–	–	–	0.21	-0.00	0.03	**1.37**	–	–	-1.32
aromatic	0.16	0.00	-0.01	-0.03	–	–	–	0.31	-0.00	0.00	-0.18	–	–	–	-0.14	-0.00	0.04	**0.10**	–	–	–
fetid	-0.09	**0.00**	-0.00	**0.27**	–	–	-0.24	-0.15	0.00	0.00	**0.53**	–	–	-0.46							
drip-tip	0.30	**0.00**	**-0.11**	**0.39**	–	–	–	0.29	**0.00**	**-0.09**	**0.67**	–	–	–	0.15	0.00	-0.14	0.24	–	–	–
terminal notch	-0.02	0.00	0.00	-0.01	–	–	–	-0.01	0.00	0.00	-0.04	–	–	–							
patterning	0.03	**0.00**	**-0.03**	-0.01	–	–	–	0.02	0.00	-0.02	0.06	–	–	–	0.04	**0.00**	**-0.04**	0.02	–	–	–
rugosity	-0.18	**0.00**	**0.03**	0.02	–	-0.00	–	-0.02	0.00	-0.00	0.05	–	–	–							
succulence	-0.21	**0.00**	0.02	**-0.31**	-0.00	–	–	0.35	-0.00	-0.00	**-0.39**	–	–	–	-0.07	0.00	0.01	-0.09	–	–	–
spines	0.26	**0.00**	**-0.03**	-0.05	–	–	–	0.26	0.00	-0.02	0.02	–	–	–	0.47	0.00	**-0.14**	-0.17	–	–	–

Appendix E Results from the analyses of tree and shrub plant functional types using generalized linear regression modelling.

The intercept and the slope values for each partial relationship between a given trait and climate variable are given. The plants functional types (PFTs): deciduous broadleaf tree (DBT), evergreen broadleaf tree (EBT), evergreen broadleaf shrub (EBS), and evergreen needleleaf tree (ENT). Significant linear terms are shown in bold. The quadratic term is shown only when this is significant and used in the final model. The climate variables are: growing degree days above a baseline of 0°C (GDD_0), mean temperature of the period above 5°C ($mGDD_5$) and the Cramer–Prentice index (α) of plant-available moisture. Grey shading indicates that the analysis was not made because there were insufficient observations to derive a meaningful relationship.

	DBT							EBT						
		linear term			quadratic term				linear term			quadratic term		
		GDD_0	$mGDD_5$	α	GDD_0	$mGDD_5$	α		GDD_0	$mGDD_5$	α	GDD_0	$mGDD_5$	α
Traits	intercept	slope	slope	slope	slope	slope	slope	intercept	slope	slope	slope	slope	slope	slope
broad	0.93	0.00	0.00	0.05	–	–	–							
needle	0.00	-0.00	0.00	0.02	–	–	–							
scale	0.07	0.00	-0.00	**-0.07**	–	–	–							
deciduous														
evergreen														
fleshy	0.72	0.00	-0.02	**-0.66**	–	–	–							
malacophyll	0.50	0.00	-0.01	0.39	–	–	–	0.77	0.00	-0.03	**-0.95**	–	–	–
tough	-0.22	-0.00	0.04	0.27	–	–	–	0.23	-0.00	0.03	**0.95**	–	–	–
dark green above	0.52	0.00	-0.08	-0.02	–	–	–	0.67	0.00	-0.03	-0.19	–	–	–
green above	-0.56	**-0.00**	0.09	**1.12**	–	–	–	0.33	-0.00	0.03	0.19	–	–	–
yellow green above	-0.03	-0.00	0.00	-0.00	–	–	–							
glaucous above	1.07	0.00	-0.02	**-1.09**	–	–	–							
dark green below	0.26	0.00	-0.02	-0.10	–	–	–	-0.09	0.00	-0.00	0.05	–	–	–
green below	-0.25	-0.00	0.04	**1.10**	–	–	–	-4.51	0.00	-0.00	**12.46**	–	–	-7.56
yellow green below	-0.06	-0.00	0.01	0.02	–	–	–	0.15	0.00	-0.01	-0.10	–	–	–
glaucous below	1.02	0.00	-0.02	**-1.02**	–	–	–	0.46	-0.00	0.08	0.09	–	–	–
red green below	0.02	0.00	-0.00	-0.00	–	–	–	-0.20	0.00	-0.01	0.19	–	–	–
picophyll	0.39	0.00	-0.01	**-0.36**	–	–	–							
leptophyll	0.21	-0.00	0.02	**-0.40**	–	–	–	0.24	-0.00	0.01	**-0.25**	–	–	–
nanophyll	0.59	0.00	-0.01	**-0.44**	–	–	–							
microphyll	-0.06	0.00	-0.00	**0.37**	–	–	–	0.74	-0.00	0.01	0.25	–	–	–
notophyll	-0.18	-0.00	0.02	**0.50**	–	–	–	0.60	-0.00	0.04	0.09	–	–	–
mesophyll	-0.08	-0.00	0.00	**0.33**	–	–	–	-6.63	-0.00	0.04	**15.62**	–	–	-9.38
macrophyll	-0.16	**0.00**	-0.01	-0.01	-0.00	–	–	-7.73	0.00	0.03	**17.92**	–	–	-10.67
thick	-0.03	0.00	0.00	-0.02	–	–	–	0.49	-0.00	0.07	0.39	–	–	–
medium	1.25	0.00	-0.04	**-0.64**	–	–	–	0.92	0.00	-0.02	-0.35	–	–	–
thin	-0.22	-0.00	0.04	**0.66**	–	–	–	-6.53	0.00	0.02	**14.89**	–	–	-8.90
erect	0.40	0.00	-0.00	**-0.51**	–	–	–	-2.22	0.00	-0.04	**8.53**	–	–	-6.24
normal	0.40	-0.00	-0.01	**1.60**	–	–	-0.88	-1.12	-0.00	0.09	**2.01**	–	–	–
pendent	0.06	0.00	-0.00	-0.03	–	–	–	0.05	0.00	-0.00	-0.07	–	–	–
entire	0.95	**0.00**	-0.03	**-1.01**	–	–	–	-0.32	**0.00**	**-0.10**	0.09	–	–	–
round toothed	-0.12	0.00	0.00	0.08	–	–	–	0.38	0.00	-0.05	-0.21	–	–	–
finely toothed	0.58	**0.00**	**-0.08**	-0.10	–	–	–	1.18	**-0.00**	**0.08**	**-0.53**	–	–	–
toothed	-0.43	**-0.00**	0.06	**1.00**	–	–	–	-0.24	-0.00	0.06	0.64	–	–	–
dissected	0.02	**-0.00**	0.04	0.03	–	–	–							
linear	0.08	0.00	0.00	-0.08	–	–	–	-0.01	0.00	-0.00	-0.01	–	–	–
lanceolate	0.04	-0.00	0.03	-0.07	–	–	–	0.08	-0.00	0.09	0.40	–	–	–
elliptic	0.35	0.00	-0.06	0.07	–	–	–	1.17	0.00	-0.11	-0.78	–	–	–
round	0.17	**-0.00**	0.07	0.21	–	–	–	-0.14	-0.00	0.03	0.33	–	–	–
other shape	0.36	0.00	-0.04	-0.13	–	–	–	-0.09	0.00	-0.00	0.06	–	–	–
hairs	0.08	**-0.00**	0.03	0.10	–	–	–	-0.14	0.00	-0.01	0.11	–	–	–
pubescence	-0.05	0.00	0.00	-0.04	–	–	–	0.33	0.00	0.01	-0.41	–	–	–
pruinose	-0.37	**-0.00**	0.07	0.18	–	–	–	-0.26	-0.00	0.00	0.33	–	–	–
waxy	-0.32	-0.00	0.03	0.23	–	–	–	0.45	-0.00	0.06	1.13	–	–	–
hypostomatic	0.12	-0.00	0.01	-0.13	–	–	–	0.08	0.00	-0.03	0.48	–	–	–
revolute	-0.15	0.00	0.00	0.75	–	–	-0.63	0.53	0.00	-0.00	**-0.56**	–	–	–
involute	-0.01	-0.00	0.03	-0.01	–	–	–	0.38	**-0.00**	**0.03**	**-0.13**	–	–	–
aromatic	0.28	-0.00	0.00	-0.23	–	–	–	0.17	0.00	-0.02	-0.04	–	–	–
fetid	-0.34	-0.00	**0.04**	0.06	–	–	–	0.61	-0.00	0.01	**-0.61**	–	–	–
drip-tip	0.46	0.00	-0.09	**0.64**	–	–	–	-4.40	0.00	-0.01	**11.70**	–	–	-6.37
terminal notch	-0.16	-0.00	0.02	0.00	–	–	–	0.29	-0.00	0.01	**-0.29**	–	–	–
patterning	-0.23	-0.00	0.02	0.20	–	–	–	-7.99	-0.00	0.03	**19.77**	–	–	-12.11
rugosity	0.45	**0.00**	**-0.06**	-0.10	–	–	–	-0.02	-0.00	0.01	0.02	–	–	–
succulence	0.53	0.00	-0.02	**-0.44**	–	–	–							
spines	0.04	-0.00	0.01	0.13	–	–	–	0.77	-0.00	0.06	-0.29	–	–	–

	EBS							ENT						
		linear term			quadratic term				linear term			quadratic term		
		GDD_0	$mGDD_5$	α	GDD_0	$mGDD_5$	α		GDD_0	$mGDD_5$	α	GDD_0	$mGDD_5$	α
Traits	intercept	slope	slope	slope	slope	slope	slope	intercept	slope	slope	slope	slope	slope	slope
broad														
needle														
scale														
deciduous														
evergreen														
fleshy														
malacophyll	0.40	-0.00	0.05	-0.34	–	–	–							
tough	0.60	0.00	-0.05	0.34	–	–	–							
dark green above	1.20	0.00	-0.09	-0.87	–	–	–							
green above	-0.10	-0.00	0.08	0.80	–	–	–							
yellow green above														
glaucous above	-0.10	-0.00	0.01	0.07	–	–	–							
dark green below	0.12	-0.00	0.00	-0.13	–	–	–							
green below	0.45	0.00	0.00	0.04	–	–	–							
yellow green below	-4.44	0.00	-0.00	**9.94**	–	–	-5.51							
glaucous below	0.38	-0.00	0.00	0.16	–	–	–							
red green below	-0.17	0.00	-0.01	0.15	–	–	–							
picophyll														
leptophyll	-20.88	0.00	-0.00	**45.66**	–	–	-24.81							
nanophyll	-0.36	-0.00	0.02	0.31	–	–	–							
microphyll	-1.40	0.00	-0.05	**2.16**	–	–	–							
notophyll	0.10	-0.00	0.00	0.45	–	–	–							
mesophyll	1.67	-0.00	0.06	**-1.89**	–	–	–							
macrophyll	0.87	0.00	-0.02	**-0.90**	–	–	–							
thick	-2.13	0.00	-0.02	**2.31**	–	–	–							
medium	2.52	-0.00	0.10	**-1.57**	–	–	–							
thin	0.61	0.00	-0.08	-0.74	–	–	–							
erect	1.72	-0.00	0.00	**-1.74**	–	–	–							
normal	-1.24	-0.00	0.02	**2.24**	–	–	–							
pendent	-83.52	0.00	-0.00	**182.63**	–	–	-99.26							
entire	-0.19	0.00	-0.06	0.30	–	–	–							
round toothed	0.05	0.00	-0.02	-0.14	–	–	–							
finely toothed	1.72	-0.00	0.03	-1.09	–	–	–							
toothed	-0.58	-0.00	0.05	0.93	–	–	–							
dissected														
linear	-4.44	0.00	-0.00	**9.94**	–	–	-5.51							
lanceolate	-0.90	-0.00	0.04	**0.84**	–	–	–							
elliptic	1.05	0.00	-0.08	-0.51	–	–	–							
round	0.79	-0.00	0.06	-0.24	–	–	–							
other shape	-0.16	0.00	-0.02	0.12	–	–	–							
hairs	-0.60	0.00	-0.04	0.46	–	–	–							
pubescence	1.12	-0.00	0.02	-0.85	–	–	–							
pruinose	-0.09	0.00	-0.00	0.06	–	–	–							
waxy	-1.60	0.00	-0.06	**2.51**	–	–	–							
hypostomatic	-0.35	0.00	-0.01	0.38	–	–	–							
revolute	0.38	0.00	-0.00	-0.40	–	–	–							
involute	0.06	-0.00	0.00	-0.02	–	–	–							
aromatic	0.10	-0.00	0.02	0.06	–	–	–							
fetid	0.09	-0.00	0.00	-0.09	–	–	–							
drip-tip	0.85	-0.00	0.09	0.09	–	–	–							
terminal notch	-20.88	0.00	-0.00	**45.66**	–	–	-24.81							
patterning	1.76	-0.00	0.08	-1.55	–	–	–							
rugosity	-0.12	0.00	-0.05	0.19	–	–	–							
succulence														
spines	0.42	-0.00	-0.03	0.21	–	–	–							

Appendix F Relationships between the abundance of different traits related to quantitative leaf economics traits (evergreen, nanophyll, notophyll, tough, malacophyll, fleshy, thick, thin, dark green above, glaucous above) and climate for woody and non-woody plant functional types.

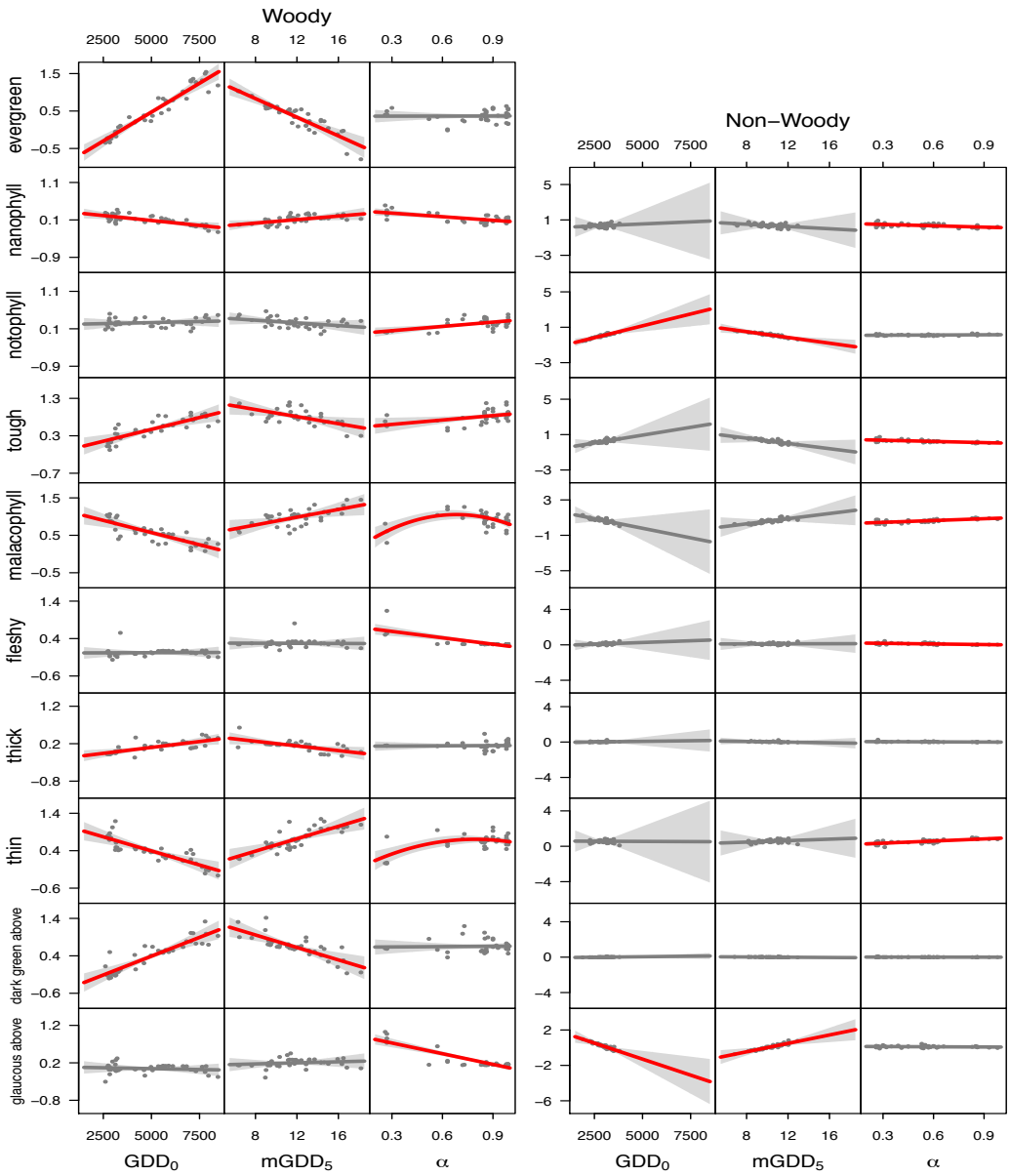

The climate variables are: growing degree days above a baseline of 0°C (GDD_0), mean temperature of the period above 5°C ($mGDD_5$) and the Cramer–Prentice index (α) of plant-available moisture. The plots show the partial residuals from the generalized linear model, which shows the relationship between a given trait and the specific climate variable after taking into account the influence of the other climate variables. Significant relationships are shown in red, non-significant relationships in grey.

Appendix G Relationships between leaf margin categories (entire, round toothed, finely toothed, toothed, dissected) and climate.

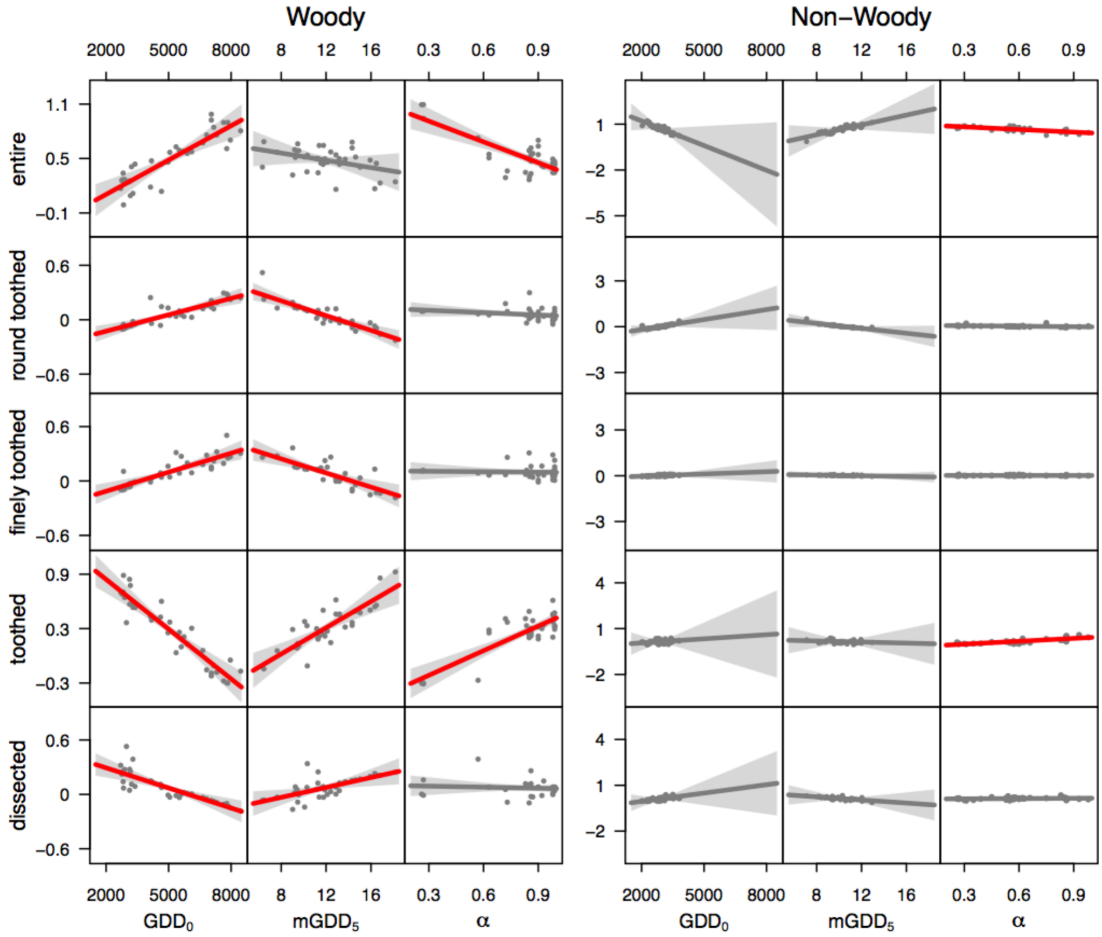

The climate variables are: growing degree days above a baseline of 0°C (GDD_0), mean temperature of the period above 5°C ($mGDD_5$) and the Cramer–Prentice index (α) of plant-available moisture for woody and non-woody plant functional types. The plots show the partial residuals from the generalized linear model, which shows the relationship between a given trait and the specific climate variable after taking into account the influence of the other climate variables. Significant relationships are shown in red, non-significant relationships in grey.

Appendix H Relationships between the abundance of different leaf traits related to protection against high levels of radiation and/or water conservation (waxy, hypostomatic, surface patterning, rugosity, drip tip, hairs, pubescence, pruinosity, revolute, involute, normal orientiation, erect orientation) and climate for woody and non-woody plant functional types.

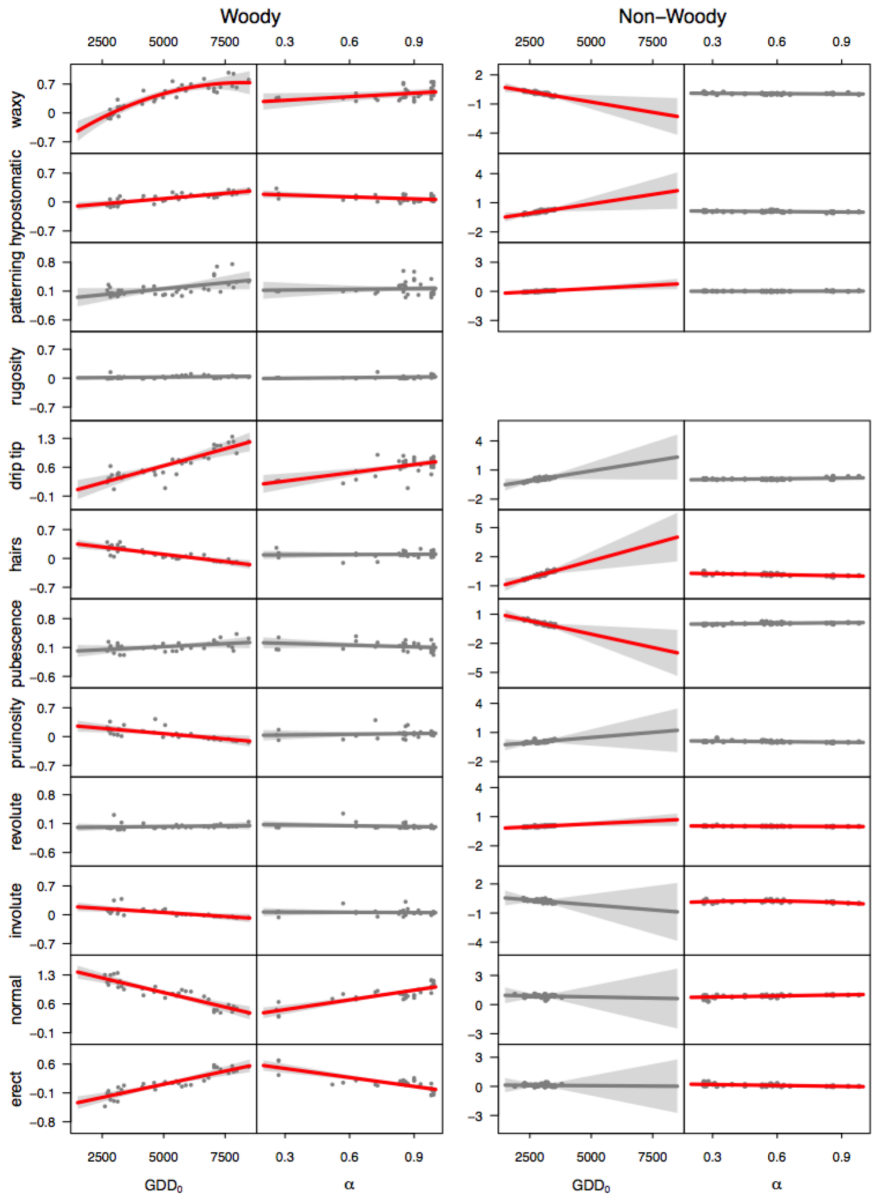

The climate variables are: growing degree days above a baseline of 0°C (GDD_0), and the Cramer–Prentice index (α) of plant-available moisture. The plots show the partial residuals from the generalized linear model, which shows the relationship between a given trait and the specific climate variable after taking into account the influence of the other climate variables. Significant relationships are shown in red, non-significant relationships in grey.

References

Agrawala, S., Ota, T., Ahmed, A. U., Smith, J., and Aalst, M. V.: Development and climate change in Bangladesh: focus on coastal flooding and the Sundarbans. Organisation for Economic Co-operation and Development (OECD). France: OECD, p70, 2003.

An, Z. S., Kutzbach, J. E., Prell, W. L., and Porter, S. C.: Evolution of Asian monsoons and phased uplift of the Himalaya–Tibetan plateau since Late Miocene times, Nature, 411, 62-66, 2001.

Araujo, M. B. and Pearson, R. G.: Equilibrium of species' distributions with climate, Ecography, 28, 693-695, 2005.

Archetti, M., Richardson, A. D., O'Keefe, J., and Delpierre, N.: Predicting Climate Change Impacts on the Amount and Duration of Autumn Colors in a New England Forest, Plos One, 8, 2013.

Atkin, O. K., Bloomfield, K. J., Reich, P. B., Tjoelker, M. G., Asner, G. P., Bonal, D., Bönisch, G., Bradford, M. G., Cernusak, L. A., and Cosio, E. G.: Global variability in leaf respiration in relation to climate, plant functional types and leaf traits, New Phytol., 206, 614-636, 2015.

Atkinson, T. C., Briffa, K. R., and Coope, G. R.: Seasonal temperatures in Britain during the past 22,000 years, reconstructed using beetle remains, Nature, 325, 587-592, 1987.

Austin, M., Nicholls, A., and Margules, C. R.: Measurement of the realized qualitative niche: environmental niches of five *Eucalyptus* species, Ecol. Monogr., 60, 161-177, 1990.

Bailey, I. W. and Sinnott, E. W.: A botanical index of Cretaceous and Tertiary climates, Science, 41, 831-834, 1915.

Bailey, I. W. and Sinnott, E. W.: The climatic distribution of certain types of angiosperm leaves, Am. J. Bot., 3, 24-39, 1916.

Barboni, D., Harrison, S., Bartlein, P., Jalut, G., New, M., Prentice, I., Sanchez-Goni, M., Spessa, A., Davis, B., and Stevenson, A.: Relationships between plant traits and climate in the Mediterranean region: a pollen data analysis, Journal of Vegetation Science, 15, 635-646, 2004.

Barras, J. A., J.C. Bernier, and Morton, R. A.: Land area changes in coastal Louisiana- A multi decadal perpective (from 1956-2006). U.S. Geological Survey Scientific Investigations Map 3019, 14 scale 1:250,000., 2008.

Bartlein, P. J., Harrison, S. P., Brewer, S., Connor, S., Davis, B. A. S., Gajewski, K., Guiot, J., Harrison-Prentice, T. I., Henderson, A., Peyron, O., Prentice, I. C., Scholze, M., Seppa, H., Shuman, B., Sugita, S., Thompson, R. S., Viau, A. E., Williams, J., and Wu, H.: Pollen-based continental climate reconstructions at 6 and 21 ka: a global synthesis, Climate Dynamics, 37, 775-802, 2011.

Bartlein, P. J., Prentice, I. C., and Webb III, T.: Climatic response surfaces from pollen data for some eastern North American taxa, J. Biogeogr., 13, 35-57, 1986.

Bartoli, G., Honisch, B., and Zeebe, R. E.: Atmospheric CO_2 decline during the Pliocene intensification of Northern Hemisphere glaciations, Paleoceanography, 26, 2011.

Beerling, D. J. and Royer, D. L.: Convergent cenozoic CO_2 history, Nature Geoscience, 4, 418-420, 2011.

Bell, E.: Life at extremes: Environments, organisms, and strategies for survival, Cabi, 2012.

Bharathan, G., Goliber, T. E., Moore, C., Kessler, S., Pham, T., and Sinha, N. R.: Homologies in leaf form inferred from KNOXI gene expression during development, Science, 296, 1858-1860, 2002.

Birks, H. J. B. and Birks, H. H.: Quaternary palaeoecology, Edward Arnold London, 1980.

Birks, H. J. B., Heiri, O., Seppä, H., and Bjune, A. E.: Strengths and weaknesses of quantitative climate reconstructions based on late-Quaternary biological proxies, The Open Ecology Journal, 2010.

Bistinas, I., Harrison, S., Prentice, I., and Pereira, J.: Causal relationships vs. emergent patterns in the global controls of fire frequency, Biogeosci. Disc., 11, 3865-3892, 2014.

Blanco, G., R. Gerlagh, S. Suh, J. Barrett, H. C. de Coninck, C. F. Diaz Morejon, R. Mathur, N. Nakicenovic, A. Ofosu Ahenkora, J. Pan, H. Pathak, J. Rice, R. Richels, S. J. Smith, D. I. Stern, F. L. Toth, and Zhou, P.: Drivers, Trends and Mitigation. In: Climate Change 2014: Mitigation of Climate Change. Contribution of Working Group III to the Fifth Assessment Report of the Intergovernmental Panel on Climate Change [Edenhofer, O., R. Pichs-Madruga, Y. Sokona, E. Farahani, S. Kadner, K. Seyboth, A. Adler, I. Baum, S. Brunner, P. Eickemeier, B. Kriemann, J. Savolainen, S. Schlömer, C. von Stechow, T. Zwickel and J.C. Minx (eds.)]. Cambridge University Press, Cambridge, United Kingdom and New York, NY, USA., 2014.

Blisniuk, P. M., Hacker, B. R., Glodny, J., Ratschbacher, L., Bi, S., Wu, Z., McWilliams, M. O., and Calvert, A.: Normal faulting in central Tibet since at least 13.5 Myr ago, Nature, 412, 628-632, 2001.

Bloom, A. J., Chapin, F. S., and Mooney, H. A.: Resource limitation in plants--an economic analogy, Annu. Rev. Ecol. Syst., 1985. 363-392, 1985.

Böhme, M.: The Miocene climatic optimum: evidence from ectothermic vertebrates of Central Europe, Palaeogeogr., Palaeoclimatol., Palaeoecol., 195, 389-401, 2003.

Böhme, M., Bruch, A. A., and Selmeier, A.: The reconstruction of Early and Middle Miocene climate and vegetation in Southern Germany as determined from the fossil wood flora, Palaeogeogr., Palaeoclimatol., Palaeoecol., 253, 91-114, 2007.

Bohra-Mishra, P., Oppenheimer, M., and Hsiang, S. M.: Nonlinear permanent migration response to climatic variations but minimal response to disasters, Proceedings of the National Academy of Sciences of the United States of America, 111, 9780-9785, 2014.

Bolch, T., Kulkarni, A., Kaab, A., Huggel, C., Paul, F., Cogley, J. G., Frey, H., Kargel, J. S., Fujita, K., Scheel, M., Bajracharya, S., and Stoffel, M.: The State and Fate of Himalayan Glaciers, Science, 336, 310-314, 2012.

Bonan, G. B., Levis, S., Kergoat, L., and Oleson, K. W.: Landscapes as patches of plant functional types: An integrating concept for climate and ecosystem models, Global Biogeochemical Cycles, 16, 2002.

Bond, W. J., Woodward, F. I., and Midgley, G. F.: The global distribution of ecosystems in a world without fire, New Phytol., 165, 525-537, 2005.

Bondarenko, O. V., Blokhina, N. I., and Utescher, T.: Quantification of Calabrian climate in southern Primory'e, Far East of Russia—An integrative case study using multiple proxies, Palaeogeogr., Palaeoclimatol., Palaeoecol., 386, 445-458, 2013.

Braconnot, P., Harrison, S. P., Kageyama, M., Bartlein, P. J., Masson-Delmotte, V., Abe-Ouchi, A., Otto-Bliesner, B., and Zhao, Y.: Evaluation of climate models using palaeoclimatic data, Nature Climate Change, 2, 417-424, 2012.

Breedlovestrout, R. L., Evraets, B. J., and Parrish, J. T.: New Paleogene paleoclimate analysis of western Washington using physiognomic characteristics from fossil leaves, Palaeogeogr Palaeocl, 392, 22-40, 2013.

Bruch, A., Utescher, T., Mosbrugger, V., Gabrielyan, I., and Ivanov, D.: Late Miocene climate in the circum-Alpine realm—a quantitative analysis of terrestrial palaeofloras, Palaeogeogr., Palaeoclimatol., Palaeoecol., 238, 270-280, 2006.

Budyko, M. I. and Sedunov, Y. S.: Anthropogenic climatic changes. In Conf. Climatic Change and Variability and Resulting Social, Economic and Technological Implications, Hamburg, Germany., 1988.

Burchfiel, B., Zhang, P., Wang, Y., Zhang, W., Song, F., Deng, Q., Molnar, P., and Royden, L.: Geology of the Haiyuan fault zone, Ningxia‐Hui Autonomous Region, China, and its relation to the evolution of the northeastern margin of the Tibetan Plateau, Tectonics, 10, 1091-1110, 1991.

Burnham, K. P. and Anderson, D. R.: Model selection and multimodel inference: a practical information-theoretic approach, Springer Science & Business Media, 2002.

Butzin, M., Lohmann, G., and Bickert, T.: Miocene ocean circulation inferred from marine carbon cycle modeling combined with benthic isotope records, Paleoceanography, 26, 2011.

Campbell, G. S. and Norman, J. M.: An introduction to environmental biophysics, 2th edn. Springer, NY., Springer Science & Business Media, 1998.

Cao, X. Y., Herzschuh, U., Ni, J., Zhao, Y., and Bohmer, T.: Spatial and temporal distributions of major tree taxa in eastern continental Asia during the last 22,000 years, Holocene, 25, 79-91, 2015.

Carey, M., Huggel, C., Bury, J., Portocarrero, C., and Haeberli, W.: An integrated socio-environmental framework for glacier hazard management and climate change

adaptation: lessons from Lake 513, Cordillera Blanca, Peru, Clim. Change, 112, 733-767, 2012.

Carrión, J. S.: A taphonomic study of modern pollen assemblages from dung and surface sediments in arid environments of Spain, Rev. Palaeobot. Palynol., 120, 217-232, 2002.

Information Department of Beijing Meteorological Center: Land climate data of China (1951–1980). China Meteorological Press, Beijing., 1983.

Chaloner, W. G. and Creber, G. T.: Do fossil plants give a climatic signal?, Journal of the Geological Society, 147, 343-350, 1990.

Chang, D.H.S.: The vegetation zonation of the Tibetan Plateau, Mt Res Dev, 29-48, 1981.

Cheddadi, R., Yu, G., Guiot, J., Harrison, S. P., and Prentice, I. C.: The climate of Europe 6000 years ago, Climate Dynamics, 13, 1-9, 1996.

Chen, D. G. and Pen, Z. C.: K-Ar ages and Pb, Sr isotopic characteristics of Cenozoic volcanic ropcks in Shandong, China, Geochimica, 4, 293-303, 1985.

Chen, W.-Y., Su, T., Adams, J. M., Jacques, F. M., Ferguson, D. K., and Zhou, Z.-K.: Large-scale dataset from China gives new insights into leaf margin–temperature relationships, Palaeogeogr., Palaeoclimatol., Palaeoecol., 402, 73-80, 2014.

Cheng, Y., Ferguson, D. K., Li, C., Jiang, X., and Wang, Y.: *Cedreloxylon coristalliferum*, a new record of angiosperm wood of Pliocene age from Yunnan, China, IAWA journal, 27, 145, 2006.

Chirilă, G. and Ţabără, D.: Palaeofloristic study of the Volhynian from Râşca (Moldavian Platform)-Palaeoclimatic and palaeoenvironment implications, Acta Palaeontologica Romaniae, VI, 29-42, 2008.

Church, J. A. and White, N. J.: Sea-level rise from the late 19th to the early 21st century, Surveys in Geophysics, 32, 585-602, 2011.

Coleman, M. and Hodges, K.: Evidence for Tibetan plateau uplift before 14 Myr ago from a new minimum age for east-west extension, Nature, 374, 49-52, 1995.

Collins, D. N.: Climatic warming, glacier recession and runoff from Alpine basins after the Little Ice Age maximum, Ann Glaciol, 48, 119-124, 2008.

Collins, M., R. Knutti, J. Arblaster, J.-L. Dufresne, T. Fichefet, and P. Friedlingstein, X. G., W.J. Gutowski, T. Johns, G. Krinner, M. Shongwe, C. Tebaldi, A.J. Weaver and M. Wehner: Long-term Climate Change: Projections, Commitments and Irreversibility. In: Climate Change 2013: The Physical Science Basis. Contribution of Working Group I to the Fifth Assessment Report of the Intergovernmental Panel on Climate Change [Stocker, T.F., D. Qin, G.-K. Plattner, M. Tignor, S.K. Allen, J. Boschung, A. Nauels, Y. Xia, V. Bex and P.M. Midgley (eds.)]. Cambridge University Press, Cambridge, United Kingdom and New York, NY, USA., 2013.

Collinvaux, P. A., De Oliveira, P. E., and Moreno, E.: Amazon: Pollen Manual and Atlas: Pollen Manual and Atlas, CRC Press, 2003.

Comiso, J. C.: Large Decadal Decline of the Arctic Multiyear Ice Cover, J. Clim., 25, 1176-1193, 2012.

Comiso, J. C., Parkinson, C. L., Gersten, R., and Stock, L.: Accelerated decline in the Arctic Sea ice cover, Geophys. Res. Lett., 35, 2008.

Cour, P., Zheng, Z., Duzer, D., Calleja, M., and Yao, Z.: Vegetational and climatic significance of modern pollen rain in northwestern Tibet, Rev. Palaeobot. Palynol., 104, 183-204, 1999.

Davis, B. A. S., Brewer, S., Stevenson, A. C., Guiot, J., and Contributors, D.: The temperature of Europe during the Holocene reconstructed from pollen data, Quaternary Science Reviews, 22, 1701-1716, 2003.

Davis, J. and Taylor, S.: Leaf physiognomy and climate: a multivariate analysis, Quatern. Res., 14, 337-348, 1980.

DeFries, R., Hansen, M., Townshend, J., Janetos, A., and Loveland, T.: A new global 1-km dataset of percentage tree cover derived from remote sensing, Global Change Biol., 6, 247-254, 2000.

Denton, F., T.J. Wilbanks, A.C. Abeysinghe, I. Burton, Q. Gao, M.C. Lemos, T. Masui, K.L. O'Brien, and Warner, K.: Climate-resilient pathways: adaptation, mitigation, and sustainable development. In: Climate Change 2014: Impacts, Adaptation, and Vulnerability. Part A: Global and Sectoral Aspects. Contribution of Working Group II to the Fifth Assessment Report of the Intergovernmental Panel on Climate Change [Field, C.B.,V.R. Barros, D.J. Dokken, K.J. Mach, M.D. Mastrandrea, T.E. Bilir, M. Chatterjee, K.L. Ebi, Y.O. Estrada,R.C. Genova, B. Girma, E.S. Kissel, A.N. Levy, S. MacCracken, P.R. Mastrandrea, and L.L. White (eds.)]. Cambridge University Press, Cambridge, United Kingdom and New York, NY, USA, pp. 1101-1131., 2014.

Diaz, S., Cabido, M., and Casanoves, F.: Plant functional traits and environmental filters at a regional scale, Journal of Vegetation Science, 9, 113-122, 1998.

Diaz, S., Noy-Meir, I., and Cabido, M.: Can grazing response of herbaceous plants be predicted from simple vegetative traits?, J. Appl. Ecol., 38, 497-508, 2001.

Dlugokencky, E. J., Myers, R. C., Lang, P. M., Masarie, K. A., Crotwell, A. M., Thoning, K. W., Hall, B. D., Elkins, J. W., and Steele, L. P.: Conversion of NOAA atmospheric dry air CH_4 mole fractions to a gravimetrically prepared standard scale, J Geophys Res-Atmos, 110, 2005.

Dolph, G. E. and Dilcher, D. L.: Variation in leaf size with respect to climate in Costa Rica, Biotropica, 91-99, 1980.

Dong, N., Prentice, I. C., Evans, B. J., Caddy-Retalic, S., Lowe, A. J., and Wright, I. J.: Leaf nitrogen from first principles: field evidence for adaptive variation with climate, Biogeosci. Disc., doi: 10.5194/bg-2016-89. , 2016a.

Dong, N., Prentice, I. C., Harrison, S. P., Song, Q. H., and Zhang, Y. P.: Biophysical homoeostasis of leaf temperature: a neglected process for vegetation and land-surface modelling, Global Ecol. Biogeogr., 2016b.

Dong, W.: Upper Cenozoic stratigraphy and palaeoenvirionment of Xiaolongtan basin, Kaiyuan, Yunnan Province. In: Deng, T., Wang, Y. (Eds.), Proceedings of the Eighth Annual Meeting of the Chinese Society of Vertebrate Paleontology. China Ocean Press, Beijing, pp. 91–100 (in Chinese with English abstract). 2001.

Dowsett, H., Robinson, M., Haywood, A., Salzmann, U., Hill, D., Sohl, L., Chandler, M., Williams, M., Foley, K., and Stoll, D.: The PRISM3D paleoenvironmental reconstruction, Stratigraphy, 7, 123-139, 2010.

Dowsett, H. J., Cronin, T. M., Poore, R. Z., Thompson, R. S., Whatley, R. C., and Wood, A. M.: Micropaleontological Evidence for Increased Meridional Heat-Transport in the North-Atlantic Ocean during the Pliocene, Science, 258, 1133-1135, 1992.

Dowsett, H. J., Robinson, M. M., Haywood, A. M., Hill, D. J., Dolan, A. M., Stoll, D. K., Chan, W.-L., Abe-Ouchi, A., Chandler, M. A., and Rosenbloom, N. A.: Assessing confidence in Pliocene sea surface temperatures to evaluate predictive models, Nature Climate Change, 2, 365-371, 2012.

Dulvy, N. K., Rogers, S. I., Jennings, S., Stelzenmuller, V., Dye, S. R., and Skjoldal, H. R.: Climate change and deepening of the North Sea fish assemblage: a biotic indicator of warming seas, J. Appl. Ecol., 45, 1029-1039, 2008.

Duque-Caro, H.: Neogene stratigraphy, paleoceanography and paleobiogeography in northwest South America and the evolution of the Panama Seaway, Palaeogeogr., Palaeoclimatol., Palaeoecol., 77, 203-234, 1990.

Ellenberg, H.: Site Conditions under Which Leaves Develop So-Called Drip Tips, Flora, 176, 169-188, 1985.

Erdei, B. and Bruch, A.: A climate analysis of Late Oligocene (Egerian) macrofloras from Hungary, Studia Botanica Hungarica, 34, 5-23, 2004.

Erdei, B., Hably, L., Kázmér, M., Utescher, T., and Bruch, A. A.: Neogene flora and vegetation development of the Pannonian domain in relation to palaeoclimate and palaeogeography, Palaeogeogr., Palaeoclimatol., Palaeoecol., 253, 115-140, 2007.

Etheridge, D. M., Steele, L. P., Francey, R. J., and Langenfelds, R. L.: Atmospheric methane between 1000 AD and present: Evidence of anthropogenic emissions and climatic variability, J Geophys Res-Atmos, 103, 15979-15993, 1998.

Etheridge, D. M., Steele, L. P., Langenfelds, R. L., Francey, R. J., Barnola, J. M., and Morgan, V. I.: Natural and anthropogenic changes in atmospheric CO_2 over the last 1000 years from air in Antarctic ice and firn, J Geophys Res-Atmos, 101, 4115-4128, 1996.

Fang, J., Wang, Z., and Tang, Z.: Atlas of woody plants in China: distribution and climate, Springer Science & Business Media, 2011.

Farr, T. G., Rosen, P. A., Caro, E., Crippen, R., Duren, R., Hensley, S., Kobrick, M., Paller, M., Rodriguez, E., Roth, L., Seal, D., Shaffer, S., Shimada, J., Umland, J., Werner, M., Oskin, M., Burbank, D., and Alsdorf, D.: The shuttle radar topography mission, Rev. Geophys., 45, 2007.

Fauquette, S., Guiot, J., and Suc, J. P.: A method for climatic reconstruction of the Mediterranean Pliocene using pollen data, Palaeogeogr Palaeocl, 144, 183-201, 1998.

Fauquette, S., Suc, J.-P., Guiot, J., Diniz, F., Feddi, N., Zheng, Z., Bessais, E., and Drivaliari, A.: Climate and biomes in the West Mediterranean area during the Pliocene, 152, 15-36, 1999.

Feng, S. Z., Krueger, A. B., and Oppenheimer, M.: Linkages among climate change, crop yields and Mexico-US cross-border migration, Proceedings of the National Academy of Sciences of the United States of America, 107, 14257-14262, 2010.

Ferguson, D. K., Zetter, R., and Paudayal, K. N.: The need for the SEM in palaeopalynology, Comptes Rendus Palevol, 6, 423-430, 2007.

Flato, G., J. Marotzke, B. Abiodun, P. Braconnot, S.C. Chou, W. Collins, P. Cox, F. Driouech, S. Emori, V. Eyring, C. Forest, P. Gleckler, E. Guilyardi, C. Jakob, V. Kattsov, Reason, C., and Rummukainen, M.: Evaluation of Climate Models. In: Climate Change 2013: The Physical Science Basis. Contribution of Working Group I to the Fifth Assessment Report of the Intergovernmental Panel on Climate Change [Stocker, T.F., D. Qin, G.-K. Plattner, M. Tignor, S.K. Allen, J. Boschung, A. Nauels, Y. Xia, V. Bex and P.M. Midgley (eds.)]. Cambridge University Press, Cambridge, United Kingdom and New York, NY, USA., 2013.

Fletcher, T. L.: Paleoclimate of the Dinosaur-Bearing, Mid-Cretaceous Winton Formation, Central-Western Queensland, Australia: New Observations Based on Leaf Margin Analysis, Climate Leaf Analysis Multivariate Program, Bioclimatic Analysis and Fossil Wood Growth Indices, J. Vert. Paleontol., 32, 94-95, 2012.

Fletcher, W. J., Goni, M. F. S., Peyron, O., and Dormoy, I.: Abrupt climate changes of the last deglaciation detected in a Western Mediterranean forest record, Climate of the Past, 6, 245-264, 2010.

Fonseca, C. R., Overton, J. M., Collins, B., and Westoby, M.: Shifts in trait-combinations along rainfall and phosphorus gradients, J. Ecol., 88, 964-977, 2000.

Foster, G.: Seawater pH, pCO_2 and [CO_3^{2-}] variations in the Caribbean Sea over the last 130 kyr: a boron isotope and B/Ca study of planktic foraminifera, Earth and Planetary Science Letters, 271, 254-266, 2008.

Foster, G. L., Lear, C. H., and Rae, J. W. B.: The evolution of pCO_2, ice volume and climate during the middle Miocene, Earth and Planetary Science Letters, 341, 243-254, 2012.

Franklin, J.: Mapping Species Distributions: Spatial Inference and Prediction, Cambridge University Press, Cambridge, UK, 2010.

Fricke, H. C. and Wing, S. L.: Oxygen isotope and paleobotanical estimates of temperature and $\delta^{18}O$–latitude gradients over North America during the early Eocene, Am. J. Sci., 304, 612-635, 2004.

Friedlingstein, P., Cox, P., Betts, R., Bopp, L., Von Bloh, W., Brovkin, V., Cadule, P., Doney, S., Eby, M., and Fung, I.: Climate-carbon cycle feedback analysis: Results from the C4MIP model intercomparison, J. Clim., 19, 3337-3353, 2006.

Gallego-Sala, A. V., Clark, J. M., House, J. I., Orr, H. G., Prentice, I. C., Smith, P., Farewell, T., and Chapman, S. J.: Bioclimatic envelope model of climate change impacts on blanket peatland distribution in Great Britain, Clim. Res., 45, 151-162, 2010.

Gao, Q., Li, X. B., and Yang, X. S.: Responses of vegetation and primary production in north-south transect of eastern China to global change under land use constraint, Acta Botanica Sinica, 45, 1274-1284, 2003.

Gardner, A. S.: A reconciled estimate of glacier contributions to sea level rise: 2003 to 2009, Science, 340, 1168-1168, 2013.

Gardner, A. S., Moholdt, G., Cogley, J. G., Wouters, B., Arendt, A. A., Wahr, J., Berthier, E., Hock, R., Pfeffer, W. T., Kaser, G., Ligtenberg, S. R. M., Bolch, T., Sharp, M. J., Hagen, J. O., van den Broeke, M. R., and Paul, F.: A Reconciled Estimate of Glacier Contributions to Sea Level Rise: 2003 to 2009, Science, 340, 852-857, 2013.

Gates, D. M.: Transpiration and Leaf Temperature, Ann Rev Plant Physio, 19, 211-238, 1968.

Gavin, D. G. and Hu, F. S.: Spatial variation of climatic and non-climatic controls on species distribution: the range limit of *Tsuga heterophylla*, J. Biogeogr., 33, 1384-1396, 2006.

Gebka, M., Mosbrugger, V., Schilling, H.-D., and Utescher, T.: Regional-scale palaeoclimate modelling on soft proxy-data basis—an example from the Upper Miocene of the Lower Rhine Embayment, Palaeogeogr., Palaeoclimatol., Palaeoecol., 152, 225-258, 1999.

Gedney, N., Cox, P. M., Betts, R. A., Boucher, O., Huntingford, C., and Stott, P. A.: Detection of a direct carbon dioxide effect in continental river runoff records, Nature, 439, 835-838, 2006.

Gerten, D., Rost, S., von Bloh, W., and Lucht, W.: Causes of change in 20th century global river discharge, Geophys. Res. Lett., 35, 2008.

Givnish, T.: Leaf and canopy adaptations in tropical forests. In: Physiological ecology of plants of the wet tropics, Springer, 1984.

Givnish, T. J. and Vermeij, G. J.: Sizes and shapes of liane leaves, Am. Nat., 110, 743-778, 1976.

Goldner, A., Huber, M., and Caballero, R.: Does Antarctic glaciation cool the world?, Climate of the Past, 9, 173-189, 2013.

Google: Earth V 6.2.2.6613. (September 30, 2010). The Tibetan Plateau 25–45°N, 70–105°E, Eye Alt 7136.38 km. http://www.earth.google.com [April 26, 2012]. 2012.

Green, W. A.: Loosening the clamp: An exploratory graphical approach to the Climate Leaf Analysis Multivariate Program, Palaeontologia Electronica, 9, 2006.

Greenwood, D.: Palaeobotanical evidence for Tertiary climates, History of the Australian vegetation cretaceous to recent, pp. 44-59, 1994.

Greenwood, D. R.: Leaf form and the reconstruction of past climates, New Phytol., 166, 355-357, 2005.

Greenwood, D. R.: Taphonomic constraints on foliar physiognomie interpretations of Late Cretaceous and tertiary palaeoeclimates, Rev. Palaeobot. Palynol., 71, 149-190, 1992.

Greenwood, D. R., Archibald, S. B., Mathewes, R. W., and Moss, P. T.: Fossil biotas from the Okanagan Highlands, southern British Columbia and northeastern Washington State: climates and ecosystems across an Eocene landscape, Canadian Journal of Earth Sciences, 42, 167-185, 2005.

Greenwood, D. R., Wilf, P., Wing, S. L., and Christophel, D. C.: Paleotemperature estimation using leaf-margin analysis: is Australia different?, Palaios, 19, 129-142, 2004.

Greenwood, D. R. and Wing, S. L.: Eocene continental climates and latitudinal temperature gradients, Geology, 23, 1044-1048, 1995.

Gregory, K. M. and Chase, C. G.: Tectonic Significance of Paleobotanically Estimated Climate and Altitude of the Late Eocene Erosion Surface, Colorado, Geology, 20, 581-585, 1992.

Gregory-Wodzicki, K. M.: Relationships between leaf morphology and climate, Bolivia: implications for estimating paleoclimate from fossil floras, Paleobiology, 26, 668-688, 2000.

Grein, M., Utescher, T., Wilde, V., and Roth-Nebelsick, A.: Reconstruction of the middle Eocene climate of Messel using palaeobotanical data, Neues Jahrb Geol P-A, 260, 305-318, 2011.

Grichuk, V.: An attempt of reconstruction of certain climatic indexes of the Northern hemisphere during the Atlantic stage of the Holocene, 1969.

Grimm, G., Denk, T., Bouchal, J. M., and Potts, A. J.: Fables and foibles: a critical analysis of the Palaeoflora database and the Coexistence approach for palaeoclimate reconstruction, bioRxiv, doi: 10.1101/016378, 2015.

Grimm, G. W. and Denk, T.: Reliability and resolution of the coexistence approach—a revalidation using modern-day data, Rev. Palaeobot. Palynol., 172, 33-47, 2012.

Grímsson, F. and Zetter, R.: Combined LM and SEM study of the Middle Miocene (Sarmatian) palynoflora from the Lavanttal Basin, Austria: Part II. Pinophyta (Cupressaceae, Pinaceae and Sciadopityaceae), Grana, 50, 262-310, 2011.

Guiot, J.: Methodology of the Last Climatic Cycle Reconstruction in France from Pollen Data, Palaeogeogr Palaeocl, 80, 49-69, 1990.

Guiot, J.: Statistical analyses of biospherical variability. In: Long-Term Climatic Variations, Springer, 1994.

Guiot, J., Boreux, J. J., Braconnot, P., Torre, F., and PMIP Participants: Data-model comparison using fuzzy logic in paleoclimatology, Climate Dynamics, 15, 569-581, 1999.

Hancock, P. A. and Hutchinson, M. F.: Spatial interpolation of large climate data sets using bivariate thin plate smoothing splines, Environ. Model. Software, 21, 1684-1694, 2006.

Hansen, J., Ruedy, R., Sato, M., and Lo, K.: Global Surface Temperature Change, Rev. Geophys., 48, 2010.

Hao, H., Ferguson, D. K., Feng, G.-P., Ablaev, A., Wang, Y.-F., and Li, C.-S.: Early Paleocene vegetation and climate in Jiayin, NE China, Clim. Change, 99, 547-566, 2010.

Haque, C. E.: Atmospheric hazards preparedness in Bangladesh: A study of warning, adjustments and recovery from the April 1991 cyclone, Nat. Hazards, 16, 181-202, 1997.

Harris, I., Jones, P. D., Osborn, T. J., and Lister, D. H.: Updated high-resolution grids of monthly climatic observations–the CRU TS3. 10 Dataset, International Journal of Climatology, 34, 623-642, 2014.

Harrison, S., Bartlein, P., Izumi, K., Li, G., Annan, J., Hargreaves, J., Braconnot, P., and Kageyama, M.: Evaluation of CMIP5 palaeo-simulations to improve climate projections, Nature Climate Change, 5, 735-743, 2015.

Harrison, S. P., Prentice, I. C., Barboni, D., Kohfeld, K. E., Ni, J., and Sutra, J. P.: Ecophysiological and bioclimatic foundations for a global plant functional classification, Journal of Vegetation Science, 21, 300-317, 2010.

Harrison, T. M., Copeland, P., Kidd, W. S. F., and Lovera, O. M.: Activation of the Nyainqentanghla Shear Zone: Implications for uplift of the southern Tibetan Plateau, Tectonics, 14, 658-676, 1995.

Hartmann, D. L., Tank, A. M. G. K., Rusticucci, M., Alexander, L. V., Brönnimann, S., Charabi, Y., Dentener, F. J., Easterling, E. J. D. D. R., Kaplan, A., Soden, B. J., Thorne, P. W., Wild, M., and Zhai, P. M.: Observations: Atmosphere and Surface. In: Climate Change 2013: The Physical Science Basis. Contribution of Working Group I to the Fifth Assessment Report of the Intergovernmental Panel on Climate Change [Stocker, T.F., D. Qin, G.-K. Plattner, M. Tignor, S.K. Allen, J. Boschung, A. Nauels, Y. Xia, V. Bex and P.M. Midgley (eds.)]. Cambridge University Press, Cambridge, United Kingdom and New York, NY, USA., 2013.

Haywood, A. M., Dowsett, H. J., Otto-Bliesner, B., Chandler, M. A., Dolan, A. M., Hill, D. J., Lunt, D. J., Robinson, M. M., Rosenbloom, N., Salzmann, U., and Sohl, L. E.: Pliocene Model Intercomparison Project (PlioMIP): experimental design and boundary conditions (Experiment 1), Geoscientific Model Development, 3, 227-242, 2010.

Haywood, A. M., Dowsett, H. J., Robinson, M. M., Stoll, D. K., Dolan, A. M., Lunt, D. J., Otto-Bliesner, B., and Chandler, M. A.: Pliocene Model Intercomparison Project (PlioMIP): experimental design and boundary conditions (Experiment 2), Geoscientific Model Development, 4, 571-577, 2011.

Haywood, A. M., Hill, D. J., Dolan, A. M., Otto-Bliesner, B. L., Bragg, F., Chan, W. L., Chandler, M. A., Contoux, C., Dowsett, H. J., Jost, A., Kamae, Y., Lohmann, G., Lunt, D. J., Abe-Ouchi, A., Pickering, S. J., Ramstein, G., Rosenbloom, N. A., Salzmann, U., Sohl, L., Stepanek, C., Ueda, H., Yan, Q., and Zhang, Z.: Large-scale features of Pliocene climate: results from the Pliocene Model Intercomparison Project, Climate of the Past, 9, 191-209, 2013.

Heinemann, M., Jungclaus, J. H., and Marotzke, J.: Warm Paleocene/Eocene climate as simulated in ECHAM5/MPI-OM, Climate of the Past, 5, 785-802, 2009.

Herold, N., Huber, M., and Müller, R.: Modeling the Miocene Climatic Optimum. Part I: Land and Atmosphere, J. Clim., 24, 6353-6372, 2011.

Herold, N., Müller, R., and Seton, M.: Comparing early to middle Miocene terrestrial climate simulations with geological data, Geosphere, 6, 952-961, 2010.

Herzschuh, U.: Reliability of pollen ratios for environmental reconstructions on the Tibetan Plateau, J. Biogeogr., 34, 1265-1273, 2007.

Herzschuh, U., Birks, H. J. B., Mischke, S., Zhang, C. J., and Böhner, J.: A modern pollen–climate calibration set based on lake sediments from the Tibetan Plateau and its application to a Late Quaternary pollen record from the Qilian Mountains, J. Biogeogr., 37, 752-766, 2010.

Hesse, M., Halbritter, H., Weber, M., Buchner, R., Frosch-Radivo, A., and Ulrich, S.: Pollen terminology: an illustrated handbook, Springer Science & Business Media, 2009.

Hickey, L. J.: Stratigraphy and paleobotany of the Golden Valley Formation (early Tertiary) of western North Dakota, Geological Society of America Memoirs, 150, 1-296, 1977.

Hinojosa, L. F., Pérez, F., Gaxiola, A., and Sandoval, I.: Historical and phylogenetic constraints on the incidence of entire leaf margins: insights from a new South American model, Global Ecol. Biogeogr., 20, 380-390, 2011.

Hjelmroos, M. and Franzen, L. G.: Implications of recent long-distance pollen transport events for the interpretation of fossil pollen records in Fennoscandia, Rev. Palaeobot. Palynol., 82, 175-189, 1994.

Ho, K., Chen, J., Lo, C., and Zhao, H.: ^{40}Ar–^{39}Ar dating and geochemical characteristics of late Cenozoic basaltic rocks from the Zhejiang–Fujian region, SE China: eruption ages, magma evolution and petrogenesis, Chemical Geology, 197, 287-318, 2003.

Hodell, D. A. and Woodruff, F.: Variations in the Strontium Isotopic Ratio of Seawater during the Miocene - Stratigraphic and Geochemical Implications, Paleoceanography, 9, 405-426, 1994.

Holmes, M. G. and Keiller, D. R.: Effects of pubescence and waxes on the reflectance of leaves in the ultraviolet and photosynthetic wavebands: a comparison of a range of species, Plant, Cell Environ., 25, 85-93, 2002.

Hong, Y.: Discovery of new fossil Pseudoscorpionids in amber. Bulletin of the Tianjin Institute of Geology and Mineral Resources. Chinese Academy of Geological Sciences 8, 23–29 (in Chinese, with English abstract). W. Szafer Institute of Botany, Polish Acadamy of Sciences, 1983.

Hong, Y., Guo, X., and Ren, D.: A new genus-Eopalpomyitis gen. nov. from Eocene Fushun amber and discussion of its taxonomic position, Acta Parasitologica et Medica Entomologica Sinica, 7, 225-234, 2000.

Hong, Y., Yang, T., Wang, S., Wang, S., Li, Y., Sun, M., Sun, H., and Tu, N.: Stratigraphy and palaeontology of Fushun coal-field, Liaoning Province. Acta Geologica Sinica 48 (2), 113–150 (pls. 8 (in Chinese with English abstract)). W. Szafer Institute of Botany, Polish Acadamy of Sciences, 1974.

Hong, Y. C., Yang, Z. Q., Wang, S. T., Sun, X. J., Du, N. Q., Sun, M. R., and Li, Y. G.: A Research on the Strata and Palaeontology of the Fushun Coal Field in Liaoning Province. Science Press, Beijing. (in Chinese). 1980.

Hönisch, B., Hemming, N. G., Archer, D., Siddall, M., and McManus, J. F.: Atmospheric carbon dioxide concentration across the mid-Pleistocene transition, Science, 324, 1551-1554, 2009.

Hoorn, C., Straathof, J., Abels, H. A., Xu, Y., Utescher, T., and Dupont-Nivet, G.: A late Eocene palynological record of climate change and Tibetan Plateau uplift (Xining Basin, China), Palaeogeogr., Palaeoclimatol., Palaeoecol., 344, 16-38, 2012.

Hu, Y. Q.: The vegetation and quantitative climate reconstruction of early pliocene in Shengzhou, Zhejiang, Eastern China, State Key Laboratory of Systematic and Evolutionary Botany. Institute of Botany, Chinese Academy of Sciences, Beijing (in Chinese), 2007.

Huang, C. X., Van Compo, E., and Dobremez, J. F.: A study on pollen in surface soil from the western Xizang, Arid Land Geography, 16, 75-84, 1993.

Huber, M. and Caballero, R.: The early Eocene equable climate problem revisited, Climate of the Past, 7, 603-633, 2011.

Huber, M. and Sloan, L. C.: Heat transport, deep waters, and thermal gradients: Coupled simulation of an Eocene greenhouse climate, Geophys. Res. Lett, 28, 3481-3484, 2001.

Huggel, C., L. Blaškovičová, H. Breien, P. Dobesberger, R. Frauenfelder, B.G. Kalsnes, A. Solheim, M. Stankoviansky, K. Hagen, and Kronholm, K.: Landslide and rock slope failures. In: Impacts of Climate Change on Snow, Ice, and Permafrost in Europe: Observed Trends, Future Projections, and Socio-Economic Relevance [Voigt, T., H.M.

Füssel, I. Gärtner-Roer, C. Huggel, C. Marty, and M. Zemp (eds.)]. ETC/ACC Technical Paper 2010/13, Prepared by the European Topic Centre on Air and Climate Change (ETC/ACC) with the Department of Geography of the University of Zuerich, the WSL Institute for Snow and Avalanche Research (SLF) Davos and others for the European Environment Agency (EEA), ETC/ACC, Bilthoven, Netherlands, pp. 95-101., 2011.

Huntley, B., Spicer, R. A., Chaloner, W. G., and Jarzembowski, E. A.: The Use of Climate Response Surfaces to Reconstruct Palaeoclimate from Quaternary Pollen and Plant Macrofossil Data [and Discussion], Philosophical Transactions of the Royal Society of London B: Biological Sciences, 341, 215-224, 1993.

Hyland, E. G. and Sheldon, N. D.: Coupled CO_2-climate response during the Early Eocene Climatic Optimum, Palaeogeogr Palaeocl, 369, 125-135, 2013.

IEA: CO_2 Emissions from Fuel Combustion. Beyond 2020 Online Database. Available at: http://data.iea.org., 2012.

Ivanov, D., Ashraf, A., Mosbrugger, V., and Palamarev, E.: Palynological evidence for Miocene climate change in the Forecarpathian Basin (central Paratethys, NW Bulgaria), Palaeogeogr., Palaeoclimatol., Palaeoecol., 178, 19-37, 2002.

Iversen, J.: Viscum, Hedera and Ilex as climate indicators: A contribution to the study of the post-glacial temperature climate, GFF, 66, 463-483, 1944.

Izumi, K., Bartlein, P. J., and Harrison, S. P.: Consistent behaviour of the climate system in response to past and future forcing, Geophys. Res. Lett., 40, 1-7, 2013.

Jackson, J. E.: A User's Guide to Principal Components. Wiley, New York., 1991.

Jacobs, B. F.: Estimation of low-latitude paleoclimates using fossil angiosperm leaves: examples from the Miocene Tugen Hills, Kenya, Paleobiology, 28, 399-421, 2002.

Jacques, F. M., Su, T., Spicer, R. A., Xing, Y., Huang, Y., Wang, W., and Zhou, Z.: Leaf physiognomy and climate: Are monsoon systems different?, Global Planet. Change, 76, 56-62, 2011a.

Jacques, F. M. B., Guo, S. X., Su, T., Xing, Y. W., Huang, Y. J., Liu, Y. S., Ferguson, D. K., and Zhou, Z. K.: Quantitative reconstruction of the Late Miocene monsoon climates of southwest China: A case study of the Lincang flora from Yunnan Province, Palaeogeogr Palaeocl, 304, 318-327, 2011b.

Jevrejeva, S., Moore, J., Grinsted, A., and Woodworth, P.: Recent global sea level acceleration started over 200 years ago?, Geophys. Res. Lett., 35, 2008.

Jiang, H. and Ding, Z.: Spatial and temporal characteristics of Neogene palynoflora in China and its implication for the spread of steppe vegetation, J. Arid Environ., 73, 765-772, 2009.

Jiménez Cisneros, B. E., T. Oki, N.W. Arnell, G. Benito, J.G. Cogley, P. Döll, T. Jiang, and Mwakalila, S. S.: Impacts, Adaptation, and Vulnerability. Part A: Global and Sectoral Aspects. Contribution of Working Group II to the Fifth Assessment Report of the Intergovernmental Panel on Climate Change [Field, C.B., V.R. Barros, D.J. Dokken, K.J.

Mach, M.D. Mastrandrea, T.E. Bilir, M. Chatterjee, K.L. Ebi, Y.O. Estrada, R.C. Genova, B. Girma, E.S. Kissel, A.N. Levy, S. MacCracken, P.R. Mastrandrea, and L.L. White (eds.)]. Cambridge University Press, Cambridge, United Kingdom and New York, NY, USA, pp. 229-269., 2014.

Jobson, J. D.: Applied Multivariate Data Analysis, Vol. 2. Springer-Verlag, New York., 1992.

Johnson, E. A.: Geology of the Fushun coalfield, Liaoning province, People's Republic of China, International Journal of Coal Geology, 14, 217-236, 1990.

Johnson, H. B.: Plant Pubescence - Ecological Perspective, Bot. Rev., 41, 233-258, 1975.

Jolley, D. W. and Widdowson, M.: Did Paleogene North Atlantic rift-related eruptions drive early Eocene climate cooling?, Lithos, 79, 355-366, 2005.

Jones, P., Lister, D., Osborn, T., Harpham, C., Salmon, M., and Morice, C.: Hemispheric and large ‐ scale land ‐ surface air temperature variations: An extensive revision and an update to 2010, Journal of Geophysical Research: Atmospheres (1984–2012), 117, 2012.

Joos, F. and Spahni, R.: Rates of change in natural and anthropogenic radiative forcing over the past 20,000 years, Proceedings of the National Academy of Sciences, 105, 1425-1430, 2008.

Jordan, G. J.: Uncertainty in palaeoclimatic reconstructions based on leaf physiognomy, Aust. J. Bot., 45, 527-547, 1997.

Jost, A., Lunt, D., Kageyama, M., Abe-Ouchi, A., Peyron, O., Valdes, P. J., and Ramstein, G.: High-resolution simulations of the last glacial maximum climate over Europe: a solution to discrepancies with continental palaeoclimatic reconstructions?, Climate Dynamics, 24, 577-590, 2005.

Joussaume, S., Taylor, K. E., Braconnot, P., Mitchell, J. F. B., Kutzbach, J. E., Harrison, S. P., Prentice, I. C., Broccoli, A. J., Abe-Ouchi, A., Bartlein, P. J., Bonfils, C., Dong, B., Guiot, J., Herterich, K., Hewitt, C. D., Jolly, D., Kim, J. W., Kislov, A., Kitoh, A., Loutre, M. F., Masson, V., McAvaney, B., McFarlane, N., de Noblet, N., Peltier, W. R., Peterschmitt, J. Y., Pollard, D., Rind, D., Royer, J. F., Schlesinger, M. E., Syktus, J., Thompson, S., Valdes, P., Vettoretti, G., Webb, R. S., and Wyputta, U.: Monsoon changes for 6000 years ago: Results of 18 simulations from the Paleoclimate Modeling Intercomparison Project (PMIP), Geophys. Res. Lett., 26, 859-862, 1999.

JRC/PBL: Emission Database for Global Atmospheric Research (EDGAR), Release Version 4.2 FT2010. European Commission, Joint Research Centre (JRC)/PBL Netherlands Environmental Assessment Agency. Available at: http://edgar.jrc.ec.europa.eu., 2013.

Karim, M. F. and Mimura, N.: Impacts of climate change and sea-level rise on cyclonic storm surge floods in Bangladesh, Global Environ Chang, 18, 490-500, 2008.

Kattge, J., Diaz, S., Lavorel, S., Prentice, C., Leadley, P., Bonisch, G., Garnier, E., Westoby, M., Reich, P. B., Wright, I. J., Cornelissen, J. H. C., Violle, C., Harrison, S. P., van Bodegom,

P. M., Reichstein, M., Enquist, B. J., Soudzilovskaia, N. A., Ackerly, D. D., Anand, M., Atkin, O., Bahn, M., Baker, T. R., Baldocchi, D., Bekker, R., Blanco, C. C., Blonder, B., Bond, W. J., Bradstock, R., Bunker, D. E., Casanoves, F., Cavender-Bares, J., Chambers, J. Q., Chapin, F. S., Chave, J., Coomes, D., Cornwell, W. K., Craine, J. M., Dobrin, B. H., Duarte, L., Durka, W., Elser, J., Esser, G., Estiarte, M., Fagan, W. F., Fang, J., Fernandez-Mendez, F., Fidelis, A., Finegan, B., Flores, O., Ford, H., Frank, D., Freschet, G. T., Fyllas, N. M., Gallagher, R. V., Green, W. A., Gutierrez, A. G., Hickler, T., Higgins, S. I., Hodgson, J. G., Jalili, A., Jansen, S., Joly, C. A., Kerkhoff, A. J., Kirkup, D., Kitajima, K., Kleyer, M., Klotz, S., Knops, J. M. H., Kramer, K., Kuhn, I., Kurokawa, H., Laughlin, D., Lee, T. D., Leishman, M., Lens, F., Lenz, T., Lewis, S. L., Lloyd, J., Llusia, J., Louault, F., Ma, S., Mahecha, M. D., Manning, P., Massad, T., Medlyn, B. E., Messier, J., Moles, A. T., Muller, S. C., Nadrowski, K., Naeem, S., Niinemets, U., Nollert, S., Nuske, A., Ogaya, R., Oleksyn, J., Onipchenko, V. G., Onoda, Y., Ordonez, J., Overbeck, G., Ozinga, W. A., Patino, S., Paula, S., Pausas, J. G., Penuelas, J., Phillips, O. L., Pillar, V., Poorter, H., Poorter, L., Poschlod, P., Prinzing, A., Proulx, R., Rammig, A., Reinsch, S., Reu, B., Sack, L., Salgado-Negre, B., Sardans, J., Shiodera, S., Shipley, B., Siefert, A., Sosinski, E., Soussana, J. F., Swaine, E., Swenson, N., Thompson, K., Thornton, P., Waldram, M., Weiher, E., White, M., White, S., Wright, S. J., Yguel, B., Zaehle, S., Zanne, A. E., and Wirth, C.: TRY - a global database of plant traits, Global Change Biol., 17, 2905-2935, 2011.

Keddy, P. A.: Assembly and response rules: two goals for predictive community ecology, Journal of Vegetation Science, 3, 157-164, 1992.

Kirtman, B., S.B. Power, J.A. Adedoyin, G.J. Boer, R. Bojariu, I. Camilloni, F.J. Doblas-Reyes, A.M. Fiore, M. Kimoto, G.A. Meehl, M. Prather, A. Sarr, C. Schär, R. Sutton, G.J. van Oldenborgh, G. Vecchi, and Wang, H. J.: Near-term Climate Change: Projections and Predictability. In: Climate Change 2013: The Physical Science Basis. Contribution of Working Group I to the Fifth Assessment Report of the Intergovernmental Panel on Climate Change [Stocker, T.F., D. Qin, G.-K. Plattner, M. Tignor, S.K. Allen, J. Boschung, A. Nauels, Y. Xia, V. Bex and P.M. Midgley (eds.)]. Cambridge University Press, Cambridge, United Kingdom and New York, NY, USA., 2013.

Kou, X. Y., Ferguson, D. K., Xu, J. X., Wang, Y. F., and Li, C. S.: The reconstruction of paleovegetation and paleoclimate in the Late Pliocene of West Yunnan, China, Clim. Change, 77, 431-448, 2006.

Kovar-Eder, J., Kvaček, Z., Martinetto, E., and Roiron, P.: Late Miocene to Early Pliocene vegetation of southern Europe (7–4Ma) as reflected in the megafossil plant record, Palaeogeogr., Palaeoclimatol., Palaeoecol., 238, 321-339, 2006.

Kowalski, E. A. and Dilcher, D. L.: Warmer paleotemperatures for terrestrial ecosystems, Proceedings of the National academy of Sciences, 100, 167-170, 2003.

Krakauer, N. Y. and Fung, I.: Mapping and attribution of change in streamflow in the coterminous United States, Hydrol Earth Syst Sc, 12, 1111-1120, 2008.
Krawchuk, M. A., Cumming, S. G., and Flannigan, M. D.: Predicted changes in fire weather suggest increases in lightning fire initiation and future area burned in the mixedwood boreal forest, Clim. Change, 92, 83-97, 2009.

Kundzewicz, Z. W., L.J. Mata, N.W. Arnell, P. Döll, P. Kabat, B. Jiménez, K.A. Miller, T. Oki, Sen, Z., and Shiklomanov, I. A.: Freshwater resources and their management. Climate Change 2007: Impacts, Adaptation and Vulnerability. Contribution of Working Group II

to the Fourth Assessment Report of the Intergovernmental Panel on Climate Change, M.L. Parry, O.F. Canziani, J.P. Palutikof, P.J. van der Linden and C.E. Hanson, Eds., Cambridge University Press, Cambridge, UK, 173-210., 2007.

Kunreuther, H., S. Gupta, V. Bosetti, R. Cooke, V. Dutt, M. Ha-Duong, H. Held, J. Llanes-Regueiro, A. P., and E. Shittu, a. E. W.: Integrated Risk and Uncertainty Assessment of Climate Change Response Policies. In: Climate Change 2014: Mitigation of Climate Change. Contribution of Working Group III to the Fifth Assessment Report of the Intergovernmental Panel on Climate Change [Edenhofer, O., R. Pichs-Madruga, Y. Sokona, E. Farahani, S. Kadner, K. Seyboth, A. Adler, I. Baum, S. Brunner, P. Eickemeier, B. Kriemann, J. Savolainen, S. Schlömer, C. von Stechow, T. Zwickel and J.C. Minx (eds.)]. Cambridge University Press, Cambridge, United Kingdom and New York, NY, USA., 2014.

Kurschner, W. M., Kvacek, Z., and Dilcher, D. L.: The impact of Miocene atmospheric carbon dioxide fluctuations on climate and the evolution of terrestrial ecosystems, Proc. Natl. Acad. Sci. USA, 105, 449-453, 2008.

Kutzbach, J., Guetter, P., Ruddiman, W., and Prell, W.: Sensitivity of climate to late Cenozoic uplift in southern Asia and the American west: numerical experiments, Journal of Geophysical Research: Atmospheres (1984–2012), 94, 18393-18407, 1989.

Kutzbach, J., Prell, W., and Ruddiman, W. F.: Sensitivity of Eurasian climate to surface uplift of the Tibetan Plateau, The Journal of Geology, 177-190, 1993.

Labat, D., Godderis, Y., Probst, J. L., and Guyot, J. L.: Evidence for global runoff increase related to climate warming, Adv Water Resour, 27, 631-642, 2004.

Lange, O. L.: Untersuchungen über Wärmehaushalt und Hitzeresistenz mauretanischer Wüsten-und Savannenpflanzen, Flora. Gustav Fischer Verlag, Jena, 1959.

Lapola, D. M., Oyama, M. D., Nobre, C. A., and Sampaio, G.: A new world natural vegetation map for global change studies, An Acad Bras Cienc, 80, 397-408, 2008.

Larsen, W. A. and McCleary, S. J.: The use of partial residual plots in regression analysis, Technometrics, 14, 781-790, 1972.

Lavorel, S., Díaz, S., Cornelissen, J. H. C., Garnier, E., Harrison, S. P., McIntyre, S., Pausas, J. G., Pérez-Harguindeguy, N., Roumet, C., and Urcelay, C.: Plant functional types: are we getting any closer to the Holy Grail? In: Terrestrial ecosystems in a changing world, Springer, 2007.

Lavorel, S. and Garnier, E.: Predicting changes in community composition and ecosystem functioning from plant traits: revisiting the Holy Grail, Funct. Ecol., 16, 545-556, 2002.

Lawrimore, J. H., Menne, M. J., Gleason, B. E., Williams, C. N., Wuertz, D. B., Vose, R. S., and Rennie, J.: An overview of the Global Historical Climatology Network monthly mean temperature data set, version 3, J Geophys Res-Atmos, 116, 2011.

Levitus, S., Antonov, J., Boyer, T., Locarnini, R., Garcia, H., and Mishonov, A.: Global ocean heat content 1955–2008 in light of recently revealed instrumentation problems, Geophys. Res. Lett., 36, 2009.

Li, G., Harrison, S., and Prentice, I.: A model analysis of climate and CO_2 controls on tree growth in a semi-arid woodland, Biogeosci. Disc., 12, 4769-4800, 2015a.

Li, G., Harrison, S. P., Bartlein, P. J., Izumi, K., and Colin Prentice, I.: Precipitation scaling with temperature in warm and cold climates: An analysis of CMIP5 simulations, Geophys. Res. Lett., 40, 4018-4024, 2013.

Li, J.-F., Ferguson, D. K., Yang, J., Feng, G.-P., Ablaev, A. G., Wang, Y.-F., and Li, C.-S.: Early Miocene vegetation and climate in Weichang District, North China, Palaeogeogr., Palaeoclimatol., Palaeoecol., 280, 47-63, 2009.

Li, J.-F., Hu, Y.-Q., Ferguson, D. K., Wang, Y.-F., and Li, C.-S.: An Early Pliocene lake and its surrounding vegetation in Zhejiang, East China, J. Paleolimnol., 43, 751-769, 2010.

Li, J.-J., Fang, X.-M., Van der Voo, R., Zhu, J.-J., Mac Niocaill, C., Cao, J.-X., Zhong, W., Chen, H.-L., Wang, J., and Wang, J.-M.: Late Cenozoic magnetostratigraphy (11–0 Ma) of the Dongshanding and Wangjiashan sections in the Longzhong Basin, western China, Geologie en Mijnbouw, 76, 121-134, 1997.

Li, S. F., Mao, L. M., Spicer, R. A., Lebreton-Anberree, J., Su, T., Sun, M., and Zhou, Z. K.: Late Miocene vegetation dynamics under monsoonal climate in southwestern China, Palaeogeogr Palaeocl, 425, 14-40, 2015b.

Li, T. Q.: Pollen Flora of China Woody Plants by SEM, Science Press, 2011.

Li, X., Li, C., Lu, H., Dodson, J., and Wang, Y.: Paleovegetation and paleoclimate in middle–late Pliocene, Shanxi, central China, Palaeogeogr., Palaeoclimatol., Palaeoecol., 210, 57-66, 2004.

Li, X. Q. and Du, N. Q.: The acid-alkali-free analysis of Quaternary pollen, Acta Botanica Sinica, 41, 782-784, 1998.

Liang, M. M., Bruch, A., Collinson, M., Mosbrugger, V., Li, C. S., Sun, Q. G., and Hilton, J.: Testing the climatic estimates from different palaeobotanical methods: an example from the Middle Miocene Shanwang flora of China, Palaeogeogr Palaeocl, 198, 279-301, 2003.

Linacre, E.: A note on a feature of leaf and air temperatures, Agricultural Meteorology, 1, 66-72, 1964.

Little, S. A., Kembel, S. W., and Wilf, P.: Paleotemperature proxies from leaf fossils reinterpreted in light of evolutionary history, PLoS One, 5, e15161, 2010.

Liu, C. L., Golding, D., and Gong, G.: Farmers' coping response to the low flows in the lower Yellow River: A case study of temporal dimensions of vulnerability, Global Environ Chang, 18, 543-553, 2008.

Lobell, D. B., Schlenker, W., and Costa-Roberts, J.: Climate Trends and Global Crop Production Since 1980, Science, 333, 616-620, 2011.

Losada, I. J., Reguero, B. G., Mendez, F. J., Castanedo, S., Abascal, A. J., and Minguez, R.: Long-term changes in sea-level components in Latin America and the Caribbean, Global Planet. Change, 104, 34-50, 2013.

Lowenstein, T. K. and Demicco, R. V.: Elevated Eocene atmospheric CO_2 and its subsequent decline, Science, 313, 1928-1928, 2006.

Lu, H. Y., Wu, N. Q., Liu, K. B., Zhu, L. P., Yang, X. D., Yao, T. D., Wang, L., Li, Q. A., Liu, X. Q., Shen, C. M., Li, X. Q., Tong, G. B., and Jiang, H.: Modern pollen distributions in Qinghai-Tibetan Plateau and the development of transfer functions for reconstructing Holocene environmental changes, Quaternary Science Reviews, 30, 947-966, 2011.

Lu, H. Y., Wu, N. Q., Yang, X. D., Shen, C. M., Zhu, L. P., Wang, L., Li, Q. A., Xu, D. K., Tong, G. B., and Sun, X. J.: Spatial pattern of *Abies* and *Picea* surface pollen distribution along the elevation gradient in the Qinghai-Tibetan Plateau and Xinjiang, China, Boreas, 37, 254-262, 2008.

Lu, X. M., Chen, H., and Xu, Q. H.: Surface pollen and its relationship to vegetation on the southern slope of the eastern Qilian Mountains, Journal of Geographical Sciences, 16, 215-222, 2006.

Lu, X. M., Herrmann, M., Mosbrugger, V., Yao, T. D., and Zhu, L. P.: Airborne pollen in the Nam Co Basin and its implication for palaeoenvironmental reconstruction, Rev. Palaeobot. Palynol., 163, 104-112, 2010.

Lunt, D. J., Dunkley Jones, T., Heinemann, M., Huber, M., LeGrande, A., Winguth, A., Loptson, C., Marotzke, J., Roberts, C., and Tindall, J.: A model–data comparison for a multi-model ensemble of early Eocene atmosphere–ocean simulations: EoMIP, Climate of the Past, 8, 1717-1736, 2012.

Lunt, D. J., Valdes, P. J., Dunkley Jones, T., Ridgwell, A., Haywood, A. M., Schmidt, D. N., Marsh, R., and Maslin, M.: CO_2-driven ocean circulation changes as an amplifier of Paleocene-Eocene thermal maximum hydrate destabilization, Geology, 38, 875-878, 2010.

MacGinitie, H. D.: Middle Eocene flora from the central Sierra Nevada, 1941.

Macknick, J.: Energy and CO_2 emission data uncertainties, Carbon Manag, 2, 189-205, 2011.

Maire, V., Wright, I. J., Prentice, I. C., Batjes, N. H., Bhaskar, R., Bodegom, P. M., Cornwell, W. K., Ellsworth, D., Niinemets, Ü., and Ordonez, A.: Global effects of soil and climate on leaf photosynthetic traits and rates, Global Ecol. Biogeogr., 24, 706-717, 2015.

Marchiori, L., Maystadt, J.-F., and Schumacher, I.: The impact of weather anomalies on migration in sub-Saharan Africa, J. Environ. Econ. Manage., 63, 355-374, 2012.

Masson-Delmotte, V., M Schulz, A Abe-Ouchi, J Beer, A Ganopolski, JF González Rouco, E. Jansen, K. Lambeck, J. Luterbacher, T. Naish, T. Osborn, B. Otto-Bliesner, T. Q., R.

Ramesh, M. Rojas, Shao, X., and Timmermann, A.: Information from Paleoclimate Archives. In: Climate Change 2013: The Physical Science Basis. Contribution of Working Group I to the Fifth Assessment Report of the Intergovernmental Panel on Climate Change [Stocker, T.F., D. Qin, G.-K. Plattner, M. Tignor, S.K. Allen, J. Boschung, A. Nauels, Y. Xia, V. Bex and P.M. Midgley (eds.)]. Cambridge University Press, Cambridge, United Kingdom and New York, NY, USA., 2013.

Mc Millen, G. G. and Mc Clendon, J. H.: Leaf angle: an adaptive feature of sun and shade leaves, Botanical Gazette, 437-442, 1979.

McFadden, D.: Conditional logit analysis of qualitative choice behavior, in P. Zarembka (ed.), Frontiers in Econometrics, Academic Press, pp. 105-142, 1974.

McIntyre, S., Lavorel, S., Landsberg, J., and Forbes, T.: Disturbance response in vegetation–towards a global perspective on functional traits, Journal of Vegetation Science, 10, 621-630, 1999.

McLeod, E., Moffitt, R., Timmermann, A., Salm, R., Menviel, L., Palmer, M. J., Selig, E. R., Casey, K. S., and Bruno, J. F.: Warming Seas in the Coral Triangle: Coral Reef Vulnerability and Management Implications, Coast. Manage., 38, 518-539, 2010.

Medlyn, B. E., Duursma, R. A., Eamus, D., Ellsworth, D. S., Prentice, I. C., Barton, C. V. M., Crous, K. Y., de Angelis, P., Freeman, M., and Wingate, L.: Reconciling the optimal and empirical approaches to modelling stomatal conductance, Global Change Biol., 17, 2134-2144, 2011.

Meehl, G. A., T.F. Stocker, W.D. Collins, P. Friedlingstein, A. T. G., and J.M. Gregory, A. K., R. Knutti, J.M. Murphy, A. Noda, S.C.B. Raper, I.G. Watterson, A.J. Weaver and Z.-C. Zhao: Global climate projections. In: Climate Change 2007: The Physical Science Basis. Contribution of Working Group I to the Fourth Assessment Report of the Intergovernmental Panel on Climate Change [Solomon, S., D. Qin, M. Manning, Z. Chen, M. Marquis, K. B. Averyt, M. Tignor and H. L. Miller (eds.)] Cambridge University Press, Cambridge, United Kingdom and New York, NY, USA, 2007.

Meng, T. T., Ni, J., and Harrison, S. P.: Plant morphometric traits and climate gradients in northern China: a meta-analysis using quadrat and flora data, Ann. Bot., 104, 1217-1229, 2009.

Meng, T. T., Wang, H., Harrison, S. P., Prentice, I. C., Ni, J., and Wang, G.: Responses of leaf traits to climatic gradients: adaptive variation vs. compositional shifts, Biogeosci. Disc., 12, 2015.

Métivier, F., Gaudemer, Y., Tapponnier, P., and Meyer, B.: Northeastward growth of the Tibet plateau deduced from balanced reconstruction of two depositional areas: the Qaidam and Hexi Corridor basins, China, Tectonics, 17, 823-842, 1998.

Michaletz, S. T., Weiser, M. D., Zhou, J., Kaspari, M., Helliker, B. R., and Enquist, B. J.: Plant Thermoregulation: Energetics, Trait–Environment Interactions, and Carbon Economics, Trends Ecol. Evol., 30, 714-724, 2015.

Miller, I. M., Brandon, M. T., and Hickey, L. J.: Using leaf margin analysis to estimate the mid-Cretaceous (Albian) paleolatitude of the Baja BC block, Earth and Planetary Science Letters, 245, 95-114, 2006.

Minckley, T. A., Bartlein, P. J., Whitlock, C., Shuman, B. N., Williams, J. W., and Davis, O. K.: Associations among modern pollen, vegetation, and climate in western North America, Quaternary Science Reviews, 27, 1962-1991, 2008.

Moles, A. T., Perkins, S. E., Laffan, S. W., Flores-Moreno, H., Awasthy, M., Tindall, M. L., Sack, L., Pitman, A., Kattge, J., and Aarssen, L. W.: Which is a better predictor of plant traits: temperature or precipitation?, Journal of vegetation science, 25, 1167-1180, 2014.

Moore, P. D., Webb, J. A., and Collison, M. E.: Pollen analysis, Blackwell scientific publications, 1991.

Morris, J.: The limits of salt marsh adaptation to rising sea level. Sea-level rise 2010 Conference, March 1–3, 2010, Corpus Christi, Texas. Harte Research Institute and Texas A&M University. http://www.sealevelrise2010.org/Morris,James. pdf, last viewed June 9, 2010.

Morton, R. A., Bernier, J. C., Barras, J. A., and Ferina, N.F.: Rapid Subsidence and Historical Wetland Loss in the Mississippi Delta Plain: Likely Causes and Future Implications. Open File Report 2005-1216, U.S. Department of Interior and U.S. Geological Survey (USGS), p124 , 2005.

Morzadec-Kerfourn, M. T.: Dinoflagellate cysts and the paleoenvironment of Late-Pliocene Early-Pleistocene deposits of Brittany, northwest France, Quaternary Science Reviews, 16, 883-898, 1997.

Mosbrugger, V. and Utescher, T.: The coexistence approach—a method for quantitative reconstructions of Tertiary terrestrial palaeoclimate data using plant fossils, Palaeogeogr., Palaeoclimatol., Palaeoecol., 134, 61-86, 1997.

Mosbrugger, V., Utescher, T., and Dilcher, D. L.: Cenozoic continental climatic evolution of Central Europe, Proceedings of the National Academy of Sciences of the United States of America, 102, 14964-14969, 2005.

Moss, R., Babiker, M., Brinkman, S., Calvo, E., Carter, T., Edmonds, J., Elgizouli, I., Emori, S., Erda, L., Hibbard, K., Jones, R., Kainuma, M., Kelleher, J., Manning, J. F. L. M., Matthews, B., Meehl, J., Meyer, L., Mitchell, J., Nakicenovic, N., O'Neill, B., Pichs, R., Riahi, K., Rose, S., Runci, P., Stouffer, R., Vuuren, D. v., Weyant, J., Wilbanks, T., Ypersele, J. P. v., and Zurek, M.: Towards New Scenarios for Analysis of Emissions, Climate Change, Impacts, and Response Strategies. Technical Summary. Intergovernmental Panel on Climate Change, Geneva, 25 pp., 2008.

Murty, T. S., Flather, R. A., and Henry, R. F.: The Storm-Surge Problem in the Bay of Bengal, Prog. Oceanogr., 16, 195-233, 1986.

Myhre, G., D. Shindell, F.-M. Bréon, W. Collins, J. Fuglestvedt, J. Huang, D. Koch, and J.-F. Lamarque, D. L., B. Mendoza, T. Nakajima, A. Robock, G. Stephens, T. Takemura and H. Zhang: Anthropogenic and Natural Radiative Forcing. In: Climate Change 2013: The

Physical Science Basis. Contribution of Working Group I to the Fifth Assessment Report of the Intergovernmental Panel on Climate Change [Stocker, T.F., D. Qin, G.-K. Plattner, M. Tignor, S.K. Allen, J. Boschung, A. Nauels, Y. Xia, V. Bex and P.M. Midgley (eds.)]. Cambridge University Press, Cambridge, United Kingdom and New York, NY, USA., Cambridge University Press, 2013.

Neinhuis, C. and Barthlott, W.: Characterization and distribution of water-repellent, self-cleaning plant surfaces, Ann. Bot., 79, 667-677, 1997.

Nelder, J. and Wedderburn, R.: Generalized Linear Models. J, Journal of the Royal Statistical Society, A135, 370–384, 1972.

Ni, J. and Wang, G. H.: Northeast China Transect (NECT): Ten-year synthesis and future challenges, Acta Botanica Sinica, 46, 379-391, 2004.

Nicotra, A. B., Leigh, A., Boyce, C. K., Jones, C. S., Niklas, K. J., Royer, D. L., and Tsukaya, H.: The evolution and functional significance of leaf shape in the angiosperms, Funct. Plant Biol., 38, 535-552, 2011.

Niinemets, Ü.: Global-scale climatic controls of leaf dry mass per area, density, and thickness in trees and shrubs, Ecology, 82, 453-469, 2001.

Nye, J. A., Link, J. S., Hare, J. A., and Overholtz, W. J.: Changing spatial distribution of fish stocks in relation to climate and population size on the Northeast United States continental shelf, Mar. Ecol. Prog. Ser., 393, 111-129, 2009.

Ortu, E., Brewer, S., and Peyron, O.: Pollen-inferred palaeoclimate reconstructions in mountain areas: problems and perspectives, J Quaternary Sci, 21, 615-627, 2006.

Ortu, E., David, F., and Peyron, O.: Pollen-inferred palaeoclimate reconstruction in the Alps during the Lateglacial and the early Holocene: how to estimate the effect of elevation and local parameters, J Quaternary Sci, 25, 651-661, 2010.

Overpeck, J. T., Webb, T., and Prentice, I. C.: Quantitative interpretation of fossil pollen spectra: dissimilarity coefficients and the method of modern analogs, Quatern. Res., 23, 87-108, 1985.

Pagani, M., Liu, Z. H., LaRiviere, J., and Ravelo, A. C.: High Earth-system climate sensitivity determined from Pliocene carbon dioxide concentrations, Nature Geoscience, 3, 27-30, 2010.

Pall, P., Aina, T., Stone, D. A., Stott, P. A., Nozawa, T., Hilberts, A. G. J., Lohmann, D., and Allen, M. R.: Anthropogenic greenhouse gas contribution to flood risk in England and Wales in autumn 2000, Nature, 470, 382-385, 2011.

Pan, Y. F., Yan, S., Behling, H., and Mu, G. J.: Transport of airborne *Picea schrenkiana* pollen on the northern slope of Tianshan Mountains (Xinjiang, China) and its implication for paleoenvironmental reconstruction, Aerobiologia, 29, 161-173, 2013.

Papke, L. E. and Wooldridge, J. M.: Econometric methods for fractional response variables with an application to 401(k) plan participation rates, Journal of Applied Econometrics, 11, 619-632, 1996.

Parkhurst, D. F. and Loucks, O.: Optimal leaf size in relation to environment, J. Ecol., 60, 505-537, 1972.

Parrish, J. T. and Spicer, R. A.: Late Cretaceous Terrestrial Vegetation - a near-Polar Temperature Curve, Geology, 16, 22-25, 1988.

Pearson, P. N., Ditchfield, P. W., Singano, J., Harcourt-Brown, K. G., Nicholas, C. J., Olsson, R. K., Shackleton, N. J., and Hall, M. A.: Warm tropical sea surface temperatures in the Late Cretaceous and Eocene epochs, Nature, 413, 481-487, 2001.

Pearson, R. G. and Dawson, T. P.: Predicting the impacts of climate change on the distribution of species: are bioclimate envelope models useful?, Global Ecol. Biogeogr., 12, 361-371, 2003.

Peppe, D. J., Lemons, C. R., Royer, D. L., Wing, S. L., Wright, I. J., Lusk, C. H., and Rhoden, C. H.: Biomechanical and leaf-climate relationships: a comparison of ferns and seed plants, Am. J. Bot., 101, 338-347, 2014.

Peppe, D. J., Royer, D. L., Cariglino, B., Oliver, S. Y., Newman, S., Leight, E., Enikolopov, G., Fernandez-Burgos, M., Herrera, F., and Adams, J. M.: Sensitivity of leaf size and shape to climate: global patterns and paleoclimatic applications, New Phytol., 190, 724-739, 2011.

Peppe, D. J., Royer, D. L., Wilf, P., and Kowalski, E. A.: Quantification of large uncertainties in fossil leaf paleoaltimetry, Tectonics, 29, 2010.

Perez-Sanz, A., Li, G., Gonzalez, P., and Harrison, S. P.: Evaluation of seasonal climates of northern Africa and the Mediterranean in the CMIP5 simulations., Climate of the Past, 10, 551–568, 2014.

Perry, A. L., Low, P. J., Ellis, J. R., and Reynolds, J. D.: Climate change and distribution shifts in marine fishes, Science, 308, 1912-1915, 2005.

Piao, S. L., Ciais, P., Huang, Y., Shen, Z. H., Peng, S. S., Li, J. S., Zhou, L. P., Liu, H. Y., Ma, Y. C., Ding, Y. H., Friedlingstein, P., Liu, C. Z., Tan, K., Yu, Y. Q., Zhang, T. Y., and Fang, J. Y.: The impacts of climate change on water resources and agriculture in China, Nature, 467, 43-51, 2010.

Pien, S., Wyrzykowska, J., McQueen-Mason, S., Smart, C., and Fleming, A.: Local expression of expansin induces the entire process of leaf development and modifies leaf shape, Proceedings of the National Academy of Sciences, 98, 11812-11817, 2001.

Pigliucci, M.: Phenotypic integration: studying the ecology and evolution of complex phenotypes, Ecol. Lett., 6, 265-272, 2003.

Pillar, V. D. and Sosinski, E. E.: An improved method for searching plant functional types by numerical analysis, Journal of Vegetation Science, 14, 323-332, 2003.

Pinsky, M. L. and Fogarty, M.: Lagged social-ecological responses to climate and range shifts in fisheries, Clim. Change, 115, 883-891, 2012.

Poorter, H., Niinemets, U., Poorter, L., Wright, I. J., and Villar, R.: Causes and consequences of variation in leaf mass per area (LMA): a meta-analysis, New Phytol., 182, 565-588, 2009.

Poorter, L. and Bongers, F.: Leaf traits are good predictors of plant performance across 53 rain forest species, Ecology, 87, 1733-1743, 2006.

Porter, J. R., L. Xie, A.J. Challinor, K. Cochrane, S.M. Howden, M.M. Iqbal, D.B. Lobell, and Travasso, M. I.: Food security and food production systems. In: Climate Change 2014: Impacts, Adaptation, and Vulnerability. Part A: Global and Sectoral Aspects. Contribution of Working Group II to the Fifth Assessment Report of the Intergovernmental Panel on Climate Change [Field, C.B., V.R. Barros, D.J. Dokken, K.J. Mach, M.D. Mastrandrea, T.E. Bilir, M. Chatterjee, K.L. Ebi, Y.O. Estrada, R.C. Genova, B. Girma, E.S. Kissel, A.N. Levy, S. MacCracken, P.R. Mastrandrea, and L.L. White (eds.)]. Cambridge University Press, Cambridge, United Kingdom and New York, NY, USA, pp. 485-533., 2014.

Poulter, B., Ciais, P., Hodson, E., Lischke, H., Maignan, F., Plummer, S., and Zimmermann, N. E.: Plant functional type mapping for earth system models, Geoscientific Model Development, 4, 993-1010, 2011.

Pound, M. J., Haywood, A. M., Salzmann, U., and Riding, J. B.: Global vegetation dynamics and latitudinal temperature gradients during the Mid to Late Miocene (15.97–5.33 Ma), Earth-Sci. Rev., 112, 1-22, 2012.

Prather, M. J., Holmes, C. D., and Hsu, J.: Reactive greenhouse gas scenarios: Systematic exploration of uncertainties and the role of atmospheric chemistry, Geophys. Res. Lett., 39, 2012.

Prentice, I. C., Bartlein, P. J., and Webb, T.: Vegetation and Climate Change in Eastern North-America since the Last Glacial Maximum, Ecology, 72, 2038-2056, 1991.

Prentice, I. C., Bartlein, P. J., and Webb, T.: Vegetation and Climate-Change in Eastern North-America since the Last Glacial Maximum (Vol 72, Pg 2038, 1993), Ecology, 74, 998-998, 1993.

Prentice, I. C., Bondeau, A., Cramer, W., Harrison, S. P., Hickler, T., Lucht, W., Sitch, S., Smith, B., and Sykes, M. T.: Dynamic global vegetation modeling: quantifying terrestrial ecosystem responses to large-scale environmental change. In: Terrestrial ecosystems in a changing world, Springer, 2007.

Prentice, I. C., Dong, N., Gleason, S. M., Maire, V., and Wright, I. J.: Balancing the costs of carbon gain and water transport: testing a new theoretical framework for plant functional ecology, Ecol. Lett., 17, 82-91, 2014.

Prentice, I. C. and Jolly, D.: Mid-Holocene and glacial-maximum vegetation geography of the northern continents and Africa, J. Biogeogr., 27, 507-519, 2000.

Prentice, I. C., Meng, T. T., Wang, H., Harrison, S. P., Ni, J., and Wang, G. H.: Evidence of a universal scaling relationship for leaf CO_2 drawdown along an aridity gradient, New Phytol., 190, 169-180, 2011.

Price, C. A., Wright, I. J., Ackerly, D. D., Niinemets, U., Reich, P. B., and Veneklaas, E. J.: Are leaf functional traits 'invariant' with plant size and what is 'invariance' anyway?, Funct. Ecol., 28, 1330-1343, 2014.

Pross, J., Klotz, S., and Mosbrugger, V.: Reconstructing palaeotemperatures for the Early and Middle Pleistocene using the mutual climatic range method based on plant fossils, Quaternary Science Reviews, 19, 1785-1799, 2000.

Punt, W., Blackmore, S., Hoen, P., and Stafford, P.: The northwest European pollen flora, Elsevier, 2003.

Punt, W., Hoen, P., Blackmore, S., Nilsson, S., and Le Thomas, A.: Glossary of pollen and spore terminology, Rev. Palaeobot. Palynol., 143, 1-81, 2007.

Qiang, X., Li, Z., Powell, C. M., and Zheng, H.: Magnetostratigraphic record of the Late Miocene onset of the East Asian monsoon, and Pliocene uplift of northern Tibet, Earth and Planetary Science Letters, 187, 83-93, 2001.

Qin, F., Ferguson, D. K., Zetter, R., Wang, Y. F., Syabryaj, S., Li, J. F., Yang, J. A., and Li, C. S.: Late Pliocene vegetation and climate of Zhangcun region, Shanxi, North China, Global Change Biol., 17, 1850-1870, 2011.

Qiu, Z. X.: The Chinese Neogene mammalian biochronology—its correlation with the European Neogene mammalian zonation. In: European Neogene mammal chronology, Springer, 1989.

Quan, C., Liu, Y. S., and Utescher, T.: Paleogene Evolution of Precipitation in Northeastern China Supporting the Middle Eocene Intensification of the East Asian Monsoon, Palaios, 26, 743-753, 2011.

Rabassa, J.: Impact of global climate change on glaciers and permafrost of South America, with emphasis on Patagonia, Tierra del Fuego, and the Antarctic Peninsula, Developments in Earth Surface Processes, 13, 415-438, 2009.

Rabatel, A., Francou, B., Soruco, A., Gomez, J., Caceres, B., Ceballos, J. L., Basantes, R., Vuille, M., Sicart, J. E., Huggel, C., Scheel, M., Lejeune, Y., Arnaud, Y., Collet, M., Condom, T., Consoli, G., Favier, V., Jomelli, V., Galarraga, R., Ginot, P., Maisincho, L., Mendoza, J., Menegoz, M., Ramirez, E., Ribstein, P., Suarez, W., Villacis, M., and Wagnon, P.: Current state of glaciers in the tropical Andes: a multi-century perspective on glacier evolution and climate change, Cryosphere, 7, 81-102, 2013.

Ray, R. D. and Douglas, B. C.: Experiments in reconstructing twentieth-century sea levels, Prog. Oceanogr., 91, 496-515, 2011.

Reagan, M. K., McClelland, W. C., Girard, G., Goff, K. R., Peate, D. W., Ohara, Y., and Stern, R. J.: The geology of the southern Mariana fore-arc crust: Implications for the scale of Eocene volcanism in the western Pacific, Earth and Planetary Science Letters, 380, 41-51, 2013.

Regional Geology of Zhejiang Province: Tertiary. In: Bureau of Geology and Mineral Resources of Zhejiang Province (Ed.), Geological Memoirs. Ser., vol. 1. Geological Publishing House, Beijing, China, pp. 189–204., 1982.

Reich, P. B.: The world‐wide ‘fast‐slow’ plant economics spectrum: a traits manifesto, J. Ecol., 102, 275-301, 2014.

Reich, P. B., Walters, M. B., and Ellsworth, D. S.: From tropics to tundra: global convergence in plant functioning, Proceedings of the National Academy of Sciences, 94, 13730-13734, 1997.

Rhein, M., S.R. Rintoul, S. Aoki, E. Campos, D. Chambers, and R.A. Feely, S. G., G.C. Johnson, S.A. Josey, A. Kostianoy, C. Mauritzen, D. Roemmich, L.D. Talley and F. Wang: Observations: Ocean. In: Climate Change 2013: The Physical Science Basis. Contribution of Working Group I to the Fifth Assessment Report of the Intergovernmental Panel on Climate Change [Stocker, T.F., D. Qin, G.-K. Plattner, M. Tignor, S.K. Allen, J. Boschung, A. Nauels, Y. Xia, V. Bex and P.M. Midgley (eds.)]. Cambridge University Press, Cambridge, United Kingdom and New York, NY, USA., 2013.

Rind, D. and Chandler, M.: Increased Ocean Heat Transports and Warmer Climate, J Geophys Res-Atmos, 96, 7437-7461, 1991.

Robinson, M. and Dowsett, H.: Why Study Paleoclimate?, Report 2010-3021, 2010.

Rohde, R., Muller, R., Jacobsen, R., Muller, E., Perlmutter, S., Rosenfeld, A., Wurtele, J., Groom, D., and Wickham, C.: A new estimate of the average Earth surface land temperature spanning 1753 to 2011. Geoinfor Geostat: An Overview, 1(1), 2013.

Rosen, R.: Optimality principles in biology, Plenum Publishing Corp., New York, 40-52, 1967.

Roth, A., Mosbrugger, V., Belz, G., and Neugebauer, H.: Hydrodynamic modelling study of angiosperm leaf venation types, Botanica Acta, 108, 121-126, 1995.

Roth-Nebelsick, A., Utescher, T., Mosbrugger, V., Diester-Haass, L., and Walther, H.: Changes in atmospheric CO_2 concentrations and climate from the Late Eocene to Early Miocene: palaeobotanical reconstruction based on fossil floras from Saxony, Germany, Palaeogeogr., Palaeoclimatol., Palaeoecol., 205, 43-67, 2004.

Royer, D. L.: Climate reconstruction from leaf size and shape: new developments and challenges, The Paleontological Society Papers 18, 195-212, 2012.

Royer, D. L.: CO_2-forced climate thresholds during the Phanerozoic, Geochim. Cosmochim. Acta, 70, 5665-5675, 2006.

Royer, D. L., Meyerson, L. A., Robertson, K. M., and Adams, J. M.: Phenotypic plasticity of leaf shape along a temperature gradient in Acer rubrum, PLoS One, 4, e7653, 2009.

Royer, D. L. and Wilf, P.: Why do toothed leaves correlate with cold climates? Gas exchange at leaf margins provides new insights into a classic paleotemperature proxy, Int. J. Plant Sci., 167, 11-18, 2006.

Royer, D. L., Wilf, P., Janesko, D. A., Kowalski, E. A., and Dilcher, D. L.: Correlations of climate and plant ecology to leaf size and shape: potential proxies for the fossil record, Am. J. Bot., 92, 1141-1151, 2005.

Ryser, P. and Eek, L.: Consequences of phenotypic plasticity vs. interspecific differences in leaf and root traits for acquisition of aboveground and belowground resources, Am. J. Bot., 87, 402-411, 2000.

Saito, Y., N., Chaimanee, T., Jarupongsakul, and Syvitski, J. P. M.: Shrinking megadeltas in Asia: sea-level rise and sediment reduction impacts from case study of the Chao Phraya Delta. Land-Ocean Interaction in the Coastal Zone (LOICZ) INPRINT, 2007/2, 3-9., 2007.

Salonen, J. S., Seppa, H., and Birks, H. J. B.: The effect of calibration data set selection on quantitative palaeoclimatic reconstructions, Holocene, 23, 1650-1654, 2013.

Scheiter, S. and Higgins, S. I.: Impacts of climate change on the vegetation of Africa: an adaptive dynamic vegetation modelling approach, Global Change Biol., 15, 2224-2246, 2009.

Schilt, A., Baumgartner, M., Blunier, T., Schwander, J., Spahni, R., Fischer, H., and Stocker, T. F.: Glacial-interglacial and millennial-scale variations in the atmospheric nitrous oxide concentration during the last 800,000 years, Quaternary Science Reviews, 29, 182-192, 2010.

Schimper, A. F. W.: Pflanzen-geographie auf physiologischer Grundlage, G. Fischer, 1898.

Schmidt, G. A., J.D. Annan, P.J. Bartlein, B.I. Cook, E. Guilyardi, J.C. Hargreaves, S.P. Harrison, M. Kageyama, A.N. LeGrande, B. Konecky, S. Lovejoy, M.E. Mann, V. Masson-Delmotte, C. Risi, D. Thompson, A. Timmermann, L.-B. Tremblay, and Yiou, P.: Using paleo-climate comparisons to constrain future projections in CMIP5, Clim. Past, 10, 221–250, 2014.

Seki, O., Foster, G. L., Schmidt, D. N., Mackensen, A., Kawamura, K., and Pancost, R. D.: Alkenone and boron-based Pliocene pCO_2 records, Earth and Planetary Science Letters, 292, 201-211, 2010.

Seneviratne, S. I., Nicholls, N., Easterling, D. R., Goodess, C. M., Kanae, S., Kossin, J., Luo, Y., Marengo, J., McInnes, K., Rahimi, N., Reichstein, M., Sorteberg, A., Vera, C., and Zhang, X.: Changes in climate extremes and their impacts on the natural physical environment, in: Managing the Risks of Extreme Events and Disasters to Advance Climate Change Adaptation, edited by: Field, C. B., Barros, V., Stocker, T. F., Qin, D., Dokken, D. J., Ebi, K., Mastrandrea, D. M., Mach, K. J., Plattner, G.-K., Allen, S. K., Tignor, M., and Midgley, G. F., Cambridge University Press, Cambridge, UK, and New York, NY, USA, 109–230, 2012.

Sexton, J. P., McIntyre, P. J., Angert, A. L., and Rice, K. J.: Evolution and Ecology of Species Range Limits, Annu Rev Ecol Evol S, 40, 415-436, 2009.

Shaver, G. S.: Leaf angle and light absorbance of *Arctostaphylos* species (Ericaceae) along elevational gradients, Madrono, 25, 218-226, 1978.

Shen, C. M., Liu, K. B., Tang, L. Y., and Overpeck, J. T.: Numerical analysis of modern and fossil pollen data from the Tibetan Plateau, Ann Assoc Am Geogr, 98, 755-772, 2008.

Shen, C. M., Liu, K. B., Tang, L. Y., and Overpeck, J. T.: Quantitative relationships between modern pollen rain and climate in the Tibetan Plateau, Rev. Palaeobot. Palynol., 140, 61-77, 2006.

Shevenell, A. E., Kennett, J. P., and Lea, D. W.: Middle Miocene ice sheet dynamics, deep-sea temperatures, and carbon cycling: A Southern Ocean perspective, Geochemistry, Geophysics, Geosystems, 9, 2008.

Shipley, B., Lechowicz, M. J., Wright, I., and Reich, P. B.: Fundamental trade-offs generating the worldwide leaf economics spectrum, Ecology, 87, 535-541, 2006.

Sloan, L. C.: Equable Climates during the Early Eocene−Significance of Regional Paleogeography for North-American Climate, Geology, 22, 881-884, 1994.

Sloan, L. C. and Barron, E. J.: Equable Climates during Earth History, Geology, 18, 489-492, 1990.

Sloan, L. C., Walker, J. C., Moore, T. C., Jr., Rea, D. K., and Zachos, J. C.: Possible methane-induced polar warming in the early Eocene, Nature, 357, 320-322, 1992.

Smith, K. R., A. Woodward, D. Campbell-Lendrum, D.D. Chadee, Y. Honda, Q. Liu, J.M. Olwoch, Revich, B., and Sauerborn, R.: Human health: impacts, adaptation, and co-benefits. In: Climate Change 2014: Impacts, Adaptation, and Vulnerability. Part A: Global and Sectoral Aspects. Contribution of Working Group II to the Fifth Assessment Report of the Intergovernmental Panel on Climate Change [Field, C.B., V.R. Barros, D.J. Dokken, K.J. Mach, M.D. Mastrandrea, T.E. Bilir, M. Chatterjee, K.L. Ebi, Y.O. Estrada, R.C. Genova, B. Girma, E.S. Kissel, A.N. Levy, S. MacCracken, P.R. Mastrandrea, and L.L. White (eds.)]. Cambridge University Press, Cambridge, United Kingdom and New York, NY, USA, pp. 709-754., 2014.

Smith, W. K.: Temperatures of desert plants: another perspective on the adaptability of leaf size, Science, 201, 614-616, 1978.

Song, Z. C.: Fossil Spores and Pollen of China 1: The Late Cretaceous and Tertiary Spores and Pollen, Science Press, Beijing (in Chinese with English abstract). 1999.

Spicer, R. A.: CLAMP online. http://clamp.ibcas.ac.cn/. 2012.

Spicer, R. A., Herman, A. B., Liao, W. B., Spicer, T. E. V., Kodrul, T. M., Yang, J., and Jin, J. H.: Cool tropics in the Middle Eocene: Evidence from the Changchang Flora, Hainan Island, China, Palaeogeogr Palaeocl, 412, 1-16, 2014.

Spicer, R. A. and Parrish, J. T.: Paleobotanical Evidence for Cool North Polar Climates in Middle Cretaceous (Albian-Cenomanian) Time, Geology, 14, 703-706, 1986.

Stahl, E.: Über den Einfluß der Lichtintensität auf Struktur und Anordnung des Assimilationsparenchyms, Bot. Zeitung, 38, 868-874, 1880.

Steininger, F. F., Berggren, W. A., Kent, D. V., Bernor, R. L., Sen, S., and Agust., J.: Circum-Mediterranean Neogene (Miocene and Pliocene) marine–continental chronologic correlations of European mammal units. In R. L. Bernor, V. Fahlbusch, and H. W.

Mittmann [eds.], The evolution of eastern Eurasian Neogene mammal faunas, 7– 46. Columbia University Press, New York, USA., 1996.

Stuchlik, L.: Atlas of pollen and spores of the Polish Neogene, W. Szafer Institute of Botany, Polish Acadamy of Sciences, 2001.

Stuchlik, L.: Atlas of pollen and spores of the Polish Neogene, Angiosperms, vol. 3, W. Szafer Institute of Botany, Polish Acadamy of Sciences, 2009.

Stuchlik, L.: Atlas of pollen and spores of the Polish Neogene, Gymnosperms, vol. 2, W. Szafer Institute of Botany, Polish Acadamy of Sciences, 2002.

Su, T., Jacques, F. M. B., Spicer, R. A., Liu, Y. S., Huang, Y. J., Xing, Y. W., and Zhou, Z. K.: Post-Pliocene establishment of the present monsoonal climate in SW China: evidence from the late Pliocene Longmen megaflora, Climate of the Past, 9, 1911-1920, 2013.

Su, T., Xing, Y. W., Liu, Y. S., Jacques, F. M. B., Chen, W. Y., Huang, Y. J., and Zhou, Z. K.: Leaf Margin Analysis: A New Equation from Humid to Mesic Forests in China, Palaios, 25, 234-238, 2010.

Suc, J. P., Diniz, F., Leory, S., Poumont, C., Bertini, A., Dupont, L., Clet, M., Bessais, E., Zheng, Z., Fauquette, S., and Ferrier, J.: Zanclean (~Brunssumian) to early Piacenzian (~early-middle Reuverian) climate from 4° to 54° north latitude (West Africa, West Europe and West Mediterranean areas): Mededelingen Rijks Geologische Dienst, no. 52, p. 43–56., 1995.

Sun, N. and Li, X. Q.: The quantitative reconstruction of the palaeoclimate between 5200 and 4300 cal yr BP in the Tianshui Basin, NW China, Climate of the Past, 8, 625-636, 2012.

Sun, Q. G., Collinson, M. E., Li, C. S., Wang, Y. F., and Beerling, D. J.: Quantitative reconstruction of palaeoclimate from the Middle Miocene Shanwang flora, eastern China, Palaeogeogr., Palaeoclimatol., Palaeoecol., 180, 315-329, 2002.

Sun, T. X., Ablaev, A. G., Wang, Y. F., and Li, C. S.: *Cyclocarya* cf. *paliurus* (Batal.) Iljinskaja (Juglandaceae) from the Hunchun Formation (Eocene), Jilin Province, China, Journal of Integrative Plant Biology, 47, 1281-1287, 2005.

Sun, W. X., Liang, S. L., Xu, G., Fang, H. L., and Dickinson, R.: Mapping plant functional types from MODIS data using multisource evidential reasoning, Remote Sens. Environ., 112, 1010-1024, 2008.

Sun, X. and Wang, P.: How old is the Asian monsoon system?—Palaeobotanical records from China, Palaeogeogr., Palaeoclimatol., Palaeoecol., 222, 181-222, 2005.

Swenson, N. G. and Enquist, B. J.: Ecological and evolutionary determinants of a key plant functional trait: Wood density and its community-wide variation across latitude and elevation, Am. J. Bot., 94, 451-459, 2007.

Tang, Y. N., Li, X., Yao, Y. F., Ferguson, D. K., and Li, C. S.: Environmental reconstruction of Tuyoq in the fifth fentury and its bearing on Buddhism in Turpan, Xinjiang, China, PLoS One, 9, e86363, 2014.

Tao, J., Zhou, Z., and Liu, Y.: The evolution of the Late cretaceous Cenozoic flora of China, (in Chinese), 2000.

Taylor, S. E.: Optimal leaf form. In: Perspectives of biophysical ecology, Springer, 1975.

Teodoridis, V., Kvaček, Z., and Uhl, D.: Pliocene palaeoenvironment and correlation of the Sessenheim–Auenheim floristic complex (Alsace, France), Palaeodiversity, 2, 1-17, 2009.

ter Braak, C. J.: Canonical correspondence analysis: a new eigenvector technique for multivariate direct gradient analysis, Ecology, 67, 1167-1179, 1986.

Thiel, C., Klotz, S., and Uhl, D.: Palaeoclimate Estimates for Selected Leaf Floras from the Late Pliocene (Reuverian) of Central Europe Based on Different Palaeobotanical Techniques, Turk J Earth Sci, 21, 263-287, 2012.

Thompson, R., Anderson, K., Pelltier, R., Strickland, L., Bartlein, P., and Shafer, S.: Quantitative estimation of climatic parameters from vegetation data in North America by the mutual climatic range technique, Quaternary Science Reviews, 51, 18-39, 2012.

Thompson, R. S.: Atlas of relations between climatic parameters and distributions of important trees and shrubs in North America: Alaska species and ecoregions, US Dept. of the Interior, US Geological Survey, 2006.

Thompson, R. S., Anderson, K. H., and Bartlein, P. J.: Atlas of relations between climatic parameters and distributions of important trees and shrubs in North America, US Department of the Interior, US Geological Survey, 1999.

Thompson, R. S., Anderson, K. H., and Bartlein, P. J.: Quantitative estimation of bioclimatic parameters from presence/absence vegetation data in North America by the modern analog technique, Quaternary Science Reviews, 27, 1234-1254, 2008.

Tindall, J., Flecker, R., Valdes, P., Schmidt, D. N., Markwick, P., and Harris, J.: Modelling the oxygen isotope distribution of ancient seawater using a coupled ocean-atmosphere GCM: Implications for reconstructing early Eocene climate, Earth and Planetary Science Letters, 292, 265-273, 2010.

Tomsich, C. S., McCarthy, P. J., Fowell, S. J., and Sunderlin, D.: Paleofloristic and paleoenvironmental information from a late Cretaceous (Maastrichtian) flora of the lower Cantwell Formation near Sable Mountain, Denali National Park, Alaska, Palaeogeogr., Palaeoclimatol., Palaeoecol., 295, 389-408, 2010.

Traiser, C., Klotz, S., Uhl, D., and Mosbrugger, V.: Environmental signals from leaves–a physiognomic analysis of European vegetation, New Phytol., 166, 465-484, 2005.

Trninic, V., Jelaska, I., and Štalec, J.: appropriateness and limitations of factor analysis methods utilised in psychology and kinesiology -part i, Physical culture, 66, 77-87, 2012.

Trninic, V., Jelaska, I., and Štalec, J.: appropriateness and limitations of factor analysis methods utilised in psychology and kinesiology -part ii, Physical culture, 67, 5-17, 2013.

Tsukui, K. and Clyde, W. C.: Fine-tuning the calibration of the early to middle Eocene geomagnetic polarity time scale: Paleomagnetism of radioisotopically dated tuffs from Laramide foreland basins, Geological Society of America Bulletin, 124, 870-885, 2012.

Uhl, D., Mosbrugger, V., Bruch, A., and Utescher, T.: Reconstructing palaeotemperatures using leaf floras–case studies for a comparison of leaf margin analysis and the coexistence approach, Rev. Palaeobot. Palynol., 126, 49-64, 2003.

Uhl, D., Traiser, C., Griesser, U., and Denk, T.: Fossil leaves as palaeoclimate proxies in the Palaeogene of Spitsbergen (Svalbard), Acta Palaeobotanica, 47, 89-107, 2007.

Upchurch, D. R. and Mahan, J. R.: Maintenance of constant leaf temperature by plants—II. Experimental observations in cotton, Environ. Exp. Bot., 28, 359-366, 1988.

Upchurch Jr, G. and Wolfe, J.: Mid-Cretaceous to Early Tertiary vegetation and climate: evidence from fossil leaves and woods, Origins of angiosperms and their biological consequences/edited by EM Friis, WG Chaloner, and PR Crane, 1987.

Utescher, T., Bruch, A. A., Erdei, B., François, L., Ivanov, D., Jacques, F. M. B., Kern, A. K., Liu, Y. S., Mosbrugger, V., and Spicer, R. A.: The Coexistence Approach—Theoretical background and practical considerations of using plant fossils for climate quantification, Palaeogeogr., Palaeoclimatol., Palaeoecol., 410, 58-73, 2014.

Utescher, T., Djordjevic-Milutinovic, D., Bruch, A., and Mosbrugger, V.: Palaeoclimate and vegetation change in Serbia during the last 30 Ma, Palaeogeogr., Palaeoclimatol., Palaeoecol., 253, 141-152, 2007.

Utescher, T. and Mosbrugger, V.: The Palaeoflora database, Available online at http://www.palaeoflora.de/. 2013.

Utescher, T., Mosbrugger, V., and Ashraf, A. R.: Terrestrial climate evolution in northwest Germany over the last 25 million years, Palaios, 15, 430-449, 2000.

Van Bodegom, P. M., Douma, J. C., Witte, J. P. M., Ordonez, J. C., Bartholomeus, R. P., and Aerts, R.: Going beyond limitations of plant functional types when predicting global ecosystem-atmosphere fluxes: exploring the merits of traits-based approaches, Global Ecol. Biogeogr., 21, 625-636, 2012.

Vaughan, D. G., J.C. Comiso, I. Allison, J. Carrasco, G. Kaser, R. Kwok, P. Mote, T. Murray, F. Paul, J. Ren, E. Rignot, O. Solomina, Steffen, K., and Zhang, T.: Observations: Cryosphere. In: Climate Change 2013: The Physical Science Basis. Contribution of Working Group I to the Fifth Assessment Report of the Intergovernmental Panel on Climate Change [Stocker, T.F., D. Qin, G.-K. Plattner, M. Tignor, S.K. Allen, J. Boschung, A. Nauels, Y. Xia, V. Bex and P.M. Midgley (eds.)]. Cambridge University Press, Cambridge, United Kingdom and New York, NY, USA., 2013.

Verheijen, L. M., Brovkin, V., Aerts, R., Bonisch, G., Cornelissen, J. H. C., Kattge, J., Reich, P. B., Wright, I. J., and van Bodegom, P. M.: Impacts of trait variation through observed trait-climate relationships on performance of an Earth system model: a conceptual analysis, Biogeosciences, 10, 5497-5515, 2013.

Viau, A., Gajewski, K., Sawada, M., and Fines, P.: Mean-continental July temperature variability in North America during the past 14,000 years, Journal of Geophysical Research: Atmospheres, 111, D09102, 2006.

Wang, F. and Jin, L.: Petrological and geo-chemistry characteristics of Cenozic basalts from Shanwang area, Shandong. Collections of mineralogy and petrology, vol. II, 43–65. Geological Publishing House, Beijing, China, 1986.

Wang, F. X., Qian, N. F., Zhang, Y. L., and Yang, H. Q.: Pollen flora of China, Beijing: Science Press, 325, 326, 1995.

Wang, H., Ni, J., and Prentice, I. C.: Sensitivity of potential natural vegetation in China to projected changes in temperature, precipitation and atmospheric CO_2, Regional Environmental Change, 11, 715-727, 2011.

Wang, H., Prentice, I., and Ni, J.: Data-based modelling and environmental sensitivity of vegetation in China, Biogeosciences, 10, 5817-5830, 2013.

Wang, H., Prentice, I. C., and Ni, J.: Primary production in forests and grasslands of China: contrasting environmental responses of light- and water-use efficiency models, Biogeosciences, 9, 4689-4705, 2012.

Wang, Q., Ferguson, D. K., Feng, G. P., Ablaev, A. G., Wang, Y. F., Yang, J. A., Li, Y. L., and Li, C. S.: Climatic change during the Palaeocene to Eocene based on fossil plants from Fushun, China, Palaeogeogr., Palaeoclimatol., Palaeoecol., 295, 323-331, 2010.

Wang, W.: A palynological survey of Neogene strata in Xiaolongtan basin, Yunnan Province of South China. Acta Bot. Sin. 38, 743–748 (in Chinese with English abstract). 1996.

Wang, Y.-F., Li, C.-S., Collinson, M. E., Lin, J., and Sun, Q.-G.: *Eucommia* (Eucommiaceae), a potential biothermometer for the reconstruction of paleoenvironments, Am. J. Bot., 90, 1-7, 2003.

Wei, Z., Wang, H., Gao, L., Zhang, X., Zhou, L., and Feng, Y.: Pollen flora of seed plants, Yunnan Science and Technology Press, 2003. pp131, 2003.

Werger, M. and Ellenbroek, G.: Leaf size and leaf consistence of a riverine forest formation along a climatic gradient, Oecologia, 34, 297-308, 1978.

Westra, S., Alexander, L. V., and Zwiers, F. W.: Global Increasing Trends in Annual Maximum Daily Precipitation, J. Clim., 26, 3904-3918, 2013.

WGCPC: Cenozoic Plants of China. Science Press, Beijing, 1978.

Wiegand, K. M.: The relation of hairy and cutinized coverings to transpiration, Botanical Gazette, 49, 0430-0444, 1910.

Wiemann, M. C., Manchester, S. R., Dilcher, D. L., Hinojosa, L. F., and Wheeler, E. A.: Estimation of temperature and precipitation from morphological characters of dicotyledonous leaves, Am. J. Bot., 85, 1796-1802, 1998.

Wilf, P.: When are leaves good thermometers? A new case for leaf margin analysis, Paleobiology, 23, 373-390, 1997.

Wilf, P., Johnson, K. R., and Huber, B. T.: Correlated terrestrial and marine evidence for global climate changes before mass extinction at the Cretaceous–Paleogene boundary, Proceedings of the National Academy of Sciences, 100, 599-604, 2003.

Wilf, P., Wing, S. L., Greenwood, D. R., and Greenwood, C. L.: Using fossil leaves as paleoprecipitation indicators: An Eocene example, Geology, 26, 203-206, 1998.

Wing, S. L., Bao, H., and Koch, P. L.: An early Eocene cool period? Evidence for continental cooling during the warmest part of the Cenozoic, Warm climates in Earth history. Cambridge University Press, Cambridge, 2000. 197-237, 2000.

Wing, S. L. and Greenwood, D. R.: Fossils and fossil climate: the case for equable continental interiors in the Eocene, Philosophical Transactions of the Royal Society of London B: Biological Sciences, 341, 243-252, 1993.

Winguth, A., Shellito, C., Shields, C., and Winguth, C.: Climate Response at the Paleocene-Eocene Thermal Maximum to Greenhouse Gas Forcing-A Model Study with CCSM3, J. Clim., 23, 2562-2584, 2010.

Wohlfahrt, J., Harrison, S. P., and Braconnot, P.: Synergistic feedbacks between ocean and vegetation on mid- and high-latitude climates during the mid-Holocene, Climate Dynamics, 22, 223-238, 2004.

Wolfe, J. and Hopkins, D.: Climatic changes recorded by Tertiary land floras in northwestern North America. In: Tertiary correlations and climatic changes in the Pacific, Sasaki Sendai, 1967.

Wolfe, J. A.: A method of obtaining climatic parameters from leaf assemblages, US Geological Survey Bulletin (USA), 1993.

Wolfe, J. A.: Palaeobotanical Evidence for a Marked Temperature Increase Following the Cretaceous Tertiary Boundary, Nature, 343, 153-156, 1990.

Wolfe, J. A.: A paleobotanical interpretation of Tertiary climates in the Northern Hemisphere: Data from fossil plants make it possible to reconstruct Tertiary climatic changes, which may be correlated with changes in the inclination of the earth's rotational axis, Am. Sci., 1978. 694-703, 1978.

Wolfe, J. A.: Paleoclimatic estimates from Tertiary leaf assemblages, Annual Review of Earth and Planetary Sciences, 23, 119-142, 1995.

Wolfe, J. A.: Temperature parameters of humid to mesic forests of Eastern Asia and relation to forests of other regions of the Northern Hemisphere and Australasia: analysis of temperature data from more than 400 stations in Eastern Asia, United States. Geological Survey. Professional paper (USA), 1979.

Wolfe, J. A.: Tertiary climatic fluctuations and methods of analysis of Tertiary floras, Palaeogeogr., Palaeoclimatol., Palaeoecol., 9, 27-57, 1971.

Wolfe, J. A. and Upchurch, G. R.: North American nonmarine climates and vegetation during the Late Cretaceous, Palaeogeogr., Palaeoclimatol., Palaeoecol., 61, 33-77, 1987.

Woodward, F. I.: Climate and plant distribution, Cambridge University Press, 1987.

Woodward, F. I. and Cramer, W.: Plant functional types and climatic change: introduction, Journal of Vegetation Science, 7, 306-308, 1996.

Wright, I. J., Reich, P. B., Cornelissen, J. H., Falster, D. S., Garnier, E., Hikosaka, K., Lamont, B. B., Lee, W., Oleksyn, J., and Osada, N.: Assessing the generality of global leaf trait relationships, New Phytol., 166, 485-496, 2005a.

Wright, I. J., Reich, P. B., Cornelissen, J. H., Falster, D. S., Groom, P. K., Hikosaka, K., Lee, W., Lusk, C. H., Niinemets, Ü., and Oleksyn, J.: Modulation of leaf economic traits and trait relationships by climate, Global Ecol. Biogeogr., 14, 411-421, 2005b.

Wright, I. J., Reich, P. B., Westoby, M., Ackerly, D. D., Baruch, Z., Bongers, F., Cavender-Bares, J., Chapin, T., Cornelissen, J. H., and Diemer, M.: The worldwide leaf economics spectrum, Nature, 428, 821-827, 2004.

Wright, I. J. and Westoby, M.: Leaves at low versus high rainfall: coordination of structure, lifespan and physiology, New Phytol., 155, 403-416, 2002.

Wu, H. B., Guiot, J., Brewer, S., and Guo, Z. T.: Climatic changes in Eurasia and Africa at the last glacial maximum and mid-Holocene: reconstruction from pollen data using inverse vegetation modelling, Climate Dynamics, 29, 211-229, 2007.

Wu, Z. Y. and Ding, T. Y.: Seed plants of China, Yunnan Science and Technology Press, Kunming, China (Electronic publication in Chinese). 1999.

Xi, Y. Z. and Ning, J. C.: Pollen morphology of plants from dry and semi-dry area in China, Yushania, 11, 119–191, 1994.

Xia, K., Su, T., Liu, Y. S. C., Xing, Y. W., Jacques, F. M., and Zhou, Z. K.: Quantitative climate reconstructions of the late Miocene Xiaolongtan megaflora from Yunnan, southwest China, Palaeogeogr., Palaeoclimatol., Palaeoecol., 276, 80-86, 2009.

Yang, H. and Yang, S.: The Shanwang fossil biota in eastern China: a Miocene Konservat‐Lagerstätte in lacustrine deposits, Lethaia, 27, 345-354, 1994.

Yang, J., Spicer, R. A., Spicer, T. E., and Li, C.-S.: 'CLAMP Online': a new web-based palaeoclimate tool and its application to the terrestrial Paleogene and Neogene of North America, Palaeobiodiversity and Palaeoenvironments, 91, 163-183, 2011.

Yang, J., Spicer, R. A., Spicer, T. E. V., Arens, N. C., Jacques, F. M. B., Su, T., Kennedy, E. M., Herman, A. B., Steart, D. C., Srivastava, G., Mehrotra, R. C., Valdes, P. J., Mehrotra, N. C., Zhou, Z. K., and Lai, J. S.: Leaf form-climate relationships on the global stage: an ensemble of characters, Global Ecol. Biogeogr., doi: 10.1111/geb.12334, 2015.

Yang, J., Wang, Y. F., Spicer, R. A., Mosbrugger, V., Li, C. S., and Sun, Q. G.: Climatic reconstruction at the miocene shanwang basin, China, using leaf margin analysis,

CLAMP, coexistence approach, and overlapping distribution analysis, Am. J. Bot., 94, 599-608, 2007.

Yao, Y.-F., Bera, S., Ferguson, D. K., Mosbrugger, V., Paudayal, K. N., Jin, J.-H., and Li, C.-S.: Reconstruction of paleovegetation and paleoclimate in the Early and Middle Eocene, Hainan Island, China, Clim. Change, 92, 169-189, 2009.

Yao, Y. F., Bruch, A. A., Cheng, Y. M., Mosbrugger, V., Wang, Y. F., and Li, C. S.: Monsoon versus uplift in southwestern China–late Pliocene climate in Yuanmou Basin, Yunnan, PloS one, 7, e37760, 2012.

Yao, Y. F., Bruch, A. A., Mosbrugger, V., and Li, C. S.: Quantitative reconstruction of Miocene climate patterns and evolution in Southern China based on plant fossils, Palaeogeogr., Palaeoclimatol., Palaeoecol., 304, 291-307, 2011.

Yu, G., Tang, L. Y., Yang, X. D., Ke, X. K., and Harrison, S. P.: Modern pollen samples from alpine vegetation on the Tibetan Plateau, Global Ecol. Biogeogr., 10, 503-520, 2001.

Zachos, J., Pagani, M., Sloan, L., Thomas, E., and Billups, K.: Trends, rhythms, and aberrations in global climate 65 Ma to present, Science, 292, 686-693, 2001.

Zachos, J. C., Dickens, G. R., and Zeebe, R. E.: An early Cenozoic perspective on greenhouse warming and carbon-cycle dynamics, Nature, 451, 279-283, 2008.

Zangerl, A. R.: Energy Exchange Phenomena, Physiological Rates and Leaf Size Variation, Oecologia, 34, 107-112, 1978.

Zhang, Q. Q., Ferguson, D. K., Mosbrugger, V., Wang, Y. F., and Li, C. S.: Vegetation and climatic changes of SW China in response to the uplift of Tibetan Plateau, Palaeogeogr., Palaeoclimatol., Palaeoecol., 363, 23-36, 2012.

Zhang, Q. Q., Smith, T., Yang, J., and Li, C.-S.: Evidence of a Cooler Continental Climate in East China during the Warm Early Cenozoic, PLoS ONE, 11, e0155507, 2016.

Zhang, X. S., Sun, S., Yong, S., Zhou, Z., and Wang, R.: Vegetation map of the People's Republic of China (1: 1000000). Geological Publishing House: Beijing, China, 2007.

Zhang, Y. L., Xi, Y. Z., Zhang, J. T., Gao, G. Z., Du, N. Q., Sun, X. J., and Kong, Z. C.: Sporae Pteridophytorum Sinicorum, Science Press, Beijing., 1976.

Zhang, Z. Y., Harrison, S. P., Mosbrugger, V., Ferguson, D. K., Paudayal, K. N., Trivedi, A., and Li, C. S.: Evaluation of the realism of climate reconstruction using the Coexistence Approach with modern pollen samples from the Qinghai–Tibetan Plateau, Rev. Palaeobot. Palynol., 219, 172-182, 2015.

Zhao, Y. and Harrison, S. P.: Mid-Holocene monsoons: a multi-model analysis of the inter-hemispheric differences in the responses to orbital forcing and ocean feedbacks, Climate Dynamics, 39, 1457-1487, 2012.

Zhao, Y. and Herzschuh, U.: Modern pollen representation of source vegetation in the Qaidam Basin and surrounding mountains, north-eastern Tibetan Plateau, Vegetation History and Archaeobotany, 18, 245-260, 2009.

Zhao, Y. and Yu, Z. C.: Vegetation response to Holocene climate change in East Asian monsoon-margin region, Earth-Sci. Rev., 113, 1-10, 2012.

Zheng, H. B., Powell, C. M., An, Z. S., Zhou, J., and Dong, G. R.: Pliocene uplift of the northern Tibetan Plateau, Geology, 28, 715-718, 2000.

Zheng, Z., Huang, K. Y., Xu, Q. H., Lu, H. Y., Cheddadi, R., Luo, Y. L., Beaudouin, C., Luo, C. X., Zheng, Y. W., Li, C. H., Wei, J. H., and Du, C. B.: Comparison of climatic threshold of geographical distribution between dominant plants and surface pollen in China, Sci China Ser D, 51, 1107-1120, 2008.

Zhu, M., Hu, G., Zhao, D., Liu, S., Hu, X., Ma, Z., and Jian, W.: Potassium argon dating of Neogene basalt in Shanwang area, Shandong Province, Petrological Research, 5, 47-59, 1985.

Zubakov, V. A. and Borzenkova, I. I.: Pliocene Paleoclimates - Past Climates as Possible Analogs of Mid-21st Century Climate, Palaeogeogr., Palaeoclimatol., Palaeoecol., 65, 35-49, 1988.